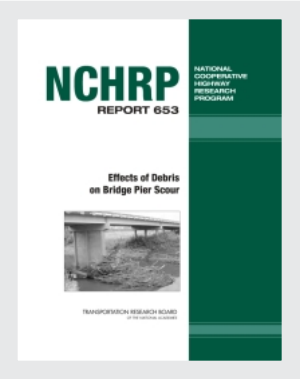

Effects of Debris on Bridge Pier Scour

DETAILS

166 pages | | PAPERBACK
ISBN 978-0-309-11834-7 | DOI 10.17226/22955

AUTHORS

NATIONAL COOPERATIVE HIGHWAY RESEARCH PROGRAM

NCHRP REPORT 653

Effects of Debris on Bridge Pier Scour

P. F. Lagasse
P. E. Clopper
L. W. Zevenbergen
W. J. Spitz
L. G. Girard
AYRES ASSOCIATES, INC.
Fort Collins, CO

Subscriber Categories
Bridges and Other Structures • Geotechnology • Hydraulics and Hydrology

Research sponsored by the American Association of State Highway and Transportation Officials
in cooperation with the Federal Highway Administration

TRANSPORTATION RESEARCH BOARD

WASHINGTON, D.C.
2010
www.TRB.org

NATIONAL COOPERATIVE HIGHWAY RESEARCH PROGRAM

Systematic, well-designed research provides the most effective approach to the solution of many problems facing highway administrators and engineers. Often, highway problems are of local interest and can best be studied by highway departments individually or in cooperation with their state universities and others. However, the accelerating growth of highway transportation develops increasingly complex problems of wide interest to highway authorities. These problems are best studied through a coordinated program of cooperative research.

In recognition of these needs, the highway administrators of the American Association of State Highway and Transportation Officials initiated in 1962 an objective national highway research program employing modern scientific techniques. This program is supported on a continuing basis by funds from participating member states of the Association and it receives the full cooperation and support of the Federal Highway Administration, United States Department of Transportation.

The Transportation Research Board of the National Academies was requested by the Association to administer the research program because of the Board's recognized objectivity and understanding of modern research practices. The Board is uniquely suited for this purpose as it maintains an extensive committee structure from which authorities on any highway transportation subject may be drawn; it possesses avenues of communications and cooperation with federal, state and local governmental agencies, universities, and industry; its relationship to the National Research Council is an insurance of objectivity; it maintains a full-time research correlation staff of specialists in highway transportation matters to bring the findings of research directly to those who are in a position to use them.

The program is developed on the basis of research needs identified by chief administrators of the highway and transportation departments and by committees of AASHTO. Each year, specific areas of research needs to be included in the program are proposed to the National Research Council and the Board by the American Association of State Highway and Transportation Officials. Research projects to fulfill these needs are defined by the Board, and qualified research agencies are selected from those that have submitted proposals. Administration and surveillance of research contracts are the responsibilities of the National Research Council and the Transportation Research Board.

The needs for highway research are many, and the National Cooperative Highway Research Program can make significant contributions to the solution of highway transportation problems of mutual concern to many responsible groups. The program, however, is intended to complement rather than to substitute for or duplicate other highway research programs.

NCHRP REPORT 653

Project 24-26
ISSN 0077-5614
ISBN 978-0-309-11834-7
Library of Congress Control Number 2010926176

COPYRIGHT INFORMATION

NOTICE

The project that is the subject of this report was a part of the National Cooperative Highway Research Program, conducted by the Transportation Research Board with the approval of the Governing Board of the National Research Council.

The members of the technical panel selected to monitor this project and to review this report were chosen for their special competencies and with regard for appropriate balance. The report was reviewed by the technical panel and accepted for publication according to procedures established and overseen by the Transportation Research Board and approved by the Governing Board of the National Research Council.

The opinions and conclusions expressed or implied in this report are those of the researchers who performed the research and are not necessarily those of the Transportation Research Board, the National Research Council, or the program sponsors.

The Transportation Research Board of the National Academies, the National Research Council, and the sponsors of the National Cooperative Highway Research Program do not endorse products or manufacturers. Trade or manufacturers' names appear herein solely because they are considered essential to the object of the report.

Published reports of the

NATIONAL COOPERATIVE HIGHWAY RESEARCH PROGRAM

are available from:

Transportation Research Board
Business Office
500 Fifth Street, NW
Washington, DC 20001

and can be ordered through the Internet at:

http://www.national-academies.org/trb/bookstore

Printed in the United States of America

THE NATIONAL ACADEMIES

Advisers to the Nation on Science, Engineering, and Medicine

The **National Academy of Sciences** is a private, nonprofit, self-perpetuating society of distinguished scholars engaged in scientific and engineering research, dedicated to the furtherance of science and technology and to their use for the general welfare. On the authority of the charter granted to it by the Congress in 1863, the Academy has a mandate that requires it to advise the federal government on scientific and technical matters. Dr. Ralph J. Cicerone is president of the National Academy of Sciences.

The **National Academy of Engineering** was established in 1964, under the charter of the National Academy of Sciences, as a parallel organization of outstanding engineers. It is autonomous in its administration and in the selection of its members, sharing with the National Academy of Sciences the responsibility for advising the federal government. The National Academy of Engineering also sponsors engineering programs aimed at meeting national needs, encourages education and research, and recognizes the superior achievements of engineers. Dr. Charles M. Vest is president of the National Academy of Engineering.

The **Institute of Medicine** was established in 1970 by the National Academy of Sciences to secure the services of eminent members of appropriate professions in the examination of policy matters pertaining to the health of the public. The Institute acts under the responsibility given to the National Academy of Sciences by its congressional charter to be an adviser to the federal government and, on its own initiative, to identify issues of medical care, research, and education. Dr. Harvey V. Fineberg is president of the Institute of Medicine.

The **National Research Council** was organized by the National Academy of Sciences in 1916 to associate the broad community of science and technology with the Academy's purposes of furthering knowledge and advising the federal government. Functioning in accordance with general policies determined by the Academy, the Council has become the principal operating agency of both the National Academy of Sciences and the National Academy of Engineering in providing services to the government, the public, and the scientific and engineering communities. The Council is administered jointly by both the Academies and the Institute of Medicine. Dr. Ralph J. Cicerone and Dr. Charles M. Vest are chair and vice chair, respectively, of the National Research Council.

The **Transportation Research Board** is one of six major divisions of the National Research Council. The mission of the Transportation Research Board is to provide leadership in transportation innovation and progress through research and information exchange, conducted within a setting that is objective, interdisciplinary, and multimodal. The Board's varied activities annually engage about 7,000 engineers, scientists, and other transportation researchers and practitioners from the public and private sectors and academia, all of whom contribute their expertise in the public interest. The program is supported by state transportation departments, federal agencies including the component administrations of the U.S. Department of Transportation, and other organizations and individuals interested in the development of transportation. **www.TRB.org**

www.national-academies.org

COOPERATIVE RESEARCH PROGRAMS

CRP STAFF FOR NCHRP REPORT 653

Christopher W. Jenks, *Director, Cooperative Research Programs*
Crawford F. Jencks, *Deputy Director, Cooperative Research Programs*
David A. Reynaud, *Senior Program Officer*
Megan A. Chamberlain, *Senior Program Assistant*
Eileen P. Delaney, *Director of Publications*
Natalie Barnes, *Editor*

NCHRP PROJECT 24-26 PANEL
Field of Soils and Geology—Area of Mechanics and Foundations

William Oliva, *Wisconsin DOT, Madison, WI (Chair)*
Brian L. Beucler, *Federal Highway Administration, Sterling, VA*
Merril E. Dougherty, *Indiana DOT, Indianapolis, IN*
Robert Ettema, *University of Wyoming, Laramie, WY*
Kevin Scott Flora, *California DOT, Sacramento, CA*
James Lane, *New Jersey DOT, Trenton, NJ*
Jon K. Zirkle, *Tennessee DOT, Nashville, TN*
David D. Zwernemann, *Texas DOT, Austin, TX*
Kornel Kerenyi, *FHWA Liaison*
Frank N. Lisle, *TRB Liaison*

FOREWORD

By David A. Reynaud
Staff Officer
Transportation Research Board

This report provides guidelines for practitioners to estimate the quantity of accumulated, flow event debris, based on the density and type of woody vegetation and river bank condition upstream and analytical procedures to quantify the effects of resulting debris-induced scour on bridge piers. The report should be of interest to bridge engineers, maintenance personnel and operations staff at state and local agencies.

As every organization that designs, operates, and maintains bridges is well aware, bridge scour is a problem that can have catastrophic effects. It is well known, since the 1980 collapse of a part of the Perkins Road Bridge over Nonconnah Creek in Memphis, Tennessee, that the accumulation of floating debris in the form of tree trunks and limbs during flood events plays a critical role in the occurrence of scour at bridge piers. In the investigation that followed the Perkins Road collapse, engineers found that a 20% blockage between piers would alter flow conditions and undermine the 12 ft of embedment on the piles supporting the pier that failed. The best information to provide to these bridge owners, to help them cut this problem down to manageable size, is improved prediction techniques to foresee the development and shape of debris accumulation and the resulting extent of scour at the bridge piers. This research performed by Ayres Associates Inc. under NCHRP Project 24-26, "Effects of Debris on Bridge Pier Scour," provides methods to create these prediction techniques.

The research methods employed during the course of this study include a literature review, a survey of bridge owners to determine current practices, and creation of a photographic archive to help predict the size and shape of accumulated debris. Results of a flume study are provided to establish relationships between the size and shape of accumulated debris and the resulting pier scour. These methods are all illustrated by example problem solutions and case studies to facilitate understanding. In addition to this published report, the debris photographic archive, the survey questionnaire and list of respondents, and the report on the field pilot study are available on the TRB website (www.trb.org) as *NCHRP Web-Only Document 148* (search for "NCHRP Web-Only Document 148").

AUTHOR ACKNOWLEDGMENTS

This work was sponsored by the American Association of State Highway and Transportation Officials (AASHTO), in cooperation with the Federal Highway Administration (FHWA), and was conducted through the National Cooperative Highway Research Program (NCHRP), which is administered by the Transportation Research Board (TRB) of the National Academies.

The research reported herein was performed under NCHRP Project 24-26 by Ayres Associates Inc., Fort Collins, Colorado. Dr. P.F. Lagasse, Senior Vice President, served as Principal Investigator and Mr. P.E. Clopper, Senior Water Resources Engineer, served as Co-Principal Investigator. They were assisted by Dr. L.W. Zevenbergen, Manager River Engineering; Mr. W. J. Spitz, Senior Geomorphologist; and Ms. L.G. Girard, Hydraulic Engineer.

Mr. G.R. Price of ETI Instrument Systems, Fort Collins, Colorado, provided support for adapting the instrumentation for the articulated arm to measure the geometry of debris clusters and accompanied the research team on the field pilot study in Kansas. A special acknowledgment is due Mr. Bradford Rognlie, Bridge Squad Leader, Kansas Department of Transportation (DOT), for his enthusiastic response to the survey, his invaluable support for the field pilot study of debris-prone bridges in Kansas, and his interest throughout the project. The core of the photographic archive in Appendix A, which provided a cost-effective substitute for extensive field work, was provided by Mr. Mike Collier, Debris Free, Inc., Ojai, California, from a collection of photographs he assembled during site visits around the United States. The research team would also like to thank the 88 respondents to the survey, which included 30 state DOTs and Puerto Rico. Your interest underscores the pervasive nature of the debris problem at bridges. Hopefully the results of this research will justify the time you invested in your responses. We must also recognize the pioneering work by Mr. Tim Diehl of the United States Geological Survey and Dr. Bruce Melville and Mr. D.M.S. Dongol of the University of Auckland, New Zealand, that provided the foundation for the advances made in this study.

All laboratory testing was performed at the Colorado State University Engineering Research Center Hydraulics Laboratory under the direction of Dr. Chris Thornton and Mr. Michael Robison. The assistance of Mr. Sean Kimbrel, graduate student; Mr. Matt Stockton, lab technician; and Mr. Mick Ursic, undergraduate student is also acknowledged.

The participation, advice, and support of NCHRP Project 24-26 panel members throughout this project are gratefully acknowledged.

CONTENTS

SUMMARY

Effects of Debris on Bridge Pier Scour

Overview

This research accomplished its basic objectives of developing guidelines for predicting the size and geometry of debris accumulations at bridge piers and methods for quantifying scour at bridge piers resulting from debris accumulations. The project produced results on two related problems: (1) predicting the accumulation characteristics of debris from potentially widely varying source areas, in rivers with different geomorphic characteristics, and on bridges with a variety of substructure geometries and (2) developing improved methods for quantifying the depth and extent of scour at bridge piers considering both the accumulation variables and the range of hydraulic factors involved.

Waterborne debris (or drift), composed primarily of tree trunks and limbs, often accumulates on bridges during flood events. Debris accumulations can obstruct, constrict, or redirect flow through bridge openings resulting in flooding, damaging loads, or excessive scour at bridge foundations. The size and shape of debris accumulations vary widely, ranging from a small cluster of debris on a bridge pier to a near complete blockage of a bridge waterway opening. Debris accumulation geometry is dependent on the characteristics and supply of debris transported to bridges, on flow conditions, and on bridge and channel geometry. The effects of debris accumulation can vary from minor flow constrictions to severe flow contraction resulting in significant bridge foundation scour.

Qualitatively, the impacts of debris have been well documented; however, a pressing need remains for state DOTs and other bridge owners to have improved prediction methods for the geometry (size and shape) of typical debris accumulations, the conditions under which debris can be expected to develop, and the resulting depth and extent of scour at bridge piers. Currently, only limited guidance is available on which to base critical public safety decisions during flooding on debris-prone rivers. There is a need for accurate methods of quantifying the effects of debris on scour at bridge pier foundations for use by departments of transportation (DOTs) and other agencies in the design, operation, and maintenance of highway bridges.

Research Approach

The research approach involved the following steps:

1. Completion of a literature review and evaluation of current practice with a survey of state DOTs and other bridge owners.
2. A field pilot study to evaluate instrumentation for obtaining data at debris-prone bridges and costs associated with debris-related field studies.

3. Development of a photographic database (archive) as an alternative to field work for assessing typical debris shapes and geometry relationships, nationally.
4. Development of detailed guidelines and flowcharts for estimating the potential for debris production and delivery to a bridge site, and a case study to illustrate the application of the guidelines.
5. Extensive laboratory testing of the most common debris shapes and geometries to determine the relationships between debris shape and dimensions and the depth and extent of bridge pier scour.
6. Development of methods for predicting the depth, shape, and extent of scour at bridge piers resulting from debris accumulation. Application of the methodology is illustrated with example problems.
7. Discussion of approaches and limitations for incorporating debris in one- and two-dimensional hydraulic computer models.
8. Discussion of inspection, monitoring, and maintenance issues at debris-prone bridges.
9. Suggestions for implementation activities to enhance the state of practice for estimating scour at bridge piers under debris loading.

Appraisal of Research Results

As an extension of the original work by Diehl (1997) for the Federal Highway Administration (FHWA), guidelines and flowcharts were developed for estimating (1) the potential for debris production and delivery from the contributing watershed of a selected bridge and (2) the potential for accumulation on individual bridge elements. The application of the guidelines is illustrated by a case study of a debris-prone bridge on the South Platte River in Colorado (summarized in Chapter 3 and presented in detail in Appendix D). The case study introduces and illustrates the use of field data sheets for evaluating the potential for debris production and delivery from a given watershed.

As a basis for laboratory testing, the photographic archive introduced in Chapter 2 (see also Appendix A), the field pilot study of debris sites in Kansas (see Appendix C), and the South Platte River case study (see Appendix D) were examined to develop a limited number of debris shapes that would represent the maximum number of configurations found in the field. Simplified, yet realistic, shapes that could be constructed and replicated with a reasonable range of geometric variables were needed for laboratory testing. Rectangular and triangular shapes with varying planform and profile dimensions were selected to represent prototype debris accumulations. To account for additional variables thought to be relevant to debris clusters in the field, a method to simulate both the porosity and roughness of the clusters was developed. However, porosity and roughness were found to be, at most, second order factors in estimating scour at bridge piers under debris loading.

The laboratory testing program included the use of a large indoor flume at Colorado State University and model bridge pier shapes, development of state-of-the-art instrumentation for data acquisition, and a wide range of materials to fabricate the debris clusters. Baseline tests were conducted and results were compared with several pier scour prediction equations. A series of tests under clear-water conditions with the various debris shapes were completed. The results are illustrated with tabular data, photographs, and post-test contour plots.

An appraisal of testing results supported the development of an improved algorithm for predicting the scour anticipated at bridge piers from debris accumulations with rectangular and triangular planforms and varying length, width, and depth geometries. In Chapter 3, application of the methodology is presented to integrate the debris accumulation guidelines with the equation for predicting debris scour at bridge piers using the South Platte River case study as an example.

Finally, guidelines for inspection, monitoring, and maintenance for debris-prone bridges are considered and an implementation plan for the results of this research is suggested. Conclusions from this research and recommendations for future research are presented in Chapter 4.

As a result of this research, bridge owners now have documentation, guidelines, and analytical procedures to quantify the effects of debris-induced scour on bridge piers:

- A fully documented database on debris and case studies, photographs, and data related to debris generation, movement, accumulation, and scour at bridges that can be used to inform and train design and maintenance personnel on debris-related hazards
- Necessary guidelines for predicting the size, location, and geometry of debris accumulations at bridge piers
- Methods for quantifying scour at bridge piers resulting from debris accumulations
- Guidance for incorporating debris effects in one- and two-dimensional hydraulic modeling
- Worked example problems and a case study illustrating the application of the guidelines and analytical methods

The end results of this research are practical, implementable guidelines for bridge owners that enhance their ability to predict debris-related hazards at bridges and design, operate, inspect, and maintain bridges considering those hazards.

CHAPTER 1

Introduction and Research Approach

1.1 Scope and Research Objectives

1.1.1 Background

On Sunday, March 16, 1980, a portion of the Perkins Road Bridge over Nonconnah Creek in Memphis, Tennessee, collapsed during high flow (Figure 1.1). The bridge failure resulted in one death and litigation was brought against numerous defendants. Investigation showed that at about 11:00 p.m. during a rainstorm, the two northbound lanes of spans 3 and 4 of the Perkins Road Bridge had collapsed. Inspection of the bridge after the collapse was conducted by a Shelby County bridge inspection crew. Initial inspection found (1) large drifts of debris on the upstream side of the bridge, (2) at least one pile that was broken but still in place, and (3) other piles completely missing.

To address the charge of negligence and other issues and to provide a basis for litigation support, detailed hydrologic, hydraulic, and scour analyses were completed. The objectives were to establish the hydraulic, erosion, and sedimentation characteristics of the Nonconnah Creek system. The analyses involved application of basic hydrologic, hydraulic, geomorphic, and sediment transport principles and yielded estimates of the contribution of degradation, contraction scour, local scour, and the impact of debris (Lagasse and Schall 1980).

The investigation focused on the impacts of debris on pier scour (Figure 1.2). Calculation procedures for scour predated but paralleled the current recommendations in FHWA's Hydraulic Engineering Circular No. 18, known as HEC-18 (Richardson and Davis 2001), and resulted in the estimates shown in Table 1.1 for local and contraction scour. To estimate the impact of debris on local pier scour, the pier width was increased incrementally to represent blockages that would reduce conveyance through the bridge opening by 20% up to 45%. It was concluded that increasing the "blockage" by assuming that the debris would increase pier width to reduce conveyance through the bridge by more than 40% to 50% would radically alter the flow conditions implicit in the pier scour equation. The results clearly showed that a 20% blockage would undermine the estimated 12 ft of embedment on the pile foundation of the pier that failed.

Surprisingly, this crude model of debris scour has not been changed substantially in the 28 years since this bridge failure. The approach of increasing the width of the pier using engineering judgment to account for debris is still suggested in the fourth edition of HEC-18 (Richardson and Davis 2001), which represents the current state of the practice in the United States.

1.1.2 Objectives

Waterborne debris (or drift), composed primarily of tree trunks and limbs, often accumulates on bridges during flood events. Debris accumulations can obstruct, constrict, or redirect flow through bridge openings resulting in flooding, damaging loads, or excessive scour at bridge foundations. The size and shape of debris accumulations vary widely, ranging from a small cluster of debris on a bridge pier to a near complete blockage of a bridge waterway opening. Debris accumulation geometry is dependent on the characteristics and supply of debris transported to bridges, on flow conditions, and on bridge and channel geometry. The effects of debris accumulation can vary from minor flow constrictions to severe flow contraction resulting in significant bridge foundation scour.

Qualitatively, the impacts of debris have been well documented (see for example, Chang and Shen 1979, Diehl 1997, Parola et al. 2000). However, a pressing need remains for state DOTs and other bridge owners to have improved prediction methods for the geometry (size and shape) of typical debris accumulations, the conditions under which debris can be expected to develop, and the resulting depth and extent of scour at bridge piers. Currently, only limited guidance is available on which to base critical public safety decisions during flooding on debris-prone rivers. There is a need for accurate methods of quantifying the effects of debris on scour at bridge

Figure 1.1. Perkins Road Bridge, March 17, 1980 (flow from right to left).

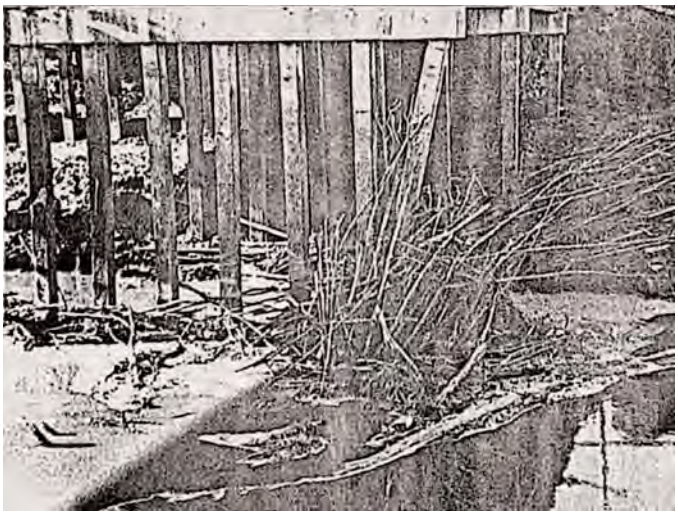

Figure 1.2. Debris at Perkins Road Bridge, March 16, 1980.

pier foundations for use by DOTs and other agencies in the design, operation, and maintenance of highway bridges.

The objectives of this research were to develop (1) guidelines for predicting the size and geometry of debris accumulations at bridge piers and (2) methods for quantifying scour at bridge piers resulting from debris accumulations.

1.2 Research Approach

1.2.1 Overview

This research project produced results on two related problems: (1) predicting the accumulation characteristics of debris from potentially widely varying source areas, in rivers with different geomorphic characteristics, and on bridges with a variety of substructure geometries and (2) developing improved methods for quantifying the depth and extent of scour at bridge piers considering both the accumulation variables and the range of hydraulic factors involved.

One might infer from previous studies, as well as the geomorphic characteristics of rivers in different physiographic regions and the different characteristics of woody vegetation and river bank erosion processes, that there might be some regional bias in debris characteristics and in debris impact on bridges. These regional characteristics were investigated during Phase 1 in the Task 1 literature search and in the Task 2 site reconnaissance and survey. The evidence available does not support the hypothesis that there is a regional bias in debris characteristics. In fact, a photographic archive of debris at bridges across the United States assembled to assess typical debris geometry relationships demonstrates that debris accumulations can be grouped into a finite number of common shapes that can be found in most physiographic regions.

For Task 3, Diehl's extensive study "Potential Drift Accumulation at Bridges" (1997) for FHWA was the obvious starting point. The preliminary guidelines for Task 3 expanded on the three major phases suggested by Diehl for assessing the potential for debris production and accumulation at a bridge site: (1) estimate the potential for debris production and delivery, (2) estimate the potential for debris accumulation on individual bridge elements, and (3) calculate the hypothetical accumulations for the entire bridge.

The Task 4 laboratory plan considered different accumulation configurations (e.g., floating raft, submerged wedge, etc.) to develop a matrix of alternatives for laboratory testing. Thus, the Task 1 and Task 2 results and the debris photographic archive were used to determine the number of alternatives that must be included in the Task 4 laboratory plan to investigate a full range of debris characteristics.

Table 1.1. Total erosion potential at Perkins Bridge for 1980 flood.

Debris Blockage (%)	Local Scour Depth (ft)	Contraction Scour Depth (ft)	Degradation Depth (ft)	Total Erosion (ft)	(m)
0	6.2	1.5	0.5	8.2	2.5
20	12.5	1.5	0.5	14.5	4.4
45	18.8	1.5	0.5	20.8	6.3

1.2.2 Research Plan Modifications

The Interim Report (Task 5) provided all findings and recommendations from Phase 1, including the suggested laboratory test plan for Phase 2. At the Interim Report panel meeting, the following topics were presented and discussed:

- Survey and field pilot study results
- Photographic archive—sources, distribution, and applications
- Preliminary guidelines for debris production and prediction
- Laboratory test plan
- Conceptual framework for predicting debris scour at piers

Panel guidance was requested on the following topics:

- Requirements for additional field work
- Guidelines for predicting size and geometry of debris
- Laboratory testing matrix and priorities (including scaling factors)
- Debris scour prediction—conceptual framework

As a result of the Interim Report meeting with the panel, several significant changes were made to the research approach based on findings of the field pilot study during Phase 1:

- Plans for extensive field work at debris sites were eliminated.
- The photographic archive of debris sites should be expanded and examined for all relevant information on trends or patterns that could be used as a guide by the practitioner.
- A case study should be developed to illustrate the application of the final guidelines (Task 6) for production of debris and accumulation at bridges.
- Considering the testing budget, laboratory tests should be conducted at a single scale.
- Guidelines for inspection, monitoring, and maintenance related to debris at bridges should be developed.

1.3 Research Tasks

Considering the research approach discussed and outlined previously, the following specific tasks were completed to accomplish project objectives. These tasks incorporate panel guidance and parallel, with some modifications, those suggested in the original research project statement.

1.3.1 Phase 1 Tasks

Task 1, Review the Technical Literature

The research team conducted a thorough review of the technical literature from foreign and domestic sources to assess the adequacy and extent of existing information on debris accumulations and the effect of these accumulations on bridge scour. The literature review identified research in progress as well as completed work.

As part of the literature review, a photographic archive was compiled to assess typical debris geometry relationships. Photographs of debris at bridges were acquired from a number of contributors. The primary contributor was Debris Free, Inc. of Ojai, California, who provided almost 50% of the photos. Numerous photographs were provided by 22 state DOT personnel in response to the project survey. The remaining photographs were acquired from in-house sources, Internet sites, and referenced publications. A total of 1,079 photographs were acquired from the various sources.

Task 2, Conduct Survey and Site Reconnaissance

The research team determined typical debris accumulations by surveying state DOTs and other agencies and by site reconnaissance of debris accumulations at bridge piers. The site reconnaissance (pilot study) included field measurements, photographs, geomorphologic information, channel types and flow patterns, and associated bridge and pier geometrics.

Task 2 required determination of typical debris accumulations by surveying state DOTs and other agencies. The results of the survey are analyzed in Chapter 2 and included in Appendix B.

The field pilot study to bridge sites in southeastern Kansas was completed during the period April 25–28, 2005. Overall coordination was provided by Kansas DOT. A detailed field trip report is included as Appendix C. Results and recommendations are summarized in Chapter 2. The panel concurred with the recommendation that no additional field work should be conducted to obtain additional measurements of the geometry of debris accumulations. The panel directed that the remaining field work budget be allocated to developing a case study for application of the final guidelines (Task 6).

Task 3, Develop Preliminary Guidelines

Based on the Task 1 literature search and the empirical data collected in Task 2, the research team developed preliminary guidelines for predicting the size and geometry of debris accumulations at bridge piers. Here, Diehl's extensive study "Potential Drift Accumulation at Bridges" (1997) for FHWA was the starting point.

Task 4, Develop Phase 2 Laboratory Plan

The research team developed a detailed description of the Phase 2 laboratory experiments proposed for assessing the effects of debris accumulations on scour at bridge piers. Typical configurations of debris accumulations identified in Tasks 1

and 2 were categorized, and selected debris configurations were prioritized for use in the Phase 2 laboratory experiments. A testing program was proposed to address three main objectives:

1. Effect of debris accumulation on local hydraulic conditions at bridge piers
2. Quantification of scour resulting from predicted debris accumulations
3. Sensitivity of hydraulic conditions, and resulting scour patterns, to variations in debris accumulation geometries

All laboratory testing was completed at the Colorado State University Engineering Research Center Hydraulics Laboratory.

Task 5, Submit Interim Report

The research team prepared and submitted an Interim Report documenting the information developed in Tasks 1 through 5. The Interim Report contained a detailed discussion of the typical debris configurations to be used in the Phase 2 laboratory experiments and the preliminary guidelines for predicting the size and geometry of debris accumulations. The research team met with the NCHRP 24-26 panel to discuss the Interim Report and the revised work plan.

1.3.2 Phase 2 Tasks

Task 6, Finalize Task 3 Guidelines

Based on panel comments and guidance during the Interim Report meeting, the research team finalized the Task 3 preliminary guidelines for predicting the size and geometry of debris accumulations.

Case Study. A case study was developed to provide an example of how the practitioner should apply the guidelines for assessing debris production and predicting debris accumulation at a bridge site. Developing the case study also assisted in refining and finalizing the guidelines.

The intent of the case study is to provide practitioners with an example that documents the step-by-step process used to apply the guidelines for a specific bridge site. The final guidelines include procedures for documenting:

- Geomorphic factors that affect stream stability
- Debris production from the watershed and tributary network
- Transport and delivery to the bridge. The guidelines also provide guidance on how to use the information collected at a bridge site to estimate potential accumulation sizes and geometry, and from that, apply the appropriate scour prediction relationship.

For the case study, field data sheets specific to the debris problem were developed. The sheets can be used to document site characteristics such as channel type and size, channel instability, bank erosion and retreat, and bank vegetation characteristics in detail. The sheets were designed to document potential or existing debris size, production, transport, and storage characteristics. The field data sheets were incorporated into the final guidelines. Guidance is also provided on obtaining supplemental information such as watershed size, channel planform, land use conditions, and peak discharges, which can be documented from aerial photography and gage data that are readily available (e.g., TerraServer and U.S. Geological Survey Water Resources websites).

Debris Photographic Archive. The panel instructed the research team to extract as much additional information from the debris photographic archive as possible with the resources remaining in Task 6. The database was developed on Microsoft® Excel spreadsheets, which were expanded in Task 6. The existing photographs in the database were reviewed and additional fields of the database were populated with National Bridge Inventory (NBI) data, aerial photography, bridge plans, and inspection reports for a selected subset of bridges. The photographic archive also contains case studies to illustrate the use of these data sources to expand the archive for a typical bridge.

Task 7, Laboratory Studies

Using the typical debris configurations agreed on during the Interim Report meeting, the research team conducted the laboratory experiments according to the approved work plan. The goal of the laboratory testing was to provide sufficient data for a range of debris accumulations to develop adjustment factors to the HEC-18 pier scour equation (see Task 8). The adjustment factors considered included a correction factor to the overall equation (such as the K_w factor for wide piers) and an adjustment to the pier width used as an input variable to the equation (similar to the HEC-18 complex pier approach).

The goal of the laboratory plan was to develop a series of tests for a wide range of debris configurations that could be run quickly and efficiently. The tests were performed for single debris clusters at individual piers, which is the primary type of debris accumulation identified by all regions in the (Task 2) survey. The majority of the testing was performed for clear-water sediment transport conditions. The testing encompassed a range of debris characteristics including debris accumulation shape, thickness, width, length, porosity, and roughness. The range of debris accumulation size that was tested in the laboratory is related to actual debris accumulations observed by the research team in the field or from the survey sources and the photographic archive.

Task 8, Develop Scour Prediction Methods

Based on the results of Task 7, the research team developed methods for predicting the depth, shape, and lateral extent of scour at bridge piers resulting from debris accumulations. The methods are suitable for incorporation into HEC-18.

Task 9, Submit Final Report

The research team submitted a final report that documents the entire research effort. They also provided a companion executive summary that outlines the research results.

1.4 Research Results

As a result of this research, bridge owners now have documentation, guidelines, and analytical procedures to quantify the effects of debris-induced scour on bridges:

- A fully documented database on debris and case studies, photographs, and data related to debris generation, movement, accumulation, and scour at bridges that can be used to inform and train design and maintenance personnel on debris-related hazards
- Necessary guidelines for predicting the size and geometry of debris accumulations at bridge piers
- Methods for quantifying scour at bridge piers resulting from debris accumulations
- Guidance for incorporating debris effects in one- and two-dimensional hydraulic modeling
- Worked example problems and a case study illustrating the application of the guidelines and analytical methods

The end results are practical, implementable guidelines for bridge owners that enhance their ability to predict debris-related hazards at bridges and to design, operate, inspect, and maintain bridges considering those hazards.

1.5 Documentation Organization

Findings from this research are available in three documents:

- ***NCHRP Report 653***
  - Findings from the review of current practice and site reconnaissance
  - Overview of laboratory testing results
  - Interpretation and appraisal of findings and results
  - Conclusions and recommendations
  - Suggested research
  - Guidelines for predicting size and geometry of debris accumulations at bridge piers
  - Methodology for predicting scour at bridge piers with debris loading
- ***NCHRP Web-Only Document 148*** [available on the TRB website (www.trb.org) by searching for "NCHRP Web-Only Document 148"]
  - Photographic archive of debris at bridge piers
  - Survey of practitioners
  - Field pilot study report
- **Reference Document** [available from the NCHRP Project 24-26 web page (http://144.171.11.40/cmsfeed/TRBNetProjectDisplay.asp?ProjectID=725)], which contains detailed laboratory testing results from Colorado State University

CHAPTER 2

Findings

2.1 Review of Current Practice

2.1.1 Introduction

Debris (or drift), for the purposes of this project, is defined as floating woody debris that is delivered to and transported along a stream or river. The effects of debris on bridges have been well documented (see for example Chang and Shen 1979, Diehl 1997, Parola et al. 2000). Debris problems are most common on rivers and streams with active bank erosion and that drain wooded or forested areas or corridors. As discussed in Chapter 1, there is a pressing need for state DOTs and other bridge owners to have improved prediction methods for the geometry (size and shape) of typical debris accumulations; the conditions under which debris can be expected to be recruited, transported, and deposited on a bridge; and the resulting depth and extent of scour at bridge piers. Currently, only limited guidance is available on which to base critical public safety decisions during flooding on debris-prone rivers. Consequently, there is a need for accurate methods of quantifying the effects of debris on scour at bridge pier foundations for use by DOTs and other agencies in the design, operation, and maintenance of highway bridges.

Both FHWA (Diehl 1997) and NCHRP (Parola et al. 2000) have published recent debris-related studies that have excellent reference source lists. These sources were screened and a preliminary working bibliography of the most relevant references was assembled. Additional sources were evaluated as well. For example, a laboratory and field study on single-pier debris accumulation was completed at Purdue University in 2001 and presented at the TRB 82nd Annual Meeting (Lyn et al. 2003a). The Purdue study was subsequently published through the University's Civil Engineering Joint Transportation Research program (Lyn et al. 2003b). Of course, studies such as the initial work by Laursen and Toch (1956)—which characterize the scour pattern at a pier for floating, submerged, and buried debris—were revisited as well.

The international literature was also reviewed, but little information or data were forthcoming. For example, following the devastating damage to infrastructure by Hurricane Mitch in 1998 in Honduras, Nicaragua, and Guatemala, a major international relief and recovery effort was launched. Emphasis was on replacement of infrastructure, particularly bridges, as hundreds of bridges had been lost because of scour and debris accumulation. Although a number of universities in Central and South America conducted research on the debris problem to develop improved design procedures for debris, the results of this work have not made the mainstream literature in the United States.

Some studies have been conducted in Australia and New Zealand (see for example Dongol 1989, Young 1991, Shields and Gippel 1995, and Gippel et al. 1996). In Europe, very few studies on debris have been conducted because the lack of significant riparian forest corridors have made large woody debris rare. Also, debris accumulations are seen as a river management problem and are routinely cleared from river channels (Piégay and Gurnell 1997).

Much of the recent literature pertains to large woody debris (LWD) or coarse woody debris (CWD) and is associated with riparian forest ecology and aquatic habitat concerns and the influence of LWD on flow patterns, stream morphology, and alluvial processes (Hickin 1984, Fetherston et al. 1995, Wallerstein et al. 1997, Abt et al. 1998, Dudley et al. 1998, Duncan 2000, Manga and Kirchner 2000, Ringgold et al. 2000, Haga et al. 2002, Rollerson and McGourlick 2002, Hygelund and Manga 2003, Kraft and Warren 2003, Montgomery et al. 2003, Simon et al. 2004). As a result, much of the literature on LWD in streams and rivers is associated with these types of studies and most studies are associated with work conducted in old-growth coniferous forests of the Pacific Northwest. Some studies, such as the one conducted by Robinson (2003) on the White River in Indiana, attempt to document existing debris production, transport, and storage conditions. Yet, other than the reviews by Gippel (1995), Diehl (1997), and Parola

et al. (2000), there is still a paucity of literature on the processes associated with debris delivery to bridge sites.

Three primary processes are associated with debris accumulation at bridges: (1) debris source loading, distribution, and recruitment, which is defined as drift generation by Diehl (1997); (2) debris transport; and (3) debris accumulation, deposition, and storage. Diehl (1997) provides a relatively concise review of the literature on these processes. The following is an expanded review covering the literature that was not included in or was subsequent to the reviews conducted by Chang and Shen (1979), Diehl (1997) and Parola et al. (2000). The References section provides a bibliography of current practice.

2.1.2 Debris Source Loading, Distribution, and Recruitment

Montgomery and Piégay (2003) indicate that the geomorphological effects of wood in streams and rivers are highly variable and are reflected in the differences in wood size, density, and shape that are partly controlled by wood availability, depending on external factors controlling wood recruitment, and the character of the surrounding forest as well as on stream size, characteristics, and processes. However, the observations of Lyn et al. (2003b) and many other researchers would suggest that the recruitment, transport, and accumulation of debris appears to be a somewhat random process while the results of Manners et al. (2007) show that "the relationship between individual logs and complete debris jams is complex and nonlinear."

Woody debris recruitment pertains to the processes by which live trees and standing snags fall along a stream corridor or where existing forest deadfall and residues from logging and clearing activities are delivered to the stream channel for potential transport downstream to a bridge site. The availability of wood for recruitment is, in part, dependent on the distribution, density, and health of forested hillslopes, flood plains, and riparian corridors along a stream. Most woody debris delivered to streams originates from that part of the riparian forest closest to the channel. For example, based on work conducted in the Pacific Northwest, Fetherston et al. (1995) noted that 70% to 90% of riparian input of LWD occurs within 100 ft (30 m) of the channel edge. Most studies to date confirm that LWD recruitment is driven by a fluvial process through channel meandering and attendant bank undercutting, mass failure, and input of trees.

In upland, low order streams, landslides and debris flows are the principal mechanism by which trees and other organic debris are delivered to a stream channel. Although windthrow in some areas can be a significant contributor of woody debris to streams and rivers, in medium to high order streams and rivers, which may or may not have flood plains, the primary methods of delivery are associated with stream meandering and bank erosion/undercutting. Nakamura and Swanson (1994) concluded that channel width and sinuosity are the primary factors that influence distribution of storage sites for LWD. But Wallerstein et al. (1997) suggest that reach stability and channel sinuosity are probably better measures of debris volume and frequency of debris jams because these factors, to a large extent, determine the rate of debris input.

Empirical and theoretical analyses of the probability of input of woody debris to a channel as a function of distance from the streambank have been developed (Murphy and Koski 1989, Robison and Beschta 1990, Van Sickle and Gregory 1990, Andrus and Lorenzen 1992, Downs and Simon 2001, Teply 2001). Robison and Beschta (1990) indicate that the possible surface area that could be impacted is defined by the area of a circle whose radius is equal to the effective tree height (H_e) (Figure 2.1), assuming that a tree has an equal chance of falling in any direction. The effective tree height of a conifer is considered to be the total tree height minus about the last 5 ft (1.5 m) since the crown of the tree is not considered to qualify as coarse woody debris.

According to Robison and Beschta (1990), the probability, P, of a tree's falling and delivering coarse woody debris to the channel is proportional to the ratio of the arc distance, AD, along the stream to the total arc distance (circumference) of the circle:

$$P = \frac{AD}{2\pi H_e} = \frac{\cos^{-1}\left(D/H_e\right)}{180^\circ} \tag{2.1}$$

where D is the distance of the tree from the stream (Figure 2.2). Robison and Beschta (1990) suggest that the integration of

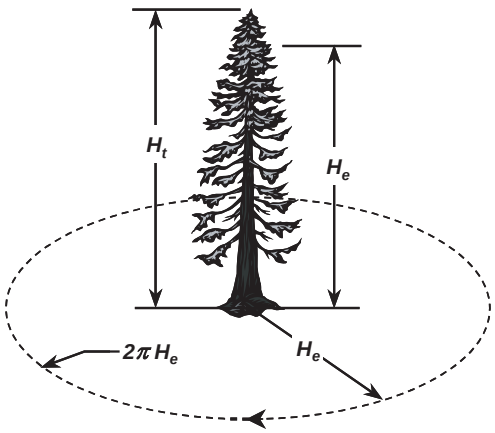

Source: after Robison and Beschta (1990)

Figure 2.1. Potential tree fall area showing total tree height, H_t; effective tree height, H_e (used to determine CWD delivery from conifers); and total arc distance, $2\pi H_e$.

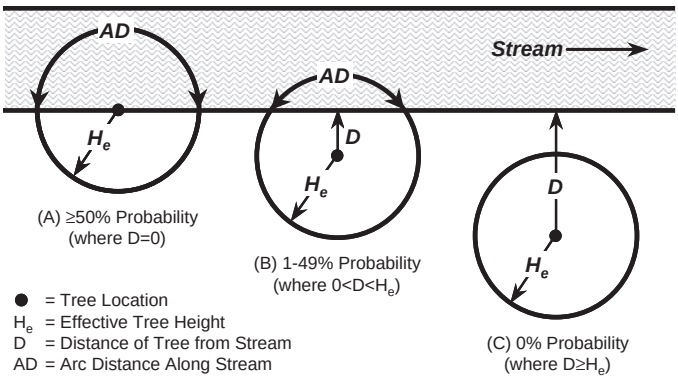

Source: after Robison and Beschta 1990

Figure 2.2. Schematic illustrating the probability of coarse woody debris falling into a stream from a tree located (A) at the edge of the stream, (B) at a distance less than the effective tree height, and (C) at a distance greater than the effective tree height.

this model with tree-growth and "fall-down" (risk-rating) models may be useful for identifying trees that will have a high probability of providing coarse woody debris to a stream in later years.

Once a tree falls, its limbs and branches may break off, adding to the debris litter on the flood plain. In addition, the tree trunk may break into smaller pieces when hitting the ground or other large upright trees. The broken limbs and small branches, twigs, and leaves are available for recruitment as well. Often, when a tree falls, its rootwad (or root bole) is still attached, particularly if the tree is a product of bank erosion. Woody debris that is available for transport may be found in all positions and orientations on the flood plain, on top of and along the stream bank, in the channel, and on bars and islands.

Gregory (1991) reports that the majority of woody debris along streams in the McKenzie River basin in Oregon is retained along channel margins and flood plains with less than 30% of the debris volume occurring within the active channel. He also indicates that reaches with broad flood plains and complex channels make up less than 20% of the channel length, but contain more than 50% of the large woody debris. However, Andrus et al. (1988) found no correlation between riparian stand volume in sample plots and the volume of new debris in adjacent channel reaches. In a similar plot survey, Robison (1988) found that while the riparian stand, stream morphology, and debris in the channel were interrelated, there was too much variability to distinguish definite relationships. Gippel et al. (1996) suggest that "the general lack of correlation between the distribution of debris in streams and the distribution of adjacent riparian trees is indicative of the importance of re-distribution of debris by flood events, the potentially long residence time of wood in streams, and the re-exposure of ancient wood buried in flood plain sediments as rivers alter their course."

Some studies have also been conducted to evaluate debris recruitment on incised or degrading streams in the southern United States (Downs and Simon 2001, Wallerstein et al. 1997, Wallerstein and Thorne 2004). In these studies, the authors suggest that debris recruitment can be tied directly to channel stability and sinuosity. Through an understanding of incised channel evolution, they suggest that the spatial density of debris jams in degrading rivers can be qualitatively predicted on the basis of location and migration of headcuts and degradational processes. Based on studies conducted on degrading streams in northern Mississippi, Wallerstein et al. (1997) and Wallerstein and Thorne (2004) note that debris input was found to be the result of the following key mechanisms (percentages are rounded):

- 37% due to outer bank erosion in channel bends
- 36% due to bank mass-wasting in degrading reaches
- 12% due to windthrow
- 7% resulting from paleodebris (material introduced into the channel from old alluvial deposits containing preserved debris)
- 5% initiated by large logs floated in from upstream
- 4% from beaver dams

Wallerstein and Thorne (2004) suggest that the possibility exists for developing a geomorphic tool to predict the distribution of debris inputs and jams on the basis of the Incised Channel Evolution Model (ICEM).

The species composition of the riparian vegetation influences the amount and distribution of LWD; species that achieve large size produce more stable, longer-lived debris than smaller species. For example, in the Pacific Northwest, channels located in younger communities, which are often dominated by smaller hardwood species, have smaller average-size pieces of LWD compared to streams flowing through mature stands of conifer (Bilby and Ward 1991). Table 2.1 presents a list of the characteristics and distribution of LWD for various geographic and channel network locations as compiled by Lassettre and Harris (2001).

2.1.3 Debris Transport

The mobilization and transport of woody debris is dependent on the physical characteristics of the piece as it relates to channel width; diameter of the piece as it relates to flow depth; orientation of the piece within the channel; and, to a lesser degree, channel slope. The size of LWD accumulations increases downstream while the frequency decreases (Swanson et al. 1982, Bilby and Ward 1989) because LWD on small, low order streams generally tends to be longer than the channel

Table 2.1. Characteristics and distribution of LWD.

Location	Channel Network Position	Results	References
Western Oregon	• 0.10 to 0.30 channel gradients	• LWD in small streams randomly distributed • LWD easily transported in larger rivers leading to size sorting and accumulations in distinct jams	Swanson et al. 1976
Western Oregon	• 0.02 to 0.50 channel gradients	• Debris loading highest in small, steep streams, decreasing downstream • In 1st and 2nd order streams, LWD randomly located because streams too small to redistribute • In 3rd to 5th order streams, flows large enough to redistribute debris from distinct accumulations that directly affect channel width • In large rivers, LWD thrown on islands or on banks, having little influence on channel, except during high flows	Swanson and Lienkaemper 1978
Indiana, North Carolina, Oregon	• 0.001 to 0.40 channel gradients	• Loading (kg/m^2) decreased with increasing channel width, watershed area, stream order, and decreasing channel gradient	Keller and Swanson 1979
Northwest California	• 0.01 to 0.40 channel gradients • 1.0 km^2 to 27 km^2 drainage areas • 2nd through 4th order streams	• Redwood debris usually dominates total loading • Loading (m^3/m^2) decreased as drainage area and width increased • Debris accumulations in lower reaches larger, more complex, and spaced further apart than in upper reaches	Keller and Tally 1979, Tally 1980, Keller and MacDonald 1983, Keller et al. 1985
New England	• 1.5 m to 7 m wide channels	• Frequency of debris dams decreased from 1st order (20 to 40 dams per 100 m) to 2nd order (10 to 15 dams per 100 m) to 3rd order (1 to 6 dams per 100 m) streams	Likens and Bilby 1982
Western Oregon	• 0.03 to 0.37 channel gradients • 3.5 m to 24 m bankfull widths • 0.1 km^2 to 61 km^2 drainage areas • 1st through 5th order streams	• Amount of LWD generally decreased from small to large channels	Lienkaemper and Swanson 1987
Western Washington	• 0.13 channel gradient (<7 m channel width) • 0.08 channel gradient (7 m to 10 m channel width) • 0.03 channel gradient (>10 m channel width)	• Mean diameter, length, and volume of LWD increased with increasing channel width • Frequency of occurrence (number of pieces/m) decreased with increasing channel width • Changes related to increased capacity of larger streams to move wood downstream • Higher proportion of wood input remained in the stream channel as stream size decreased	Bilby and Ward 1989
Southeast Alaska	• <0.03 channel gradients • 0.7 km^2 to 55 km^2 drainage areas • 1st through 4th order streams	• Abundance of LWD and volume per channel length (m^3/m) increased with increasing stream size • LWD loading (m^3/m^2) decreased with increasing bankfull width	Robison and Beschta 1990
Western Washington	• 3 m to 24 m bankfull channel widths	• Average LWD volume increased with increasing stream size (bankfull width) • LWD abundance (number of pieces/m) decreased with increasing bankfull width	Bilby and Ward 1991
United Kingdom	• 110 km^2 drainage area	• Density of LWD jams (number of dams per 100 m and number of dams per 500 m) decreased downstream from headwaters and with increasing channel width • Abundance of partial spanning dams increased in downstream direction • Debris loading (kg/m^2) decreased in downstream direction	Gregory et al. 1993

Table 2.1. (Continued).

Location	Channel Network Position	Results	References
Southeastern France	• 0.0012 to 0.0018 channel gradients • 3700 km^2 drainage area • 6th order river	• LWD differentially deposited on banks depending on flow and forest conditions	Piégay 1993
Western Oregon	• 0.022 average channel gradient • 23 m average channel width • 60 km^2 drainage area • 5th order channel	• Channel width and sinuosity were main factors controlling LWD supply and distribution • Number and volume of LWD highest in wide sinuous reaches	Nakamura and Swanson 1994
Southwest Alaska, Western Washington	• 0.002 to 0.085 channel gradients • 2.5 m to 38 m channel widths	• Number of LWD pieces per m^2 decreased with increasing channel width • Logs in larger channels were more readily transported • Inverse proportionality between pool spacing and LWD frequency	Montgomery et al. 1995
North Central Colorado	• 0.005 to 0.065 channel gradients • 4 m to 10 m bankfull width • 2 km^2 to 30 km^2 drainage areas • 1st through 3rd order streams	• LWD abundance (number of pieces/m) greater in smaller streams when sorted by drainage area and width • Lower percentage of pieces spanned channel in larger streams (sorted by drainage area and width) than in smaller streams • Percentage of LWD lying perpendicular to stream channel decreased with increasing drainage area • Percentage of debris pieces in wetted channel decreased in larger streams • Percentage of LWD above wetted channels increased in smaller streams • LWD randomly distributed in streams <5.0 m width and clumped into jams in streams >5.0 m in width	Richmond and Fausch 1995
Northwest Washington	• 0.002 to 0.05 channel gradients • 5 m to 20 m channel widths • 2 km^2 to 120 km^2 drainage areas	• Loading and abundance decreased with increasing channel width • Channel width is dominant influence on number of pieces of LWD/m^2	Beechie and Sibley 1997
Southeastern France	• 0.0012 to 0.0018 channel gradients • 3700 km^2 drainage area • 6th order river	• LWD distribution on meander banks related to angle of bank to flow, height of flow, and presence of secondary channels	Piégay and Marston 1998
Spain	• 0.08 to 0.1575 channel gradients • 3 m to 8 m channel widths • 0.4 km^2 to 64 km^2 drainage areas • 1st through 3rd order streams	• Abundance and loading decreased in downstream direction	Elosegi et al. 1999
Southeastern France	• 0.003 to 0.008 channel gradients • 1650 km^2 drainage area	• Most LWD in active channel on high bars • LWD deposit controlled by deposit site morphology and proximity of LWD sources	Piégay et al. 1999

Source: Lassettre and Harris (2001)

width and remains in place during most flow events whereas wood in larger, higher order streams is generally shorter than the channel width and is, therefore, more easily transported, leading to a reduction in LWD frequency due to flushing of smaller pieces and clumping of the remaining LWD pieces. Evidence suggests that pieces shorter than bankfull width and with a diameter less than bankfull depth are more likely to be transported downstream (Bilby 1984, Bilby and Ward 1989). Rootwads increase the stability of logs by increasing the potential for snagging on instream obstructions and potentially increasing the log diameter to greater than the average bankfull depth (Sedell et al. 1988).

Log position and orientation also influence the potential mobilization and transportability of a piece. The percentage of the piece anchored to the bank either by the rootwad or by burial, the proportion of the piece in the water, and the angle of orientation to flow contribute to the stability of in-channel wood (Bryant 1983).

Once debris is available for recruitment, it generally remains in place until conditions are sufficient to mobilize and transport

the debris. In steep, low order streams, woody debris mobilization and transport is accomplished primarily by debris torrents triggered by heavy rainfall and flood flows (Swanson et al. 1976, Keller and Swanson 1979, Nakamura and Swanson 1993). In intermediate and high order streams, flotation is the main mobilization mechanism (Lassettre and Harris 2001). Diehl (1997) suggests that the depth sufficient to float a log is about the diameter of the butt plus the distance the roots extend below the butt. He notes that this is roughly 3% to 5% of the estimated log length based on observations of typical large logs at drift study sites.

Braudrick and Grant (2000) developed theoretical models of entrainment and performed flume experiments to examine thresholds for wood movement in streams. They note that piece entrainment is primarily a function of the piece angle relative to flow direction, the presence or absence of a rootwad, the density of the log, and the piece diameter. They also note, contrary to previous studies, that piece length did not significantly affect the threshold of movement for logs shorter than the channel width. Although their model reasonably predicted entrainment thresholds for pieces oriented at 45° and 90° to flow, they note that the model underestimated the flows at which pieces oriented parallel to flow moved. Because of the complexity of movement of wood in streams, they recommend that a larger number of variables need to considered in predicting entrainment and that unequal forces exerted on different parts of the log, including the effects of flotation, need to be considered in predicting wood movement. Subsequently, Alonso (2004) characterized the transport mechanics of individual logs by examining information on a number of influencing factors and using a generalized modeling concept of log motion. Based on his study, he determined that log transport by unsteady streams can be characterized by estimating the hydrodynamic forces on a single cylindrical body and noted that drag and buoyancy are the main mobilizing forces.

In general, most drift is transported as individual logs, which tend to move along the thalweg of the stream (Chang and Shen 1979, Lagasse et al. 2001). However, drift can commonly aggregate into short-lived clumps or jams, most of which are broken apart by turbulence as they move downstream or as they strike stationary objects. Using flume experiments, Braudrick et al. (1997) observed three distinct wood transport regimes: uncongested, congested, and semi-congested. They note that during uncongested transport, logs move without piece-to-piece interactions and generally occupy less than 10% of the channel, whereas in congested transport, the logs move together as a single mass and occupy more than 33% of the channel area. Semi-congested transport is intermediate between these transport regimes. Flume experiments conducted by Bocchiola et al. (2008) showed that, even though logs tended to travel individually rather than as a clump or large aggregation of material, wood pieces tended to travel further downstream when congested transport was observed.

Diehl and Bryan (1993) note, based on work in the basin of the West Harpeth River in Tennessee, that curved pieces of debris were more likely to form intertwined jams. Even though the effect of shape was not examined in their flume studies, Lyn et al. (2003b) used natural twigs because it was decided that they represented a more "realistic" model log element.

Diehl (1997) notes that most drift floats at the water surface in a zone of surface convergence (Figure 2.3) where flow is generally deepest and fastest and, as a result, is transported

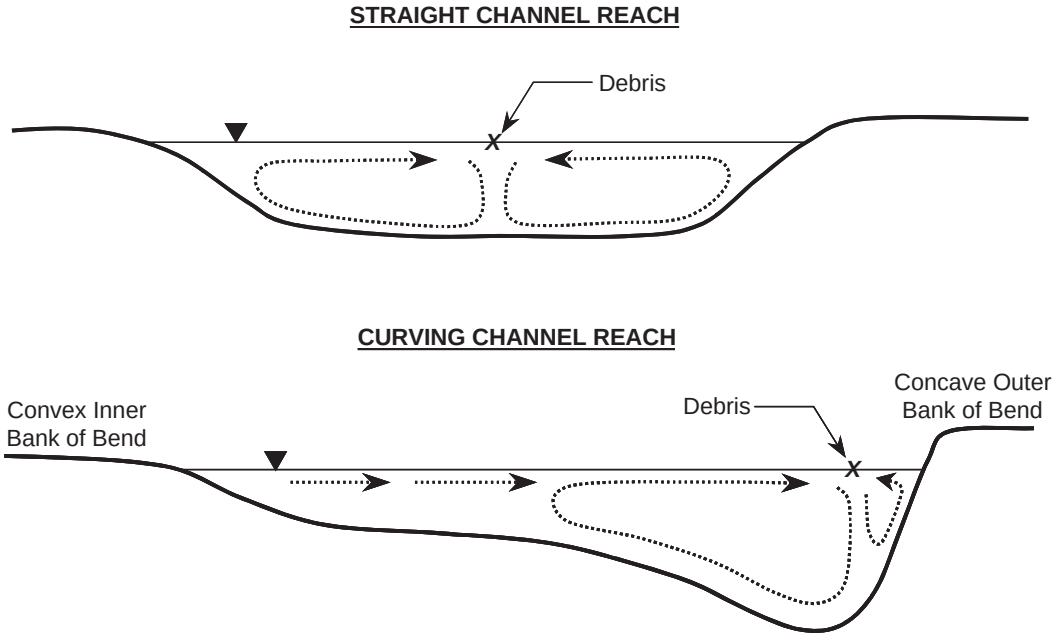

Figure 2.3. Secondary flow patterns in straight and curving channels.

at about the average water velocity. In moderate radius bends, drift is observed more often along the thread of a stream (i.e., thalweg) between the center of the channel and the outside bank than in contact with bank vegetation (Diehl 1997). In contrast, submerged debris is transported near the bed by dragging, bouncing, or tumbling and is often deposited along the banks in straight reaches and on point bars in bends by the slower, diverging flow near the bed (Diehl 1997). Lyn et al. (2003b) also indicate that stable debris piles were more likely to develop in shallower flows or flow regions and to form at lower velocities. Contact with fixed objects also tends to strip the branches and longer roots from trees as they move downstream.

Little physical research has been conducted to evaluate how far drift is transported and where it is deposited in streams. Braudrick and Grant (2001) note in a review of the literature that most studies inferred transport relations from mapped temporal changes in LWD distribution in first to fifth order streams; LWD moves farther and more frequently in larger (≥ fifth order) rather than smaller (< fifth order) streams; smaller pieces move farther than larger pieces; piece diameter, which strongly influences flow depth requirements for log entrainment and transport, influences travel distance; and channel morphology is also a factor in determining travel distance, because wide, sinuous reaches tend to promote deposition on the outside of bends and the head of bars and islands. Braudrick and Grant (2001) hypothesize that the distance logs travel may be a function of the channel's debris roughness, *DR*, a dimensionless index incorporating ratios of piece length and diameter to channel width, depth, and sinuosity:

$$DR \,\alpha \left(a_1 \frac{L_{\log}}{w_{av}} + a_2 \frac{L_{\log}}{R_c} + a_3 \frac{d_b}{d_{av}} \right) \tag{2.2}$$

where:

$L_{\log}$ = Piece length
w_{av} = Mean channel width
R_c = Radius of curvature
d_b = Buoyant depth
d_{av} = Average channel depth
a_1, a_2, a_3 = Coefficients that vary according to relative importance of each variable

However, they note that while the terms in the model were significantly correlated with distance traveled for pieces, the results as indicated by the low R^2 values were not particularly useful from a predictive standpoint.

Finally, Lyn et al. (2003b) note that the delivery of debris to a given site "seems to occur in bursts, rather than continuously, even during a flow event of extended duration" and that a possible explanation for this is that "the debris is not generated in the vicinity of the site, and the bursts result from different travel times from different contributing areas." They also conclude that "the transport of debris occurs rather intermittently with long periods of comparative inactivity punctuated by short periods of intense activity, generally on the rising limb of the hydrograph."

Table 2.2 presents a list of the mobility and transport mechanisms of LWD for various geographic locations and channel positions as compiled by Lassettre and Harris (2001).

2.1.4 Debris Deposition, Accumulation, and Storage

In intermediate channels (typically third and fourth order), drift is transported during major floods in large logjams consisting of large pieces and typically spanning the channel (Diehl and Bryan 1993). Thus, drift may be deposited in a variety of positions and accumulations throughout the channel and may be sufficient to form blockages of the channel. In contrast, in most wide streams (typically fifth order and larger), very little drift is stored within the channel, instead drift accumulates most frequently and in the greatest amounts where the path of floating drift encounters obstructions and fixed objects (Diehl 1997).

On meandering streams, debris is often deposited in wide, sinuous reaches where meander bend and alternate bar morphology promote frequent contact between the debris and the channel margins (Nakamura and Swanson 1994). In these types of channels, pieces tend to deposit on the outside of bends, at the heads of islands and bars, in flood plain forests, and in chutes and sloughs (McFadden and Stallion 1976, Sedell and Duval 1985, Malanson and Butler 1990, Chergui and Pattee 1991, Nakamura and Swanson 1994, Abbe and Montgomery 1996, 2003). Daniels and Rhoads (2003) conducted a field experiment to assess the influence of a debris obstruction located along the outer bank downstream of a bend apex on the three-dimensional (3-D) flow through a meander bend and identified pronounced influences on the flow structure through the bend.

Debris jams form where pieces lodge against obstructions such as large boulders and other immobile features (Nakamura and Swanson 1994, Diehl 1997, Abbe and Montgomery 2003, Manners et al. 2007). D'Aoust and Millar (2000) noted during an investigation of the stability of single logs, single logs with rootwads, and multiple log structures that natural debris jams are initiated by large immobile logs that act as a stable key. When the rootwad remains intact on logs, deposited logs tend to be oriented with the rootwad upstream, likely as a result of the rootwad dragging as the log is transported downstream. The rootwad can be an obstacle to other debris and can become the point of further debris accumulation, especially where they become lodged on the apex of a bar (Abbe and Montgomery 1996, 2003).

Table 2.2. Mobility and transport mechanisms of LWD.

Location	Channel Network Position	Results	References
Western Oregon	• 0.10 to 0.30 channel gradients	• Ability of streams and rivers to move LWD depends on size of river and wood dimensions • Large rivers transport most LWD, while small streams move only small debris short distances before deposition on channel obstructions • Very large debris in small channels transported through debris torrents • Torrents rare in >2nd to 3rd order streams, as steep gradients are required to move debris	Swanson et al. 1976
Western Oregon	• 0.02 to 0.50 channel gradients	• Debris moves through flotation at high flows or through debris flows • Debris flows originate in 1st and 2nd order channels (>50% gradient, <0.2 km^2 drainage areas) • 3rd to 5th order streams (4 km^2 to 60 km^2 drainage areas) wide enough to float large debris and debris jams at high flows	Swanson and Lienkaemper 1978
Eastern Washington	• 0.015 channel gradient • 11.5 m bankfull width	• LWD movement depended on length and diameter of wood • Distance traveled by LWD inversely related to piece length • Anchored pieces more stable in high flows	Bilby 1984
Indiana, North Carolina, Oregon	• 0.001 to 0.40 channel gradients	• Debris torrents main transport mechanism in small, high gradient streams • Flotation main transport mechanism in large, low gradient streams	Keller and Swanson 1979
Western Oregon	• 0.03 to 0.37 channel gradients • 3.5 m to 24 m bankfull widths • 0.1 km^2 to 61 km^2 drainage areas • 1st through 5th order streams	• Wood movement occurred in larger streams during monitoring period • Distance moved depended on piece length in relation to bankfull width • All pieces moving >10 m were shorter than bankfull width	Lienkaemper and Swanson 1987
Western Oregon	• 0.03 to 0.21 channel gradients • 7 m to 25 m bankfull widths • 2nd through 5th order streams	• Debris flows redistributed LWD in steep, low order streams • Floods redistributed LWD in medium to high order streams	Nakamura and Swanson 1993
Western Oregon	• 0.019 to 0.028 channel gradients • 9 m to 71 m channel widths • 5th order streams	• Most transported pieces shorter than bankfull width • 20% of untransported pieces longer than bankfull width • LWD length to channel width useful measure of susceptibility to transport	Nakamura and Swanson 1994
Wyoming	• 0.041 to 0.055 channel gradients • 6.4 m to 7 m low flow channel widths	• LWD less stable in burned drainage due to increased runoff and peak flows, and decreased bank stability	Young 1994
NA	• NA	• Uncongested, semi-congested, and congested wood transport based on ratio of log input (Q_{log}) to stream discharge (Q_w) • Proposed ability of channel to retain wood is function of debris roughness, which varies with channel and log dimensions	Braudrick et al. 1997
Spain	• 0.08 to 0.1575 channel gradients • 3 m to 14 m bankfull widths • 0.8 km^2 to 69 km^2 drainage areas • 1st through 3rd order streams	• Loading (m^3/m^2) decreased in downstream direction • Log mobility increased in larger streams	Elosegi et al. 1999

Source: Lassettre and Harris (2001)

Based on a study conducted in the Queets River basin in Washington, Abbe and Montgomery (2003) determined that individual pieces of woody debris in an accumulation or jam can be separated into key, racked, and loose members. They define three primary categories of woody debris jams (in-situ, transport, and combination jams) based on whether or not the constituent debris was fluvially transported. In-situ debris jams are composed of debris that has remained in place following entry to the channel, although it may have rotated or the channel may have moved. Transport jams are composed of debris that has moved downstream by fluvial processes. Combination jams are composed of both in-situ key mem-

bers and fluvially transported racked and loose members. Within these categories, Abbe and Montgomery (2003) further define 10 types of woody debris accumulation based on the mode of recruitment and the orientation of the members (Table 2.3). They found that key members usually account for a small fraction of individual logs in a jam, but they compose most of a jam's volume, and that many jams have one to four key members and 10 to 100 times as many racked pieces. They also determined that the frequency of jams generally increases with drainage area up to about 116 mi^2 (300 km^2), above which frequency gradually decreases.

Montgomery and Piégay (2003) indicate that tree type is important in the character, distribution, and type of debris accumulations. They note that widely spreading or multiple-stemmed hardwoods are more likely to form snags rather than accumulating as racked members in large log jams, whereas coniferous debris tends to produce cylindrical pieces that are more readily fluvially transported and routed downstream resulting in local concentrations or log jams along a river system.

Once a debris jam forms, fine particles and small material such as brush, leaves, twigs, tree bark, small branches, grasses and weeds, sediment, and man-made materials can fill in the interstitial spaces within the jam (Parola et al. 2000). This reduction in the permeability of the debris jam matrix may increase the scour potential of the jam. Laursen and Toch (1956) suggest that permeability may be just as important as the size of the debris mass in evaluating scour. Observations indicate that the matrix of most debris jams is at least partially filled with fine material. Still, the study conducted by Manners et al. (2007) on the Indian River in New York indicates that debris jams are still highly porous structures, even with large volumes of soil and organic matter in them.

2.1.5 Debris Accumulation at Bridge Piers

The structural components of a bridge can trap debris and may result in significant accumulations. Diehl (1997) notes that there are two classes of debris accumulation observed at bridges: single-pier accumulations and span blockages. Downs and Simon (2001) suggest that the overall "tree-trapping" potential of bridges is a function of tree height, trunk diameter, canopy or root bole diameter (whichever is greater), and pier span distance. Debris characteristics and, lacking detailed debris information, channel width upstream of the bridge site can be used to estimate the probable maximum width of debris accumulations and blocked bridge spans. Debris accumulations are generally deepest at the piers that support them and widest at the surface (Diehl 1997).

Depth of Debris Accumulation at Piers

Because flow depth controls the mobilization and transport of debris, it stands to reason that the depth of debris accumulations will be dependent, in large part, on flow depth at the time of the debris accumulation. Diehl (1997) suggests that, in the process of formation, single-pier accumulations often take on a form roughly resembling an inverted half-cone shape. He notes that drift accumulation begins at the surface, but may grow downward through accretion—"The accumulation can grow toward the river bed through accretion of logs on the underside of the raft as they are washed under it by the

Table 2.3. Basic wood debris accumulation typology.

Types	Distinguishing Characteristics
In-Situ (autochthonous)	**Key member has not moved downstream.**
• Bank input	– Some or all of key member in channel.
• Log steps	– Key member forming step in channel bed.
Combination	**In-situ key members with additional racked woody debris.**
• Valley	– Jam width exceeds channel width and influences valley bottom
• Flow deflection	– Key members may rotate, jam deflects channel course
Transport (allochthonous)	**Key members moved downstream**
• Debris flow/flood	– Chaotic debris accumulation, key members uncommon or absent, catastrophically placed.
• Bench	– Key members along channel edge forming bench-like surface.
• Bar apex	– One or more distinct key members downstream of jam, often associated with development of bar and island.
• Meander	– Several key members buttressing large accumulation of racked debris upstream. Typically found along outside of meander bend.
• Raft	– Large stable accumulation of debris capable of plugging even large channels and causing significant backwater.
• Unstable	– Unstable accumulations composed of racked debris upon bar tops or pre-existing banks.

Source: after Abbe and Montgomery (2003)

plunging flow at the upstream edge . . .”—and that “drift accumulations are typically deepest at the piers that support them, and widest at the surface.” Although he states that under **some** circumstances debris accumulations can reach from the water surface to the riverbed, observations and photographs from a number of locations suggest that debris accumulations **often** extend to the river bed and in many cases the debris may become embedded in the channel bed during high flows and flow recession. Because most debris accumulations slide down the pier and settle on the bed during flow recession and do not re-float during subsequent floods, the debris mass may potentially form a base for further accumulations. Diehl (1997) indicates that an accumulation developing on top of a pre-existing accumulation can grow more rapidly through interaction with the underlying debris and that uncleared debris has the potential to promote bar or island growth. Diehl (1997) also notes that no limit to the vertical extent of debris accumulations has been established other than the depth of flow. The maximum vertical extent of debris accumulation observed in his study was more than 40 ft (12 m).

Diehl (1997) indicates that piers on the banks have less likelihood of trapping debris than those in the channel. He found that bridges in Tennessee with one pier in the channel were several times more likely to have single-pier debris accumulations than bridges with two piers on the banks and none in the channel. Diehl (1997) and Lyn et al. (2003b) also note that large single-pier debris accumulations seem to be associated with the formation or presence of islands and mid-channel bars or the accumulation of exceptionally large debris.

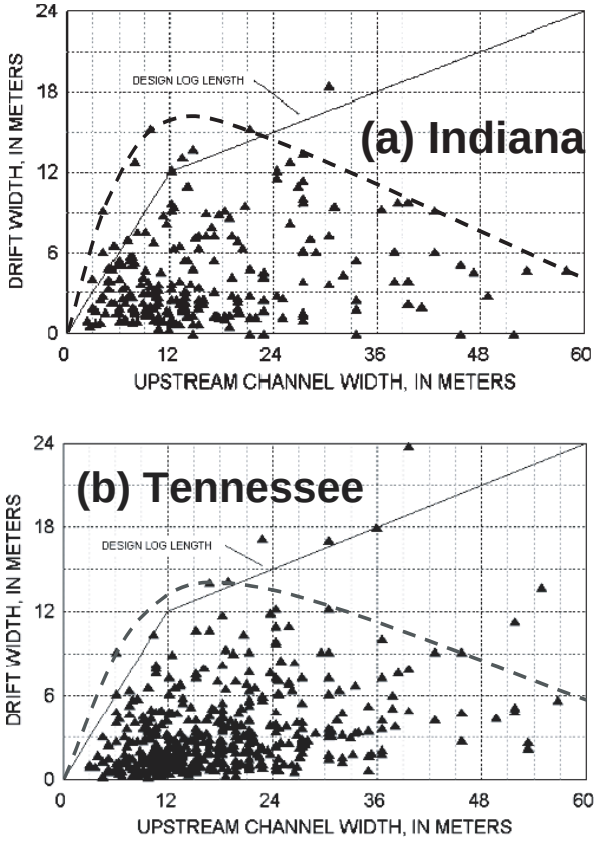

Source: after Diehl (1997)

Figure 2.4. Width of inferred single-pier drift accumulations at scour potential sites in (a) Indiana and (b) Tennessee. *Dashed lines represent curves for maximum expected width of single-pier debris accumulation.*

Width of Single-Pier Accumulations

The channel width influences the length of debris delivered to the bridge site and consequently plays an important role in determining the accumulation potential and characteristics. The length of the longest debris pieces determines the maximum width of the common types of debris accumulations. Debris accumulations resting against a single pier often contain one or more logs extending the full width of the accumulation perpendicular to flow. Large debris accumulations are held together by long logs that support the jam against lateral hydraulic forces. The full-width logs may not be visible because of the accumulation of many smaller logs and other debris, which may conceal the full-width logs. Single-pier accumulations often have a curved upstream appearance when viewed from above, and the center of the downstream side, which rests against the pier, contains the thicker part of the accumulation.

Plots compiled by Diehl (1997) of debris width versus upstream channel width for sites in Tennessee and Indiana (Figure 2.4) suggest that most debris accumulations on single piers are usually less than 50 ft (15 m) wide. The data (see Figure 2.4) also suggests that debris accumulation widths decrease with channel widths greater than about 50 to 60 ft (15 to 18 m), probably as a result of the increased hydraulic forces associated with a larger channel, which would have a greater tendency to break up or deter formation of debris rafts and large accumulations.

Width of Span Blockages

Debris accumulations between piers typically occur where the length of transported logs exceeds the effective width of the openings between piers resulting in the potential for logs to come to rest against two piers. The effective span width is dependent on the skew of the bridge piers to the approaching flow. Span blockages from debris accumulations can also occur where debris rests against and spans debris accumulated on adjacent piers. According to Diehl (1997), most pier-to-pier blockages are the result of a single log bridging the span. Where spans are short enough to be easily spanned by debris, multiple-span or nearly complete bridge-wide blockages are possible.

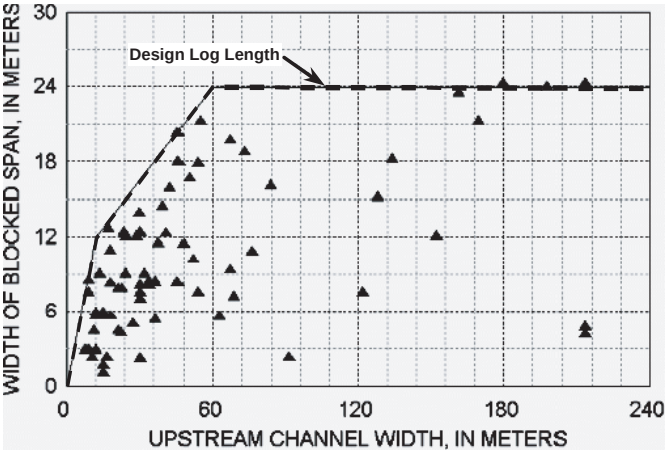

Source: Diehl (1997)

Figure 2.5. Effective width of debris-blocked spans outside of the Pacific Northwest.

In addition, accumulations between the bank or abutment and an adjacent pier are similar in structure to accumulations between piers (Diehl 1997). Often these accumulations extend diagonally upstream from the pier to the bank. Bank-to-pier accumulations are the result of one end of a large log becoming lodged against a tree or other fixed obstruction on the bank and the other end rotating into the pier.

In all cases of pier-to-pier–spanning debris accumulations that were examined for areas outside the Pacific Northwest by Diehl (1997), the effective width of the blocked openings was short enough to be spanned by a single log. Based on the data collected by Diehl (1997) and shown in Figure 2.5, it would appear that span blockages decrease significantly for spans greater than about 80 ft (24 m) for areas outside of the Pacific Northwest. Contrastingly, Diehl found that current design practice favors spans in the range of 70 to 100 ft (20 to 30 m).

Design/Key Log Length

Site investigations conducted by Diehl (1997) indicate that log length, which is closely related to channel width, is the most important factor influencing the width of debris accumulations at bridges. Key logs are those logs that extend the full width of a debris accumulation perpendicular to the approaching flow. Because single-pier drift accumulations are based on logs extending the full width of the accumulation and spans are often blocked by logs extending from pier to pier, Diehl (1997) suggests that the maximum width of these types of accumulation is about equal to the maximum length of sturdy logs delivered to bridges.

Diehl recommends that the log length that should be used in the design of bridges be inferred from the width of the largest single-pier accumulations and the longest blocked spans when estimating the potential for debris accumulations. Diehl notes that the design log length does not represent the absolute maximum length of debris pieces, but instead represents a length above which logs are insufficiently abundant or insufficiently strong throughout their full length to produce drift accumulations equal to their length. This length is also described as the sturdy-log length.

Diehl (1997) states that "the design log length, which is also the minimum effective span length for trapping potential, is intentionally set at the highest level justified by the confirmed pier-to-pier accumulations" and defines the design log length at a given site by the smallest of the following:

- Width of the channel upstream of the site
- Maximum length of sturdy logs
- In much of the United States, 30 ft (9 m) plus one-quarter of the width of the channel upstream from the site

For narrow streams, the minimum width immediately upstream of a bridge can be used as an estimate of the length of the longest logs that can be delivered to the bridge. Although the height of mature trees on the banks of wider streams determines the maximum length of the logs that may be delivered as debris to a bridge site, tree height is not identical to the maximum sturdy-log length. Diehl (1997) found that the maximum sturdy-log length seems to reach about 80 ft (24 m) throughout much of the United States, and especially much of the eastern United States, and may be as long as about 150 ft (45 m) in parts of northern California and the Pacific Northwest.

Diehl (1997) suggests that for those areas where the maximum sturdy-log length is 80 ft (24 m), it can be assumed that the design log length is less than either the upstream channel width or the maximum sturdy-log length over an intermediate range of channel width from 40 to 200 ft (12 m to 60 m). Therefore, he recommends that the design log length over this range of channel width is 30 ft (9 m) plus one-quarter of the channel width (Figure 2.6).

Where the average sturdy-log length exceeds 80 ft (24 m), as in the Pacific Northwest, the design log length is equal to the lesser of either the upstream channel width or the regional maximum sturdy-log length as shown in Figure 2.6.

2.1.6 Modeling Debris-Induced Hydrodynamic Forces and Scour

Parola et al. (2000) report that a common cause of damage to bridges subjected to forces caused by transported debris was due to the flow constriction resulting from debris accumulation. Additionally, while Parola et al. indicate that debris accumulations were typically considered to be floating rafts, observations identified conditions where debris accumulations developed through the entire flow field.

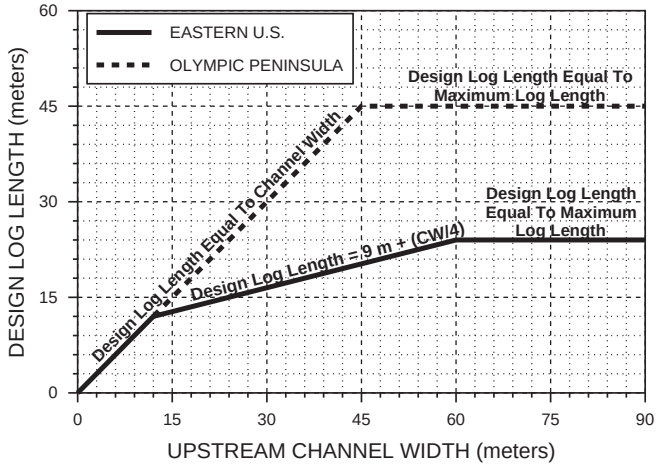

Source: after Diehl (1997)

Figure 2.6. Design log length and upstream channel width (CW) for the eastern United States and the Olympic Peninsula.

Examining the drag forces identified by Parola et al. (1998b), one can see the potential for both static and dynamic fluctuations in the hydraulic conditions around a structure as debris accumulates.

Young (1991), Cherry and Beschta (1989), Melville and Dongol (1992), Parola et al. (2000), Wallerstein et al. (2001), Lyn et al. (2003b), and Bocchiola et al. (2008) report physical model results associated with transported debris. With the exception of Parola et al. (2000) and Bocchiola et al. (2008), studies were conducted in flumes 2 ft or less in width. While numerous data can be collected from a physical model study conducted at a small scale, applying small-scale model results to prototype applications often results in overly conservative designs.

Wallerstein et al. (2002) at the University of Nottingham, U.K., developed a dynamic model for "constriction" scour caused by large woody debris. This one-dimensional (1-D) model was developed for predicting the rate and total depth of scour associated with a channel constriction. Wallerstein applied it to determine scour rates and depths associated with LWD jams and to assess debris impacts on local channel morphology.

Several studies (Prasuhn 1981, Cherry and Beschta 1989, Raudkivi 1990, Abbe and Montgomery 1996, Parola et al. 1998b, Wallerstein and Thorne 1995 and 2004, Wallerstein et al. 2001, Wallerstein 2002, Huizinga and Rydlund 2004, Manners et al. 2007, Bocchiola et al. 2008) address scour related to flow over, around, and under debris in channels. For example, studies by Cherry and Beschta (1989) and Buffington et al. (2002) suggest that scour hole formation occurs in the convergence zone off the tip of a debris jam while Manners et al. (2007) state that "only after a jam has accumulated enough material to substantially decrease its porosity will flow be sufficiently concentrated at the tip, thereby creating the predicted scour hole." They also note that localized areas of scour can develop downstream of the jam with increasing jam porosity because of flow acceleration through one of multiple holes under and/or through the debris jam. However, many of the studies indicate that the effects of constriction and obstruction can be addressed by adapting contraction and local scour equations, depending on the characteristics of the debris jam.

Other studies—including Laursen and Toch (1956), Dongol (1989), Melville and Dongol (1992), Diehl (1997), Mueller and Parola (1998), Wallerstein and Thorne (1998), and TAC (2004)—provide information on scour caused by debris accumulations at bridges. Diehl (1997) provides information on Australian and New Zealand design practices for establishing the geometry of debris masses at piers. Laursen and Toch (1956) state that debris effectively enlarges the pier obstruction, but that evaluating debris scour is very difficult because the permeability, position, and size are all important characteristics of the debris mass. Melville and Dongol (1992) indicate that a debris mass located at the water surface on a single circular pier can be evaluated using an effective pier diameter in a local pier scour equation as illustrated in Figure 2.7. Using three different idealized shapes [cylindrical, conical, and elliptical (in plan)] enveloping the pier, Dongol (1989) determined that a cylindrical shape provided the maximum clear-water scour for uniform non-rippling bed material. Diehl (1997) and TAC (2004) also indicate that debris rafts increase velocity and bed shear, which increases general (pressure) bed scour.

For local pier scour, the concept of effective pier diameter is included in the HEC-18 (Richardson and Davis 2001) complex pier scour approach. The complex pier scour approach includes the pier stem, pile cap, and pile group scour amounts as independent scour components and is illustrated in Figure 2.8 (Jones and Sheppard 2000). This complex pier approach is a more advanced treatment of the effective pier diameter approach suggested by Melville and Dongol (1992) because it addresses the pile cap separately from the pile group, whereas

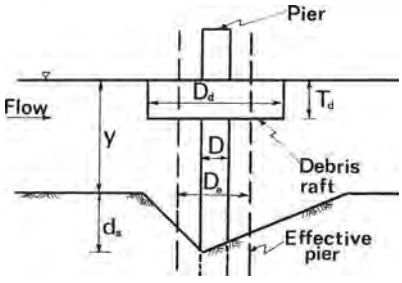

Source: Melville and Dongol (1992)

Figure 2.7. Debris raft equivalent pier diameter.

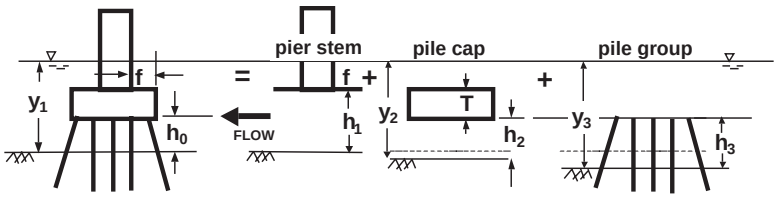

$$y_s = y_{s\,pier} + y_{s\,pc} + y_{s\,pg}$$

Source: Jones and Sheppard (2000)

Figure 2.8. Definition sketch for scour components for a complex pier.

Melville and Dongol combine the debris mass with the pile to arrive at an effective diameter.

For general scour, HEC-18 (Richardson and Davis 2001) includes live-bed and clear-water contraction scour equations as well as a pressure scour equation for submerged bridge decks. These equations may be suitable to the debris raft condition where debris extends across bridge spans or if the debris raft extends a significant distance from an individual pier. The contraction scour equations or their application may need to be modified for debris raft conditions. A modification to an equation may involve an adjusted coefficient or exponent while maintaining the original form of the equation.

Appendix D of HEC-18 (Richardson and Davis 2001) also includes an interim procedure for calculating scour for debris accumulations at the leading edge of a pier combined with a flow angle of attack. The method does not include an effective width adjustment and, therefore, appears to assume that the debris accumulates over the full depth of flow. It is important, however, to recognize that there may be combined effects of both debris accumulation and angle of attack, both of which may not be fully addressed in existing analysis and design procedures.

Another aspect of debris accumulations is the topic of *NCHRP Report 445: Debris Forces on Highway Bridges* (Parola et al. 2000). The report provides guidance on computing the additional force acting on the bridge structure. The drag force of the flow impacting the debris obstruction produces this force. Although evaluating debris forces on bridges is not a topic of this research project, this force is an additional component of the loss (or force) terms that should be included in bridge hydraulic computations. Because debris alters the bridge hydraulics (through the added drag force) and the hydraulic conditions determine the scour potential, it is important that hydraulic analyses and scour analyses are consistent and compatible.

From the Parola et al. (2000) study, it is apparent that the computation of drag force (for large accumulations) is not simply a matter of identifying a drag coefficient and an obstructed area, but also requires use of a constricted velocity rather than an approach velocity and must include the upstream and downstream hydrostatic pressure forces. Therefore, standard one- and two-dimensional (2-D) modeling approaches may not accurately represent the hydraulic effects of debris. One- and two-dimensional models may be used to determine whether the observed (experimental) hydraulic conditions can be replicated by the models.

For example, several different bridge modeling approaches are available [WSPRO, energy, momentum, Yarnell, pressure/weir in HEC-RAS (Brunner 2008)]. One method may be more applicable than others to debris simulation. In the Finite-Element Surface Water Modeling System (FESWMS) (Froehlich 2002, rev. 2003), pier drag and submerged deck routines may be applicable to debris simulation (see Section 3.8).

2.1.7 Managing Debris Accumulations at Bridges

Management of debris problems at bridges has generally focused on debris removal at bridges and in upstream channels (Brice et al. 1978, Lagasse et al. 1991, 2001), bank clearing, channel modifications (Gippel 1989, Gippel et al. 1992), and more recently, the installation of debris deflectors, guides, and traps. However, it is now recognized that debris removal can have a detrimental effect on stream ecology (Gippel 1989, Gippel et al. 1992) and, combined with bank clearing, can cause channel instability and produce a wider and shallower channel with reduced conveyance (Thorne 1990). Nonetheless, prompt and complete debris removal is greatly dependent on the accessibility of the bridge piers and substructure.

The most widely used method for dealing with debris accumulations is through removal. However, where debris removal is difficult or expensive, debris accumulations may remain in place and the potential for additional accumulations grows with the number of floods that occur. Piers with accumulated debris may not shed additional debris as effectively and new accumulations can develop more rapidly over existing accumulations as a result of the interaction with the underlying debris. Additionally, debris accumulations that remain in place for long periods of time can induce the formation of bars or islands.

Piers

The placement, type, and skew of bridge piers have a significant influence on the extent of debris accumulation at a pier. Piers placed in the path of drift movement, such as in the thalweg, will have a higher trapping potential. In narrow channels, piers placed in the center of the channel may have a greater risk of initiating a channel-wide debris accumulation. Piers placed in close proximity to the bank will have a greater trapping potential if the span between the bank and pier is less than the maximum sturdy-log length. Thus, piers placed on the banks are less likely to trap debris than those placed in the channel (Diehl 1997).

Multiple columns, pile bents, or piers with clusters or multiple rows of piles, which can result from the intentional placement of a footing above the channel bed or water surface or exposure due to erosion, can act as a debris trap unless exactly aligned with flow. Even then the gaps between columns or piles can be spanned by debris and debris can become entangled in the columns and piles, thus making removal extremely difficult and increasing the potential for damage to the bridge during clearing operations. Diehl (1997) indicates that skewed pile bents in the water were about twice as likely to have debris accumulations as those with unskewed bents in the water.

Pier shape may also influence debris trapping potential. Round-nosed piers may be more favorable than square-nosed piers, which provide a flat surface against which debris may become lodged. Although it seems intuitive that round-nosed piers should be able to shed debris more easily than square-nosed piers, Diehl (1997) found that bridges in Tennessee with round-nosed piers were no less likely to trap debris than those with square-nosed piers.

Diehl (1997) indicates that current design practice favors the use of single-column piers with rounded noses. The use of wall piers that extend upstream to the edge of the parapet are more easily cleaned of debris than other types of piers. Although hammerhead piers are an alternative to multiple-column piers, removal of debris from the top of the accumulation is more difficult because the pier nose is well under the bridge.

Spans

The potential for span blockages also depends on type, placement, and skew of bridge piers as well as on channel curvature and other channel shape features. In general, the potential for blockage of pier-to-pier, pier-to-bank, or pier-to-abutment spans is low where the effective span width is greater than the design log length.

The use of long spans provides the bridge designer the opportunity to place fewer piers in the channel and, consequently, in the path of debris or in the middle of the channel where access may be difficult. On narrow channels, the main span should bridge the entire channel in order to effectively reduce the potential for span blockage. The placement of piers at or near the base of the banks in narrow channels can create less potential for span blockage than placement in the channel (Diehl 1997).

Since transported debris tends to follow the channel thalweg, the placement of piers and spans should account for the thalweg location because debris is more likely to move along the outer bank in channel bends and along the middle of the channel in relatively straight reaches. Where the bridge crosses a bend or where the reach immediately upstream of the bridge is a long curve, the use of a span that extends from the outer (concave) bank and crosses much of the channel will have a lower trapping potential. Where a bridge is located downstream of a long straight reach, the use of a main span that bridges the center of the channel will have a lower trapping potential. However, the movement of debris should be evaluated under flood flow conditions, especially for conditions greater than bank full flow where the debris path may be short-circuited or deviate from the expected path as compared to the path during less than bank full flow.

Where the bridge is skewed to approaching flow, the effective width of horizontal gaps (span and pier-to-bank width) is reduced. The effective span or pier-to-bank width is the distance between lines parallel to the approaching flow that pass through the nose of each pier (Figure 2.9). Diehl (1997) indicates that the spans can be bridged by debris accumulations where the size of the debris exceeds the effective horizontal gap width. However, if key logs come in contact with a pier, they can rotate before coming in contact with the adjacent pier and, therefore, the pier-to-pier width (i.e., span width) should actually be equal to or greater than the design log length, not the effective horizontal gap width.

The effective pier-to-bank width should also be greater than the design log length since logs will more likely impact on the bank first and then rotate and intersect the pier at an angle equal to or greater than perpendicular to the approaching flow. Conversely, if a log impacts the pier first, it is likely that it will not intersect the bank when and if it rotates, and will probably be deflected downstream. If the log rotates inward toward the bank before passing downstream, it may become wedged between the pier and bank (depending on the bank geometry) under the bridge.

Countermeasures

Other management tools currently being used to control debris accumulation on bridges include river training or channel stabilization at the bridge site and the placement of some form of debris deflector, guide, or collector in the channel immediately upstream of the bridge. Debris deflectors, guides, or collectors have had mixed results because their effectiveness

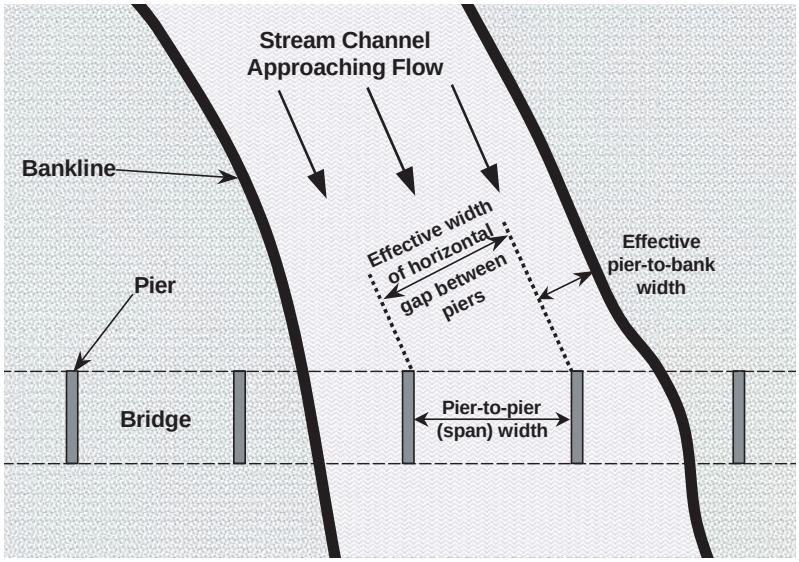

Source: after Diehl (1997)

Figure 2.9. Definition sketch of the effective width of horizontal gaps.

is dependent on the amount and frequency of debris delivered to the bridge site as well as local site conditions and structure configuration (e.g., Lyn et al. 2003b). Structural measures need to be robust enough to withstand impact and static forces and scour if they become blocked (TAC 2004).

Various methods of river training and channel stabilization at a bridge site have been well documented (Lagasse et al. 2001, Richardson et al. 2001). Although river training and channel stabilization can control the geometry of the channel at the bridge site with regard to the alignment of the structural features to the principal transport path of debris, they have little effect on the amount of debris delivered to the bridge components themselves.

A variety of methods for collecting debris or guiding debris through bridge openings has also been identified by several sources (Reihsen and Harrison 1971, Brice et al. 1978, Chang and Shen 1979, Perham 1987 and 1988, Saunders and Oppenheimer 1993, Lagasse et al. 2001, Richardson et al. 2001, Bradley et al. 2005). Three general categories of debris control structures are used on streams: (1) debris deflectors, (2) debris catchers or racks, and (3) debris fins (Reihsen and Harrison 1971, TAC 2004). The most prevalent debris control structures used today are debris deflectors and debris fins.

Debris deflectors are generally used where debris loading is moderate to heavy. They are placed immediately upstream of a bridge and are used to deflect the major portion of debris away from bridge piers or assist in guiding debris into and through wide bridge openings.

They may consist of a single piling or a series of three pilings placed such that the group forms a v-shape in planview with the apex pointing upstream. These types of deflectors have had mixed success because debris can become lodged in the deflector and may accumulate on the deflector itself. Debris that accumulates on the deflector may become dislodged and travel downstream where it can impact bridge piers as a massive cohesive unit, which can have catastrophic consequences. However, permanently installed debris deflectors can be ineffective in reaches where flow direction changes as a result of either changing flood stages (i.e., flow path changes with stage) or because of changes in channel planform (i.e., changes in flow alignment) over time. More recently, lunate-shaped hydrofoil deflectors and rotating-drum deflectors have also been developed for use on bridges.

The lunate-shaped hydrofoil deflector is designed to generate counter-rotating streamwise vortices in its wake such that the vortices migrate to the surface of the water ahead of the pier and deflect the debris around the pier (Saunders and Oppenheimer 1993). However, the hydrofoil is also fixed in the river and its success is largely stage and flow direction dependent, and it can be damaged by debris that becomes lodged underneath it during lower flows. It is not known if this type of deflector has been installed or used at any bridge locations.

Rotating drum deflectors are mounted upstream near the front of a pier and rotate such that debris that impacts on the deflector is turned away from the pier by the current and the force of the debris (Collier 2005). These types of deflectors can be mounted such that they can adjust with river stage and are generally not affected by changes in flow direction except at extreme angles. Because they are mounted near the leading edge of a pier, deflectors can be easily changed if they become damaged.

Debris racks or catchers are placed across the channel and are used to collect debris before it reaches a bridge (Perham 1987, 1988). They may be vertical or inclined and may be square or skewed to flow. Inclined racks allow for debris to ride up onto the rack and skewed racks allow debris to be partially deflected toward the bank. However, debris racks and catchers can become clogged or blocked. Completely blocked racks or catchers can produce significant backwater upstream, potentially severe scour downstream of the structure or where flow reenters the structure, contraction and local scour if the structure is immediately upstream of the bridge, and possible flanking or by-passing of the structure due to lateral erosion (Diehl 1997, TAC 2004). In addition, racks and collectors may collect significantly more debris than would be trapped by a bridge, so the cost of debris removal may be greater where these structures are used (Diehl 1997).

Cribs or timber sheathing is also used on bridge piers to deflect debris away from piers that consist of open pile bents. However, cribs with large mesh openings can trap debris and create problems and wooden cribs or sheathing can be severely damaged by large debris and ice (Chang and Shen 1979).

Debris fins are walls or rows of pilings placed upstream of bridge piers or may be upstream extensions of the piers themselves (Chang and Shen 1979, TAC 2004). The fins are aligned to flow and may be inclined to allow deflection of the debris through the bridge opening. However, as with piers, the effectiveness of fins is dependent on their alignment to flow and debris path, and they can contribute to span blockages if the span between fins is less than the design log length.

Finally, a combination of channel dredging and bank revetment may be an option where sedimentation and stream aggradation play a significant role in debris accumulation problems (Lyn et al. 2003b). However, dredging by itself would not provide a long-term solution under these circumstances because the underlying causes of sedimentation/aggradation would probably not be addressed.

2.2 Debris Photographic Archive

A photographic archive was compiled to assess typical debris geometry relationships. Photographs of debris at bridges were acquired from a number of contributors. The photographs in the archive provided the primary source that was used for evaluating debris accumulation characteristics and debris geometry from a wide range of sites located throughout the United States.

The primary contributor of debris photographs was Collier (2005), who provided almost 50% of the photographs. Numerous photographs were provided by state DOT personnel in response to the Task 2 survey. The remaining photographs were acquired from in-house sources, Internet sites, and from referenced publications. A total of 1,079 photographs at 142 sites in 31 states were acquired from the various sources, but not all the photographs are specifically of debris accumulations at bridges. The photographic archive is provided on the TRB website (see Appendix A). Table 2.4 presents a list of the sources of the debris photographs, site locations and the number of photographs available for each site (see also Figure 2.14 for a map of the photograph locations in each of the five geographic regions).

Directions for navigating the debris photographic archive are included in Appendix A. The photographs are first organized by state and finally by the river or stream. Within each subdirectory, a Microsoft® PowerPoint file has been created containing the individual photographs for the given site.

2.3 Regional Analysis of Debris

One might infer from previous studies, experience with debris problems nationally, the geomorphic characteristics of rivers in different Physiographic Regions, and the distinctly different characteristics of woody vegetation and river bank erosion processes that there should be some regional bias in debris characteristics and in debris impact on bridges. As a starting point, these regional characteristics were investigated in the Task 1 literature search and in the Task 2 site reconnaissance and survey. An attempt was made to identify common (or typical) debris characteristics that might be distinguishable by major Physiographic Region or Ecoregion.

Several studies have suggested the potential for regionalized debris generation characteristics. Chang and Shen (1979) developed a depiction of a national distribution of debris problems from severe to moderate to minor or no problem as shown in Figure 2.10. The distribution was based on a state-specific survey of debris problems at highway bridges nationwide and indicated that the Pacific Northwest and the upper and lower Mississippi River Valley experience the most severe debris problems. Diehl (1997) mapped debris sites reported by DOTs, distribution of debris field-study sites, and debris sites referenced in publications or personal communications. Diehl suggests that watersheds of high or low debris generation can be identified based on watershed characteristics such as proximity of vegetation to the stream, rate of bank erosion, and/or channel instability resulting from natural properties, climate change, fire, or human modification.

Prediction of debris accumulation might potentially be regionalized by initially dividing the land area into subdivisions based on debris-contributing characteristics such as vegetation type and geomorphic factors. Two commonly recognized systems of geomorphic and ecological subdivisions or classifications are the Physiographic Regions classification by Fenneman (1917) and Ecoregions classification by Bailey (1983).

Table 2.4. Inventory of photographs of debris at bridge piers.

Geographic Region	State	Stream	Source	Number of Photos
East	North Carolina	Deep River	Debris Free, Inc. (Mike Collier)	4
		Deep River	NCDOT (web site photos)	5
	Tennessee	Coles Creek	Web Site Photos	4
	Virginia	Appomattox River	Debris Free, Inc. (Mike Collier)	4
		Dan River	Debris Free, Inc. (Mike Collier)	2
		James River	Debris Free, Inc. (Mike Collier)	2
		Nottoway River	Debris Free, Inc. (Mike Collier)	4
	West Virginia	Mud River	Debris Free, Inc. (Mike Collier)	2
		Tug River	Debris Free, Inc. (Mike Collier)	3
Midwest	Illinois	East Skokie Ditch	Debris Free, Inc. (Mike Collier)	3
		Iroquois River	Debris Free, Inc. (Mike Collier)	4
		Mackinaw River	Debris Free, Inc. (Mike Collier)	3
		Mississippi River	Debris Free, Inc. (Mike Collier)	3
		Unknown	Debris Free, Inc. (Mike Collier)	6
	Indiana	Indian Creek	Ayres Associates Inc.	1
		Eel River	Debris Free, Inc. (Mike Collier)	8
		Eel River	Debris Free, Inc. (Mike Collier)	4
		Vermillion River	Debris Free, Inc. (Mike Collier)	11
		Wabash River	Debris Free, Inc. (Mike Collier)	3
		White River	Timothy Diehl (1997)	1
		White River	USGS (Robinson 2003)	6
	Iowa	Cedar Creek	Tim Dunlay, Iowa DOT (Survey)	14
		East Nishnabotna River	Tim Dunlay, Iowa DOT (Survey)	11
		West Nodaway River	Tim Dunlay, Iowa DOT (Survey)	3
	Kansas	Elk River	Ayres Associates Inc.	32
		Neosho River	Ayres Associates Inc.	38
		Neosho River	Ayres Associates Inc.	28
		Verdigris River	Ayres Associates Inc.	14
		Chikaskia River	Brad Rognlie, P.E. KDOT (Survey)	1
		Elk River	Brad Rognlie, P.E. KDOT (Survey)	25
		Elm Creek	Brad Rognlie, P.E. KDOT (Survey)	7
		Neosho River	Brad Rognlie, P.E. KDOT (Survey)	19
		Smoky Hill River	Brad Rognlie, P.E. KDOT (Survey)	37
		Unknown	Brad Rognlie, P.E. KDOT (Survey)	6
		Verdigris River	Brad Rognlie, P.E. KDOT (Survey)	11
		Republican River	Debris Free, Inc. (Mike Collier)	6
		Smoky Hill River	Debris Free, Inc. (Mike Collier)	34
	Kentucky	Unknown	Debris Free, Inc. (Mike Collier)	2
	Minnesota	Minnesota River	Debris Free, Inc. (Mike Collier)	9
		S. Br. Wild Rice River	Duane Hill, MnDOT (Survey)	2
		Minnesota River	Larry Cooper, MnDOT (Survey)	1
		Minnesota River	Larry Cooper, MnDOT (Survey)	1
		Mississippi River	Larry Cooper, MnDOT (Survey)	2
		Black River	MnDOT Dist. 1 (web site photos)	2
	Missouri	Florida Creek	Ayres Associates Inc.	1
		Unknown	Debris Free, Inc. (Mike Collier)	1
		Chariton River	John Holmes, MoDOT (Survey)	9
		Big Creek	Ken Foster, MoDOT (Survey)	2
		Grand River	Ken Foster, MoDOT (Survey)	1
		W. Fk. Grand River	Ken Foster, MoDOT (Survey)	8
	Nebraska	South Platte River	Ayres Associates Inc.	1
	Ohio	Great Miami River	Brandon Collett, ODOT (Survey)	9
		Unknown	Debris Free, Inc. (Mike Collier)	5
	Oklahoma	Washita River	Debris Free, Inc. (Mike Collier)	3
		North Canadian River	Debris Free, Inc. (Mike Collier)	12
	Tennessee	Harpeth River	Debris Free, Inc. (Mike Collier)	8
		Harpeth River	Jon Zirkle, TDOT (Survey)	11
		Harpeth River	Timothy Diehl (1997)	2
	Texas	Clear Fk. Brazos River	Debris Free, Inc. (Mike Collier)	6
		Clear Fk. Brazos River	Jerry Conner, TxDOT (Survey)	6
	Wisconsin	Bad River	Allan Bjorklund, WisDOT (Survey)	1
		Pikes Creek	Allan Bjorklund, WisDOT (Survey)	1

(continued on next page)

Table 2.4. (Continued).

Geographic Region	State	Stream	Source	Number of Photos
Pacific Coast	California	Bear River	Ayres Associates Inc.	2
		Harris Creek	Ayres Associates Inc.	1
		Malibu Laguna	Ayres Associates Inc.	1
		Sacramento River	Ayres Associates Inc.	6
		Sacramento River	Ayres Associates Inc.	2
		Stony Creek	Ayres Associates Inc.	1
	California (Central & South Coast)	Arroyo Grande Creek	Kevin Flora, Caltrans (Survey)	11
		Hopper Creek	Kevin Flora, Caltrans (Survey)	3
		Salsipuedes Creek	Kevin Flora, Caltrans (Survey)	5
	California (Central Valley)	Sacramento River	Kevin Flora, Caltrans (Survey)	2
		Stony Creek	Kevin Flora, Caltrans (Survey)	6
		Thomes Creek	Kevin Flora, Caltrans (Survey)	3
	California (Mountain)	North Fork Deer Creek	Kevin Flora, Caltrans (Survey)	4
	California (North Coast)	Mad River	Kevin Flora, Caltrans (Survey)	4
		Trinity River	Kevin Flora, Caltrans (Survey)	3
		Yager Creek	Kevin Flora, Caltrans (Survey)	5
	California (North)	Butte Creek	Debris Free, Inc. (Mike Collier)	9
		Navarro River	Debris Free, Inc. (Mike Collier)	13
	California (South)	Callegas Creek	Debris Free, Inc. (Mike Collier)	18
		San Antonio Creek	Debris Free, Inc. (Mike Collier)	9
		Santa Clara River	Debris Free, Inc. (Mike Collier)	26
		Ventura River	Debris Free, Inc. (Mike Collier)	29
	Oregon	Shitike Creek	Ayres Associates Inc.	1
		Calapooia River	Debris Free, Inc. (Mike Collier)	1
		North Santiam River	Debris Free, Inc. (Mike Collier)	3
	Washington	Cowlitz River	Debris Free, Inc. (Mike Collier)	7
		North Fork Skagit River	Debris Free, Inc. (Mike Collier)	6
		North Fork Skagit River	Debris Free, Inc. (Mike Collier)	2
		Skykomish River	Debris Free, Inc. (Mike Collier)	4
		South Fork Skagit River	Debris Free, Inc. (Mike Collier)	1
		Queets River	Timothy Diehl (1997)	1
South	Arkansas	St. Francis River	Debris Free, Inc. (Mike Collier)	34
	Florida	Escambia River	Debris Free, Inc. (Mike Collier)	6
	Louisiana	Bayou Boeuf	Ayres Associates Inc.	1
		Amite River	Debris Free, Inc. (Mike Collier)	10
		Red River Raft	Web Site Photos	2
	Mississippi	Abiaca Creek	Ayres Associates Inc.	1
		Jack Creek	Ayres Associates Inc.	2
		Sykes Creek	Ayres Associates Inc.	1
		Coles Creek	MDOT Bridge Design (Survey)	1
	South Carolina	Little River	Debris Free, Inc. (Mike Collier)	40
	Tennessee	Jackson District Var.	Debris Free, Inc. (Mike Collier)	121
		Wolf River	Debris Free, Inc. (Mike Collier)	3
		Wolf River	Jon Zirkle, TDOT (Survey)	3
	Texas	Brushy Creek	Blaine Laywell, TxDOT (Survey)	6
		Little River	Blaine Laywell, TxDOT (Survey)	7
		Guadalupe River	Carl O'Neil, TxDOT (Survey)	7
		Rocky Creek	H.C. Schroeder, TxDOT (Survey)	6
		Pedernales River	Jeff Howell, TxDOT (Survey)	6
		San Marcos River	Jeff Howell, TxDOT (Survey)	1
		Cocklebur Creek	Jon Kilgore, TxDOT (Survey)	7
		San Antonio River	Jon Kilgore, TxDOT (Survey)	13
		Elm Fork of Trinity River	Tim Hertel, TxDOT (Survey)	2
		Red River	Tim Hertel, TxDOT (Survey)	12
		Brazos River	Timothy Diehl (1997)	1
		Unknown	Timothy Diehl (1997)	5

Table 2.4. (Continued).

Geographic Region	State	Stream	Source	Number of Photos
West	Arizona	New River	Ayres Associates Inc.	2
	Colorado	Bijou Creek	Ayres Associates Inc.	4
	Idaho	Pack River	Ayres Associates Inc.	2
		Teton River	Ayres Associates Inc.	1
	Montana	Boulder River	Russell Brewer, PE MtDOT (Survey)	12
		Jefferson River	Russell Brewer, PE MtDOT (Survey)	14
		Regis River	Russell Brewer, PE MtDOT (Survey)	3
	Nevada	Carson River	Ayres Associates Inc.	2
		Humboldt River	Ayres Associates Inc.	1
		Carson River	Chris Miller, NDOT (Survey)	15
		Carson River	Chris Miller, NDOT (Survey)	6
		Carson River	Debris Free, Inc. (Mike Collier)	6
	New Mexico	Rio Grande	Ayres Associates Inc.	1
	Unknown	Unknown	Ayres Associates Inc.	3
	Utah	Colorado River	Debris Free, Inc. (Mike Collier)	4
		San Rafael River	Debris Free, Inc. (Mike Collier)	7
		Santa Clara River	Tim Ularich, UDOT (Survey)	6
		Virgin River	Tim Ularich, UDOT (Survey)	5
		Unknown	Various Web Sites (incl. KSL Channel 5 TV, City of St. George)	11
		Beaver Dam Creek	Various Web Sites (incl. KSL Channel 5 TV, City of St. George)	4
		Santa Clara River	Various Web Sites (incl. KSL Channel 5 TV, City of St. George)	7
		Virgin River	Various Web Sites (incl. KSL Channel 5 TV, City of St. George)	1

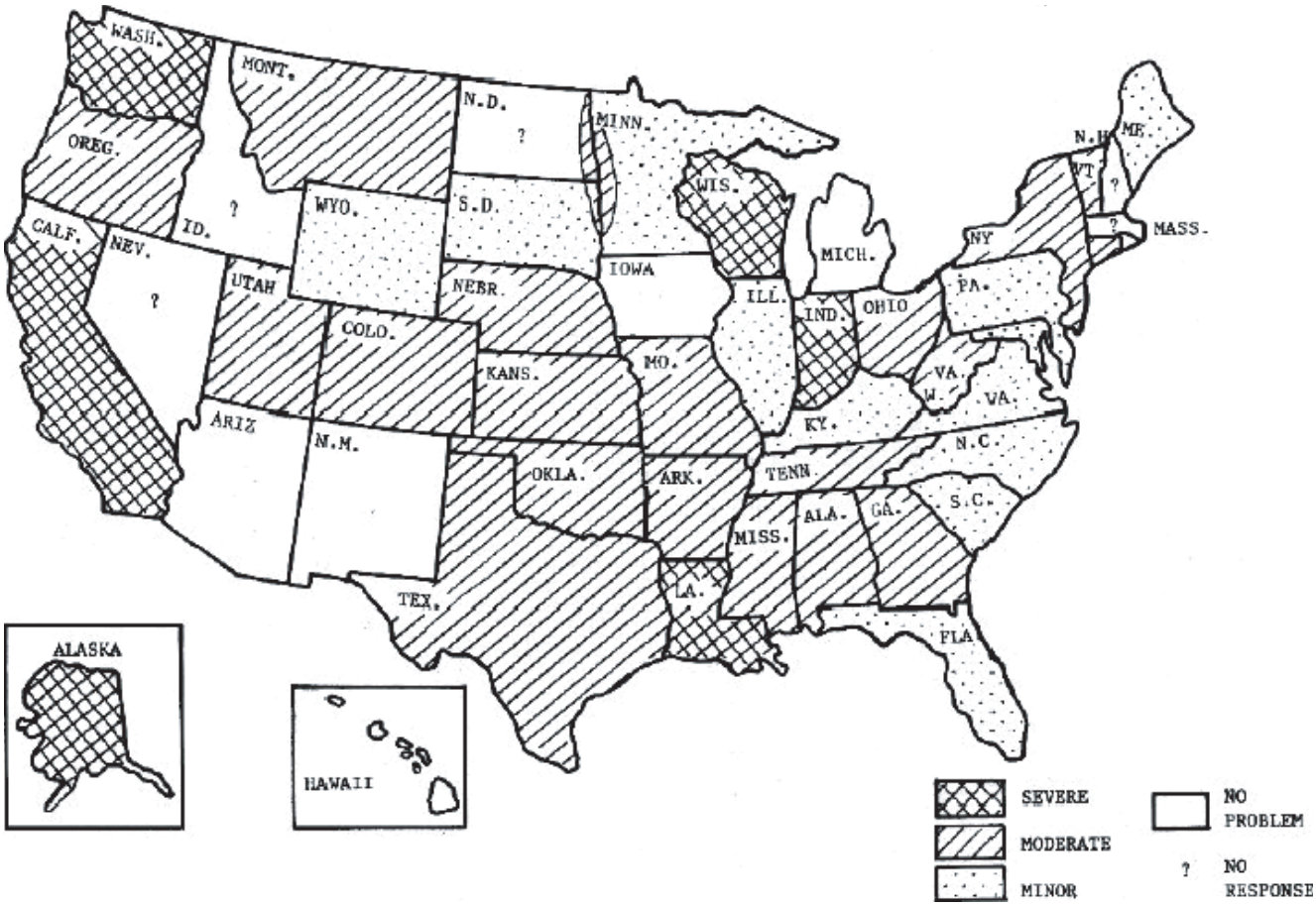

Source: Chang and Shen (1979)

Figure 2.10. Debris problem distribution.

Fenneman (1917) proposed the concept of physiographic subdivisions of the United States based on regional geomorphologic characteristics in the early 20th century. Leighty (2001) defines a physiographic unit as "an area of the Earth's surface within which the major topographic features have a single geomorphic history, a definite general structure, certain physical characteristics, and a predictable general pattern of lower order landforms." Fenneman created a three-tiered classification system consisting of divisions, provinces, and sections derived from terrain texture, rock type, and geologic structure and history (Barton et al. 2003). In the United States, there are 25 physiographic providences and 82 physiographic sections. Figure 2.11 presents a map of the Physiographic Regions of the United States (Barton et al. 2003).

Ecoregions subdivide the earth's surface into identifiable areas based on macroscale patterns of ecosystems (Bailey 2005) and the environmental factors that most likely acted in creating variation in ecosystems (Bailey 1983). The intent of the ecologically based Ecoregions classification system is to provide a foundation for estimating ecosystem productivity and potential response to varying management practices (Bailey 1983).

Ecoregions are based on a three-tiered hierarchy system. The two broadest tiers, domains and divisions (within domains), are delineated principally on the large ecological climate zones identified by Köppen (1931) and modified by Trewartha (1968). Climate is emphasized because of the prevailing effect it has on composition and productivity of an ecosystem (Bailey 1995), where moisture and temperature characteristics drive soil formation and surface topography and limit plant growth. The third tier, provinces, allows an Ecoregion to be described in terms of its dominant physical and biological characteristics such as land-surface form, climate, vegetation, soils, and fauna. Bailey's Ecoregion map contains 34 provinces and 29 mountain provinces, within 24 divisions and 4 domains. Figure 2.12 presents a map of the Ecoregions of the United States (Bailey 1995).

Ecoregions and Physiographic Regions define areas where one might expect to find similar types of vegetation and geomorphic conditions, thereby possibly providing a method of predicting regional debris generation relationships. To more closely examine the relationship among the two classification systems and general debris characteristics, the site locations described in the photographic archive and presented in Table 2.5 are delineated on the Physiographic Regions and Ecoregions maps shown in Figures 2.11 and 2.12.

An examination of the debris characteristics and accumulation geometry from the various debris site photographs relative to their locations on the Physiographic Region and Ecoregion maps reveals that there is no identifiable or well-defined relationship with regard to the individual Physiographic Regions or Ecoregions. Instead, the typical debris accumulation geometries that have been identified appear to be common throughout the United States, and any river or stream with a riparian corridor along its bank is susceptible to debris problems. For example, Figure 2.13 shows a common debris accumulation geometry found at five different sites from various parts of the country that are in distinctly different Physiographic Regions and Ecoregions. With regard to vegetation types, only general relationships exist. In most of the eastern half of the United States, large woody debris delivered to streams and rivers is primarily from riparian forests or corridors along those streams and rivers. In the arid southwest and west, vegetation can be limited to small trees and shrub-like vegetation, and the debris accumulation sizes and geometry in these areas often reflect this type of vegetation. In the Pacific Northwest, large conifers are the dominant tree species and are the controlling factor in the size of the debris accumulations and the debris geometry in this region.

However, there does appear to be a simple geographic relationship with regard to the distribution of debris problems as suggested by the site locations of the debris photographs in the photographic archive. The distribution of the photograph sites can be grouped into five general geographic regions of the United States: East, South, Midwest, West, and Pacific. The boundaries for these general geographic regions are roughly similar to some of the major physiographic boundaries with some deviation. Figure 2.14 shows the debris sites from the photographic archive in relation to the five general geographic boundaries.

As seen in Figure 2.14, the majority of the photograph sites are distributed within three of the five geographic regions: the Midwest, the Texas coast and lower Mississippi Valley portions of the South, and the Pacific. The large number of sites located in the Midwest is closely related to distribution of the major tributary drainages of the Mississippi River. The distribution of the sites in the South appears to be tied to the major tributary drainages in coastal Texas and the lower Mississippi Valley. Many of these major drainages still contain rivers and streams with abundant or extensive riparian corridors, active meanderbelts, erodible bank materials, and some form of disturbance within their watersheds that is driving channel or bank instability.

The distribution of debris sites in the Pacific is probably tied to climate and geology, since most of the sites are located within or in close proximity to forested mountains and hills. The poor geotechnical competence of the hills and mountains of the Pacific region combined with major or extreme precipitation events can result in the delivery of large volumes of debris through mass movement processes. In the valleys of the Pacific region, the delivery of debris is more closely tied to the erosion of stream and riverbanks as a result of instability induced by watershed disturbances and channel migration. Considerably fewer sites are in the West, probably as a

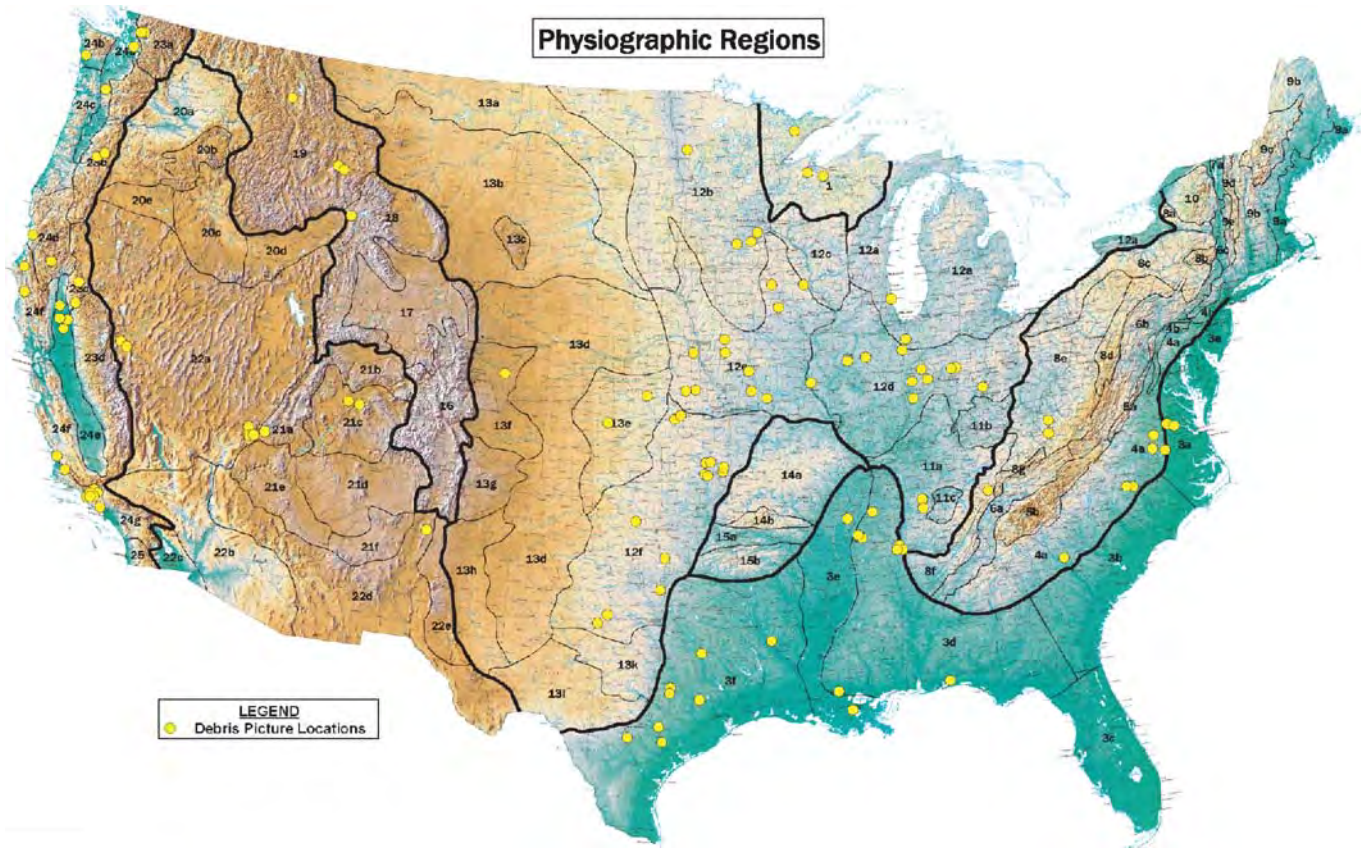

LAURENTIAN UPLAND
1. Superior Upland

ATLANTIC PLAIN
2. Continental Shelf (not on map)
3. Coastal Plain
   a. Embayed section
   b. Sea Island section
   c. Floridian section
   d. East Gulf Coastal Plain
   e. Mississippi Alluvial Plain
   f. West Gulf Coastal Plain

APPALACHIAN HIGHLANDS
4. Piedmont Province
   a. Piedmont Upland
   b. Piedmont Lowlands
5. Blue Ridge Province
   a. Northern section
   b. Southern section
6. Valley and Ridge Province
   a. Tennessee section
   b. Middle section
   c. Hudson Valley
7. St. Lawrence Valley
   a. Champlain section
   b. Northern section (not on map)
8. Appalachian Plateaus Province
   a. Mohawk section
   b. Catskill section
   c. Southern New York section
   d. Allegheny Mountain section
   e. Kanawha section
   f. Cumberland Plateau section
   g. Cumberland Mountain section
9. New England Province
   a. Seaboard Lowland section
   b. New England Upland section
   c. White Mountain section
   d. Green Mountain section
   e. Taconic section
10. Adirondack Province

INTERIOR PLAINS
11. Interior Low Plateaus
   a. Highland Rim section
   b. Lexington Plain
   c. Nashville Basin
12. Central Lowland
   a. Eastern Lake section
   b. Western Lake section
   c. Wisconsin Driftless section
   d. Till Plains
   e. Dissected Till Plains
   f. Osage Plains

INTERIOR PLAINS (continued)
13. Great Plains Province
   a. Missouri Plateau, glaciated
   b. Missouri Plateau, unglaciated
   c. Black Hills
   d. High Plains
   e. Plains Border
   f. Colorado Piedmont
   g. Raton section
   h. Pecos Valley
   i. Edwards Plateau
   j. Central Texas section
14. Ozark Plateaus
   a. Springfield-Salem plateaus
   b. Boston "Mountains"
15. Ouachita Province
   a. Arkansas Valley
   b. Ouachita Mountains

ROCKY MOUNTAIN SYSTEM
16. Southern Rocky Mountains
17. Wyoming Basin
18. Middle Rocky Mountains
19. Northern Rocky Mountains

INTERMONTANE PLATEAUS
20. Columbia Plateau
   a. Walla Walla Plateau
   b. Blue Mountain section
   c. Payette section
   d. Snake River
   e. Harney section
21. Colorado Plateaus
   a. High Plateaus of Utah
   b. Unita Basin
   c. Canyon Lands
   d. Navajo section
   e. Grand Canyon section

INTERMONTANE PLATEAUS (continued)
21. Colorado Plateaus (continued)
   f. Datil section
22. Basin and Range Province
   a. Great Basin
   b. Sonoran Desert
   c. Salton Trough
   d. Mexican Highland
   e. Sacramento section

PACIFIC MOUNTAIN SYSTEM
23. Cascade-Sierra Mountains
   a. Northern Cascade Mountains
   b. Middle Cascade Mountains
   c. Southern Cascade Mountains
   d. Sierra Nevada
24. Pacific Border Province
   a. Puget Trough

PACIFIC MOUNTAIN SYSTEM (continued)
24. Pacific Border Province (continued)
   b. Olympic Mountains
   c. Oregon Coast Range
   d. Klamath Mountains
   e. California Trough
   f. California Coast Ranges
   g. Los Angeles Ranges
25. Lower California

Source: after Barton et al. (2003)

Figure 2.11. Physiographic regions of the United States and photographic archive sites.

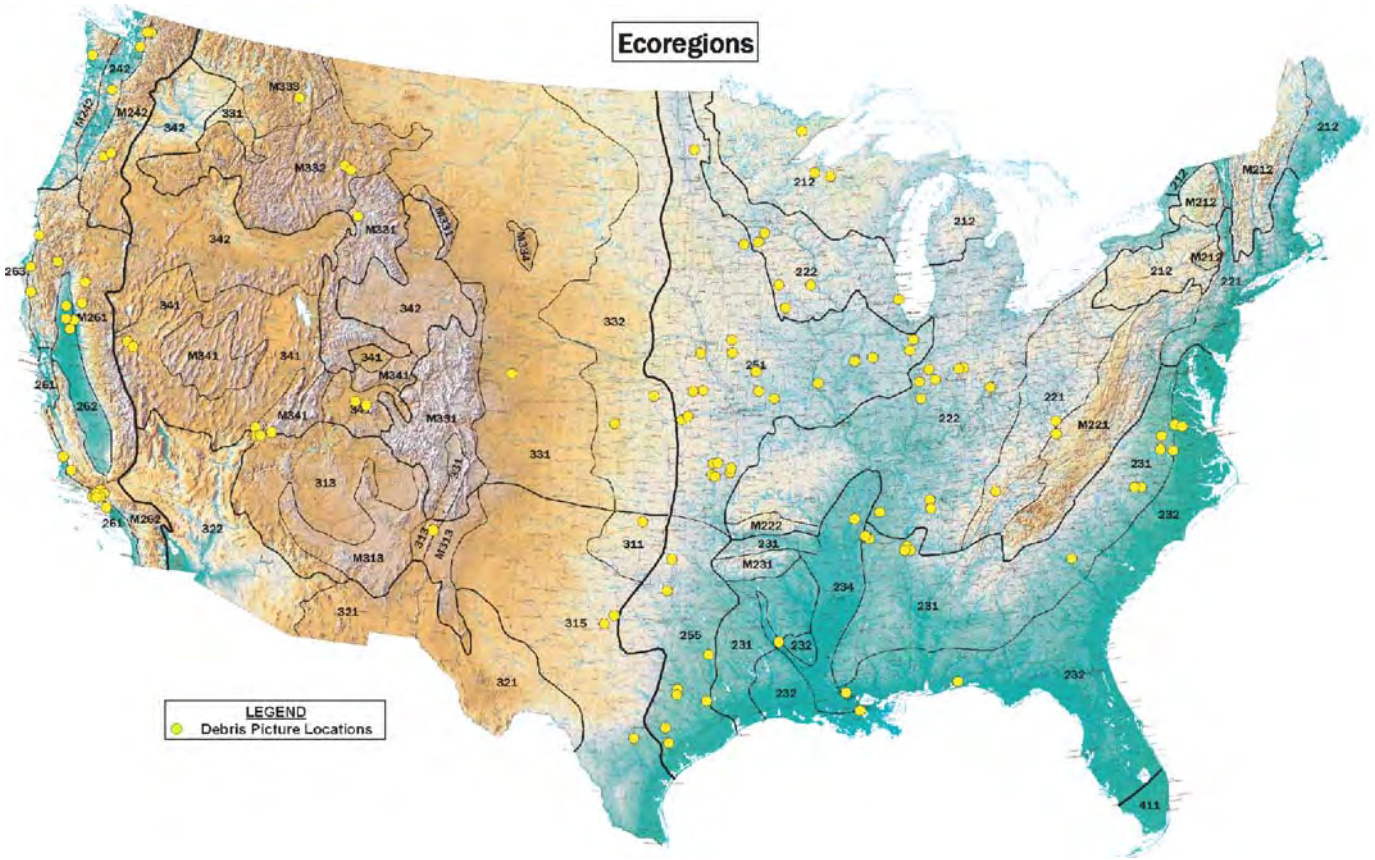

100 POLAR DOMAIN

120 Tundra Division
- 124 Arctic Tundra Province
- 125 Bering Tundra (Northern) Province
- 126 Bering Tundra (Southern) Province

M120 Tundra Division – Mountain Provinces
- M121 Brooks Range Tundra – Polar Desert Province
- M125 Seward Peninsula Tundra – Meadow Province
- M126 Ahklun Mountains Tundra – Meadow Province
- M127 Aleutian Oceanic Meadow – Heath Province

200 HUMID TEMPERATE DOMAIN

210 Warm Continental Division
- 212 Laurentian Mixed Forest Province

M210 Warm Continental Division – Mountain Provinces

M212 Adirondack-New England Mixed Forest - Coniferous Forest – Alpine Meadow Province

220 Hot Continental Division
- 221 Eastern Broadleaf Forest (Oceanic) Province
- 222 Eastern Broadleaf Forest (Continental) Province

M220 Hot Continental Division – Mountain Provinces
- M221 Central Appalachian Broadleaf Forest – Coniferous Forest – Meadow Province
- M222 Ozark Broadleaf Forest – Meadow Province

230 Subtropical Division
- 231 Southeastern Mixed Forest Province
- 232 Outer Coastal Plain Mixed Forest Province
- 234 Lower Mississippi Riverine Forest Province

M230 Subtropical Division – Mountain Provinces
- M231 Ouachita Mixed Forest – Meadow Province

M240 Marine Division
- 242 Pacific Lowland Mixed Forest Province

M240 Marine Division – Mountain Provinces
- M242 Cascade Mixed Forest – Coniferous Forest – Alpine Meadow Province

250 Prairie Division
- 251 Prairie Parkland (Temperate) Province
- 255 Prairie Parkland (Subtropical) Province

260 Mediterranean Division
- 261 California Coastal Chaparral Forest and Shrub Province
- 262 California Dry Steppe Province
- 263 California Coastal Steppe, Mixed Forest, and Redwood Forest Province

M260 Mediterranean Division – Mountain Provinces
- M261 Sierran Steppe – Mixed Forest – Coniferous Forest – Alpine Meadow Province
- M262 California Coastal Range Open Woodland-Shrub-Coniferous Forest – Meadow Province

300 DRY DOMAIN

310 Tropical/Subtropical Steppe Division
- 311 Great Plains Steppe and Shrub Province
- 313 Colorado Plateau Semidesert Province
- 315 Southwest Plateau and Plains Dry Steppe and Shrub Province

M310 Tropical/Subtropical Steppe Division – Mountain Provinces
- M313 Arizona – New Mexico Mountains Semidesert – Open Woodland – Coniferous Forest – Alpine

320 Tropical/Subtropical Desert Division
- 321 Chihuahuan Semidesert Province
- 322 American Semidesert and Desert Province

330 Temperate Steppe Division
- 331 Great Plains-Palouse Dry Steppe Province
- 332 Great Plains Steppe Province

M330 Temperate Steppe Division – Mountain Provinces
- M331 Southern Rocky Mountain Steppe – Open Woodland – Coniferous Forest – Alpine Meadow
- M332 Middle Rocky Mountain Steppe – Coniferous Forest – Alpine Meadow Province
- M333 Northern Rocky Mountain Forest Steppe – Coniferous Forest – Alpine Meadow Province
- M334 Black Hills Coniferous Forest Province

340 Temperate Desert Division
- 341 Intermountain Semidesert and Desert Province
- 342 Intermountain Semidesert Province

M340 Temperate Desert Division – Mountain Provinces
- M341 Nevada-Utah Mountains Semidesert – Coniferous Forest – Alpine Meadow Province

400 HUMID TROPICAL DOMAIN

410 Savanna Division
- 411 Everglades Province

M410 Savanna Division – Mountain Provinces
- M411 Puerto Rico Province

420 Rainforest Division

M420 Rainforest Division – Mountain Provinces
- M423 Hawaiian Islands Province

Source: after Bailey (1997)

Figure 2.12. Ecoregions of the United States and photographic archive sites.

Table 2.5. Inventory of photographs of debris at bridge sites with Physiographic Regions and Ecoregions.

Geographic Region	Source	State	Stream	No. of Photos	Physiographic Region	Ecoregion
Pacific Coast	Kevin Flora, Caltrans (Survey)	California (Central and South Coast)	Arroyo Grande	11	24	260
			Hopper Creek	3	24	M260
			Salsipuedes Creek	5	24	M260
		California (Mountain)	N. Fork Deer Creek	4	23	260
		California (North Coast)	Mad River	4	24	260
			Trinity River	1	24	260
			Yager Creek	6	24	260
		California (Central Valley)	Sacramento River	2	24	260
			Stony Creek	6	24	260
			Thomes Creek	4	24	260
	Ayres Associates Inc.	California	Malibu Laguna	1	21	260
			Harris Creek	1	25	M262
			Stony Creek	1	24	260
		Oregon	Shitike Creek	1	24a	242
	Debris Free, Inc. (Mike Collier)	California (North)	Butte Creek	9	23	260
			Navarro River	13	24	260
		California (South)	Callegas Creek	18	24	260
			Santa Clara River	26	24	260
			San Antonio Creek	9	24	260
			Adams Creek	3	24	M260
			Ventura River	29	24	260
		Oregon	Calapooia River	1	23	M240
			North Santiam River	3	23	M240
		Washington	Cowlitz River	7	24	240
			N. Fork Skagit River	6	23	M240
			N. Fork Skagit River	2	23	M240
			S. Fork Skagit River	1	23	M240
			Skykomish River	4	24	240
	Timothy Diehl (1997)	Washington	Quetts River	1	24	M240
West	Debris Free, Inc. (Mike Collier)	Nevada	Carson River	6	22	340
		Utah	Colorado River	4	21	340
			San Rafael River	7	21	340
	Russell Brewer, PE MtDOT (Survey)	Montana	Jefferson River	14	19	M330
			Boulder River	7	19	M331
			St. Regis River	3	19	M332
	Chris Miller, NDOT	Nevada	Carson River	15	22	340
	Tim Ularich, UDOT	Utah	Santa Clara & Virgin Rvs.	11	21	340
	Ayres Associates Inc.	New Mexico	Rio Grande	1	22	310
		Colorado	Bijou Creek	2	13	330
		Idaho	Teton River	1	18	M330
	Various Web Sites (incl. (KSL Channel 5 TV, City of St. George)	Utah	Santa Clara River	8	22	340
			Beaver Dam Creek	4	22	340
			Unknown	11	22	340
Midwest	Debris Free, Inc. (Mike Collier)	Illinois	East Skokie Ditch	3	12	220
			Iroquois River	4	12	250
			Mississippi River	3	12	250
			Mackinaw River	3	12	250
			Unknown	6		
		Indiana	Eel River	8	12	220
			Eel River	4	12	220
			Vermillion River	11	12	220
			Wabash River	3	12	220
		Kansas	Republican River	6	12	250
			Smoky Hill River	34	13	330
		Minnesota	Minnesota River	15	15	250
		Missouri	Unknown	1		
		Ohio	Unknown	5		
		Kentucky	Unknown	2		
		Texas	Clear Fork Brazos Rv.	6	12	310
		Tennessee	Harpeth River	8	11	220
		Oklahoma	Wild Horse River	3	12	250
			North Canadian River	12	12	310

(continued on next page)

Table 2.5. (Continued).

Geographic Region	Source	State	Stream	No. of Photos	Physiographic Region	Ecoregion
Midwest (continued)	Brad Rognlie, P.E. KDOT (Survey)	Kansas	Verdigris River	12	12	250
			Smoky Hill River	73	13	330
			Chikaskia River	1	13	330
			Elm Creek	25	13	330
			Neosho River	19	12	250
			Elk River	25	12	250
			Unknown	6		
	Ayres Associates Inc.	Kansas	Neosho River	38	12	250
			Neosho Rv. (US 400)	28	12	250
			Verdigris River	14	12	250
			Elk River	32	12	250
		Missouri	Florida Creek	1	12	250
		Nebraska	South Platte River	1	12	250
		Indiana	Indian Creek	1	12	220
	MnDOT District 1 (web site photos)	Minnesota	Black River	2	1	212
	USGS (Robinson 2003)	Indiana	White River	6	12	220
	Tim Dunlay, IDOT (Survey)	Iowa	Cedar Creek	3	12	220
		Iowa	E. Nishnabotna River	6	12	250
		Iowa	West Nodaway River	3	12	250
	J. Holmes, MoDOT (Sur)	Missouri	Chariton River	9	12	250
	Ken Foster, MoDOT (Survey)	Missouri	Big Creek	2	12	250
			W. Fork of Grand Rv.	8	12	250
	Larry Cooper, MnDOT (Survey)	Minnesota	Minnesota River	2	12	220
		Minnesota	Mississippi River	2	12	220
	D. Hill, MnDOT (Sur)	Minnesota	S. Branch, Wild Rice Rv.	2	12	250
	B. Callett, ODOT (Sur)	Ohio	Great Miami River	14	12	220
	Allan Bjorklund, WisDOT (Survey)	Wisconsin	Pikes Creek	1	1	210
			Bad River	1	1	210
	J. Conner, TxDOT (Sur)	Texas	Clear Fork, Brazos Rv.	6	12	310
	T. Hertel, TxDOT (Sur)	Texas	Red River	12	12	250
	J. Zirkle, TDOT (Survey)	Tennessee	Harpeth River	13	11	220
	Timothy Diehl (1997)	Tennessee	Harpeth River	2	11	220
		Indiana	White River	1	12	220
East	Debris Free, Inc. (Mike Collier)	North Carolina	Deep River	4	4	230
		Virginia	Appomattox River	4	4	230
			James River	2	3	230
			Meherrin River	3	4	230
			Dan River	2	4	230
			Nottoway River	4	4	230
		West Virginia	Mud River	2	8	220
			Tug River	2	8	220
	NCDOT (web site photo)	North Carolina	Deep River	5	4	230
	Web Site Photos	Tennessee	Coal Creek	4	8	220
South	Debris Free, Inc. (Mike Collier)	South Carolina	Little River	40	4	230
		Florida	Escambia River	2	3	230
		Tennessee	Wolf River	3	3	230
			Jackson District Var.	193	11	220
		Arkansas	St. Francis River	34	3	230
		Louisiana	Amite River	10	3	230
	Ayres Associates Inc.	Louisiana	Bayou Boeuf	1	3	230
		Mississippi	Abiaca Creek	1	3	230
			Jack Creek	2	3	230
			Sykes Creek	1	3	230
	Web Site Photos	Louisiana	Red River Raft	2	3	230
	MDOT Bridge Des. (Sur)	Mississippi	Coles Creek	1	3	230
	Jon Zirkle, TDOT (Sur)	Tennessee	Wolf River	3	3	230
	J. Howell, TxDOT (Sur)	Texas	San Marcos River	1	3	250
	Jon Kilgore, TxDOT (Survey)	Texas	Cocklebur Creek	7	3	310
		Texas	San Antonio River	13	3	250
	Blaine Laywell, TxDOT (Survey)	Texas	Little River	7	3	250
		Texas	Brushy Creek	6	3	250
	H. Schroeder, TxDOT (S)	Texas	Rocky Creek	6	3	250
	Timothy Diehl (1997)	Texas	Brazos River	1	12	310
		Unknown	Unknown	5		

(a) Pacific—Arroyo Grande Creek, CA; (b) Midwest—unknown location, KY; (c) Midwest—Verdigris River, KS; (d) East—Appomattox River, VA; (e) West—Santa Clara River, UT; and (f) South—St. Francis River, AR.

Figure 2.13. Photographs of similar debris geometry from sites in different regions of the United States.

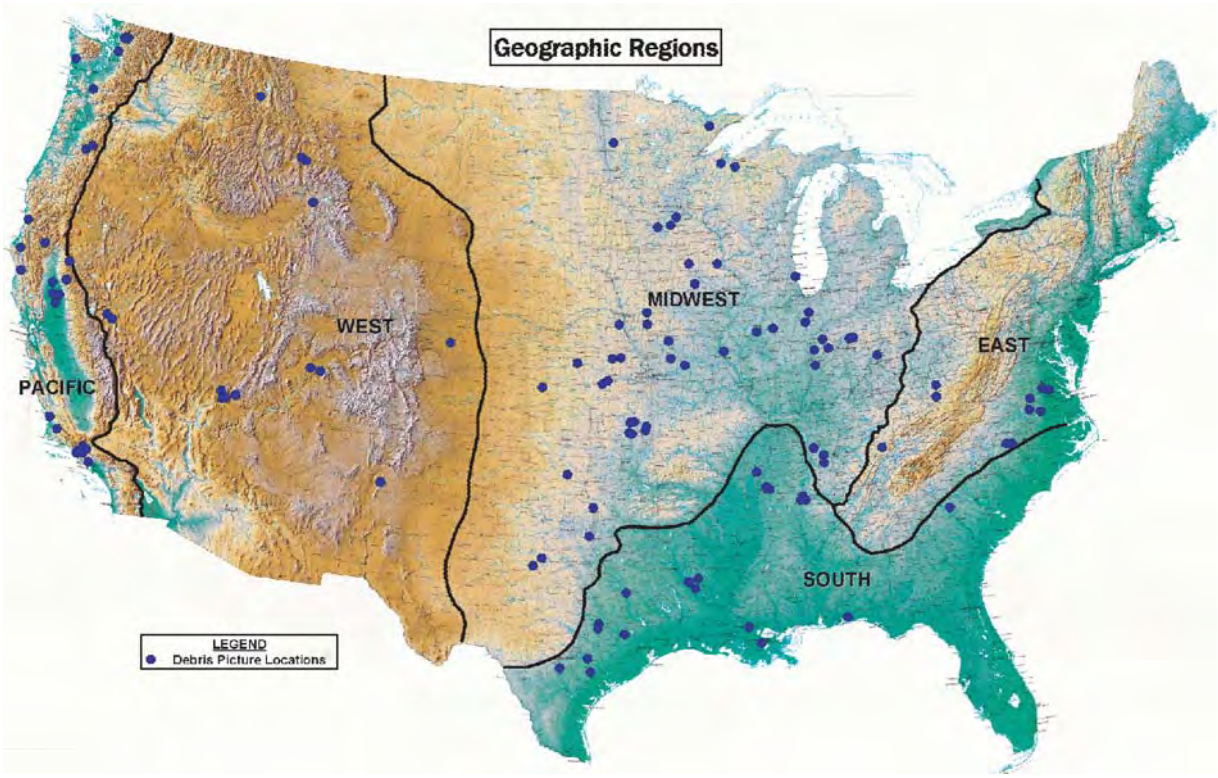

Figure 2.14. General geographic regions of the United States and photographic archive sites.

result of the more arid climate, which produces less widely distributed debris. The paucity of debris sites in the East may be tied to the greater overall stability of the streams and rivers in the region.

2.4 Survey and Site Reconnaissance

2.4.1 Survey

Task 2 required determination of typical debris accumulations by surveying state DOTs and other agencies. Since the late 1970s at least three studies related to debris conducted surveys and/or visited state DOT and other agency bridge sites. FHWA's 1979 study "Debris Problems in the River Environment" by Chang and Shen (1979) presents their literature review, a survey of debris hazards for FHWA regions and state DOTs, a debris hazard map, and a statistical analysis and observations resulting from the survey (see Figure 2.10). Responses from each DOT are compiled in an appendix. Diehl's 1997 study for FHWA compiles detailed information and maps on sources of drift (debris). Diehl also identifies debris field study sites and presents a generalized map of debris sites based on publications and written and oral communications. While Parola et al.'s study for NCHRP (2000) did not include an independent survey, they relied on and interpreted the results of Diehl's work. *NCHRP Report 417: Highway Infrastructure Damage Caused by the 1993 Upper Mississippi River Basin Flooding* (Parola et al. 1998a) contains specific information on debris problems and bridge failures for that region.

Under Task 2, a survey on debris problems was developed and distributed to DOTs and other agencies. At the suggestion of a panelist, a copy of the survey was sent to all panel members. The survey also included a request that recipients forward the survey to others within the agency who may be more knowledgeable on specific topics (e.g., bridge inspectors, maintenance personnel).

The response to the survey was outstanding. Eighty-eight responses representing 30 states and Puerto Rico were received. Appendix B contains a summary of respondents and their corresponding state and agency. Survey responses were entered into a Microsoft® Access database. A copy of the survey and instructions for viewing the survey responses are included in Appendix B. The database is available for download on the NCHRP Project 24-26 web page (http://144.171.11.40/cmsfeed/TRBNetProjectDisplay.asp?ProjectID=725).

The Microsoft® Access relational database is designed to allow rapid screening and organization of a data set based on predetermined attributes of each document. The system allows a user to examine the database using the Structured Query Language (SQL) format to obtain, in this case, a listing of all survey responses meeting the user's query criteria. From this

framework, a sublist of survey responses can be developed. The database allows the user to specify multiple query criteria, so refinements to the sublist can also be readily performed. This approach was used in the evaluation of survey responses in the next section.

2.4.2 Analysis of Survey Responses

Surveys were returned from 88 respondents, representing 30 states including Alaska and Hawaii. In addition, two responses were returned from Puerto Rico; therefore, 84 responses representing the continental United States were received. A breakdown of responses in accordance with the five geographic regions is shown in Table 2.6 and Figure 2.15 (some states may be split into more than one geographic region).

The survey was partitioned into seven categories. Five of the seven categories asked respondents to rank debris-related questions on a scale of 0 to 5 in terms of importance/severity of problem. Responses to all the questions in each of these five categories were examined using the Analysis of Variance (ANOVA) method to determine if statistically significant differences in the responses could be assigned to geographic regions.

In general, responses from different geographic regions tended to be similar in nature, indicating that there are relatively insignificant regional differences regarding the nature of drift accumulations at bridges. Similarly, the types of drift-related problems reported tended to show very few regional differences. In some instances, however, regional differences were found to be statistically significant. A discussion of the responses is provided in the following subsections. The discussion is organized to correspond to the seven categories of the survey.

Part 1. Source Areas that Produce Drift and Debris

Nationwide, respondents reported that unstable streambanks were unquestionably the single most important contributor of drift material that accumulates at bridges. ANOVA testing indicated that at a significance level $\alpha = 0.05$ (95% confidence level), there was no significant difference among the responses gathered from each of the five geographic regions. Watershed management issues were ranked second in importance, and landslides were found to be least important. Table 2.7 provides a summary of the rankings by region, and shows the nationwide results as well, for the continental United States.

Table 2.6. Breakdown of responses to survey.

Geographic Region	Responses	States Represented
Pacific Coast	8	2
West	10	7
Midwest	29	11
South	20	5
East	17	8

Part 2. Bridge Characteristics

Responses to Part 2 were mixed. This part of the survey was designed to determine if certain substructure types were more or less prone to debris-related problems. Nationwide, respondents indicated that pile bents were the substructure type most likely to be affected by debris and that skewed piers were more problematic than piers aligned with the flow.

ANOVA results indicated that some regional differences exist in the mean values of the responses to this section at a significance level $\alpha = 0.05$. Therefore, to discriminate between regions, further analysis was conducted using the two-tailed Student's t-test, also with a specified significance level $\alpha = 0.05$.

Respondents from the East region considered wall-type piers most likely to have debris problems. There was a 95% confidence level that the mean value of the responses from the East was different from all other regions. In contrast, responses from the South region were exactly the opposite: respondents from the South region reported that wall-type piers were the *least* likely to have drift accumulations. In addition, respondents from the East region along with those from the Pacific Coast region considered pile bents with cross bracing to be *least* likely to have problems with debris, at a level that is significantly different compared to the other three regions. From the data provided, it is not possible to tell whether these regional differences are due to certain types of substructures being more prevalent in some regions compared to others. Table 2.8 provides a summary of the rankings by region.

Part 3. Debris Accumulation

This part of the survey asked respondents to rank common elements that are typically used to characterize drift accumulations. Without question, debris clusters on a single pier were considered the most common problem found in all regions of the continental United States. In addition, floating material was reported to be of more concern than submerged material.

In the West region, respondents considered drift buildup between the pier and abutment to be more of a problem than did their counterparts across the rest of the country, to a statistically significant degree. However, respondents from the West region did concur that accumulations at a single pier were still the number one problem.

Although not statistically significant, it is interesting that respondents from the West region, where many streams are

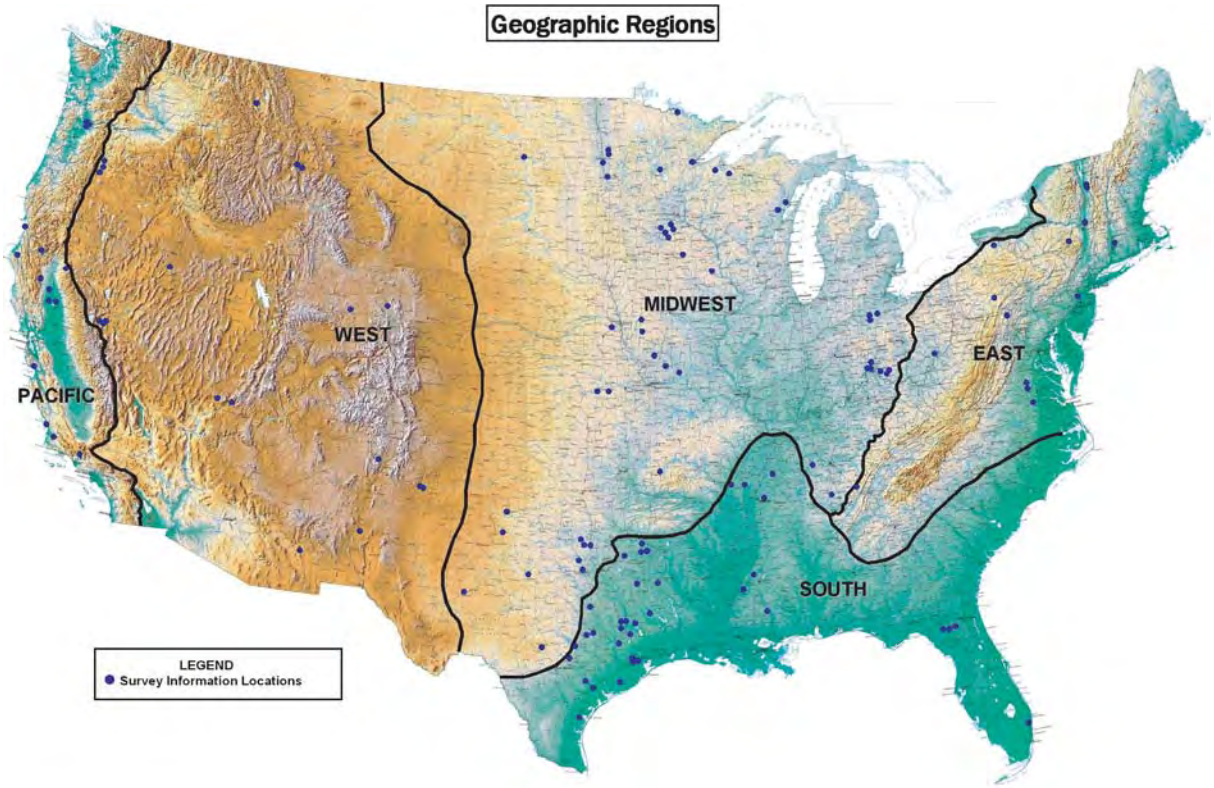

Figure 2.15. General geographic regions of the United States and survey sites.

ephemeral or intermittent, reported that submerged material was equally as common as floating material. This phenomenon may be the result of accumulations that slide to the streambed during the falling limb of a flood event. If not removed, these materials may become incorporated into the streambed sediments and are then submerged by the next event. Table 2.9 provides a summary of the rankings by region.

Part 4. Debris-Related Scour at Bridges

Respondents were asked to consider the nature of the scour problem that is created when drift accumulates at bridges. Some variability was noted in the responses, although there were no statistically significant differences between the five geographic regions.

In general, local scour at the pier where the drift cluster has accumulated was considered the most common scour issue. Bank instability in the vicinity of the bridge, caused by redirection of the flow due to debris blockage, was considered the next most common problem.

Table 2.10 provides a summary of the rankings by region.

Part 5. Maintenance

This part of the survey asked respondents to provide an estimate of the percentage of the average annual maintenance budget that was expended on removing debris, or repairing

Table 2.7. Survey results ranking source areas that produce drift.

Region	Q1. Unstable Streambanks	Q2. Landslides in Watershed	Q3. Watershed Management
Pacific Coast	a	b	c
West	a	c	b
Midwest	a	c	b
South	a	c	b
East	a	c	b
Nationwide	**a**	**c**	**b**

Note: An “a” ranking is highest in importance/severity

Table 2.8. Survey results ranking substructure types that accumulate drift.

Region	Q1. Drilled Shaft Piers	Q2. Pile Bents	Q3. Pile Bents with Cross Bracing	Q4. Pile Cap/ Pile Group	Q5. Wall-Type Pier	Q6. Pier Skewed to Flow Direction
Pacific Coast	e	a	f	b	d	b
West	f	b	c	c	e	a
Midwest	f	a	b	e	d	c
South	c	a	b	e	f	c
East	d	c	f	e	a	b
Nationwide	**f**	**a**	**d**	**e**	**c**	**b**

Note: An "a" ranking is highest in importance/severity

damage caused by debris at bridges. Only about half of the respondents answered this question. Many accompanied their estimate with a comment such as "Unknown," "Minimal," or "After large floods."

Estimates for maintenance costs associated with drift and debris ranged from 0% of the annual maintenance budget up to 15%. One respondent reported that 100% of the annual maintenance budget was spent on debris; this particular response is most certainly an outlier. The most typical responses were "1%" or "less than 1%."

This part of the survey had the most uncertainty in the nature of the responses. This uncertainty may be due in large measure to the sporadic nature of drift recruitment in waterways and its subsequent accumulation at bridges. For example, the magnitude and frequency of flood events over a period of wet years compared to dry years, coupled with the timing of debris removal activities, can create a virtually infinite combination of scenarios for maintenance crews and their budgets as related to debris at bridges.

Part 6. Characteristics of Debris

This part of the survey requested information on the type of drift that triggers the beginning of the process of debris accumulation at an initially clean pier. The intent here was to follow up on concepts developed by previous investigators, such as the "key log" mechanism described by Diehl (1997), as discussed in Section 2.1.

Table 2.9. Survey results ranking characteristics of drift accumulation.

Region	Q1. Cluster on a Single Pier	Q2. Raft Spanning Two or More Piers	Q3. Debris on Superstructure (deck/railing)	Q4. Debris Spanning from Pier to Bank	Q5. Submerged Debris	Q6. Floating Debris
Pacific Coast	a	d	f	c	e	b
West	a	f	f	b	b	b
Midwest	a	c	f	e	c	b
South	a	c	f	e	d	b
East	a	d	d	f	c	b
Nationwide	**a**	**d**	**f**	**e**	**c**	**b**

Note: An "a" ranking is highest in importance/severity

Table 2.10. Survey results ranking scour and stream instability problems caused by accumulated drift.

Region	Q1. Local Scour at One or More Piers	Q2. Local Scour at Abutment(s)	Q3. Contraction Scour Caused by Debris Constriction	Q4. Overtopping of Approach Abutments Due to Flow Blockage	Q5. Streambank Instability Due to Flow Redirection
Pacific Coast	b	e	b	e	a
West	b	d	c	e	a
Midwest	a	b	c	e	d
South	a	d	b	e	b
East	a	c	d	e	b
Nationwide	**a**	**d**	**c**	**e**	**b**

Note: An "a" ranking is highest in importance/severity

Table 2.11. Survey results ranking drift characteristics that initiate the accumulation process.

Region	Q1. Key Log Less Than 25 ft (7.6 m) Long	Q2. Key Log Greater Than 25 ft (7.6 m) but Less Than 75 ft (23 m)	Q3. Key Log Greater Than 75 ft (23 m)	Q4. Primarily Shrubs and Bushy Vegetation	Q5. Construction Debris/Manmade Material
Pacific Coast	a	c	d	b	e
West	b	c	e	a	d
Midwest	a	b	d	c	e
South	a	b	e	c	d
East	a	c	e	b	d
Nationwide	**a**	**c**	**e**	**b**	**d**

Note: An "a" ranking is highest in importance/severity

Respondents reported that key logs less than 25 ft (7.6 m) in length are most often the initiators of drift accumulation. Shrubs and brush-type vegetation was ranked second nationwide, and in fact, respondents from the West ranked shrubs and brushy vegetation as being the most important contributor initiating debris accumulation. This observation was confirmed by t-test at $\alpha = 0.05$ level of significance. Table 2.11 provides a summary of the rankings by region.

Part 7. Potential Sites for Monitoring

Many respondents provided information on specific sites in their regions that exemplified either typical or chronic drift-related problems. In most cases, these respondents also provided supporting information, which usually consisted of bridge plans accompanied by photographs, and sometimes inspection records as well. These types of additional information were noted in the database; when photographs were provided, they were added to the photographic archive.

Respondents in 16 states offered one or more sites for field study, as indicated in Table 2.12.

In particular, Kansas DOT provided detailed information on 21 bridges, primarily located in eastern Kansas, where drift has been a documented and recurring problem. As a result of this information, four sites in southeastern Kansas were selected for a field pilot study (see Section 2.5).

Summary

Based on the 84 surveys received from five regions representing the continental United States, a qualitative interpretation of the survey responses, combined with an analysis of statistical variance of the numerical rankings by region, indicates the following:

- Drift material is derived primarily from unstable stream banks.
- It is most common for drift problems to occur at pile bents compared to other pier configurations. A possible exception may be in the East region, where wall-type piers are reported to have the most problems.
- Large logs are not necessary for drift to begin accumulating at bridge piers. Most commonly, drift accumulation is initiated by logs 25 ft (7.6 m) or less in length or, in the West region, by shrubs and brushy vegetation (e.g., willows, Tamarisk).
- Nationwide, the most common drift configuration at bridges is that of an individual cluster of material on a single pier.
- Drift is most likely to exacerbate scour at bridges by causing either (1) local scour at an individual pier or (2) stream instability due to flow redirection.
- Highway departments typically do not collect cost data associated with drift removal and associated bridge repairs. Maintenance needs are sporadic in nature and are most often related to larger flood events. A reasonable range of cost estimates might be 0.5% to 1% of the total annual maintenance

Table 2.12. Sites offered for field study by region and state.

Geographic Region	Contacts	States Represented
Pacific Coast	3	CA
West	4	AZ, MT, NM, UT
Midwest	11	IA, KS, MN, MO, OH, TN, TX
South	6	LA, TX
East	3	NY, PA, VA

budget in years with little flooding and perhaps 2% to 5% in years that experience one or more significant events.
- Relatively high standard deviation from the mean numerical responses within each region indicate that it is possible to experience the full range of drift-related problems in any given region; however, ranking the responses does provide an indication that some problems or issues are more common than others, as noted in the preceding subsections.

2.5 Site Reconnaissance

2.5.1 Equipment and Preparation

The objectives of the site reconnaissance were to obtain field measurements, photographs, geomorphologic information, channel types and flow patterns, associated bridge and pier geometrics, and historical scour depths, where available. These data were then used with the photographic archive to characterize debris accumulations at bridge piers in the field as a basis for Phase 2 laboratory studies and prediction methods. For the field pilot study in southeastern Kansas, the following equipment resources were used:

- Articulated-arm truck developed under NCHRP Project 21-07 (Schall and Price 2004) to deploy portable scour-monitoring instrumentation (probes, sonar) at bridges under flood flow conditions including high sediment concentrations and floating debris.
- Hydrographic survey equipment and experienced engineer/survey personnel, a Differential Global Positioning System (DGPS), and survey-grade fathometer. The Ayres' hydrographic survey boat is equipped with this equipment as well as a computer and software to accurately and efficiently collect bathymetric data.
- Standard surveying instruments, including a total station and laser range finder.
- Interphase Twinscope™, a forward-scanning sonar using phased array technology, originally tested for NCHRP 21-07.
- Mounting brackets for a single-beam sonar to permit backward-looking and side-looking underwater measurements obtained by the articulated-arm truck.

The goal was to assemble the best available equipment using current technology for the field pilot study to determine the feasibility and accuracy of both above water and underwater measurements of debris characteristics.

2.5.2 Field Pilot Study

In response to the survey (Section 2.4), many DOTs also identified possible field sites. Kansas DOT, in particular, offered support in the field, including identifying sites, coordination for access, and on-site support such as traffic control. As a result, the research team coordinated with Kansas DOT to be in a flood-watch mode ready to mobilize the articulated arm truck and equipment in the mid-April to end of May 2005 time frame for sites along the I-70 corridor in Kansas. Kansas DOT personnel began tracking numerous sites in Kansas and provided a continuous flow of information on debris conditions throughout the state. The field pilot study at bridge sites in southeastern Kansas was scheduled for the period April 25–28, 2005. During the week of April 25, 2005, close coordination was maintained with Kansas DOT personnel for site access, traffic control, etc. A detailed trip report for the field pilot study is included in Appendix C.

2.5.3 Field Pilot Study Results

The field pilot study was an expensive undertaking. Preparation for and completion of the 5-day field pilot study consumed approximately 35% of the Task 2 budget. A substantial effort was required to assemble, recondition, or reconfigure the necessary equipment, particularly the NCHRP 21-07 articulated arm truck. The following paragraphs provide a brief summary of instrument performance during the pilot study.

The **articulated-arm truck,** as modified, performed well. The truck has a telescoping articulated arm, which can be positioned over the side of a bridge deck to determine surface characteristics of a debris pile. The truck is a 1-ton dual wheeled Ford F-450 with a Palfinger articulating knuckle-boom telescoping crane mounted on the bed and chassis. The crane is operated from the flat bed of the truck and is able to take direct measurements from a water level just below the bridge deck downward to about 30 ft (9 m). The crane can be articulated to allow positioning around the perimeter of the debris pile.

A method of recording data around the debris pile and taking topographical shots on the actual debris pile was developed for this study. In this application, a chain of known length was attached to the end of the articulated arm and was positioned at locations on and around the pile to take measurements and provide an above water map of the debris pile. The known length of the chain was added as a "rod height" to the vertical position.

Another method that was developed for the field study used the same chain method as just described, but a prism cluster was hung from the chain. The prism was shot with a total station at each position, and the debris pile was mapped using the total station and data logger for positioning of the end of the chain. This procedure provided another relatively accurate method of mapping the debris pile in relation to the bridge.

For underwater measurements of debris, separate streamlined heads were built to house a wireless sonar. Instead of the

sonar having to be mounted to point straight down, the side-looking or backward-looking heads allow the transducer to be mounted to look horizontally under the debris pile. The head was attached to the articulating arm and positioned around the pile in the same manner as the downward-pointing sonar.

Computer software for sonar measurements with the crane allowed point measurements or continuous recording. The user can select from two data collection modes: Point Data collects one data point at a specific location; Continuous Recording collects data at 1-second intervals continuously as the articulating arm is moved around the debris pile.

The **hydrographic survey boat** was used for documenting geomorphic conditions, such as bank stability, debris source areas, overall channel type, and flow patterns. The boat is a 16 ft flat bottom Jon Boat with a 50 hp jet drive outboard motor. The jet motor is very maneuverable and allows the boat to be operated in shallow water without risk of damaging a standard prop. The boat and motor can be operated in less than 1 ft (0.3 m) of water.

A **Leica total station** with data logger was used to measure horizontal and vertical angles of the debris pile from the bank. The total station displays a digital readout of the angles from the instrument to the points being surveyed. The total station was also used to take electronic distance measurements (EDM) of the bridge deck and adjacent bank line.

Similarly, a **laser range finder** was used to measure distance, height, and width of objects. The range finder gives accurate distances of an object up to 2,000 ft (610 m) without a prism. It also has a built in inclinometer to measure vertical angles.

The **Interphase Twinscope™,** used as a handheld measurement system, was tested. The Twinscope™ is a continuously scanning sonar that displays a 90° underwater view in front of the sonar. The Twinscope™ is designed to be mounted to the hull of a boat and has been used successfully in ocean applications. In this application, the instrumentation was lowered into the water and pointed in the direction of the debris pile to get an underwater view of the debris pile shape. The results were inconclusive. Echos, scatter, and interference in a shallow water environment rendered the interpretation of results speculative, at best.

2.5.4 Recommendations

The field pilot study to southeastern Kansas provided a reality check on the cost and technical limitations, primarily instrumentation, of obtaining debris-related data in the field. It was concluded that debris accumulations are highly variable in the field and depend not only on watershed conditions, but also on bridge type and geometry. The temporal variability of debris accumulations in relation to the flow hydrograph adds to this complexity. Thus, no two debris clusters are alike and determining or classifying "typical" debris configurations based on limited field data would be difficult.

A variety of instruments were deployed during the field pilot study, representing the range of technology currently available, with mixed results. While surveying and measuring the surface expression (above water) of a debris cluster is easily accomplished, obtaining detailed information on the underwater characteristics of debris is extremely difficult and time consuming, and the results are inconclusive.

During the Task 1 literature review and the Task 2 survey, an extensive archive of photographs of debris at bridge piers was assembled (see Section 2.2 and Appendix A). The original effort to obtain these photographs extended over many years and covered the Pacific Coast, Western, Midwestern, Eastern, and Southern regions of the country. This exceptional collection of debris photographs provides a resource that was not available when the original work plan was developed (see Section 1.2.2). **Consequently, the NCHRP 24-26 panel concurred with the research team that additional field work should not be conducted for this study. Rather, resources should be reallocated to additional analysis of the photographic archive of debris for interpreting regional characteristics of debris (see Section 2.3) and characterizing debris accumulations for laboratory testing (see Section 3.5).**

CHAPTER 3

Guidelines, Testing, Appraisal, and Results

3.1 Introduction

This chapter presents guidelines for assessing the potential for debris production and accumulation at a given bridge site, an overview of laboratory testing of a variety of debris configurations on model bridge piers, and an appraisal of the results. The summary of the current state of practice in Chapter 2 is combined with the testing results to provide an improved methodology for quantifying the depth and extent of scour at bridge piers resulting from the accumulation of organic debris.

As an extension of the original work by Diehl (1997) for the FHWA, guidelines and flowcharts are developed for estimating the potential for debris production and delivery from the contributing watershed of a selected bridge, and the potential for accumulation on individual bridge elements. The application of the guidelines is illustrated by a case study of a debris-prone bridge on the South Platte River in Colorado. The case study is summarized in this chapter and presented in detail in Appendix D. The case study introduces and illustrates the use of field data sheets for evaluating the potential for debris production and delivery from a given watershed.

As a basis for laboratory testing, the photographic archive introduced in Chapter 2 (see also Appendix A), the field pilot study of debris sites in Kansas (see Appendix C), and the South Platte River case study (see Appendix D) are examined to develop a limited number of debris shapes that would represent the maximum number of configurations found in the field. Simplified, yet realistic, shapes that can be constructed and replicated with a reasonable range of geometric variables were needed for laboratory testing. Rectangular and triangular shapes with varying planform and profile dimensions were selected to represent prototype debris accumulations. To account for additional variables thought to be relevant to debris clusters in the field, a method to simulate both the porosity and roughness of the clusters was developed.

The laboratory testing program is described in detail, including the flume and model piers, instrumentation for data acquisition, and the materials used to fabricate the debris clusters. Baseline tests are described and results are compared with several pier scour prediction equations. Tests with the various debris shapes are summarized and results are illustrated with tabular data, photographs, and post-test contour plots.

An appraisal of testing results supports the development of an algorithm for predicting the scour anticipated at bridge piers from debris accumulations with rectangular and triangular planforms and varying length, width, and depth geometries. An application methodology is presented to integrate the debris accumulation guidelines with the equation for predicting scour at bridge piers with debris loading using the South Platte River case study as an example.

Finally, guidelines for inspection, monitoring, and maintenance for debris-prone bridges are discussed. An implementation plan for the results of this research completes this chapter. Conclusions from this research and recommendations for future research are presented in Chapter 4.

3.2 Guidelines for Assessing Debris Production, Transport Delivery, and Accumulation Potential

This section provides guidelines for assessing the potential for debris production and accumulation at a given bridge site (Tasks 3 and 6 of the research work plan). These guidelines expand on those originally presented by Diehl (1997).

The following guidelines should be reviewed prior to a site evaluation and can be used to assist in the completion of the Field Data Sheets developed for this project. The Field Data Sheets (Appendix D, Part 1) have been developed to assist bridge inspectors in collecting and recording data and information that can be used in assessing the woody debris production, transport, delivery, and accumulation potential for a bridge site. The Field Data Sheets also contain brief descriptions for each of

the data sheet entries and the flowcharts that are included within the guidelines.

A considerable amount of information can be acquired prior to a site evaluation. Much of this information can be obtained from existing maps, aerial photographs, surveys, and DOT bridge records. Sections A and B of the Field Data Sheets (Lines 2-35) are used to record or identify the availability of this information. Section C of the Field Data Sheets is used to document specific information and data for a bridge site and the reach upstream that is acquired during a site visit and field examination for use in assessing the potential for debris production and accumulation at the bridge site.

As originally suggested by Diehl (1997) and modified here, there are three major phases for assessing the potential for debris production and accumulation at a bridge site: (1) estimate the potential for debris production and delivery; (2) estimate the potential for debris accumulation on individual bridge elements; and, as modified from Diehl, (3) delineate bridge segments or zones that have the same accumulation potential ratings. These major phases and the associated tasks and subtasks that are required to assess the potential for debris production and accumulation at a bridge site provide the basis for the following guidelines and are described in Table 3.1. There may be direct or indirect evidence for the degree of debris production and delivery potential at any given bridge site; however, direct evidence should be evaluated first and given greater weight than indirect evidence.

3.2.1 Phase 1: Evaluate Potential for Debris Production and Delivery

Under this phase, the potential for a stream to produce and deliver debris to a bridge site will be evaluated, the likely maximum dimensions of individual logs will be estimated, and the site will be divided among location categories that define the local potential for debris accumulation. The location categories reflect local conditions and are not dependent on bridge design.

Potential for Debris Production (Task 1a)

Observations of the channel upstream of a bridge site as well as observations and knowledge of the physical conditions of the watershed upstream of the site and nearby watersheds can assist in determining the potential for debris production and delivery at a given site. A lack of debris at a bridge site does not indicate that there is a low potential for the production and delivery of debris at a site. Even if debris is relatively sparse at a particular site, infrequent or catastrophic events may produce significant debris available for transport to the site. Thus, data and information collected under Items B1a, B1b, C1b, and C1c of the Field Data Sheets (Appendix D, Part 1) can be used to assist in estimating the potential for debris production upstream of a bridge site. Figure 3.1 provides a flowchart for use in evaluating the potential for debris production upstream of a bridge site.

Table 3.1. Major phases, tasks, and subtasks for assessing the potential for debris production and accumulation at a bridge.

Phase	Task	Subtask
1. Evaluate potential for debris production and delivery.	a. Evaluate potential for debris production upstream of the bridge site.	• Direct evidence • Indirect evidence
	b. Evaluate the potential for debris delivery to the site.	• Direct evidence • Indirect evidence
	c. Estimate the size of the largest debris that could be delivered to the site.	• Channel width and depth • Maximum design log length
	d. Assign location categories to all parts of the bridge crossing.	• Sheltered • Bank/flood plain • In the channel (bend or straight reach) • In the path (bend or straight reach)
2. Evaluate the potential for debris accumulation on individual elements.	a. Assign bridge structure characteristics to all submerged parts of the bridge.	• Horizontal and vertical gaps between fixed bridge elements • Pier and substructure in flow field
	b. Determine accumulation potential for each part of the bridge.	• Assume maximum size of potential accumulations
3. Delineate bridge segments that have the same accumulation potential ratings.	a. Identify elements with accumulation potential ratings of low, medium, high, and chronic.	• Delineate zones of low, medium, high, and chronic potential where adjacent elements have the same rating

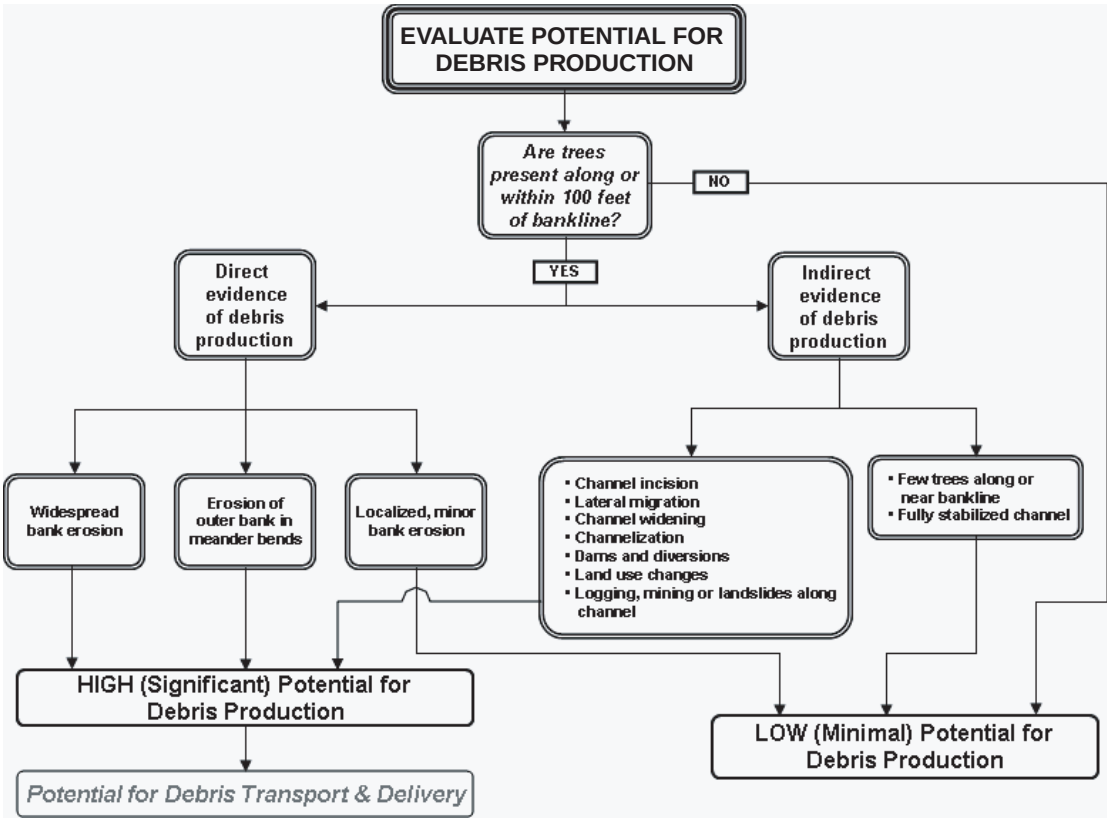

Figure 3.1. Flowchart for evaluating debris production potential.

Direct Evidence. The primary method of debris production is through bank erosion that results in woody vegetation being introduced into the channel. Therefore, existing bank erosion along forested streams provides the most direct evidence of the potential for debris production. Bank erosion may be extensive and severe or localized and minor. Extensive and severe bank erosion may be evident along straight and meandering reaches of streams that are currently unstable and undergoing incision or downcutting and/or widening. Moderate bank erosion may occur along the outer banks of actively migrating meander bends and in reaches where bars are well developed such that the bars, and any trapped debris, cause flow to impinge directly on the bank. Localized, minor bank erosion may occur at any location and is generally insufficient in magnitude to contribute a significant amount of debris.

The most direct evidence for a high potential for debris production is the presence or absence and density of a riparian forest or corridor along a stream channel upstream of a bridge site. For a river or stream corridor to produce debris that may be available for transport, the channel must contain a forested area or trees along its banks. Streams with cleared banks or sparse or intermittent riparian zones will provide little debris to a channel unless the channel has become unstable because of land use practices.

Of course, the upstream channel must have trees in proximity to the channel banks [generally within 100 ft (30 m)] for their introduction through bank erosion to occur. Trees that are leaning over the water at the bankline, incorporated in failed bank sediments at the bank toe, or lying in the water are direct indicators of ongoing bank failure and potentially high debris production.

Debris may not be present at a bridge site or in view from the site, but debris may be stored in significant quantities at sites in the upstream channel. These storage areas may not have had sufficient flows to mobilize the stored debris. Sites of debris storage include at the heads of flow splits, on bars and islands, and along the banks, especially along the outer banks of actively migrating meander bends.

Rare, large magnitude or catastrophic events such as ice storms, hurricanes, tornados, microbursts or wind shear, and extreme floods can produce considerable amounts of deadfall available for introduction into a channel. If overbank flooding occurs regularly, deadfall in proximity to the channel may be introduced to the channel as large rafts if the path of movement from the flood plain to the channel is relatively unobstructed.

Indirect Evidence. Indirect evidence for a high potential for debris production includes historic or ongoing channel changes that affect channel stability and ultimately bank

erosion, which is the primary method of debris introduction to a channel. These channel changes include the following:

- Downcutting or incision
- Lateral migration
- Channel widening
- Channelization
- Dams and diversions
- Widespread timber harvesting in the basin
- Existing or potential changes in land use practices

Some of the general upstream watershed characteristics that may have an indirect impact on debris production are documented under Item B1a, Lines 8–14, of the Field Data Sheets (Appendix D, Part 1).

Indirect evidence for a low potential for debris production includes the following:

- Woody vegetation growing along the channel and on the slopes leading down to the stream is absent or scarce.
- Channel may be fully stabilized (both vertically and laterally) and is unlikely to undergo significant change.

Potential for Debris Transport and Delivery (Task 1b)

The potential for debris transport and delivery is obviously dependent on the availability of debris and the channel geometry. If debris is readily available, the potential for transport is dependent on the size of the debris relative to the channel width, depth, and planform. Potential for transport is high if the channel width and depth exceed the maximum design log length and diameter. If there is a possibility that the width and depth of the upstream channel could increase in the future, the potential dimensions should be accounted for as well. Yet, even if the channel can accommodate the transport of debris, the channel planform may restrict delivery of the debris to the bridge site. Upstream channel geometry, including average width and depth, and flood plain characteristics are recorded under Item B1b, Lines 15–26, of the Field Data Sheets (Appendix D, Part 1). Figure 3.2 provides a flowchart for determining the potential for debris transport and delivery to a bridge site.

Direct Evidence. Observations of existing debris in the channel and at a site provide the most direct evidence for assessing the potential for debris transport and delivery to a site. Direct evidence for a high potential for debris delivery to a bridge site may include the following observations:

- Documented chronic or frequent debris accumulations at one or more bridges in the area
- Abundant debris stored in the channel and along the banks
- Ongoing or prior need for debris removal from the channel

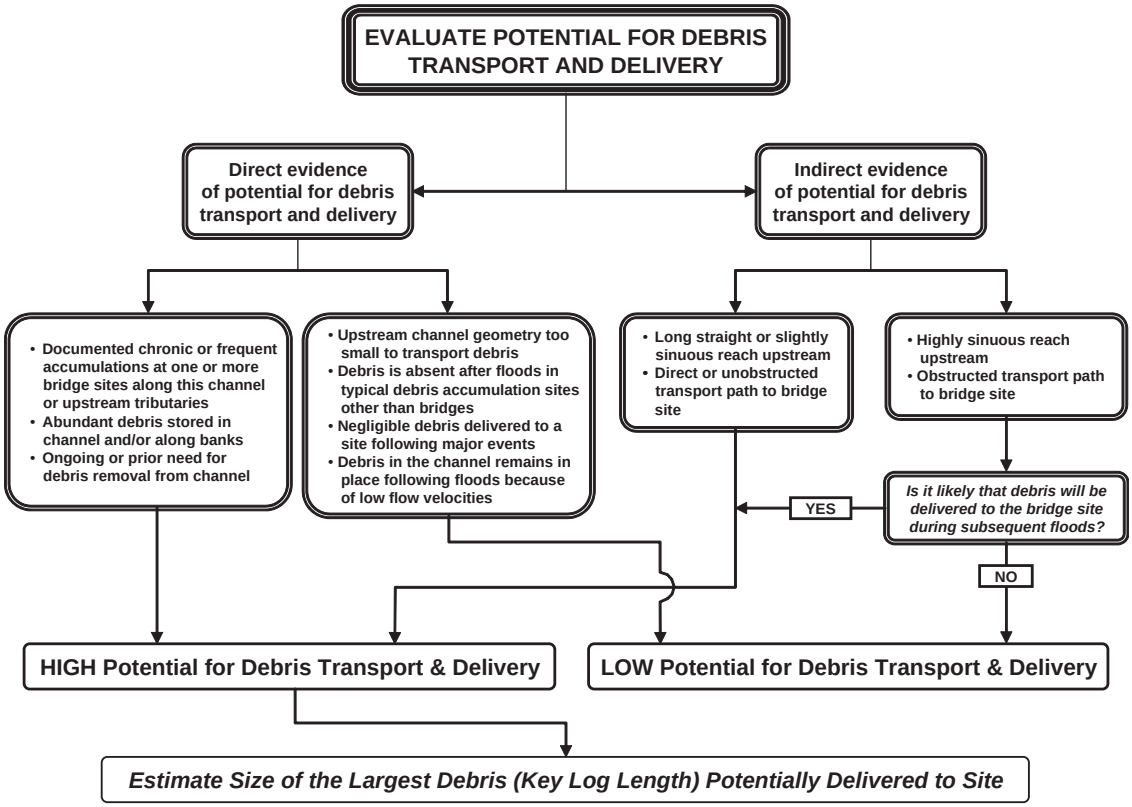

Figure 3.2. Flowchart for determining the potential for debris transport and delivery.

Direct evidence of a low potential for debris delivery includes the following:

- The upstream channel is narrower and/or shallower during flood flows than most of the debris produced.
- Debris is absent after floods in typical debris accumulation sites other than bridges (e.g., on bars and along the outer bank of meander bends).
- Negligible debris is delivered to a site following large floods or other catastrophic events.
- Debris in the channel remains in place following floods because of low flow velocities.

Indirect Evidence. Long, straight reaches upstream of a bridge site will provide the greatest potential for debris delivery. The thalweg of a straight channel is generally near the centerline and debris transported in the channel will generally follow that path. Some debris may become lodged along the banks or on bars as it moves downstream. Streams or rivers with low sinuosity or long, high radius bends can also provide a high potential for debris delivery to a bridge site because the flood path, and consequently the debris path, will generally follow a relatively straight down valley path (Figure 3.3).

On forest-lined streams or rivers, as channel sinuosity increases and bend radius decreases, the potential for debris transport and delivery during any given flood decreases because debris is generally transported along the thalweg. Consequently, debris in highly sinuous, well-forested rivers or streams will not be transported far from its source area during any given event and is often deposited along or on top of the outer bank or on the point bar of the next downstream bend. However, some of this debris may eventually be moved downstream to a bridge site during subsequent flows.

Streams with actively migrating meander bends may be fairly sinuous, but can produce substantially more debris than less sinuous or relatively straight streams because of the bank erosion associated with lateral migration processes. Yet because of the planform geometry of forested meandering streams, delivery of debris on highly sinuous streams may take longer to reach a bridge in comparison to a low sinuosity or straight channel.

Therefore, fairly sinuous streams with evident bend migration or bank erosion and significant debris production can be considered to have a moderate to high delivery potential, depending on existing conditions and sound engineering judgment.

Bankline characteristics, including evidence of vertical and lateral instability, active bank erosion, and active meander migration are documented under Item C1b, Lines 64–87 of the Field Data Sheets (Appendix D, Part 1). The general upstream riparian corridor characteristics are documented under Item C1c, Lines 88–95, of the Field Data Sheets (Appendix D, Part 1). This information can be used in conjunction with the flowcharts shown in Figures 3.1 and 3.2 to estimate the potential for debris production, transport, and delivery (Lines 96 and 97, Field Data Sheets, Appendix D, Part 1).

Estimated Size of the Largest Debris Potentially Delivered to Site (Task 1c)

The potential for a channel to deliver debris to a site will be controlled by the ability of the stream to transport it. Existing or future channel dimensions, particularly width, upstream of a site determine the size of debris that can be transported and influences the potential size of accumulations.

The maximum design (or key) log length (Figure 3.4) is estimated either by examining the largest existing logs in the channel or on the basis of the channel width upstream of the site as measured at inflection points between bends (see Figure 2.6). Diehl (1997) states that the maximum log length on wide channels for much of the United States is about 80 ft (24 m) and that channels less than 40 ft (12 m) wide transport logs with lengths equal to or less than the upstream channel width.

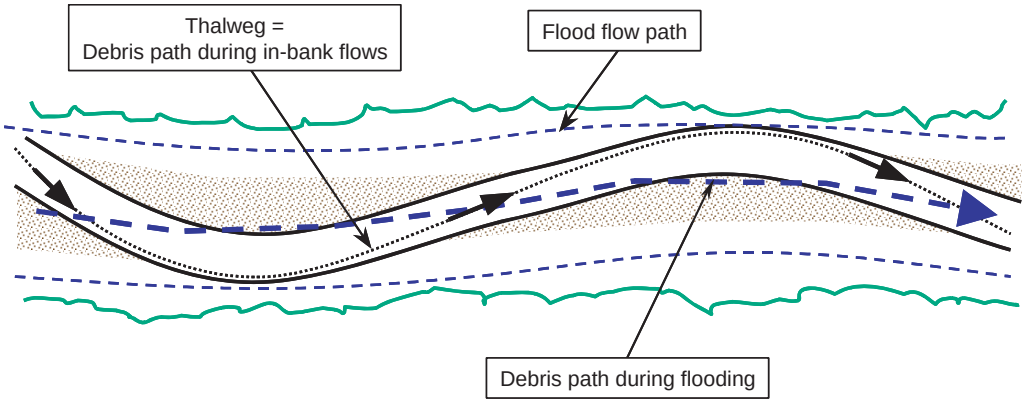

Figure 3.3. Hypothetical debris and flood flow paths during in-bank and out-of-bank flood flows for a low sinuosity channel.

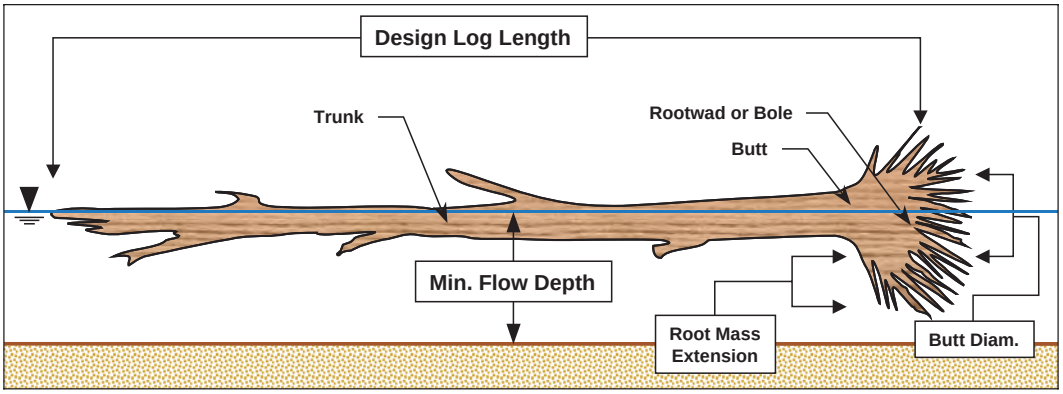

Figure 3.4. Schematic of design (or key) log length, butt diameter, and root mass extension.

In the eastern United States, channels that are 40 to 200 ft (12 to 60 m) wide transport logs with an estimated design (or key) log length of 30 ft (9 m) plus one quarter of the channel width. Depth is important as well; the depth sufficient to float logs (Figure 3.4) is the diameter of the butt of the tree plus the distance the root mass extends out from the butt, or approximately 3% to 5% of the estimated log length (Diehl 1997). Diehl also indicates that the length of transported logs with attached rootwads rarely exceeds about 30 times the maximum flow depth. The sizes of existing debris and their key log dimensions for a given site are recorded under Item C1d, Lines 101–119 of the Field Data Sheets (Appendix D, Part 1).

Location Categories for Debris Accumulation at a Bridge Crossing (Task 1d)

The delivery and accumulation of debris at a bridge crossing is generally localized. Some areas of the bridge crossing may be free of debris while other areas may receive the bulk of the debris transported to a site. Therefore, each span and pier on a bridge should be evaluated for potential debris accumulation relative to the debris delivery path(s). Figure 3.5 provides the general location categories for a meander bend and a straight reach relative to the local debris delivery path. Figure 3.6 provides a flowchart for determining the location categories.

Sheltered by Upstream Flood Plain Forest. A location that can be considered "sheltered" may lie just downstream of a flood plain forest, heavily wooded area, or other major obstruction that can trap transported debris and prevent its delivery to the site. This category may be used where the spacing between trees is much narrower than the average tree height and the tree-lined corridor or zone width perpendicular to flow is more than a single or double row of trees. If a forested corridor or zone is likely to be cleared, select a location category that assumes the location is unsheltered.

Flood Plain and Top of Bank. The flood plain and the area along the top of bank are grouped together in a single location category for the purposes of estimating the local potential for debris delivery. This location category is assigned to areas that are currently clear of trees or are currently forested, but are likely to be cleared in the future. This location category includes any area outside the channel that can be inundated in a design flood event to a depth sufficient to transport debris.

Channel. Debris can be transported anywhere in the channel as long as flow depth and channel width are sufficient to transport the debris. Piers on the bank slope or at the bank toe are just as likely to collect debris as those in the channel, especially if they are located at the outer bank of a meander bend. In many cases, piers located on the slope of the bank or at the bank toe can collect sufficient debris to cause severe scour and erosion of the bank. Diehl (1997) suggests that the "channel" location category contain the area between the bases of the banks except where judgment dictates that the bank slopes should be included in the "channel" category. However, most debris will be transported during events that have flow levels well above the base of the bank, especially in more temperate regions where flows that fill much of the channel are common. Even in arid regions where flood events are flashy and are generally of substantial magnitude, most flows that are able to transport debris often fill much of the channel well above the base of the bank. In many cases, debris can collect on the lower portions of meander bend point bars well below the top of the bank. Therefore, it is recommended that the "channel" location category include the slopes as well as the basal area of the banks and that the "flood plain" category only extend to the top of the bank.

Path of Concentrated Debris Transport. As indicated by Diehl (1997), secondary circulation currents converge at the surface, causing floating debris to be transported along a rela-

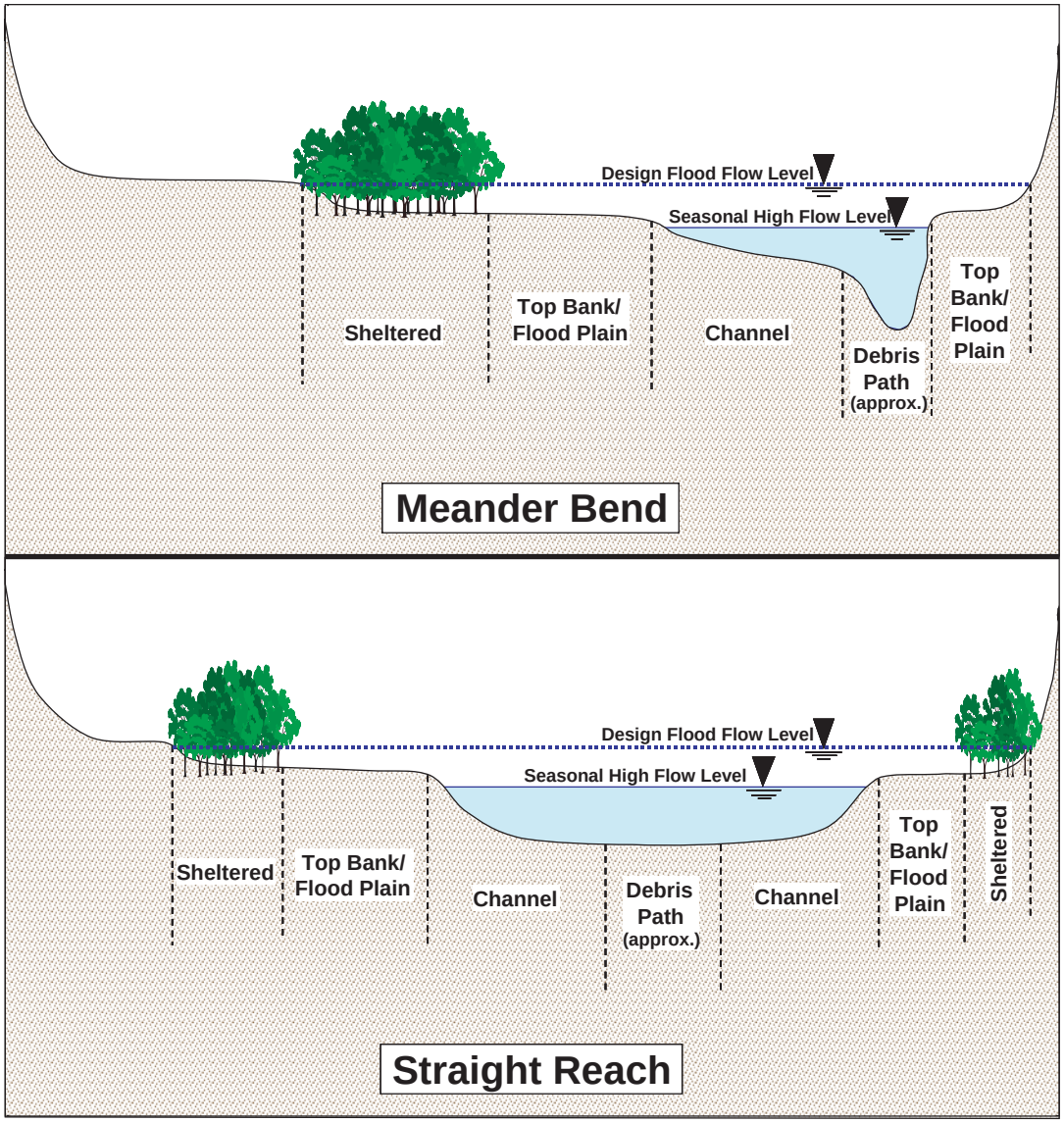

Figure 3.5. Location categories relative to local debris delivery in bends and straight reaches.

tively confined path within the channel. This path is closely related to the thalweg. On straight channels this path is generally in the middle of the channel, whereas in meander bends the path is close to the outer bank. However, the transport path during flooding can be significantly different from the path under less than flood flow conditions (see Figure 3.3). Therefore, it is recommended that debris transport during a range of flow conditions should be observed in order to evaluate the debris paths at the bridge crossing. If direct observations of the transport path of debris are not practical or are impossible to obtain, then the location category should be based on the channel characteristics and the probable flow paths under high and low flow conditions as described above. In some cases, where flood flows are out-of-bank, the top of bank and flood plain may be in the debris path, especially along the outside bank of a meander bend. In these instances, these areas may have a "debris path" location category as well.

The shape and location of existing debris accumulations on particular elements of an existing bridge are recorded under Item C1d, Lines 101–119 of the Field Data Sheets (Appendix D, Part 1). This information along with previously collected information can be used to estimate the debris accumulation potential for various elements of an existing bridge (Item C1d, Lines 120–122, Field Data Sheets, Appendix D, Part 1). For new bridges, it may be necessary to estimate the potential for debris accumulation on individual bridge elements based on their location categories as described under

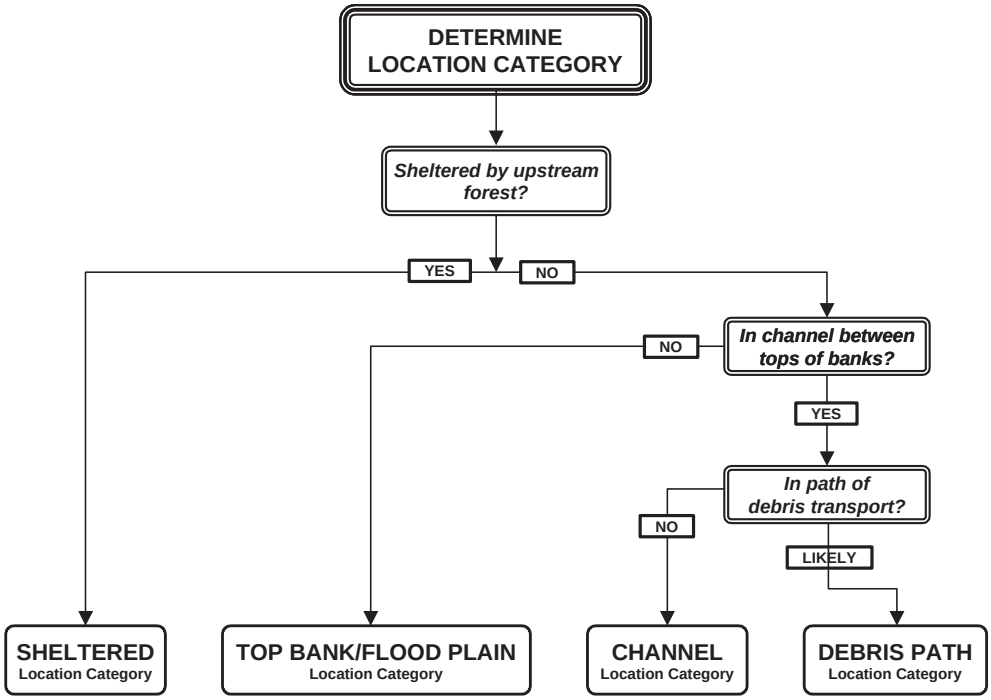

Figure 3.6. Flowchart for determining location category along bridge crossing.

Phase 2. Also, debris accumulation problems for an existing bridge can be tied to the location categories of those bridge elements identified under Phase 2 where debris accumulates, and this information could then be used to evaluate potential countermeasures and/or develop appropriate maintenance programs.

3.2.2 Phase 2: Estimate Potential for Debris Accumulation on Individual Bridge Elements

Bridge characteristics can have a significant influence on the potential accumulation of debris. The design of the substructure, piers, abutments, span widths, and bridge and pier skew all influence the location and degree of debris accumulation at the bridge. The following information along with information previously collected for the Field Data Sheets (Appendix D, Part 1) can be used to estimate the debris accumulation potential for various elements and their location categories for new and existing bridges (Item C1d, Lines 120–122, Field Data Sheets, Appendix D, Part 1).

Assign Bridge Structure Characteristics to All Submerged Parts of Bridge (Task 2a)

For existing bridges, the current location and configuration of individual components should guide the selection of values for these characteristics. For new bridges, alternative locations and designs should be developed during the design process to assess how they affect the relative potential for debris accumulation. Diehl (1997) recommends the following procedure for each design under evaluation:

1. Assign each of the following to one of the location categories as described previously:
   - Pier
   - Gap between fixed elements of the bridge crossing
   - Abutment base
   - Section of substructure where low steel is wetted by the design flood
2. Determine whether the effective width of each gap exceeds the design log length for the site.
3. Determine whether each pier or substructure section immersed in the design flood includes apertures that carry flow.

Pier and Bridge Substructure Characteristics. The characteristics of the bridge piers and substructure where they are exposed to floating debris will determine the debris-trapping potential of these features. Piers and substructure elements with narrow apertures that can pass flow during high flows are considerably more likely to trap debris than single piers or solid wall piers. These elements can include pile bents with aligned or battered piles, piers founded on footings or caps over multiple exposed pilings at or near the water surface, or even piers protected by dolphins or fenders. The skew of the flow align-

ment to these types of piers under various flow conditions can significantly influence their debris-trapping potential. Where flow is skewed, the apertures may trap debris that would normally pass between the piers if they were aligned to flow. In these cases, initiation of the debris accumulation may occur beneath the bridge well back from the upstream end of the pier or pile bent. A skewed flow alignment can produce debris accumulations that may be very large and may extend well under the bridge where access may be limited.

Open trusses and open parapets with pillars and rails are also likely to trap debris if they are located at or below the water surface. Structural arrangements that include pier caps, beams, and deck create openings that can pass flow and trap debris. Pile bents that include bracing also contain openings that can trap debris.

Wide Gaps Between Fixed Elements of the Bridge Crossing. New or existing bridges will include one or more gaps through which debris must pass. Gaps include the horizontal openings between support elements of the bridge, the banks, and/or the abutments. If submergence of the substructure is likely to occur under the design discharge, the height of vertical openings between the substructure and the streambed or flood plain should also be evaluated. The effective width and height of these gaps need to be estimated with regard to debris trapping potential.

Span or Horizontal Gaps. Horizontal gaps or spans are created by openings between the vertical support elements of the bridge as well as the stream banks and the abutments. These areas can become potential sites for debris entrapment and accumulation. Once a log or raft has become lodged across the gap at the surface, additional debris can become trapped across the gap and the rate of accumulation can increase.

A horizontal gap or span should be assigned to the most debris-prone location category occupied by fixed elements that define the gap (Diehl 1997). Therefore, a pier-to-bank or pier-to-abutment gap should have the same location category as the pier. If one of the fixed elements is sheltered and the other is not, the gap should be considered unsheltered.

If the horizontal gaps or spans are narrower than the longest debris transported by the stream, then the potential for debris accumulation at the bridge site can be high. Under some circumstances, the potential for a span blockage may be high even though the span may exceed the maximum log length. For existing bridges, this situation may be evident where large identifiable debris accumulations on adjacent piers have induced a span accumulation (Figures 3.7 and 3.8). For new bridges where one or more piers will be located in the channel and the potential for debris accumulation on the piers is determined to be high then the potential for gap spanning debris accumulations can also be high, especially where large debris accumulations on piers can induce span accumulations. This holds true for pier-to-bank and pier-to-abutment gaps as well.

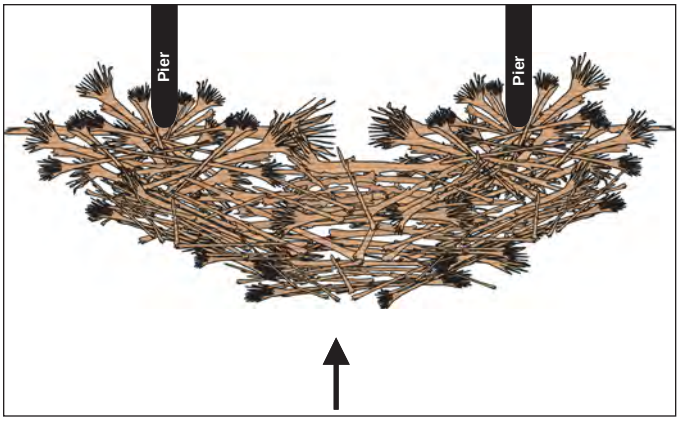

Figure 3.7. Schematic of span debris accumulation induced by adjacent pier accumulations.

Vertical Gaps. Vertical gaps are created when high flows reach the bridge substructure and debris becomes trapped between the structural elements below the bridge deck and the flood plain or streambed. Because most debris is transported at the surface, when pieces hit the substructure, most rotate to the side and are either trapped against the substructure elements at the surface or swept under the substructure. Where debris intersects the bridge structure endwise, the upstream end of the debris, if it is sufficiently long enough, may rotate downward and become wedged in the streambed or flood plain. Hammerhead or similar type piers may also act to force

Source: Mike Collier, Debris Free, Inc.

Figure 3.8. View of gap-spanning debris accumulation induced by adjacent pier on the Harpeth River in Tennessee.

one end of the debris downward toward the streambed or flood plain, which can cause the other end to project upward into the substructure as shown in Figure 3.9. For this reason, the height of the vertical gap (i.e., vertical gap width) along the bridge should be evaluated relative to the typical log length and location category. Debris that is significantly shorter than the design log length can become trapped between the bridge substructure and the ground, so a range of typical log lengths should be evaluated with regard to the vertical gap width, especially when evaluating the vertical gaps in flood plain areas. Because the width of the vertical gap is defined by the height of the gap between the low steel of the bridge substructure and the streambed or the flood plain and may vary along the gap as well as along the bridge, a vertical gap should, therefore, be assigned to the most debris-prone location category occupied by the fixed elements that define the gap (Diehl 1997).

Determine Potential for Accumulation by Location and Type (Task 2b)

The potential for debris accumulation is determined separately for each pier, each section of the submerged substructure, and each horizontal/vertical gap/span between fixed elements of the bridge following determination of the potential for delivery of debris to the site, assignment of location categories, and identification of other bridge characteristics. It should be noted that the estimation of the potential for debris delivery and accumulation does not address the potential for or likely size of debris accumulations at a given site. Depending on log dimensions, flow depth, and the number and proximity of gaps/spans and piers affected, debris accumulations can grow to maximum sizes both vertically and horizontally (Diehl 1997). Diehl suggests that estimates of debris accumulation sizes should be conservative. Therefore, he recommends assuming that the debris accumulation will extend from the water surface to the streambed, that an accumulation on a single pier will have a width equal to the design (or key) log length over its full depth, and that an accumulation across two or more piers will extend laterally half the design log length beyond the piers. Because the maximum size of debris accumulations on substructure cannot be evaluated, Diehl (1997) recommends assuming that the apertures in the bridge substructure will be completely closed by debris and that the entire vertical gap between the substructure and the streambed or flood plain could ultimately be closed by debris.

Source: Mike Collier, Debris Free, Inc.

Figure 3.9. View of large debris wedged between bridge substructure and channel bed on Carson River in Nevada.

Potential for Debris Accumulation at Each Pier and Substructure Section. The potential for debris to accumulate on each pier and section of the substructure is determined using the flowchart shown in Figure 3.10. Once the potential for delivery of debris is estimated for the entire bridge site, the location category and the presence or absence of narrow apertures that can pass flow are evaluated for each pier and section of the substructure.

Potential for Debris Accumulation Across a Span or Vertical Gap. The potential for debris to span an individual gap between fixed elements of the bridge opening is determined using the flowchart shown in Figure 3.11. Once the potential for delivery of debris is estimated for the entire bridge site, the effective length of the span/gap between fixed elements relative to the design log length and the location category of the gap are evaluated for both horizontal and vertical spans/gaps.

Effects of Accumulations That Modify Analysis. Because hydraulics and debris-trapping characteristics of a bridge can change with debris accumulation, the potential for additional trapping can increase as well. Diehl (1997) recommends that, after all possible debris accumulations at a bridge have been assigned a potential for occurrence, the analysis should be run again to determine whether some individual accumulations increase in potential or may affect the potential for adjacent accumulations elsewhere along the bridge.

3.2.3 Phase 3: Determine the Overall Debris Accumulation Potential for the Bridge

Diehl (1997) suggests that the potential for debris accumulation at a bridge is the maximum or worst case of the potentials determined for each pier, substructure section, or gap/span between fixed elements. However, this method could result in a relatively long bridge having an overall high

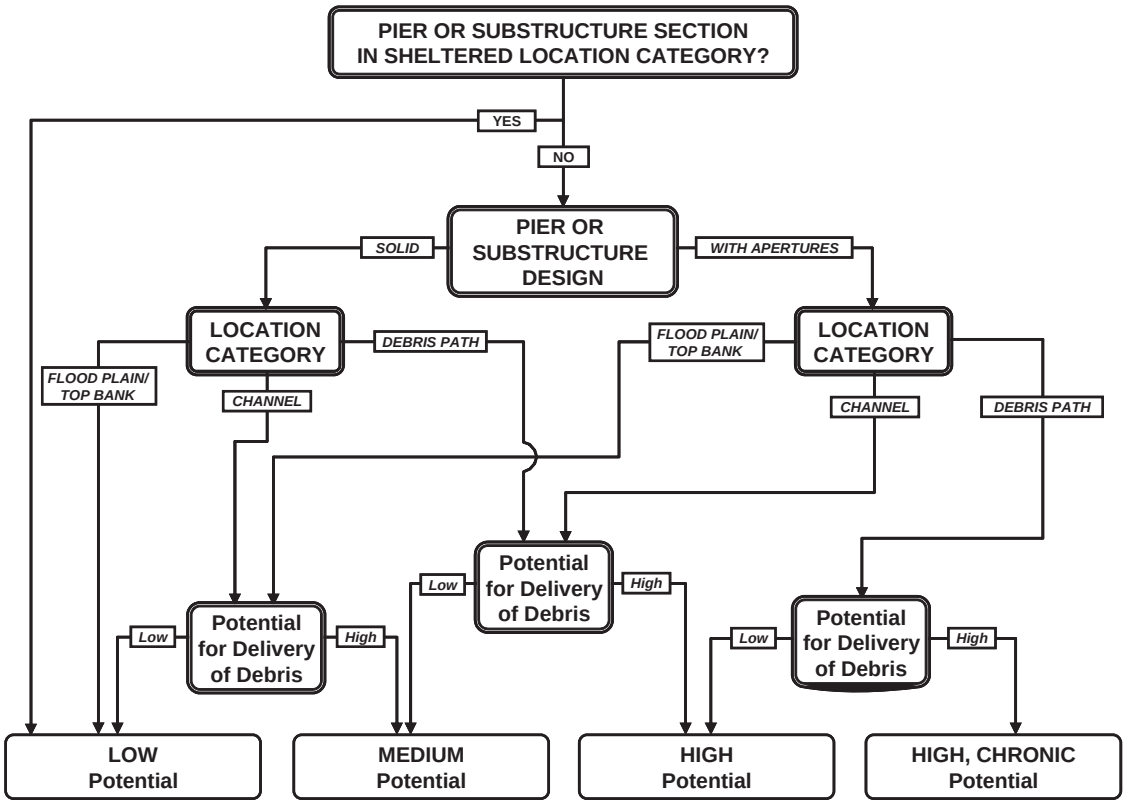

Figure 3.10. Flowchart for determining the potential for debris accumulation on a single pier or section of the bridge substructure.

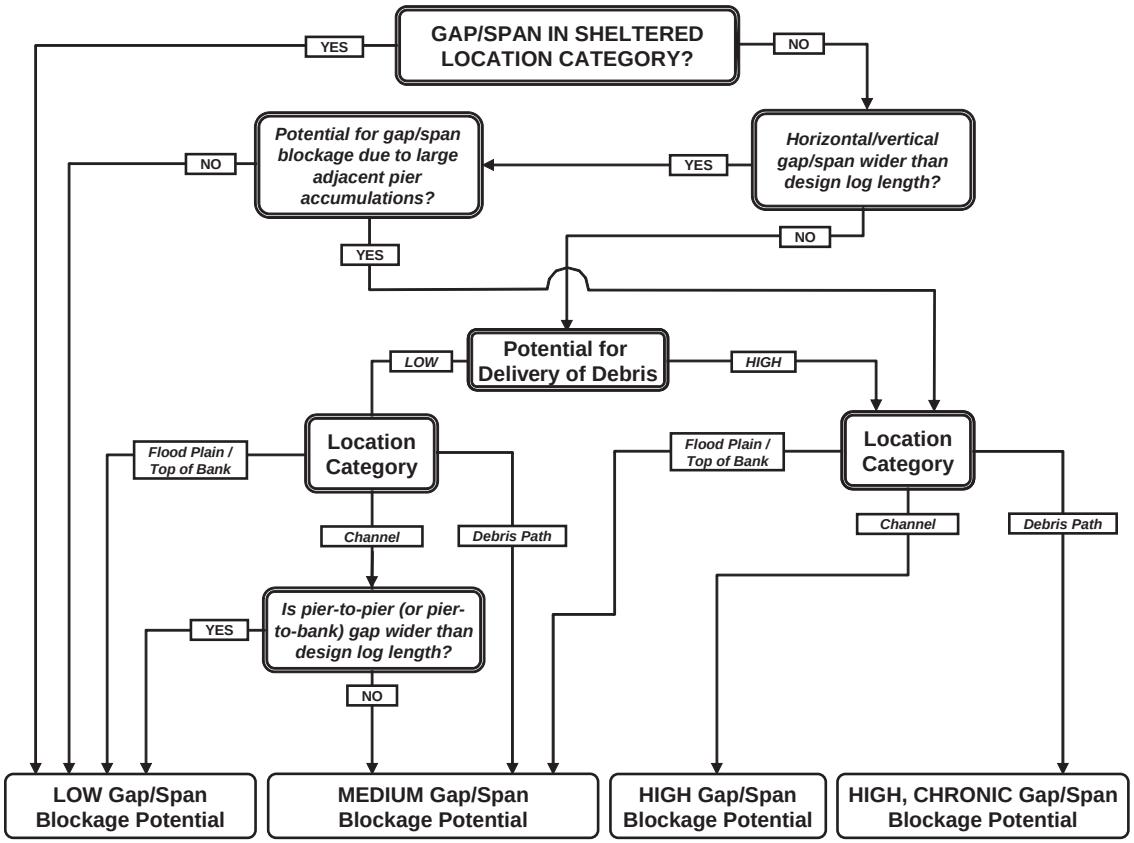

Figure 3.11. Flowchart for determining the potential for debris accumulation across a horizontal or vertical span or gap.

or chronic rating for debris accumulation potential that is based on a high or chronic rating for only one or two bridge elements. Therefore, it is recommended here that each individual element and gap/span should be treated as a separate entity in an effort to reduce design and construction costs, while maintaining structural integrity. Major bridge segments can be compartmentalized for design or maintenance purposes by identifying and delineating those zones where adjacent structural elements and gap/spans have the same debris accumulation potential rating. Construction or maintenance costs could be significantly reduced through the use of this compartmentalization or zonation of potential debris accumulation ratings.

3.3 Application of the Guidelines: South Platte River Case Study

Based on recommendations from the NCHRP 24-26 panel, a field investigation and case study were conducted as part of the revised research work plan. The intent of the field investigation was to identify potential case study locations on the South Platte River in Colorado in order to evaluate the applicability of the guidelines (see Section 3.2) and Field Data Sheets (see Part 1 of Appendix D) developed for this project. The Field Data Sheets were used to document site characteristics such as channel type and size, channel instability, bank erosion and retreat, and bank vegetation characteristics in detail. The purpose of the case study is to provide an example of how the practitioner should apply the guidelines for assessing debris production and the potential for debris accumulation at a bridge site.

3.3.1 Field Reconnaissance

Potential case study bridge sites were examined on June 7, 2006, along a stretch of the South Platte River between the cities of Greeley and Sterling, Colorado. Upstream of the potential study sites, the South Platte River Basin has a drainage area of approximately 14,600 mi^2. Headwaters of the South Platte River are located in the central Colorado mountains, where the mean annual precipitation is about 30 in. including approximately 300 in. of snowfall (USGS 2006). On the northern Colorado plains between Greely and Sterling, Colorado, where the potential study sites were located, the mean annual precipitation is about 12 in., primarily in the form of rain that typically falls April through July.

The average June flow in the South Platte River in the corridor containing the potential study sites is 1,260 ft^3/s. During the field reconnaissance, the flow was approximately 90 ft^3/s at the USGS gauge station in Fort Morgan. Unusually warm temperatures in May 2006 caused snowpack to melt faster than normal, resulting in an earlier runoff peak, which occurred on the South Platte River at Fort Morgan in early May 2006 at 182 ft^3/s, just prior to the field reconnaissance.

Land use in the corridor containing the potential study sites is primarily agriculture and some rangeland. Continuing moderate to severe drought conditions in Colorado have resulted in the need to shut off irrigation wells that draw from a shallow aquifer in the area in order to ensure minimum flow conditions in the South Platte River are maintained. During the field visit, flow depths were observed to decrease moving downstream despite the confluence with several tributaries due to what appeared to be irrigation diversion.

Sixteen bridge sites were examined during the field reconnaissance; two of the bridge sites within Weld County, Colorado, were identified as potential candidates for case study locations. These sites were the bridges carrying Weld County Road 37 (WEL 37) and Weld County Road 50/67A (WEL 50/67A) over the South Platte River. The other fourteen sites were eliminated for a number of reasons:

- Stable banks did not contribute debris to channel.
- Several bridges had relief bridges that may reduce exposure to flood flows.
- Flow diversion drastically reduced channel flow.
- Older riparian vegetation was set back from the banks minimizing large woody debris in channel.

Bridge WEL 50/67A was selected for the case study. The bridge is located on the apex of a meander bend of the South Platte River (Figure 3.12) at Hardin, Colorado. Large woody debris, composed primarily of large mature cottonwoods, was observed in the channel and on the banks upstream of the bridge. Active bank erosion and channel migration were evi-

Source: Google Earth Pro

Figure 3.12. Aerial view of the Bridge WEL 50/67A case study site.

dent on both banks upstream of the bridge and are the primary mode of debris delivery to the channel.

Bridge WEL 50/67A has three sharp-nosed piers about 18 in. (0.5 m) wide and skewed approximately 5° to high flows. Two piers had debris buildup on the nose and sides. The left and right abutments had about 12 in. (0.3 m) diameter stone riprap protection, with the riprap protection on the left bank extending about 300 ft (91 m) upstream. Pier 1 is located on a mid-channel bar that has a moderately dense cover of grass. A triangular debris pile consisting of several logs with a small [less than 1 ft (0.3 m) deep] scour hole was located on the nose of Pier 1 (Figure 3.13). Debris on Pier 2 consisted of a single log approximately 14 in. (0.36 m) in diameter with a 4 to 6 ft (1.2 to 1.8 m) diameter rootwad positioned at the upstream end. A debris pile and a scour hole, approximately 2 to 3 ft (0.6 to 0.9 m) deep and 8 to 10 ft (2.4 to 3.0 m) wide, were observed along the upstream end of the right abutment. The debris that had accumulated on the right abutment had no discernable key log, but was composed of several logs approximately 18 in. (0.5 m) in diameter with one log having a 6 to 8 ft (1.8 to 2.4 m) diameter rootwad positioned at the upstream end.

3.3.2 Development of the Case Study

Based on field conditions identified during the field reconnaissance, it was determined that Bridge WEL 50/67A was the best candidate for the case study. The case study was conducted by completing the Field Data Sheets for the bridge site both in the field and in the office following additional data collection efforts (see Part 2 of Appendix D). The completed Field Data Sheets for the bridge are provided in Part 3 of Appendix D. Once the Field Data Sheets were completed, the data and information were used with the guidelines to assess the potential for debris production, transport, delivery, and accumulation at the bridge site. Based on the data and information collected in the field and application of the guidelines, the following potentials were determined:

- Estimated potential for debris production: HIGH
- Estimated potential for debris transport and delivery: HIGH
- Estimated debris accumulation potential
  - Left Bank Abutment: LOW
  - Pier 1: MEDIUM
  - Pier 2: HIGH
  - Pier 3: HIGH
  - Right Bank Abutment: LOW
- Estimated span blockage potential:
  - Span 1: LOW
  - Span 2: LOW
  - Span 3: LOW
  - Span 4: LOW

Figure 3.13. View looking down at debris cluster and scour hole on the upstream end of Pier 1 of Bridge WEL 50/67A.

3.4 Development of Debris Characteristics for Laboratory Testing

3.4.1 Debris Accumulation Characteristics

Typical debris accumulation characteristics were identified based on the literature review (Section 2.1), an examination of the debris photographic archive (Section 2.2), the survey (Section 2.4), the field pilot study in Kansas (Section 2.5), and the field reconnaissance for the case study (Section 3.3.1). Identification of typical debris shapes and geometry was a necessary preliminary to developing a laboratory testing program. Considering laboratory testing budget constraints, the objective was to develop a limited number of debris shapes that would represent the maximum number of debris configurations found in the field. It was also necessary that the shapes be simplified so that they could be constructed and replicated with a reasonable range of geometric variables for laboratory testing.

At bridge piers, debris characteristics at a minimum might include a single-pier floating cluster, a floating raft bridging two or more piers, and submerged or sunken variations of these configurations. The debris accumulations shown in the photographs compiled in the debris photographic archive (Appendix A) were evaluated for specific geometric characteristics and guided identification of the specific geometries described in the following paragraphs. A summary of the observed planform and accumulation types—organized by region, photograph source, and location—is provided in Table 3.2. The photographs were also used to identify typical geometries of the debris piles and to provide rough estimates

Table 3.2. Inventory of photographs of debris at bridge piers classified by shape.

Source	State	Stream	Number of Photos	Physio-graphic Region	Eco-region	Single Log	Rectangular		Triangular		Profile Geometry		
							Multi	Mass	Multi	Mass	Conical	Rectangular	Inverted Cone
Pacific Coast													
Kevin Flora Caltrans (Survey)	California (Central & South Coast)	Arroyo Grande	11	24	260					X	X		
		Hopper Creek	3	24	M260								
		Salsipuedes Creek	5	24	M260		X						
	California (Mountain)	N. Fork Deer Creek	4	23	260								
	California North Coast	Mad River	4	24	260			X			X		
		Trinity River	1	24	260		X						
		Yager Creek	6	24	260		X					X	
	California (Central Valley)	Sacramento River	2	24	260		X					X	
		Stony Creek	6	24	260		X					X	
		Thomes Creek	4	24	260		X						
Ayres Assoc.	California	Malibu Laguna	1	21	260								
		Harris Creek	1	25	M262								
		Stony Creek	1	24	260		X						
	Oregon	Shitike Creek	1	24a	242								
Debris Free, Inc. (Mike Collier)	California (North)	Butte Creek	9	23	260								
		Navarro River	13	24	260			X					
	California (South	Callegas Creek	18	24	260			X				X	
		Santa Clara River	26	24	260			X				X	
		San Antonio Creek	9	24	260			X					
		Adams Creek	3	24	M260								
		Ventura River	29	24	260			X				X	
	Oregon	Calapooia River	1	23	M240								
		North Santiam River	3	23	M240		X						
	Washington	Cowitz River	7	24	240		X						
		N. Fork Skagit River	6	23	M240			X					
		N. Fork Skagit River	2	23	M240								
		S. Fork Skagit River	1	23	M240		X						
		Skykomish River	4	24	240	X							
Timothy Diehl (1997)	Washington	Queets River	1	24	M240								
West													
Debris Free, Inc. (Mike Collier)	Nevada	Carson River	6	22	340			X					
	Utah	Colorado River	4	21	340			X					
		San Rafael River	7	21	340				X		X		
Russel Brewer MtDOT (Survey)	Montana	Jefferson River	14	19	M330				X				
		Boulder River	7	19	M331								
		St. Regis River	3	19	M332	X							
C. Miller NDOT (Survey)	Nevada	Carson River	15	22	340	X							
Tim Ularich UDOT (Survey)	Utah	Santa Clara and Virgin Rivers	11	21	340			X					X
Ayres Assoc.	New Mexico	Rio Grande	1	22	310	X							X
	Colorado	Bijou Creek	2	13	330								
	Idaho	Teton River	1	18	M330								
Various Web-sites (KSL Ch. 5 TV, St. George)	Utah	Santa Clara River	8	22	340					X			
		Beaver Dam Creek	4	22	340					X			
		Unknown	11	22	340					X			
Midwest													
Debris Free, Inc. (Mike Collier)	Illinois	East Skokie Ditch	3	12	220			X					X
		Iroquois River	4	12	250								
		Mississippi River	3	12	250								
		Mackinaw River	3	12	250								
		Unknown	6										
	Indiana	Eel River	8	12	220				X				
		Eel River	4	12	220	X							
		Vermillion River	11	12	220								X
		Wabash River	3	12	220				X				
	Kansas	Republican River	6	12	250				X				
		Smoky Hill River	34	13	330			X					
	Minnesota	Minnesota River	15	15	250								
	Missouri	Unknown	1							X			

Table 3.2. (Continued).

Source	State	Stream	Number of Photos	Physio-graphic Region	Eco-region	Single Log	Rectangular		Triangular		Profile Geometry		
							Multi	Mass	Multi	Mass	Conical	Rectangular	Inverted Cone
Midwest (cont.)													
	Ohio	Unknown	5							X			
	Kentucky	Unknown	2					X			X		
	Texas	Clear Fork Brazos Rv.	6	12	310								
Debris Free, Inc. (Mike Collier)	Tennessee	Harpeth River	8	11	220								
	Oklahoma	Wild Horse River	3	12	250								
		North Canadian River	12	12	310					X		X	
Brad Rognlie KDOT (Survey)	Kansas	Verdigris River	12	12	250					X	X		
		Smoky Hill River	73	13	330			X					
		Chikaskia River	1	13	330								
		Elm Creek	25	13	330								
		Neosho River	19	12	250								
		Elk River	25	12	250								
		Unknown	6							X			
Ayres Assoc.	Kansas	Neosho River	38	12	250					X			
		Neosho River (US 400)	28	12	250						X		
		Verdigris River	14	12	250					X	X		
		Elk River	32	12	250								
	Missouri	Florida Creek	1	12	250								
	Nebraska	South Platte River	1	12	250								
	Indiana	Indian Creek	1	12	220								
MNDOT District 1 (website photos)	Minnesota	Black River	2	1	212				X				
USGS (Robinson 2003)	Indiana	White River	6	12	220			X					
Tim Dunlay Iowa DOT (Survey)	Iowa	Cedar Creek	3	12	220								
	Iowa	East Nishnabotna River	6	12	250				X				
	Iowa	West Nodoway River	3	12	250				X				
John Holmes MoDOT (Survey)	Missouri	Chariton River	9	12	250					X	X		
Ken Foster MoDOT (Survey)	Missouri	Big Creek	2	12	250				X				
		West Fork of Grand Rv.	8	12	250								X
Larry Cooper MNDot (Survey)	Minnesota	Minnesota River	2	12	220								
	Minnesota	Mississippi River	2	12	220								
Duane Hill MNDOT (Survey)	Minnesota	S. Branch of Wild Rice River	2	12	250								
Brandon Callett ODOT (Survey)	Ohio	Great Miami River	14	12	220		X						
Allan Bjorklund WisDOT (Survey)	Wisconsin	Pikes Creek	1	1	210				X				
		Bad River	1	1	210			X					
Jerry Conner TxDOT (Survey)	Texas	Clear Fork of Brazos Rv.	6	12	310								
Tim Hertel TxDOT (Survey)	Texas	Red River	12	12	250			X					
Jon Zirkle TDOT (Survey)	Tennessee	Harpeth River	13	11	220								
Timothy Diehl (1997)	Tennessee	Harpeth River	2	11	220			X					
	Indiana	White River	1	12	220								
East													
Debris Free, Inc. (Mike Collier)	N. Carolina	Deep River	4	4	230						X		
	Virginia	Appomattox River	4	4	230					X	X		
		James River	2	3	230								
		Meherrin River	3	4	230								
		Dan River	2	4	230								
		Nottoway River	4	4	230								

(continued on next page)

Table 3.2. (Continued).

Source	State	Stream	Number of Photos	Physio-graphic Region	Eco-region	Single Log	Rectangular		Triangular		Profile Geometry		
							Multi	Mass	Multi	Mass	Conical	Rectangular	Inverted Cone
East (cont.)													
	W. Virginia	Mud River	2	8	220					X			
		Tug River	2	8	220					X	X		
NCDOT Website Photos	N. Carolina	Deep River	5	4	230						X		
Website Photos	Tennessee	Coal Creek	4	8	220								
South													
Debris Free, Inc. (Mike Collier)	S. Carolina	Little River	40	4	230								
	Florida	Escambia River	2	3	230			X					
	Tennessee	Wolf River	3	3	230								
		Jackson Dist. Var.	193	11	230								
	Arkansas	St. Francis River	34	3	230					X			
	Louisiana	Amite River	10	3	230				X				
Ayres Assoc.	Louisiana	Bayou Boeuf	1	3	230								
	Mississippi	Abiaca Creek	1	3	230								X
		Jack Creek	2	3	230								
		Sykes Creek	1	3	230			X					
Website Photos	Louisiana	Red River Raft	2	3	230								
MDOT, Br. Des (Survey)	Mississippi	Coles Creek	1	3	230		X						
J. Zirkle TxDOT (Survey)	Texas	Wolf River	3	3	230								
J. Howell TxDOT (Survey)	Texas	San Marcos River	1	3	250								
J. Kilgore TxDOT (Survey)	Texas	Cocklebur Creek	7	3	310								
	Texas	San Antonio River	13	3	250								
B. Laywell TxDOT (Survey)	Texas	Little River	7	3	250				X				
	Texas	Brushy Creek	6	3	250				X				
H. Schroeder TxDOT (Survey)	Texas	Rocky Creek	6	3	250							X	
Timothy Diehl (1997)	Texas	Brazos River	1	12	310			X					
	Unknown	Unknown	5									X	

of debris accumulation length upstream of the pier and debris accumulation width relative to pier width. Table 3.3 provides a list of sites from the photographic archive that were used to acquire measurements of relative debris accumulation width and length.

Debris was observed accumulating at bridge piers as single logs, multiple logs, or a mass of logs. The single-log accumulation was composed of one or two logs that had become trapped on a pier or between spans. The multiple-log accumulation consisted of several logs that were loosely intertwined and had no filling of the interstices or matrix with finer debris, detritus, and sediment. The mass of logs accumulation was composed of a cluster of logs and other debris tightly interlocked with almost all of the matrix or interstitial openings filled with smaller debris, detritus, and sediment. Unlike the mass of logs accumulation, in almost all cases, the single-log and multiple-log types of accumulations did not extend upstream for any significant distance. Figures 3.14 through 3.16 present schematics of the three observed accumulation types as well as example photographs for each accumulation type.

Although Dongol (1989) used conical, cylindrical, and elliptical shapes in his modeling, most debris accumulations observed in the photographic archive could be considered either triangular or rectangular in planform. Triangular debris accumulations tend to have a conical shape in profile, while rectangular accumulations tend to have a rectangular profile. Figures 3.17 and 3.18 present plan view schematics of the triangular and rectangular planforms, respectively. Figures 3.19 and 3.20 illustrate the conical and rectangular profile geometries. Figure 3.21 provides a photograph of a triangular debris pile with a conical geometry after the water has receded and the pile has collapsed upon itself. Figure 3.22 presents a photograph of a rectangular debris pile with a rectangular geometry after the water has receded and the pile has collapsed upon itself. Both types of debris accumulation profiles can grow from being a surface accumulation to being partially or fully

Table 3.3. Measurements of debris pile width and length.

Geographic Region	State	Stream	W/a	L/a	L/W
Pacific Coast	California (Central Valley)	Stony Creek	10.0	6.0	0.6
Pacific Coast	California (North Coast)	Butte Creek	31.3	8.8	0.3
Pacific Coast	California (South Coast)	Callegas Creek	16.3	13.3	0.8
Pacific Coast	California (South Coast)	Callegas Creek	15.3	13.3	0.9
Pacific Coast	California (North Coast)	Navarro River	43.0	48.0	1.1
Pacific Coast	California (South Coast)	San Antonio Creek	8.0	5.0	0.6
Pacific Coast	California (Central Valley)	Sacramento River	7.1	7.1	1.0
Pacific Coast	California	Stony Creek	15.0	10.0	0.7
Pacific Coast	California (Central Valley)	Thomes Creek	7.6	6.3	0.8
Pacific Coast	Washington	Skagit River	8.3	11.7	1.4
Pacific Coast	California (Central and South Coast)	Arroyo Grande	30.0	15.0	0.5
Pacific Coast	California (North Coast)	Yager Creek	5.0	6.7	1.3
West	Utah	Santa Clara River	13.3	8.0	0.6
West	Utah	Virgin River	28.0	36.0	1.3
West	Utah	Colorado River	10.0	4.0	0.4
West	Utah	San Rafael River	5.6	4.0	0.7
West	New Mexico	Rio Grande	8.5	3.2	0.4
Midwest	Kansas	Verdigris River	13.3	11.7	0.9
Midwest	Iowa	East Nishnabotna River	17.0	16.0	0.9
Midwest	Indiana	Eel River	22.0	24.7	1.1
Midwest	Kansas	Smoky Hill River	16.0	21.7	1.4
Midwest	Ohio	Unknown	28.0	10.0	0.4
Midwest	Tennessee	Harpeth River	23.3	19.0	0.8
Midwest	Tennessee	Harpeth River	14.0	20.0	1.4
Midwest	Tennessee	Harpeth River	18.0	9.0	0.5
Midwest	Indiana	White River	12.5	20.0	1.6
Midwest	Kansas	Neosho River	17.8	8.0	0.4
Midwest	Kansas	Verdigris River	12.0	17.5	1.5
Midwest	Red River	Texas	15.7	13.8	0.9
Midwest	Red River	Texas	6.9	6.7	1.0
East	West Virginia	Tug River	6.4	17.0	2.7
East	Tennessee	Coal Creek	17.5	3.0	0.2
East	Virginia	Nottoway River	10.0	7.0	0.7
South	Louisiana	Amite River	11.0	6.0	0.5
South	Tennessee	Wolf River	15.0	6.0	0.4
South	Arkansas	St. Francis River	12.5	15.0	1.2
South	South Carolina	Little River	10.0	7.0	0.7
Unknown	Unknown	Unknown	14.3	4.9	0.3
		Average	15.1	12.4	0.9
		Range	5.2 - 43	3 - 48	0.2-2.7

NOTE: a = Pier Width, L = Length of Debris Pile, W = Width of Debris Pile

submerged, depending on flow depth. Figures 3.23 and 3.24 display schematics of the various submergence possibilities.

A third type of profile geometry is the inverted conical profile, which generally has a triangular planform. This type of accumulation is very common and usually occurs following one or more floods when an accumulation with a triangular-conical geometry settles onto the bed of the channel. The lower portion of the accumulation then becomes embedded in the bed. When the next flood occurs, the debris accumulation remains trapped on the bed, but can grow in size because of trapping of additional debris. As more debris is trapped by the existing debris pile during subsequent flows,

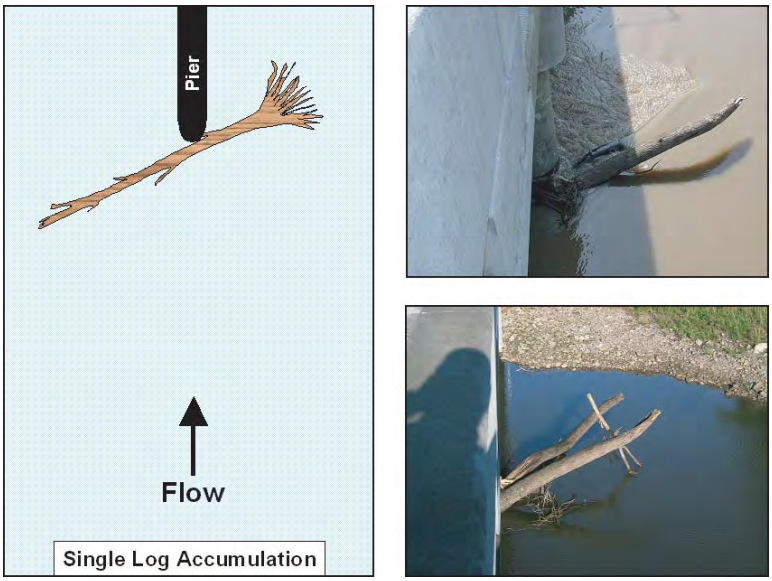

Figure 3.14. Single-log debris accumulation.

a rectangular-rectangular geometry may develop. Figure 3.25 depicts a schematic of the inverted cone scenario. Figure 3.26 presents a photograph of a debris pile with an inverted cone geometry after the water has receded and the pile has collapsed upon an existing pile embedded in the bed.

3.4.2 Laboratory Testing of Debris

Testing Requirements. The goal of the laboratory testing was to provide sufficient data for a range of debris accumulations to develop adjustment factors to the HEC-18 pier scour equation. The adjustment factors could be a correction factor to the overall equation (such as the K_w factor for wide piers) or an adjustment to the pier width used as an input variable to the equation (similar to the HEC-18 complex pier approach). The goal of the laboratory plan was to develop a series of tests for a wide range of debris configurations that can be run quickly and efficiently. The tests would be performed for single debris clusters at individual piers, which was the primary type of debris accumulation identified by all regions in the survey. These tests would then be supplemented to address specific issues related to other factors that would not be incorporated into the initial runs. The majority of the testing would be performed for clear-water

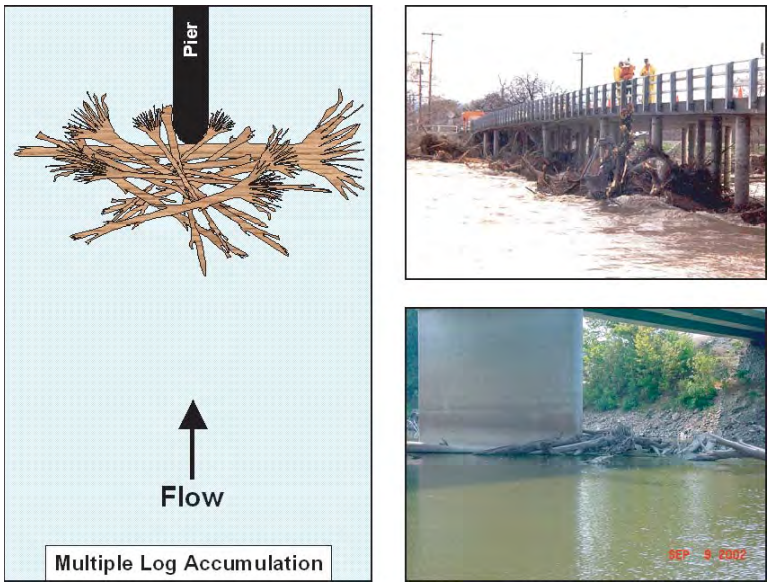

Figure 3.15. Multiple-log debris accumulation.

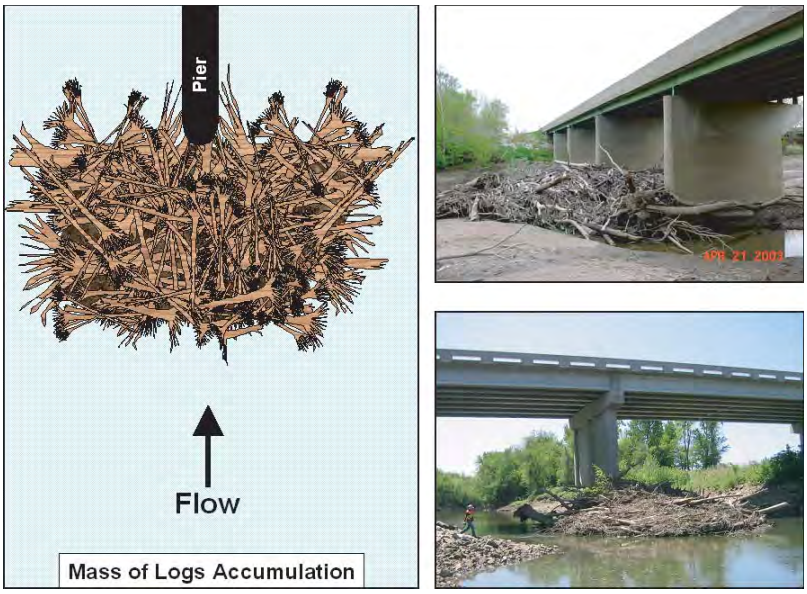

Figure 3.16. Mass of logs debris accumulation.

sediment transport conditions (approach flow velocity less than the critical velocity to initiate sediment transport) for durations much less than would be required to achieve ultimate scour. The duration will, however, be sufficient to achieve at least 60% of ultimate scour. This approach to the laboratory testing maximized the number and range of debris configurations that would be tested within the laboratory budget.

The testing should include a range of debris characteristics including debris accumulation shape, thickness, width, and length. The range of debris accumulation size that would be tested in the laboratory was related to actual debris accumulations observed by the research team in the field or from the survey sources and the photographic archive (Section 3.4.1). Figures 3.27, 3.28, and 3.29 illustrate the debris shapes (rectangular, conical, and collapsed in profile and either rectangular or triangular in planform) that were modeled and define the dimensions for the various shapes. The dimensions were varied in order to model the range of conditions typically seen in the field.

Debris Dimensions. All of the physical modeling was conducted in the 8 ft (2.4 m) wide flume at Colorado State University under clear-water flow conditions using 4 in. (10.2 cm) square piers. This scale and flow condition were selected to maximize the number of debris conditions that can be modeled because scour should develop rapidly at this scale and clear-water runs are also less time consuming.

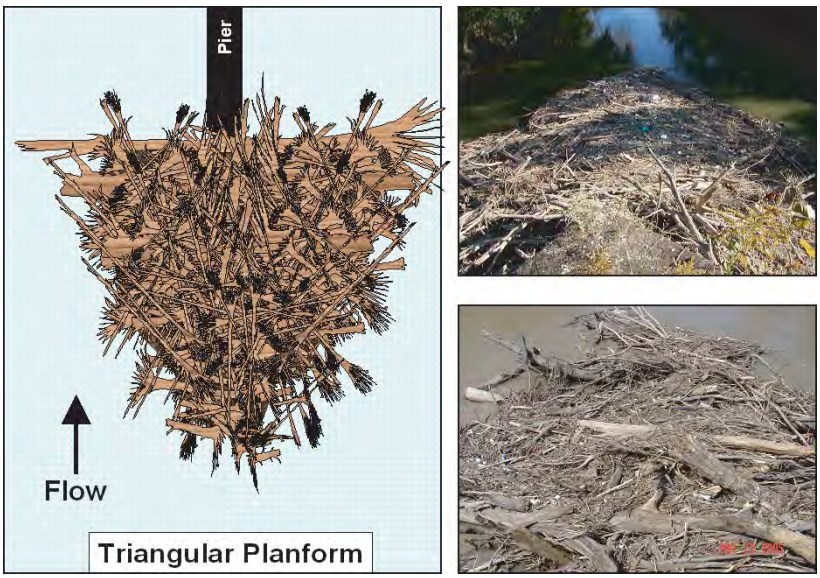

Figure 3.17. Triangular debris pile planform.

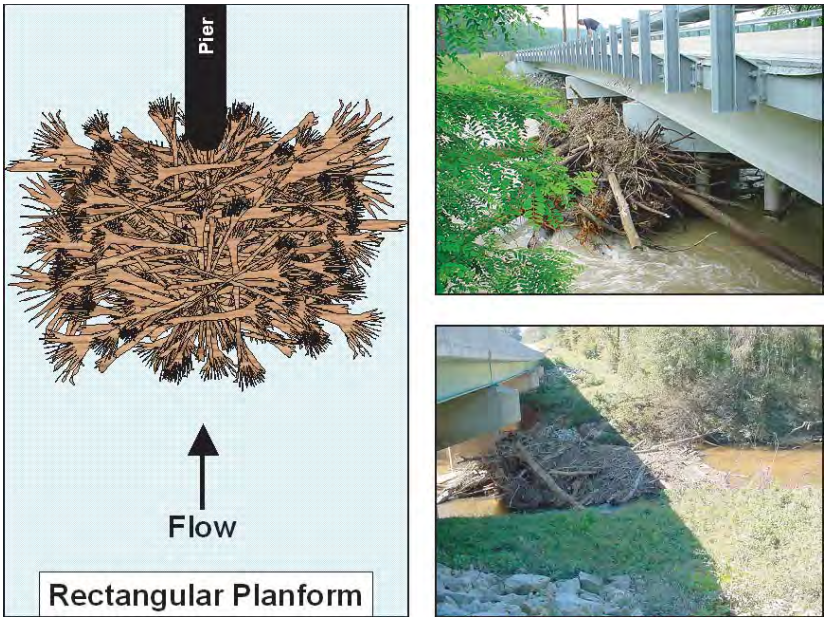

Figure 3.18. Rectangular debris pile planform.

Table 3.4 shows a summary of the observed debris dimensions contained in Table 3.3 and the range of debris dimensions for the laboratory physical modeling. All of the dimensions were normalized by the pier width so the field conditions could be used to develop a realistic range of laboratory runs. The range of debris dimensions was selected to encompass the range observed in the field +/– one standard deviation around the mean. It should be noted that W/a of 24 requires use of the 8 ft (2.5 m) wide flume using a 4 in. (10.2 cm) pier. Additional testing was conducted using 1 in. × 8 in. (2.5 cm × 20 cm) wall piers, and a pile bent having four 0.5 in. (1.3 cm) diameter columns (see Section 3.5).

3.5 Laboratory Testing Program

3.5.1 Testing Facilities and Protocols

Laboratory testing of effects of debris on bridge pier scour was conducted at the Hydraulics Laboratory at Colorado State University (CSU). An indoor recirculating flume measuring 8 ft (2.4 m) wide by 200 ft (61 m) long was utilized for all laboratory tests conducted during this research program.

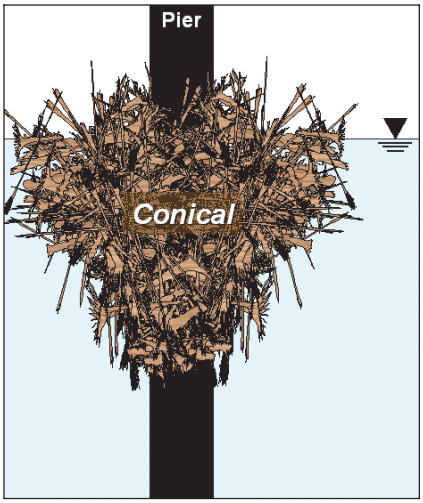

Figure 3.19. Conical profile geometry.

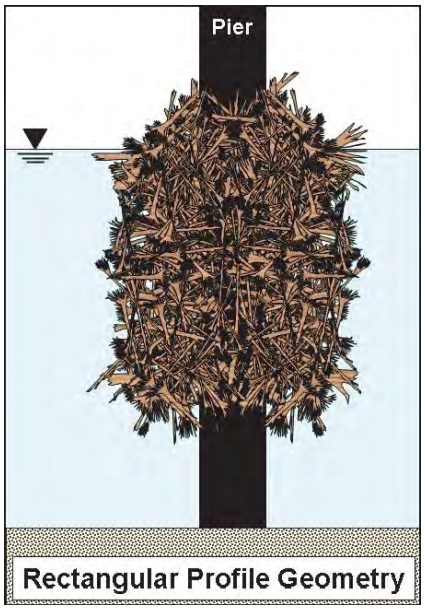

Figure 3.20. Rectangular profile geometry.

Figure 3.21. Collapsed triangular debris pile with conical profile geometry.

Figure 3.22. Collapsed rectangular debris pile with rectangular profile geometry.

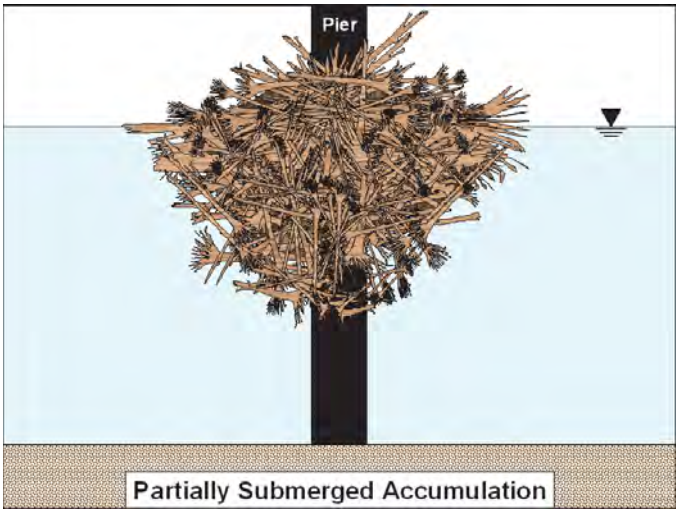

Figure 3.23. Partially submerged debris accumulation.

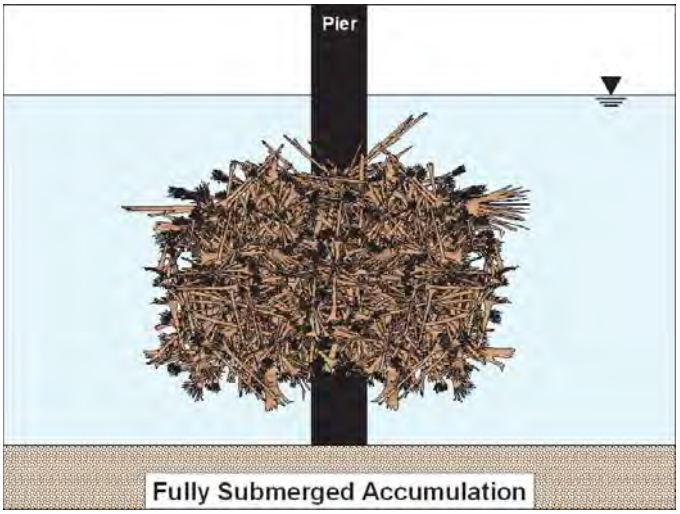

Figure 3.24. Fully submerged debris accumulation.

Flume Description

All laboratory tests were conducted under clear-water conditions with a sand bed 1.5 ft (0.46 m) thick. The sand had a median grain size d_{50} of 0.7 mm. Water was supplied by two 125-horsepower pumps, which could operate separately or in tandem to achieve a desired discharge, up to a maximum flow capacity of 55 ft^3/s (1.6 m^3/s). For all tests, the slope of the flume was kept constant at 0.1%. A flow straightening assembly was placed at the entrance to the flume to eliminate large-scale circulation and condition the flow field prior to entering the test section.

Four pier locations (A through D) were established in the flume along the centerline. All piers were designed to be constructed to a height of 3 ft (0.9 m) above the floor of the flume. Fabrication of the piers was performed by CSU shop personnel.

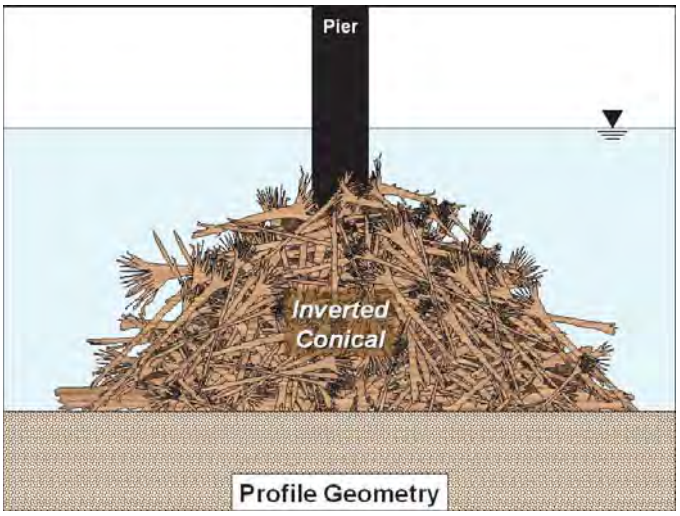

Figure 3.25. Inverted cone profile geometry.

Figure 3.26. Collapsed debris pile with an inverted cone geometry.

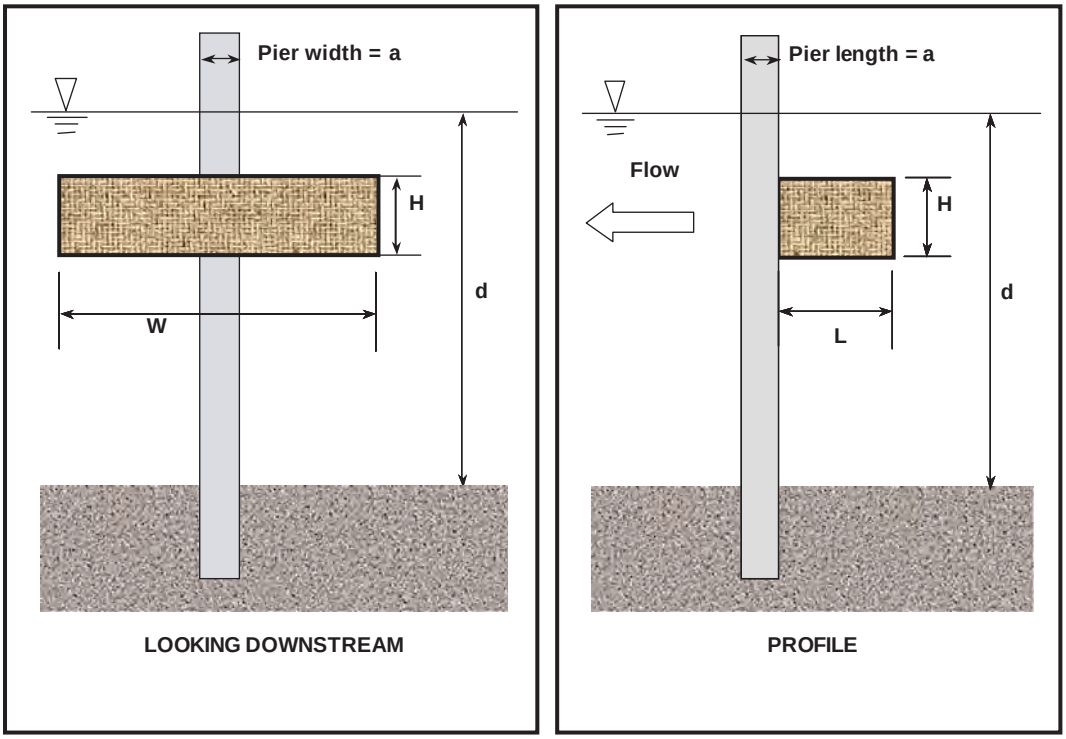

Figure 3.27. Rectangular shape definition sketch.

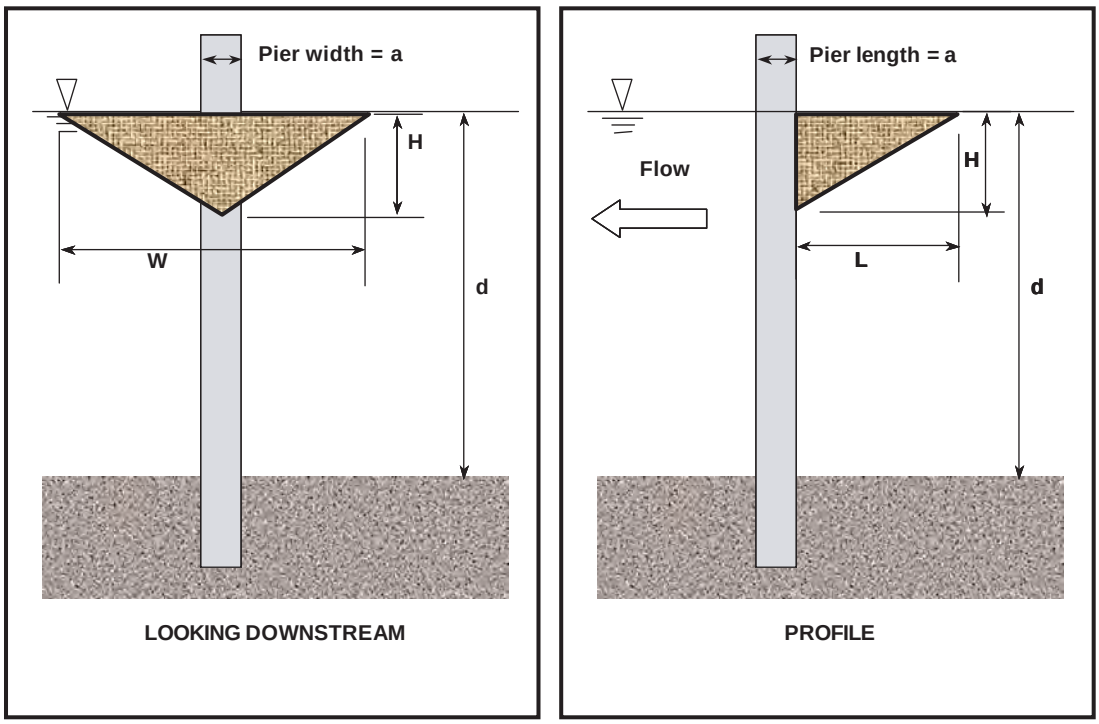

Figure 3.28. Conical shape definition sketch.

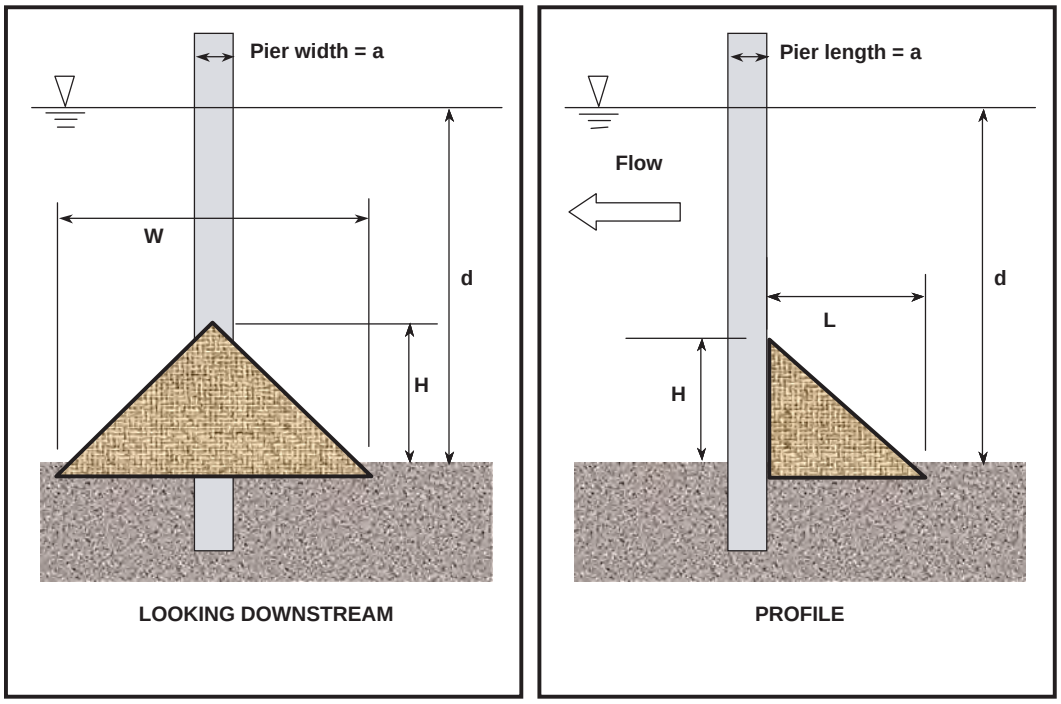

Figure 3.29. Collapsed shape (inverted cone) definition sketch.

Table 3.4. Field and laboratory debris dimensions.

	W/a	L/a	L/W
Field and Photograph Measurements			
Average	15.1	12.4	0.9
Range	5.2 – 43	3 – 48	0.2 – 2.7
St. Dev.	8.2	9.2	0.5
-/+ St. Dev.	6.9 – 23.3	3.2 – 21.5	0.4 – 1.3
Recommended Laboratory Tests			
Range	6 – 24	3 – 24	0.5 – 1.5

All piers were designed and constructed in two sections. The lower piece remained secured to the floor of the flume while the upper section could be removed at the pre-test sand level in order to easily re-level the bed after each test. A level bed surface was produced by a screed board attached to a cart and drawn across the surface of the bed. A photograph of the flume before installation of the piers is presented in Figure 3.30. A schematic of the flume showing the pier layout and ancillary features is presented in Figure 3.31.

Piers

Three types of piers were fabricated for the testing program: 4 in. (10.2 cm) square piers, 1 in. wide by 8 in. long (2.5 cm by 20 cm) wall piers, and pile bent piers having four 0.5 in. (1.3 cm) diameter columns. Before each run, four piers of predetermined shape were installed along the centerline of the flume. The piers were secured to the flume floor and extended approximately 1.5 ft (0.46 m) above the sand bed. Each pier has a removable upper section to allow automated mapping of scour holes using an array of 16 ultrasonic transducers on the data cart (further explained in the following section). Figure 3.32a shows a fully assembled 4 in. (10.2 cm) square pier, and Figure 3.32b shows the upper and lower halves of the same pier separated to allow for data collection.

Figure 3.30. Eight-foot (2.4 m) flume before pier installation.

Data Acquisition

Hydraulic Data Acquisition. Prior to each test, the tailgate was closed and the flume slowly filled with water until the target flow depth of 1 ft (30.5 cm) was established. Flow was introduced very slowly to ensure no local scour occurred during startup. During the slow filling process, air was allowed to escape from the sand bed. Figure 3.33 is a photograph of a 4 in. (10.2 cm) square pier as flow was introduced to the testing flume.

With the flume full of water, discharge was slowly increased to the target discharge, while simultaneously the tailgate was opened until steady flow at the target depth of 1 ft (30.5 cm) relative to the initial bed surface was obtained. This process ensured a very gradual acceleration of flow until the target velocity was achieved and maintained. This process took about 1.5 to 2 hours to accomplish.

Each run then proceeded for a duration of 8 hours while velocity and water surface data were collected at each pier and at designated locations between piers. For long duration tests, the duration was increased to 72 hours per run. After each test, the discharge was gradually decreased and the tailgate adjusted to ensure that no additional scour occurred during the drain-out period. Typically, the flume was allowed to drain out overnight, and the sand bed around each pier was mapped the next day.

Velocity and water surface elevation were monitored periodically at predetermined locations during each test to ensure target hydraulic conditions were maintained. A motorized cart traversed the flume along a track attached to the top of the flume and served as a platform to mount data acquisition equipment. Water surface elevations and velocity profiles were documented at designated locations along the flume. Water surface elevations were measured utilizing a point gauge assembly mounted to the mobile data acquisition cart. Accuracy of the point gauge was 0.01 ft (3 mm). Velocity acquisition equipment was mounted to the cart via the same point gauge. Measurements were recorded adjacent to each

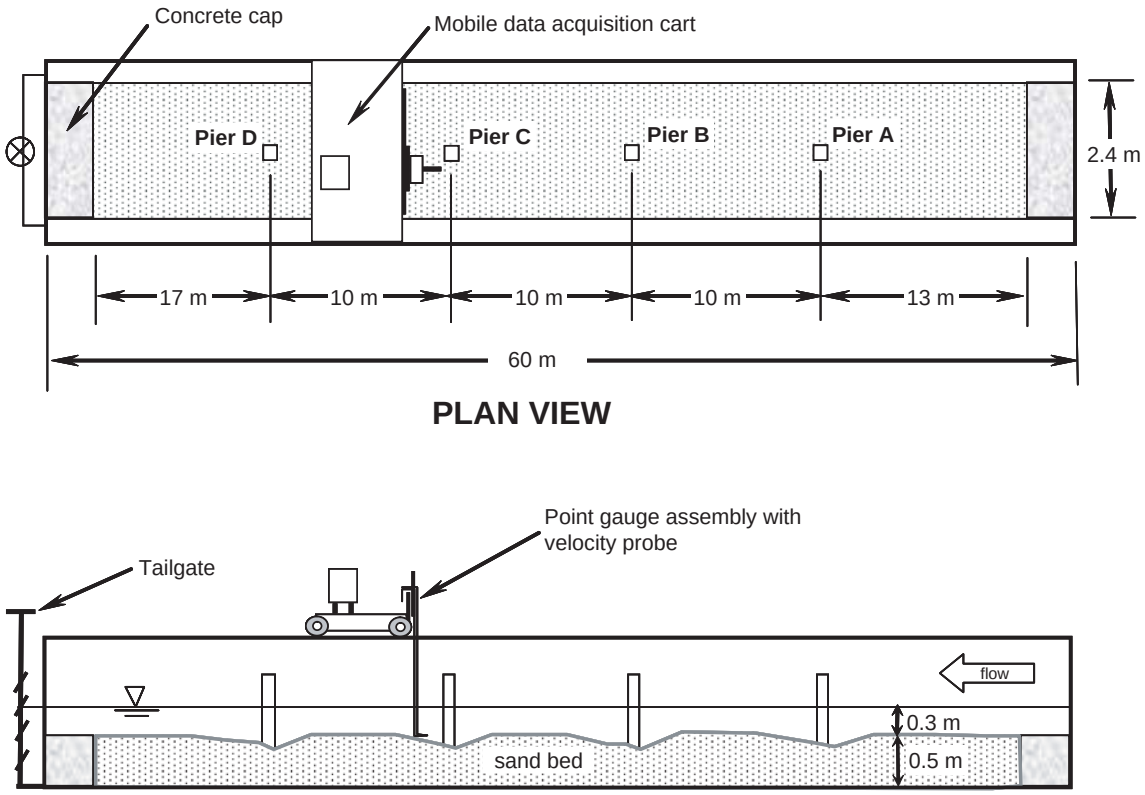

Figure 3.31. Schematic plan and profile of testing flume.

a. Four-inch square pier fully assembled.

b. Four-inch square pier separated for data collection purposes.

Figure 3.32. Four-inch square pier.

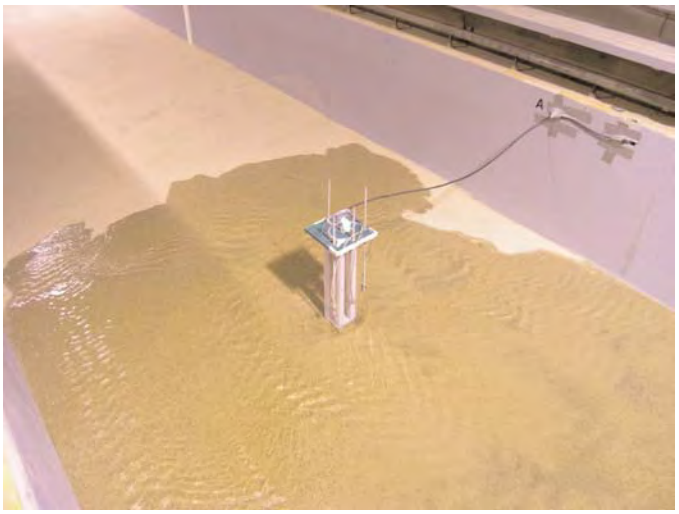

Figure 3.33. Flow initiation at the start of a test.

pier and between each pier to quantify the water surface elevation and the velocity profile.

Velocity data were collected and recorded with a SonTek Acoustic Doppler Velocimeter (ADV). Three main components made up the ADV: the probe head, the conditioning module, and the data recorder. The probe head, a three-pronged apparatus that was submerged to a predetermined depth, was attached to the point gauge assembly. Velocities were measured in a three-space coordinate system within a sampling volume located approximately 1.2 in. (5 cm) below the probe head. The data-conditioning module served as the link between the probe head and data recorder. Digital processing, necessary to interpret the Doppler signal from the probe head, was performed by the conditioning module. A personal computer was used as a data recorder. A schematic of the point gauge assembly is shown in Figure 3.34.

Hydraulic data were collected at a fixed set of 52 locations for each of the configurations considered for the specified set of piers. Flow-depth data were collected at all 52 locations. Twelve of these locations consisted of 4-point velocity profile measurements (20%, 40%, 60%, and 80% depths) in addition to the flow-depth data. The remaining 40 locations consisted of a velocity measurement taken at the 60% depth elevation in addition to the depth measurement, resulting in a total of 88 velocity measurements per data collection set. There were 13 different data collection locations at each pier. Data were generally collected at positions of 6 ft (1.8 m), 4 ft (1.2 m) (centerline), and 2 ft (0.6 m) from the right flume wall at stations 10 ft (3 m) and 4 ft (1.2 m) from each upstream pier face and 8 ft from each downstream pier face;

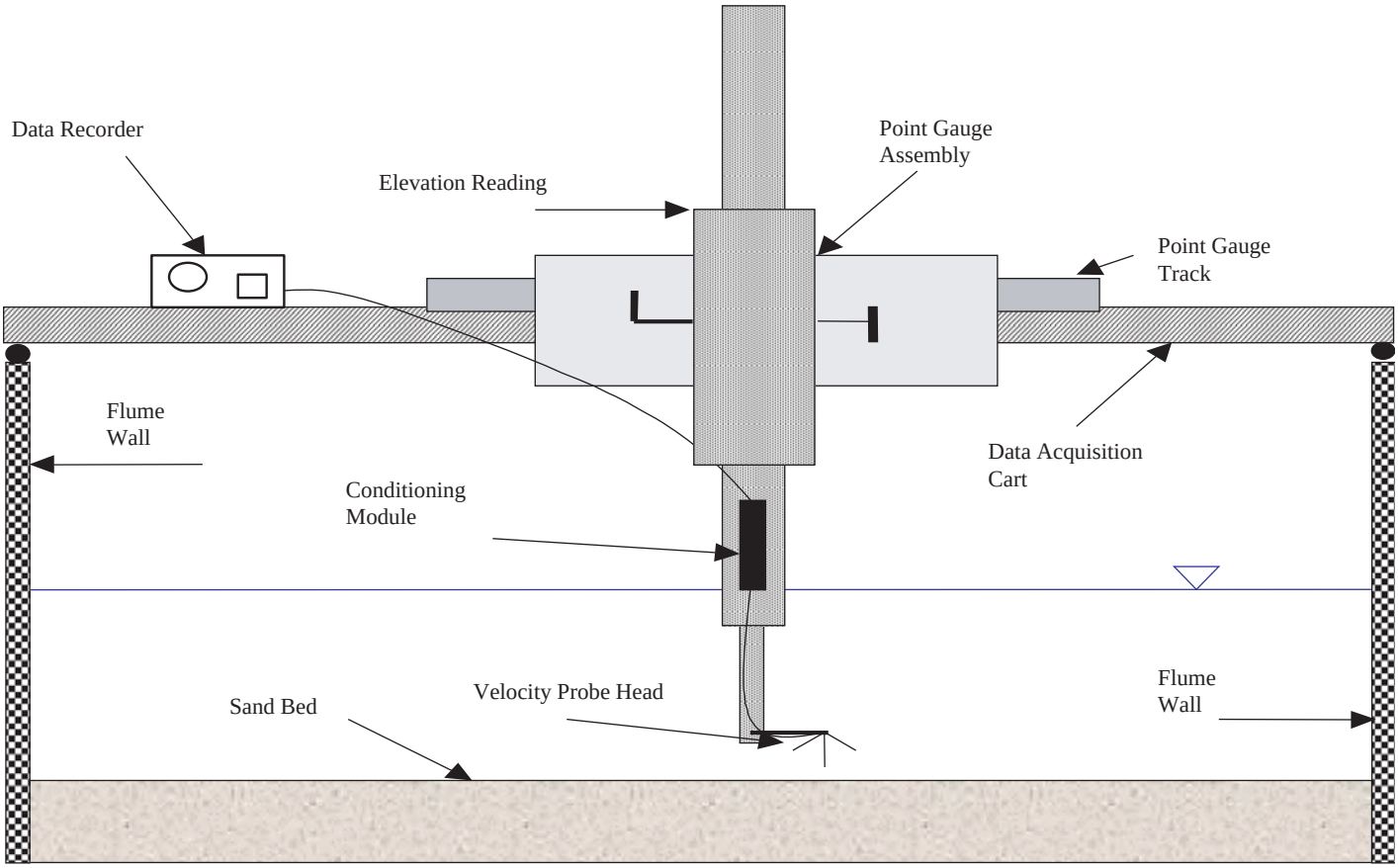

Figure 3.34. Velocity data acquisition setup.

and at positions of 7 ft (2 m), 6 ft (1.8 m), 2 ft (0.6 m), and 1 ft (0.3 m) from the right flume wall at locations aligned with each downstream pier face.

To accurately collect the velocity data for the desired locations, the ADV probe tip was set at an X-direction offset of 0.27 ft (0.08 m). This offset adjusted the X-location of where the point gauge data were collected. Table 3.5 identifies the location and description of hydraulic data collected during each test. A schematic of the hydraulic data collection locations taken in the flume is shown in Figure 3.35. A higher resolution schematic of the hydraulic data collection location taken in the vicinity of a pier is shown in Figure 3.36.

Time-Dependent Scour Measurement. Four depth transducers were mounted around a pier and/or debris cluster to track the depth of scour in real time throughout the test. Depth

Table 3.5. Hydraulic data acquisition locations and descriptions.

	Data Acquisition Point Identification #	X (ft)	Y (ft)	Data Collected
Pier A	1	31.94	6	Velocity @ 60% Depth
	2 through 5	31.94	4	Velocity @ 20%, 40%, 60%, 80% Depth
	6	31.94	2	Velocity @ 60% Depth
	7	37.94	6	Velocity @ 60% Depth
	8	37.94	4	Velocity @ 60% Depth
	9	37.94	2	Velocity @ 60% Depth
	10	42.60	7	Velocity @ 60% Depth
	11 through 14	42.60	6	Velocity @ 20%, 40%, 60%, 80% Depth
	15 through 18	42.60	2	Velocity @ 20%, 40%, 60%, 80% Depth
	19	42.60	1	Velocity @ 60% Depth
	20	50.60	6	Velocity @ 60% Depth
	21	50.60	4	Velocity @ 60% Depth
	22	50.60	2	Velocity @ 60% Depth
Pier B	23	63.94	6	Velocity @ 60% Depth
	24 through 27	63.94	4	Velocity @ 20%, 40%, 60%, 80% Depth
	28	63.94	2	Velocity @ 60% Depth
	29	69.94	6	Velocity @ 60% Depth
	30	69.94	4	Velocity @ 60% Depth
	31	69.94	2	Velocity @ 60% Depth
	32	74.60	7	Velocity @ 60% Depth
	33 through 36	74.60	6	Velocity @ 20%, 40%, 60%, 80% Depth
	37 through 40	74.60	2	Velocity @ 20%, 40%, 60%, 80% Depth
	41	74.60	1	Velocity @ 60% Depth
	42	82.60	6	Velocity @ 60% Depth
	43	82.60	4	Velocity @ 60% Depth
	44	82.60	2	Velocity @ 60% Depth
Pier C	45	95.94	6	Velocity @ 60% Depth
	46 through 49	95.94	4	Velocity @ 20%, 40%, 60%, 80% Depth
	50	95.94	2	Velocity @ 60% Depth
	51	101.94	6	Velocity @ 60% Depth
	52	101.94	4	Velocity @ 60% Depth
	53	101.94	2	Velocity @ 60% Depth
	54	106.60	7	Velocity @ 60% Depth
	55 through 58	106.60	6	Velocity @ 20%, 40%, 60%, 80% Depth
	59 through 62	106.60	2	Velocity @ 20%, 40%, 60%, 80% Depth
	63	106.60	1	Velocity @ 60% Depth
	64	114.60	6	Velocity @ 60% Depth
	65	114.60	4	Velocity @ 60% Depth
	66	114.60	2	Velocity @ 60% Depth
Pier D	67	127.94	6	Velocity @ 60% Depth
	68 through 71	127.94	4	Velocity @ 20%, 40%, 60%, 80% Depth
	72	127.94	2	Velocity @ 60% Depth
	73	133.94	6	Velocity @ 60% Depth
	74	133.94	4	Velocity @ 60% Depth
	75	133.94	2	Velocity @ 60% Depth
	76	138.60	7	Velocity @ 60% Depth
	77 through 80	138.60	6	Velocity @ 20%, 40%, 60%, 80% Depth
	81 through 84	138.60	2	Velocity @ 20%, 40%, 60%, 80% Depth
	85	138.60	1	Velocity @ 60% Depth
	86	146.60	6	Velocity @ 60% Depth
	87	146.60	4	Velocity @ 60% Depth
	88	146.60	2	Velocity @ 60% Depth

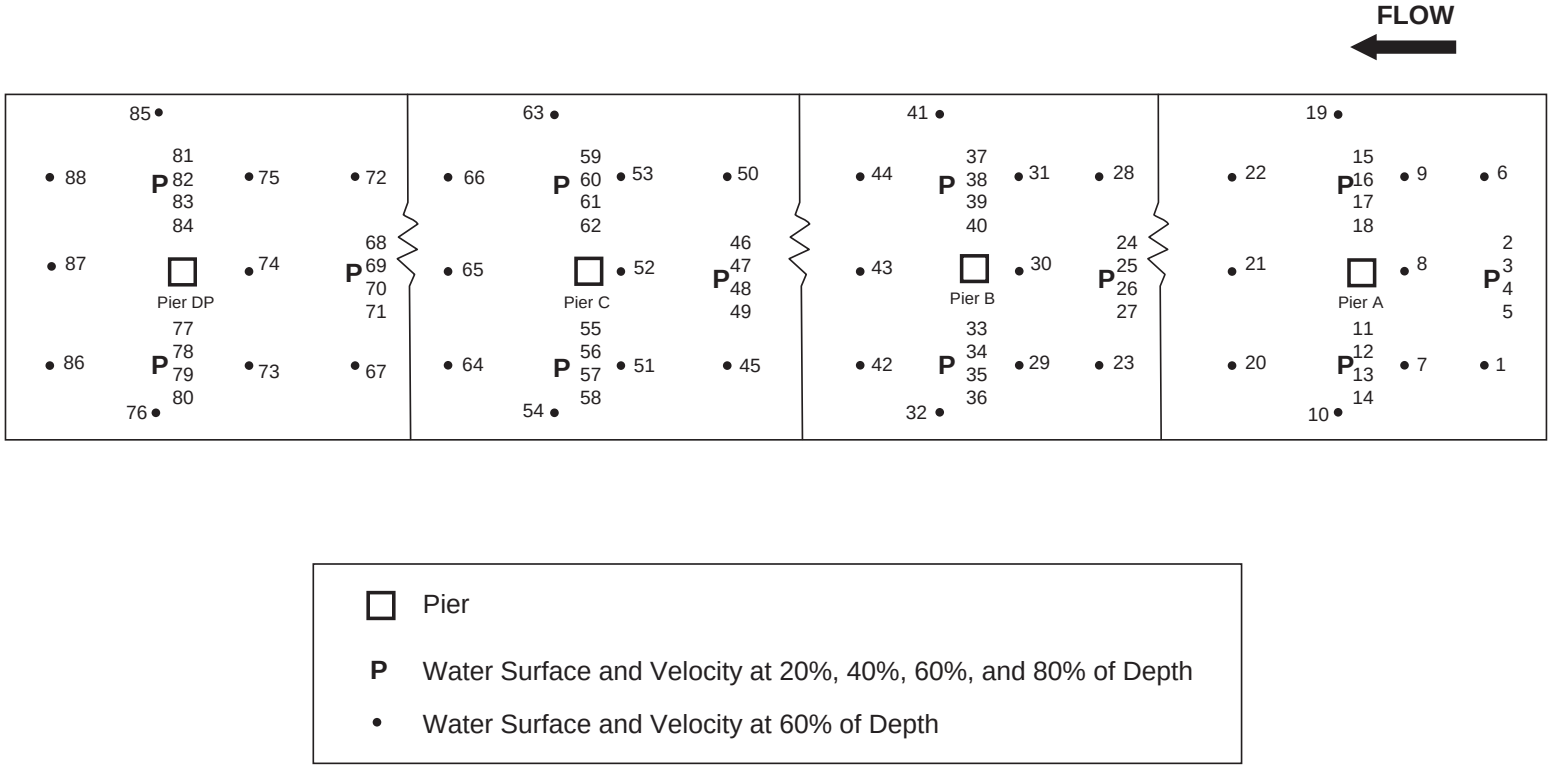

Figure 3.35. Schematic of data collection locations in 8 ft (2.4 m) flume.

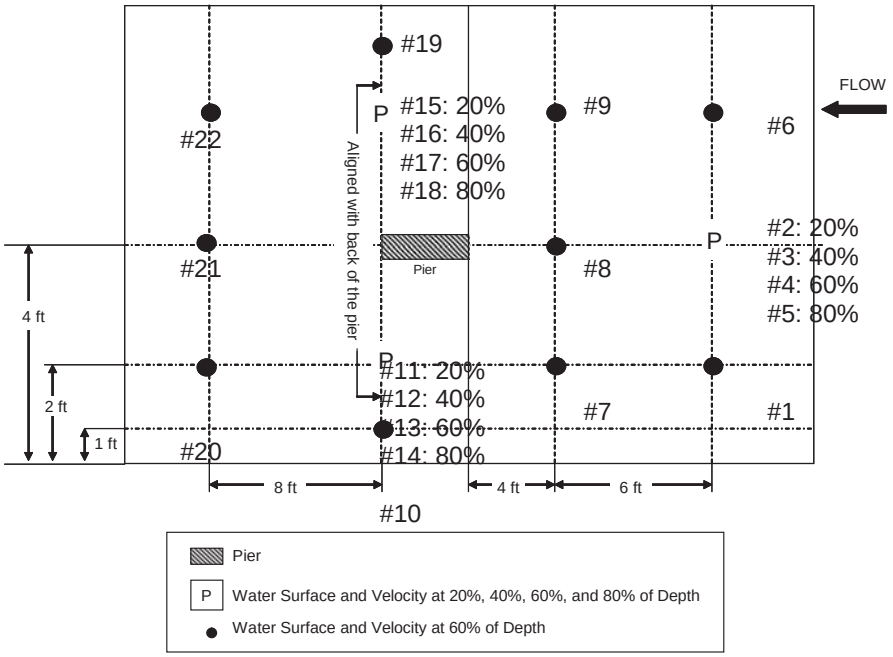

Figure 3.36. Data collection location in 8 ft (2.4 m) flume.

transducers, Figure 3.37, collected a depth measurement through the transmission of a sonar pulse from the bottom of the transducer to the surface of the sand bed every 30 seconds. The data were sent to a data logger and then saved to a computer data file. For baseline tests, where no debris cluster was mounted at the pier, the first depth transducer was mounted at the nose of the pier on the upstream face, the second depth transducer was mounted on the left upstream corner of the pier, the third depth transducer was mounted at the tail of the pier on the downstream face, and the fourth depth transducer was mounted on the right upstream corner of the pier. A schematic of the baseline depth transducer layout is shown below in Figure 3.38.

When a debris cluster was mounted such that it was suspended above the bed, the first transducer was placed upstream of the pier at a distance half the length (L/2) of the debris cluster, the second transducer was placed 1 in. (2.5 cm) from the upstream face of the pier, the third transducer was placed approximately 1 in. (2.5 cm) away from the right side of the pier and approximately flush to the upstream face, and the fourth transducer was placed directly downstream of the right edge of

Figure 3.37. Transducers used for automated scour hole mapping.

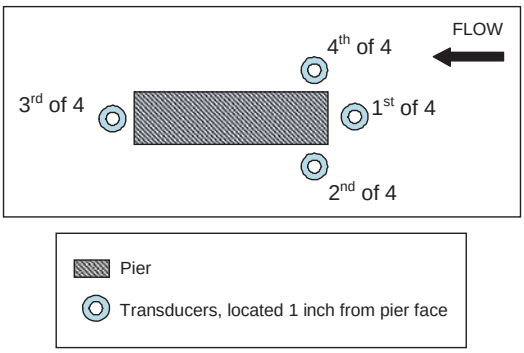

Figure 3.38. Schematic of depth transducers around baseline piers during testing.

the debris cluster. A schematic of the transducer orientation around a suspended debris cluster at a pier is presented in Figure 3.39a.

For debris clusters that were resting on the bed, the first transducer was placed approximately 1 in. (2.5 cm) away from the left side of the pier and approximately flush to the upstream face, the second transducer was placed approximately 1 in. (2.5 cm) away from the right side of the pier and approximately flush to the upstream face, the third transducer was placed directly downstream of the right edge of the debris cluster, and the fourth transducer was placed half the distance between the right corner of the debris cluster and the right flume wall. A schematic diagram of the transducer locations when the debris cluster was resting on the bed is presented in Figure 3.39b.

Post-test Bed Survey and Mapping. Post-test bed surveys were completed using Seatek® 2 MHz Ultrasonic depth transducers, a potentiometer, and a motorized cart. When necessary, survey measurements were verified manually with a point gauge.

Depth transducers were mounted on a 4 ft (1.2 m) wide frame, spaced 3 in. (7.5 cm) apart, and fixed to a rail on the data acquisition cart. A voltage-regulated potentiometer was also mounted on the data collection cart to measure the distance (X) along the flume of each depth measurement. Measurements from the depth transducers and the voltage-regulated potentiometer were recorded electronically by a data logger that was connected to a laptop computer that saved the raw data to a data file. Figure 3.40a shows the potentiometer cabled system, and Figure 3.40b shows the transducers mounted on the frame and cart.

Around each pier, depth transducers collected post-test bed data at a small change in station distance and the potentiometer would then measure the station distance for the location of each set of data. Because the depth transducer frame was only 4 ft (1.2 m) wide, two passes along the flume were necessary to collect a flume-wide post-test bed survey. Figure 3.41 presents a schematic of the ultrasonic depth transducers, potentiometer, and frame setup.

3.5.2 Debris Cluster Test Materials

All debris clusters were constructed with a 0.25 in. rolled steel frame; a 0.25 in. wire mesh was then placed around the

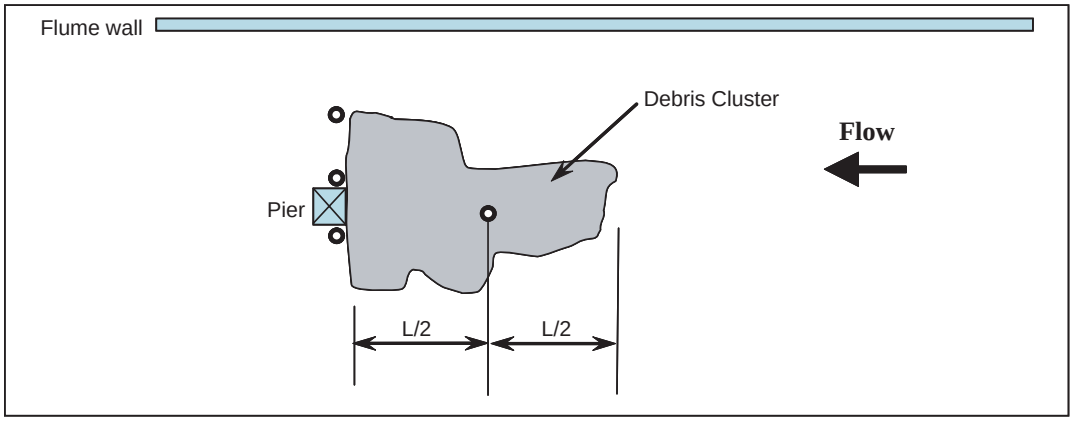

a. Debris suspended above the bed.

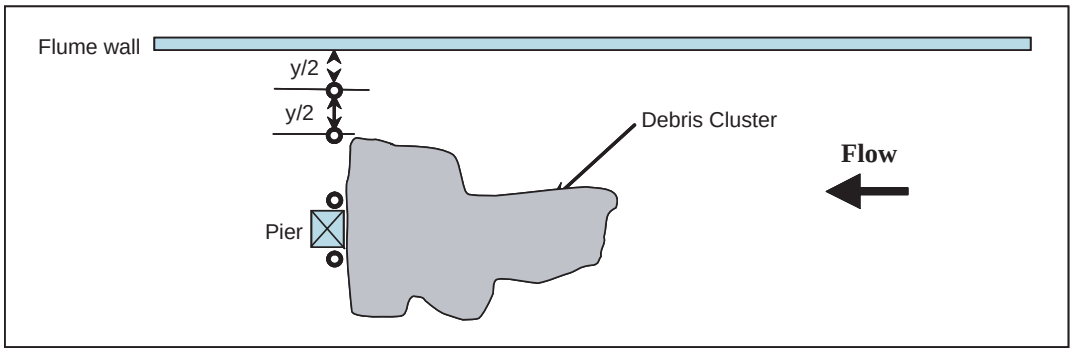

b. Debris located on the bed.

Figure 3.39. Schematic diagram showing locations of depth transducers around piers and debris during testing.

a. Data collection cable system for establishing *x* coordinate.

b. Transducer array used for automated scour hole mapping.

Figure 3.40. Post-test bed and scour hole mapping system.

steel frame. Figure 3.42 shows the basic framework and wire mesh common to all the debris clusters used in the testing program. For tests that modeled impermeable debris, the debris clusters were completely packed with 1 ft square sheets of woven geotextile (Figure 3.43).

Because the intensity of flow vortices, separation, and turbulence may depend on the surface roughness of the debris pile, variations of the surface roughness were included to test the sensitivity of scour to this variable. For tests that simulated debris with increased surface roughness, the debris clusters were artificially roughened by placing 0.25 in. (0.6 cm) diameter wood dowels around the surface of the cluster. Each dowel projected outward from the surface of the cluster a distance of 2 in. (5 cm) and was oriented orthogonally to the surface of the cluster. The average density of the dowels was one per every 4 in.^{2} (25.8 cm^2) of surface area. An example of a roughened debris cluster is shown in Figure 3.44.

To determine if porosity affects debris scour, selected debris clusters were filled with wooden dowels instead of the tightly packed geotextile. The dowels ranged in diameter from 0.25 to

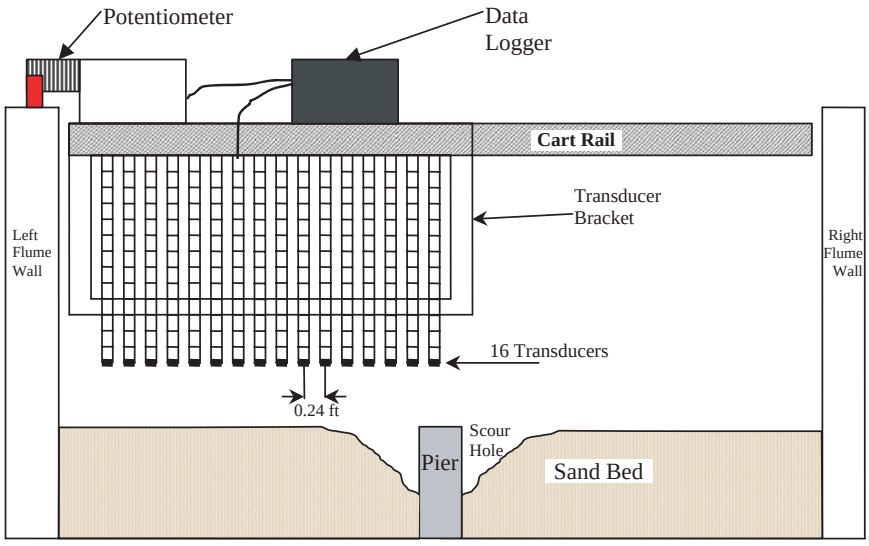

Figure 3.41. Depth transducers, potentiometer, and data logger setup for post-test mapping.

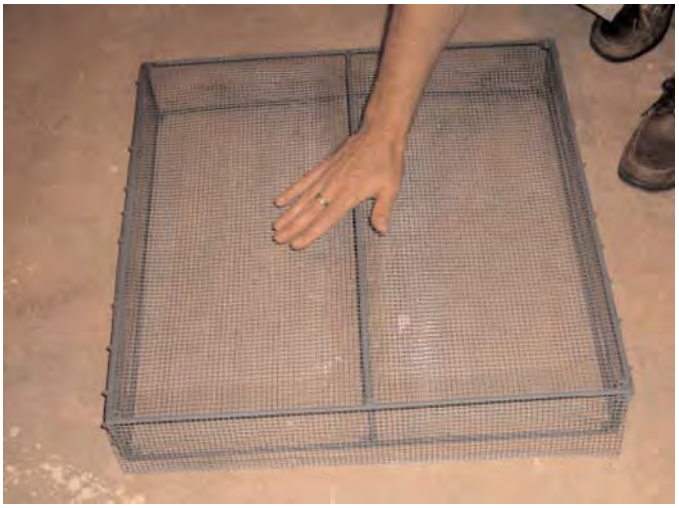

Figure 3.42. Wire framework and mesh for debris cluster construction.

2 in. (0.6 to 5 cm) and lengths ranging from 2 to 12 in. (5 to 30 cm). The dowels were placed into each debris cluster in a random orientation to achieve the overall desired porosity of 25% of the gross volume. To verify that this specification was achieved, Archimedes's principle was applied. A water tank large enough to contain all the various debris cluster sizes and shapes was filled with water, and each debris cluster was then submerged. The displaced water was measured and divided by the gross volume of the cluster to confirm the porosity. Figure 3.45 illustrates the tank and an example debris cluster being tested to determine the porosity.

3.5.3 Baseline Tests

Bed Material and Incipient Motion

The sand comprising the bed material in the test flume was characterized by a d_{50} grain size of approximately 0.70 mm. The coefficient of uniformity, C_u, defined as d_{60}/d_{10}, was 3.14. A representative grain size distribution graph is shown in Figure 3.46.

The critical velocity, V_c, for incipient motion of the bed material was estimated using the method described in HEC-18 (Richardson and Davis 2001):

$$V_c = \frac{K_s^{1/2}\left(S_s - 1\right)^{1/2} d_{50}^{1/2} y^{1/6}}{n} \tag{3.1}$$

where:

V_c = Critical velocity for the initiation of motion, m/s
K_s = Shields parameter (dimensionless)
S_s = Specific gravity of sediment (dimensionless)
d_{50} = Median particle diameter, ft (m)
y = Flow depth, ft (m)
n = Manning's resistance coefficient

Assuming that Manning's n value can be estimated from Strickler's equation as $n = 0.041(d_{50})^{1/6}$ where d_{50} is in meters, and using a range of the Shields parameter from 0.039 to

a. Woven geotextile used in filing debris clusters.

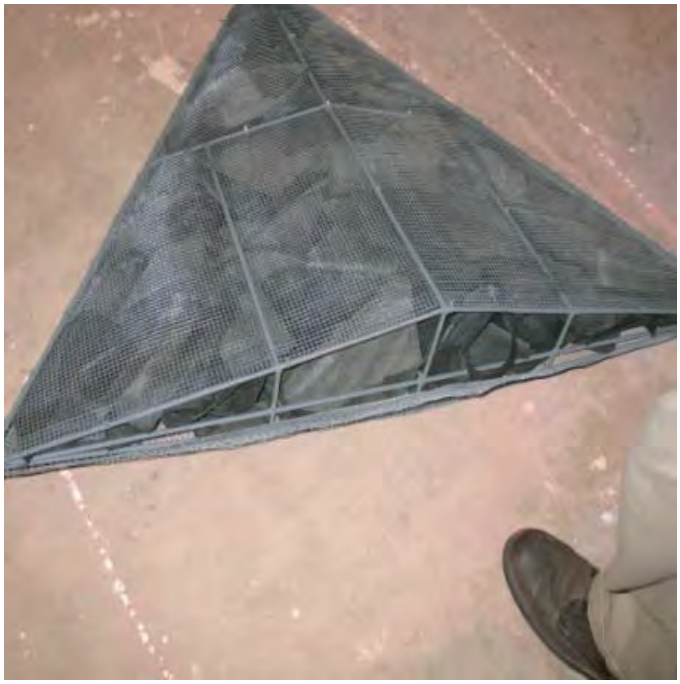

b. Wedge-shaped, impermeable debris cluster after being filled with geotextile.

Figure 3.43. Impermeable debris clusters.

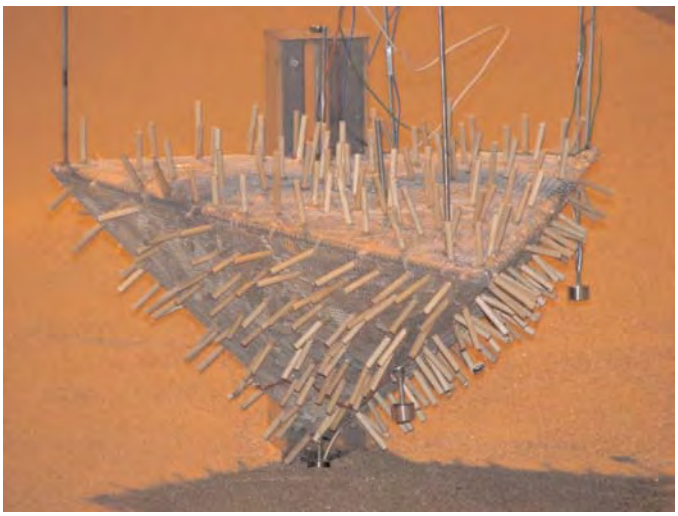

Figure 3.44. Typical photograph showing 2 in. (5 cm) wood dowels used to simulate roughness.

Figure 3.45. Determining porosity of debris cluster.

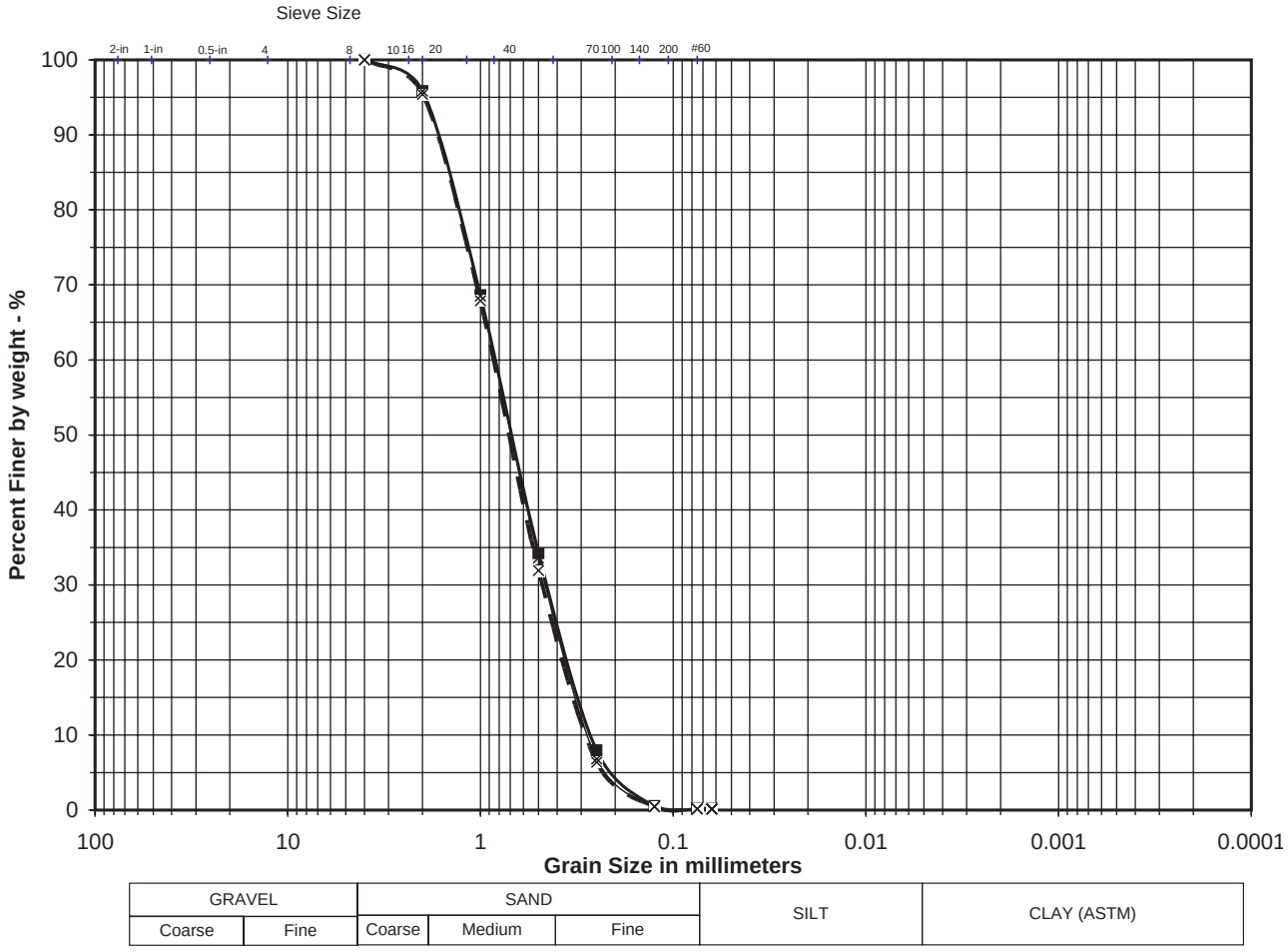

Figure 3.46. Grain size distribution of bed material.

0.047 for the initiation of movement, the critical velocity is estimated to range from 1.5 to 1.6 ft/s (0.45 to 0.49 m/s).

From this analysis, a conservative value of 1.4 ft/s (0.43 m/s) was selected for establishing the target approach velocities. The intent was to create a condition for the initial run that resulted in true clear-water conditions, with no movement of the bed material except for local scour in the immediate vicinity of the piers. Tests confirmed that an approach velocity of 1.4 ft/s (0.43 m/s) resulted in no bed material movement except for local scour.

Predicted Scour

CSU Equation. The ultimate (equilibrium) depth of local scour at a pier for clear-water conditions can be estimated using the CSU equation as presented in HEC-18 (Richardson and Davis 2001):

$$\frac{y_s}{a} = 2.0K_1K_2K_3K_4\left(\frac{y_1}{a}\right)^{0.35} Fr_1^{0.43} \tag{3.2}$$

where:

y_s = Depth of scour, ft (m)
y_1 = Flow depth directly upstream of the pier, ft (m)
K_1 = Correction factor for pier nose shape
K_2 = Correction factor for angle of attack of flow
K_3 = Correction factor for bed condition
K_4 = Correction factor for armoring by bed material size
a = Pier width, ft (m)
Fr_1 = Froude number directly upstream of the pier

For a square nose pier, $K_1 = 1.1$, and for a group of cylinders, $K_1 = 1.0$; for an angle of attack equal to zero, $K_2 = 1$. For plane bed clear-water scour, $K_3 = 1.1$, and for no armoring of the bed material, $K_4 = 1.0$. Pier widths were 4 in. (10.2 cm) for the square piers, 1 in. (2.5 cm) for the rectangular wall piers, and 0.5 in. (1.3 cm) for the multiple-column cylindrical piers.

The Froude number of the approach flow was determined by:

$$Fr_1 = \frac{V_1}{\sqrt{gy_1}} \tag{3.3}$$

where:

V_1 = Mean velocity of flow directly upstream of the pier, ft/s (m/s)
g = Acceleration of gravity, ft/s^2 (m/s^2)

The approach flow depth directly upstream of the pier was established at a depth of 1 ft (0.305 m) for all tests. The approach velocity, V_1, was found to be approximately 1.2 times the cross-sectional average velocity due to the location of the piers along the centerline of the flume. Therefore, using a target cross-sectional average velocity of 1.4 ft/s (0.43 m/s), the computed Froude number was 0.30.

Sheppard Equation. Sheppard et al. (2004) present an alternative method for predicting the ultimate depth of clear-water scour at a pier:

$$d_s = 2.5D^* f_1\left(\frac{y_0}{D^*}\right) f_2\left(\frac{V}{V_c}\right) f_3\left(\frac{D^*}{D_{50}}\right) \tag{3.4}$$

The functions f_1, f_2, and f_3 are defined as:

$$f_1\left(\frac{y_0}{D^*}\right) = \tanh\left[\left(\frac{y_0}{D^*}\right)^{0.4}\right] \tag{3.5}$$

$$f_2\left(\frac{V}{V_c}\right) = 1 - 1.75\left[\ln\left(\frac{V}{V_c}\right)\right]^2 \tag{3.6}$$

$$f_3\left(\frac{D^*}{D_{50}}\right) = \frac{\left(D^*/D_{50}\right)}{0.4\left(D^*/D_{50}\right)^{1.2} + 10.6\left(D^*/D_{50}\right)^{-0.13}} \tag{3.7}$$

where:

d_s = Equilibrium scour depth, ft (m)
D^* = Effective pier width, ft (m) where $D^* = 1.0$ times the diameter of a circular pier or 1.23 times the width of a square pier
y_0 = Depth of approach flow, ft (m)
V = Velocity of approach flow, ft/s (m/s)
V_c = Critical velocity of bed material, ft/s (m/s)
D_{50} = Median particle size, ft (m)

The computed values of local scour at a baseline pier (free from debris) using the CSU and Sheppard equations under the conditions described above are presented in Table 3.6.

Contraction Scour. A modified version of Laursen's equation, as presented in HEC-18 (Richardson and Davis 2001), was used to determine depth of scour in a contracted section under clear-water conditions.

Table 3.6. Computed local scour depths for baseline conditions.

Pier Size and Type	CSU Equation	Sheppard Equation
4" square pier	0.71 ft (0.22 m)	0.79 ft (0.24 m)
1" rectangular wall pier	0.29 ft (0.09 m)	0.25 ft (0.08 m)
0.5" cylindrical columns	0.17 ft (0.05 m)	0.09 ft (0.03 m)

$$y_2 = \left[\frac{K_u Q^2}{d_m^{2/3} w^2}\right]^{3/7} \quad (3.8)$$

$y_s = y_2 - y_o$ = average contraction scour depth, ft (m)

where:

y_2 = Average equilibrium depth in the contracted section after contraction scour, ft (m)
Q = Flow discharge through the contracted section, ft³/s (m³/s)
d_m = Diameter of the smallest non-transportable particle in the bed material in the contracted section computed from d_m (m) = (1.25 * d_{50})
W = Bottom width of the contracted section less pier widths, ft (m)
K_u = Equal to 0.025 for SI units (0.0077 for English units)
y_o = Existing depth in the contracted section before scour, ft (m)

For the square piers, using a total discharge Q = 11.2 ft³/s (0.32 m³/s) from continuity, W = width of the flume [8 ft (2.4 m)] less the width of the pier, and d_{50} = 0.7 mm (0.0023 ft), Equation 3.8 predicts that no contraction scour was anticipated for any of the piers under baseline (no-debris) conditions.

Testing

Baseline tests were designed as control tests to provide scour data for piers under clear-water conditions. No debris was affixed to the piers, allowing for determination of baseline scour for all pier shapes. Figure 3.47 shows the results for square piers after 72 hours of testing; the upper segment of the pier has been removed for data collection purposes and ambient bed elevation is represented by the top of the lower segment of the pier. Figure 3.48 shows the results for multiple-column and wall piers. Arrows indicate direction of flow on the photographs. Table 3.7 provides the results (maximum scour at the pier only), details on the run number, hydraulic conditions, duration, and location of the baseline tests. Note that all scour depth measurements in Table 3.7 were taken at the nose of the pier.

Figure 3.47. Square pier after 72-hour test with no debris (flow from right to left).

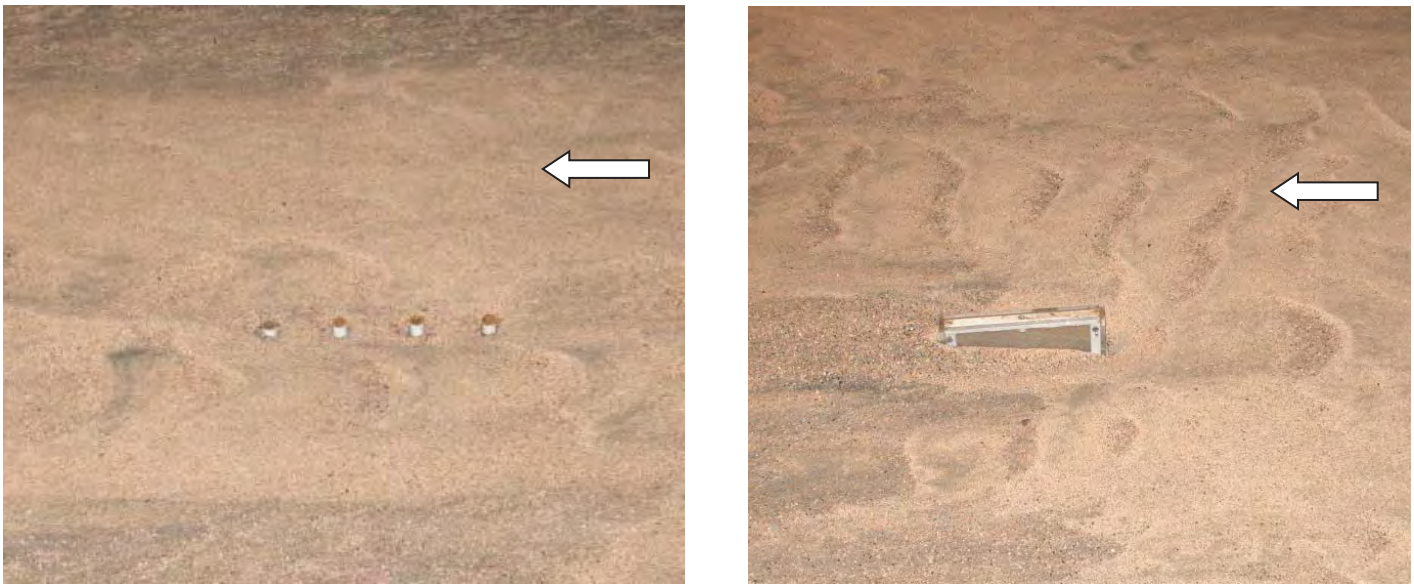

a. Multiple 0.5" column pier after 72-hour test with no debris

b. 1" wall pier after 72-hour test with no debris

Figure 3.48. Baseline tests of multiple-column and wall piers.

Table 3.7. Maximum measured scour, baseline tests.

Run No.	Pier	Nominal V/V_c	Duration (h)	Maximum Measured Scour Depth (ft)	Pier Shape
003_01	A	0.7	72	0.67	4" square
003_01	D	0.7	72	0.41	4" square
004_01	A	0.7	8	0.49	4" square
004_01	B	0.7	8	0.38	4" square
004_01	C	0.7	8	0.34	4" square
004_01	D	0.7	8	0.34	4" square
003_02	A	1.0	72	1.02	4" square
003_02	D	1.0	72	0.86	4" square
004_02	A	1.0	8	0.85	4" square
004_02	B	1.0	8	0.70	4" square
004_02	C	1.0	8	0.68	4" square
004_02	D	1.0	8	0.70	4" square
009_01	B	1.0	72	0.80	4" square
003_01	C	0.7	72	0.16	1" rectangular wall
003_02	C	1.0	72	0.26	1" rectangular wall
008_01	A	1.0	8	0.17	1" rectangular wall
003_01	B	0.7	72	0.10	0.5" cylindrical columns
003_02	B	1.0	72	0.10	0.5" cylindrical columns
008_01	B	1.0	8	0.11	0.5" cylindrical columns

3.5.4 Tests with Debris

The goal of the laboratory plan was to develop a series of tests for a wide range of debris configurations that could be run quickly and efficiently. Tests were performed for single debris clusters at individual piers. The literature review, survey results, photographic archive, and site reconnaissance were used to determine the number of alternatives that should be included to investigate a representative range of bridge-specific debris characteristics. Initial runs considered various debris geometric characteristics (see Section 3.4.2). These tests were then supplemented to address issues of porosity and roughness.

All test runs were performed for clear-water sediment transport conditions (approach flow velocity less than the critical velocity required to initiate sediment transport). Typically, the test duration was 8 hours after steady flow conditions were established. Selected pier shapes and debris cluster types were run for 72 hours.

Rectangular Debris

Nine geometrically unique rectangular (in planform and profile) debris shapes were tested. Variations in testing included location within the water column, pier type, roughness, and porosity for a total of 39 tests. Five of these tests were conducted at a nominal velocity of 0.7 V_c; the remaining 34 tests were conducted at 1.0 V_c. Figure 3.49 provides a definition sketch of the rectangular debris geometry and associated variables.

Table 3.8 shows the tests performed at 4 in. by 4 in. (10.2 cm by 10.2 cm) square piers, while Table 3.9 shows the tests performed at 1 in. (2.5 cm) rectangular wall piers (no skew) and 0.5 in. (1.3 cm) cylindrical column piers (no skew). Each letter in the table denotes a specific test and the variable examined.

Figure 3.50 shows a 1 ft wide by 1 ft long by 1 ft high rectangular debris configuration incorporating roughness and porosity prior to Test 009_01C. Figure 3.51 shows the results from the debris configuration presented in the previous figure after 72 hours of testing at 1 V_c. The upper segment of the pier has been removed for data collection purposes, and ambient bed elevation is represented by the top of the lower segment of the pier.

Figure 3.52 shows a 4 ft wide by 3 ft long by 8 in. high debris configuration incorporating roughness and porosity prior to Test 004_03C. Figure 3.53 shows the results from the debris configuration presented in the previous figure after 8 hours of testing at 0.7 V_c. The upper segment of the pier has been removed for data collection purposes, and ambient bed elevation is represented by the top of the lower segment of the pier.

Figure 3.54 shows a 2 ft wide by 1 ft high, wedge-shaped debris cluster before Test 007_02B, incorporating roughness and porosity. Figure 3.55 shows the results from the debris configuration presented in the previous figure after 8 hours of testing at 1 V_c; the upper segment of the pier has been removed for data collection purposes and ambient bed elevation is represented by the top of the lower segment of the pier.

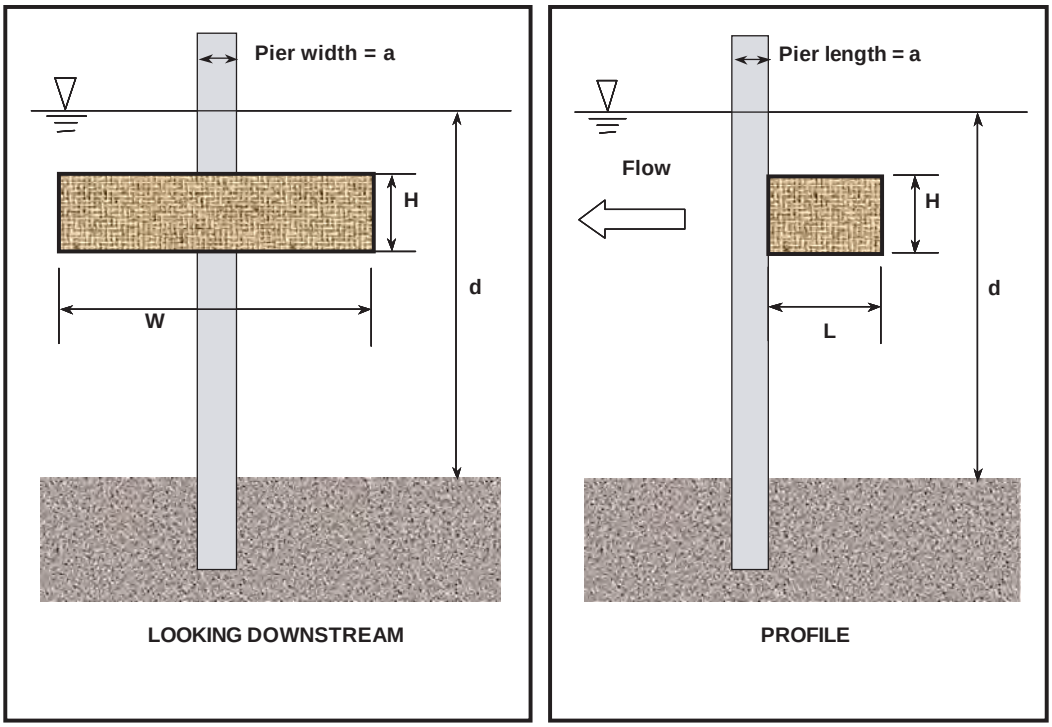

Figure 3.49. Rectangular debris geometry and associated variables.

Table 3.8. Square piers with rectangular debris.

Debris Width (ft)	Debris Length (ft)	Debris Height (ft)	W/a	L/a	H/d	Position		
						Surface	Mid-depth	Bed
1.0	1.0	1.0	3	3	3/3	**I**, **P**, **R**, **C**, **C**(72)		
2.0	1.0	0.33	6	3	1/3	**I**, **P**, **R**, **C**(72)		
2.0	1.0	0.67	6	3	2/3	**I**, **P**, **R**		**I**
2.0	2.0	0.33	6	6	1/3	**I**, **P**, **C**(72), **P**(72)	**I**	**I**
2.0	2.0	0.67	6	6	2/3	**I**	**I**, **P**, **R**	**I**
2.0	3.0	0.67	6	9	2/3	**C**		
4.0	3.0	0.67	12	9	2/3	**I**, **C**	**C**	
6.0	4.0	0.67	18	12	2/3	**I**, **I**(72)		
Wedge Shape Variant, Rectangular in Plan, Triangular in Section								
2.0	1.0	0.67	6	3	2/3	**C**, **C**(72)		

W = Debris width
L = Debris length
H = Debris height
a = Pier dimension
d = Depth of water

I = Impermeable fill, no roughness
P = Porosity tested independently, no roughness
R = Roughness tested independently, no porosity
C = Porosity and roughness tested together (combined)
(72) = Test ran for 72 hours

Table 3.9. Wall and multiple-column piers with rectangular debris.

Debris Width (ft)	Debris Length (ft)	Debris Height (ft)	W/a	L/a	H/d	Position		
						Surface	Mid-depth	Bed
1.0	1.0	1.0	12	12	3/3	**C** (1" wall pier)		
1.0	1.0	0.67	24	24	2/3	**C** (0.5" columns)		
4.0	3.0	0.67	96	72	2/3		**C** (0.5" columns)	
Wedge Shape Variant, Rectangular in Plan, Triangular in Section								
2.0	1.0	0.67	48	24	2/3	**C** (0.5" columns)		

W = Debris width
L = Debris length
H = Debris height
a = Pier dimension
d = Depth of water
C = Porosity and roughness tested together (combined)

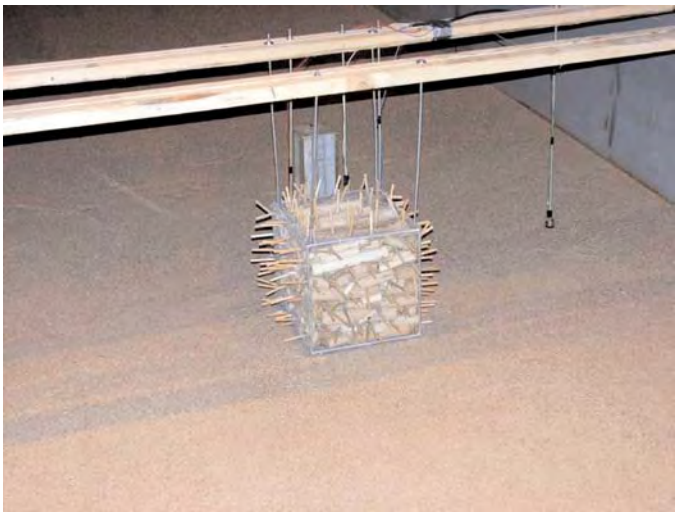

Figure 3.50. Rectangular debris cluster before Test 009_01C.

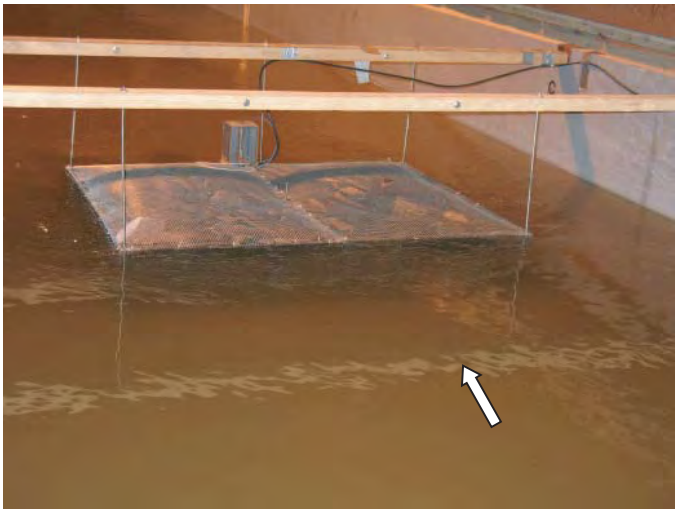

Figure 3.52. 4'W × 3'L × 8''H debris cluster located at the water surface during Test 004_03C.

Table 3.10 provides the results (maximum scour at the pier only) of tests performed with rectangular debris configurations. Most scour depth measurements in Table 3.10 were taken at the pier nose. When nose scour measurements were not possible due to location of the debris in the vicinity of the bed, data was collected at the upstream corner of the pier; this is denoted by the use of a "c" after the test number.

Triangular/Conical Debris

Seven geometrically unique conical debris shapes (triangular in planform) were tested. Variations in testing included location within the water column, pier type, roughness, and porosity for a total of 14 tests. Three of these tests were conducted at a nominal velocity of 0.7 V_c; the remaining 11 tests were conducted at 1.0 V_c. Figure 3.56 provides a definition sketch of the triangular/conical debris geometry and associated variables.

Table 3.11 shows the tests performed at 4 in. by 4 in. (10.2 cm by 10.2 cm) square piers. Table 3.12 shows the tests performed at multiple-column and wall piers. Each letter in the table denotes a specific test and the variable examined.

Figure 3.57 shows a 4 ft wide by 3 ft long by 1 ft high triangular/conical debris configuration incorporating roughness and porosity before testing. Figure 3.58 shows the results

Ambient bed elevation is represented by the top of the pier. Upper segment of the pier and the debris configuration have been removed for data collection purposes.

Figure 3.51. Scour hole resulting from Test 009_01C after 72 hours of testing at 1 V_c.

Ambient bed elevation is represented by the top of the pier. Upper segment of the pier and the debris configuration have been removed for data collection purposes. Note that the deepest scour occurred upstream and away from the pier face.

Figure 3.53. Scour hole resulting from Test 004_01C after 8 hours of testing at 0.7 V_c.

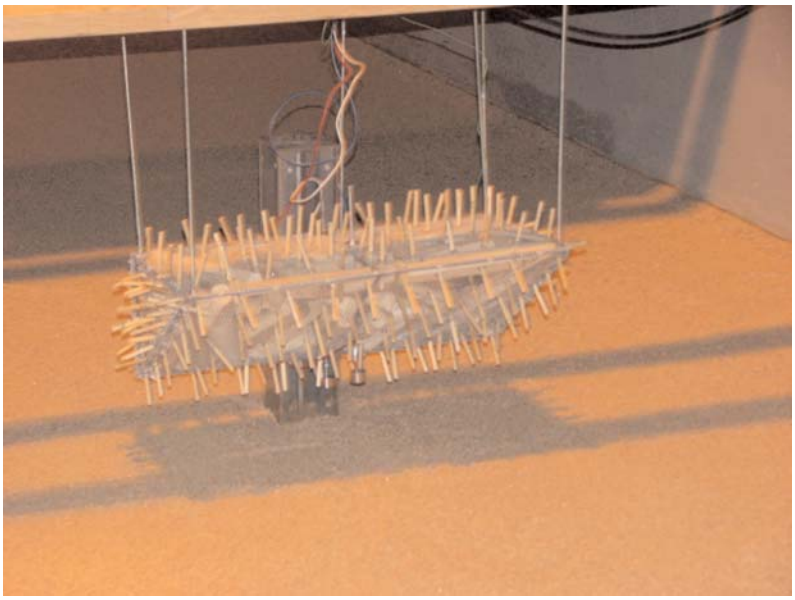

Figure 3.54. Wedge-shaped debris cluster before Test 007_02B.

from the debris configuration presented in the previous figure after 8 hours of testing at 1 V_c; the upper segment of the pier has been removed for data collection purposes and ambient bed elevation is represented by the top of the lower segment of the pier.

Table 3.13 provides the results of tests performed with triangular/conical debris configurations at a pier. Most scour depth measurements in Table 3.13 were taken at the pier nose. When nose scour measurements were not possible due to location of the debris in the vicinity of the bed, data was collected at the upstream pier corner; this is denoted by a "c" after the test number.

Figure 3.59 shows a 2 ft wide ×3 ft long ×8 in. high, impermeable, buried wedge debris configuration before Test 003_03D. Figure 3.60 shows the results from the debris configuration presented in the previous figure after 8 hours of testing at 0.7 V_c and an additional 8 hours of testing at 1 V_c; the upper segment of the pier has been removed for data collection purposes, and ambient bed elevation is represented by the top of the lower segment of the pier.

Ambient bed elevation is represented by the top of the pier. Upper segment of the pier and the debris configuration have been removed for data collection purposes. Note that the deepest scour is coincident with the pier face.

Figure 3.55. Scour hole resulting from Test 007_02B after 8 hours of testing at 1 V_c.

3.6 Appraisal of Testing Results

3.6.1 Baseline (No-Debris) Tests

Predicted vs. Measured Scour

A total of 19 baseline tests were run under clear-water scour conditions. Thirteen baseline tests were conducted using 4 in. (10.2 cm) square piers. Six of the square pier tests were conducted at a nominal (target) approach velocity of 0.7 V_{crit}, where V_{crit} was estimated to be 1.4 ft/s (0.43 m/s) for the initiation of motion of the bed material. The remaining seven square pier tests were conducted at a nominal velocity of 1.0 V_{crit}.

Three baseline tests were conducted using 1 in. by 8 in. (2.5 cm by 20 cm) rectangular wall piers with no skew angle. One of those tests was conducted at a nominal velocity of 0.7 V_{crit}, and the other two tests were run at 1.0 V_{crit}.

Three baseline tests were conducted using piers having multiple 0.5 in. (1.25 cm) cylindrical columns with no skew angle. One of those tests was conducted at a nominal velocity of 0.7 V_{crit}, and the other two tests were run at 1.0 V_{crit}.

Table 3.10. Results of Rectangular Debris Tests.

Run No.	Pier	V/V_c	Duration (h)	Max Measured Scour Depth d_s(ft)	Transducer Location	Debris Shape	Width (ft)	Length (ft)	Height (ft)	Debris Location	Pier Type	Debris Characteristic
005_02C-c	C	1.0	8	0.42	at corner	cube	1	1	1	full depth	square	impermeable
006_01C-c	C	1.0	8	0.47	at corner	cube	1	1	1	full depth	square	roughness
006_02C-c	C	1.0	8	0.47	at corner	cube	1	1	1	full depth	square	porosity
008_01C-c	C	1.0	8	0.51	at corner	cube	1	1	1	cube	wall	roughness and porosity
009_01D-c	D	1.0	72	0.75	at corner	cube	1	1	1	cube	square	roughness and porosity
005_02B	B	1.0	8	0.92	at nose	rectangle	2	1	0.33	surface	square	impermeable
006_01B	B	1.0	8	0.91	at nose	rectangle	2	1	0.33	surface	square	roughness
006_02A	B	1.0	8	1.11	at nose	rectangle	2	1	0.67	surface	square	porosity
009_02C	C	1.0	72	1.06	at nose	rectangle	2	1	0.33	surface	square	roughness and porosity
005_01A-c	A	1.0	8	0.81	at corner	rectangle	2	1	0.67	bed	square	impermeable
005_02A	A	1.0	8	1.21	at nose	rectangle	2	1	0.67	surface	square	impermeable
006_01A	A	1.0	8	1.16	at nose	rectangle	2	1	0.67	surface	square	roughness
006_02B	A	1.0	8	1.00	at nose	rectangle	2	1	0.33	surface	square	porosity
003_03A-c	A	0.7	8	0.46	at corner	rectangle	2	2	0.33	surface	square	impermeable
003_04A-c	A	1.0	8	0.75	at corner	rectangle	2	2	0.33	surface	square	impermeable
004_03A	A	0.7	8	0.42	at nose	rectangle	2	2	0.33	mid-depth	square	impermeable
004_04A	A	1.0	8	0.70	at nose	rectangle	2	2	0.33	mid-depth	square	impermeable
005_01B-c	B	1.0	8	0.35	at corner	rectangle	2	2	0.33	bed	square	impermeable
009_01A	A	1.0	72	1.14	at nose	rectangle	2	2	0.33	surface	square	roughness and porosity
009_02A	A	1.0	72	1.13	at nose	rectangle	2	2	0.33	surface	square	porosity
004_03B	B	0.7	8	0.40	at nose	rectangle	2	2	0.67	surface	square	impermeable
004_04B	B	1.0	8	0.66	at nose	rectangle	2	2	0.67	surface	square	impermeable
005_01D-c	D	1.0	8	0.35	at corner	rectangle	2	2	0.67	bed	square	impermeable
005_02D-c	D	1.0	8	0.55	at corner	rectangle	2	2	0.67	mid-depth	square	impermeable
006_01D-c	D	1.0	8	0.42	at corner	rectangle	2	2	0.67	mid-depth	square	roughness
008_01D	D	1.0	8	0.30	at nose	rectangle	2	2	0.67	surface	multiple column	roughness and porosity
007_01B	B	1.0	8	0.59	at nose	rectangle	2	3	0.67	surface	square	roughness and porosity
004_03C	C	0.7	8	0.49	at nose	rectangle	4	3	0.67	surface	square	impermeable
004_04C	C	1.0	8	0.74	at nose	rectangle	4	3	0.67	surface	square	impermeable
007_01D	D	1.0	8	0.85	at nose	rectangle	4	3	0.67	surface	square	roughness and porosity
007_02bD	D	1.0	8	0.91	at nose	rectangle	4	3	0.67	mid-depth	square	roughness and porosity
008_02D	D	1.0	8	0.72	at nose	rectangle	4	3	0.67	mid-depth	multiple column	roughness and porosity
004_03D	D	0.7	8	0.58	at nose	rectangle	6	4	0.67	surface	square	impermeable
004_04D	D	1.0	8	0.95	at nose	rectangle	6	4	0.67	surface	square	impermeable
009_02D	D	1.0	72	1.23	at nose	rectangle	6	4	0.67	surface	square	impermeable
007_02bB	B	1.0	8	0.92	at nose	wedge	4	6	0.67	surface	square	roughness and porosity
008_02B	B	1.0	8	0.45	at nose	wedge	2	1	0.67	surface	multiple column	roughness and porosity
000_01C	C	1.0	72	1.08	at nose	wedge	2	1	0.67	surface	square	roughness and porosity

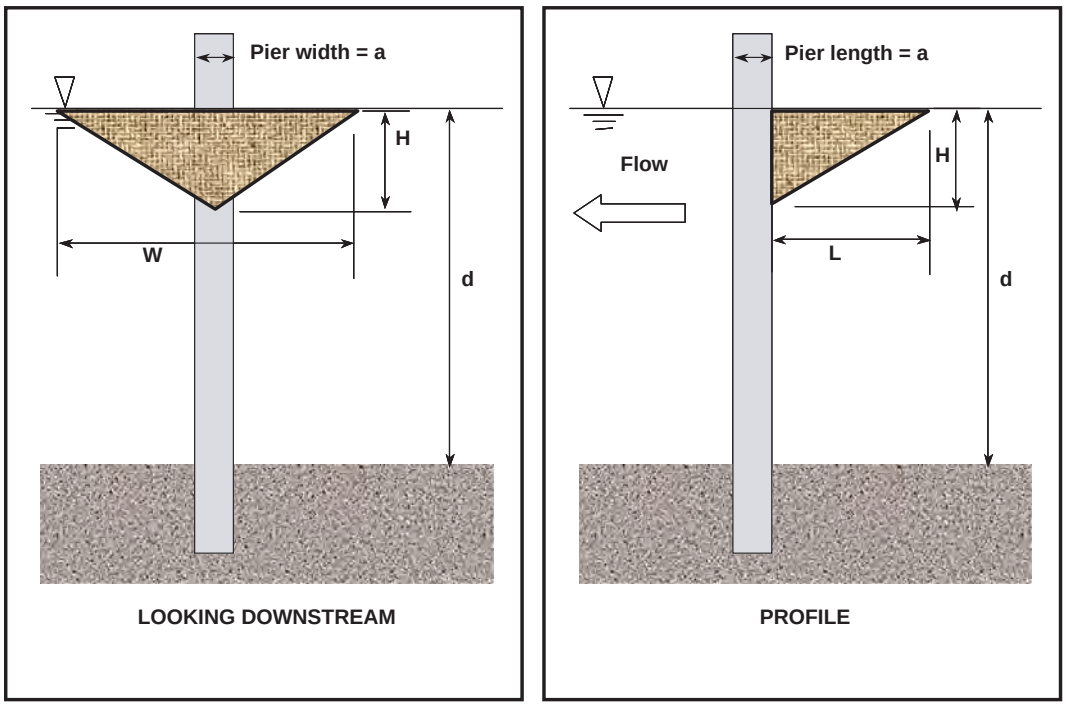

Figure 3.56. Triangular/conical debris geometry and associated variables.

Table 3.11. Square piers with triangular/conical debris.

Debris Width (ft)	Debris Length (ft)	Debris Height (ft)	W/a	L/a	H/d	Position and Shape			
						Surface	Bed	Bed (partially buried) $H_2/H_1 = 1$	Bed (partially buried) $H_2/H_1 = 0.5$
2.0	2.0	0.67	6	6	2/3	**C**			
2.0	3.0	0.33	6	9	1/3	**I**			
2.0	3.0	0.67	6	9	2/3	**I**	**I**		
2.0	3.0	1.0	6	9	3/3	**C**			
4.0	3.0	0.67	12	9	2/3				**I**
4.0	3.0	1.0	12	9	3/3	**C**, **C**(72)			
4.0	6.0	0.67	12	18	2/3	**C**			

W = Debris width
L = Debris length
H = Debris height
a = Pier dimension
d = Depth of water
I = Impermeable fill, no roughness
C = Porosity and roughness tested together (combined)
(72) = Test ran for 72 h

Table 3.12. Wall and multiple-column piers with triangular/conical debris.

Debris Width (ft)	Debris Length (ft)	Debris Height (ft)	W/a	L/a	H/d	Position and Shape			
						Surface	Bed	Bed (partially buried) $H_2/H_1 = 1$	Bed (partially buried) $H_2/H_1 = 0.5$
2.0	3.0	0.67	24	36	3/3	**C** (1" wall pier)			
4.0	3.0	0.33	48	36	3/3	**C** (1" wall pier)			

W = Debris width
L = Debris length
H = Debris height
a = Pier dimension
d = Depth of water
C = Porosity and roughness tested together (combined)

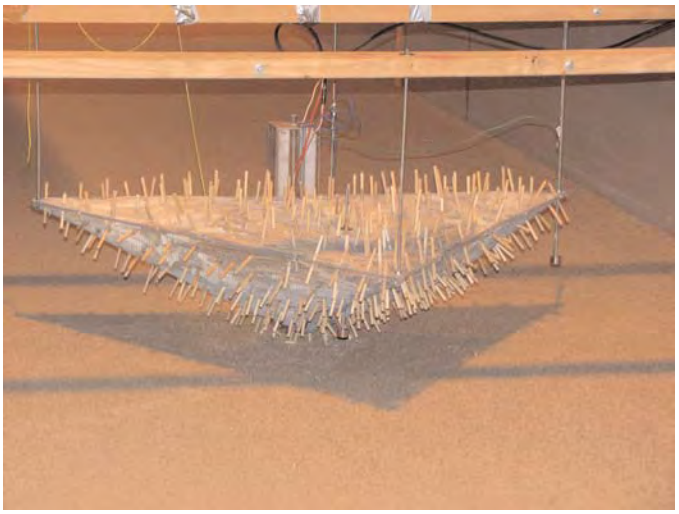

Figure 3.57. Triangular/conical debris cluster before Test 007_02A, mounted such that the top surface of the debris was located at the water surface.

Ambient bed elevation is represented by the top of the pier. Upper segment of the pier and the debris configuration have been removed for data collection purposes.

Figure 3.58. Scour hole resulting from Test 007_02A after 8 hours of testing at 1.0 V_c.

Table 3.13. Results of triangular/conical debris tests.

Run No.	Pier	V/V_c	Duration (h)	Max Measured Scour Depth d_s(ft)	Transducer Location	Debris Shape	Width (ft)	Length (ft)	Height (ft)	Debris Location	Pier Type	Debris Characteristic
007_01A	A	1.0	8	0.86	at nose	conical	2	2	0.67	surface	square	roughness and porosity
003_03B-c	B	0.7	8	0.41	at right corner	conical	2	3	0.33	surface	square	impermeable
003_04B-c	B	1.0	8	0.72	at right corner	conical	2	3	0.33	surface	square	impermeable
003_03D-c	D	0.7	8	0.41	at right corner	conical	2	3	0.67	buried	square	impermeable
003_04D-c	D	1.0	8	0.69	at right corner	conical	2	3	0.67	buried	square	impermeable
005_01C-c	C	1.0	8	0.19	at right corner	conical	2	3	0.67	bed	square	impermeable
007_02bC	C	1.0	8	0.80	at nose	conical	2	3	1	surface	square	roughness and porosity
008_02C	C	1.0	8	0.37	at nose	conical	2	3	1	surface	wall	roughness and porosity
007_02bA	A	1.0	8	1.15	at nose	conical	4	3	1	surface	square	roughness and porosity
008_02A	A	1.0	8	0.54	at nose	conical	4	3	1	surface	wall	roughness and porosity
009_02B	B	1.0	72	1.19	at nose	conical	4	3	1	surface	square	roughness and porosity
007_01C	C	1.0	8	0.77	at nose	conical	4	6	0.67	surface	square	roughness and porosity
003_03C-c	C	0.7	8	0.09	at right corner	conical	2	3	0.67	surface	square	H2/H1-0.5
003_04C-c	C	1.0	8	0.21	at right corner	conical	2	3	0.67	surface	square	H2/H1-0.6

Figure 3.59. Buried wedge debris cluster placed on the bed showing initiation of flow during test.

Most tests were run for 8 hours. However, selected tests were conducted with a duration of 72 hours. Because equations for assessing pier scour are intended to reflect ultimate (equilibrium) conditions, the observed scour depths in the laboratory flume were adjusted to reflect estimated equilibrium scour. The method provided in Melville and Coleman (2000) for estimating the time dependency of clear-water pier scour was used to develop a best estimate of the equilibrium condition, as follows:

Ambient bed elevation is represented by the top of the pier. Upper segment of the pier and the debris configuration have been removed for data collection purposes.

Figure 3.60. Scour hole resulting from Test 007_02A after 8 hours of testing at 0.7 V_c and an additional 8 hours of testing at 1.0 V_c.

$$K_t = \exp\left\{-0.03\left|\frac{V_c}{V}\ln\left(\frac{t}{t_e}\right)\right|^{1.6}\right\} \tag{3.9}$$

where:

K_t = Fraction of ultimate scour reached at time t (dimensionless)
t = Elapsed time from start of scour, days
t_e = Time to ultimate (equilibrium) scour, days
V_c = Critical velocity for the initiation of motion of bed sediment, ft/s (m/s)
V = Approach velocity upstream of pier, ft/s (m/s)

and the time to ultimate scour is given by:

$$t_e = 30.89\frac{a}{V}\left(\frac{V}{V_c} - 0.4\right)\left(\frac{y}{a}\right)^{0.25} \tag{3.10}$$

where:

a = Pier width or diameter, ft (m)
y = Depth of approach flow, ft (m)
t_e = Time to ultimate (equilibrium) scour, days

72-Hour Tests. The analysis of the time dependency of scour in the laboratory flume indicated that, for all tests, the 72-hour duration runs resulted in 98% to 100% of the expected ultimate scour depth at the pier face. Therefore, observed scour was adjusted minimally for all 72-hour tests, regardless of pier type.

8-Hour Tests. In contrast to the 72-hour tests, the 8-hour tests resulted in measured scour depths that were significantly less than the estimated ultimate scour. For the 4 in. square piers, the 8-hour tests at 0.7 V_{crit} ranged from 77% to 81% of ultimate scour, while the tests at 1.0 V_{crit} ranged from 84% to 87% of ultimate scour. The slimmer wall piers and multiple-column piers reached about 93% to 96% of ultimate scour after 8 hours.

Table 3.14 summarizes the results of the baseline (no-debris) tests. In this table, the actual approach velocity as measured by ADV and the measured approach flow depth are shown, because both velocity and depth during any particular test were typically slightly higher or lower than the target conditions. The table also shows the measured scour depths at the end of each test, the ultimate scour depth estimated by the Melville method, and the ultimate scour depth predicted by the CSU equation. Figure 3.61 presents the results of the scour predictions vs. equilibrium scour in graphical form.

For the runs conducted at a target velocity of 1.0 V_{crit}, the ratio of clear-water equilibrium scour depth, Y_{se}, to pier width, a, was slightly different depending on pier type, as follows:

4 in. square piers (7 tests): $2.4 < \frac{Y_{se}}{a} < 2.6$

Table 3.14. Pier scour for baseline tests (no debris).

Run No.	Pier	Velocity ratio V/V_c		Meas. Approach Depth (ft)	Test Duration (h)	Measured Scour[1] (ft)	Estimated Ultimate Scour (ft)	Predicted Scour, CSU Equation (ft)
		Target	Meas.					
4 in. (10 cm) Square Piers								
003_01	A	0.7	0.81	1.00	72	0.54	0.55	0.59
003_01	D	0.7	0.65	1.05	72	0.41	0.41	0.54
003_02	A	1.0	1.14	1.03	72	0.83	0.84	0.69
003_02	D	1.0	0.91	1.08	72	0.86	0.87	0.63
004_01	A	0.7	0.78	1.02	8	0.40	0.49	0.58
004_01	B	0.7	0.69	1.03	8	0.38	0.48	0.55
004_01	C	0.7	0.65	1.09	8	0.34	0.44	0.55
004_01	D	0.7	0.63	1.08	8	0.34	0.44	0.54
004_02	A	1.0	1.12	1.01	8	0.70	0.80	0.68
004_02	B	1.0	1.00	1.04	8	0.70	0.82	0.65
004_02	C	1.0	0.94	1.10	8	0.68	0.81	0.64
004_02	D	1.0	0.94	1.06	8	0.70	0.83	0.64
009_01	B	1.0	0.99	1.05	72	0.80	0.81	0.65
1 in. (2.5 cm) Wall Piers (no skew)								
003_01	C	0.7	0.64	1.08	72	0.16	0.16	0.22
003_02	C	1.0	0.90	1.09	72	0.26	0.26	0.25
008_01	A	1.0	1.02	1.04	8	0.17	0.18	0.27
Multiple 0.5 in. (1.25 cm) Cylindrical Columns (no skew)								
003_01	B	0.7	0.72	1.02	72	0.11	0.11	0.13
003_02	B	1.0	0.97	1.05	72	0.10	0.10	0.15
008_01	B	1.0	1.04	1.06	8	0.11	0.12	0.16

[1] Measured scour at Pier A was reduced by a factor of 1.23 to account for the observation that baseline scour was consistently larger at this pier.

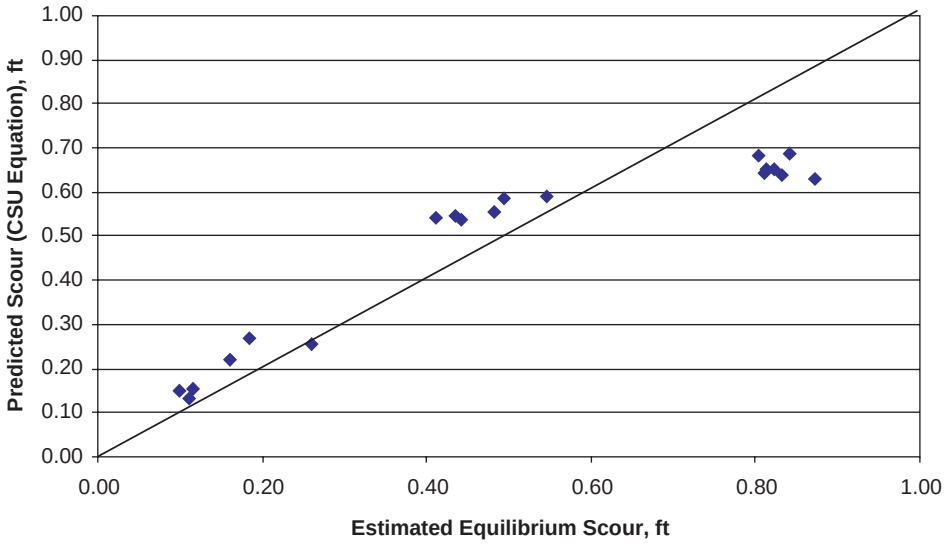

Figure 3.61. Predicted scour vs. equilibrium scour for all baseline tests.

1 in. wall piers (2 tests): $2.2 < \frac{Y_{se}}{a} < 3.1$

0.5 in. multiple columns (2 tests): $2.4 < \frac{Y_{se}}{a} < 2.7$

Equilibrium scour depths for baseline (no-debris) conditions must be identified for each of these pier types in order to assess the effect of debris on scour. The 1.0 V_{crit} condition was used to define baseline scour, as this condition represents the upper limit of clear-water scour, and because almost all of the laboratory tests with debris clusters used this condition.

The average of the equilibrium scour depths from tests on square, wall, and multiple-column piers used in this study were 0.83 ft, 0.22 ft, and 0.11 ft, respectively. These values were used as baseline values in the assessment of debris effects on pier scour for the remainder of the laboratory testing program.

Baseline tests typically resulted in a very symmetric elliptical scour hole (in plan view) for all pier shapes investigated. Figure 3.62 is a photograph of a typical scour hole for a baseline run at a 4 in. square pier. The resulting contour map of the scour from that test is provided in Figure 3.63. The lateral extent of the scour hole from the sides of the piers typically ranged from 2.0 to 2.5 times the depth of scour for all pier shapes.

3.6.2 Tests with Debris

Rectangular Debris Clusters

A total of 39 tests were run under clear-water scour conditions with rectangular (in plan and profile) debris clusters affixed to the upstream face of the piers. Five of those tests were conducted at a nominal (target) approach velocity of 0.7 V_{crit}, where V_{crit} was estimated to be 1.4 ft/s (0.43 m/s) for the initiation of motion of the bed material. The remaining 34 tests were conducted at a nominal velocity of 1.0 V_{crit}. All tests were conducted with a nominal approach flow depth of 1.0 ft.

(Test 009-01, Pier B)

Figure 3.62. Typical scour pattern at square pier with no debris.

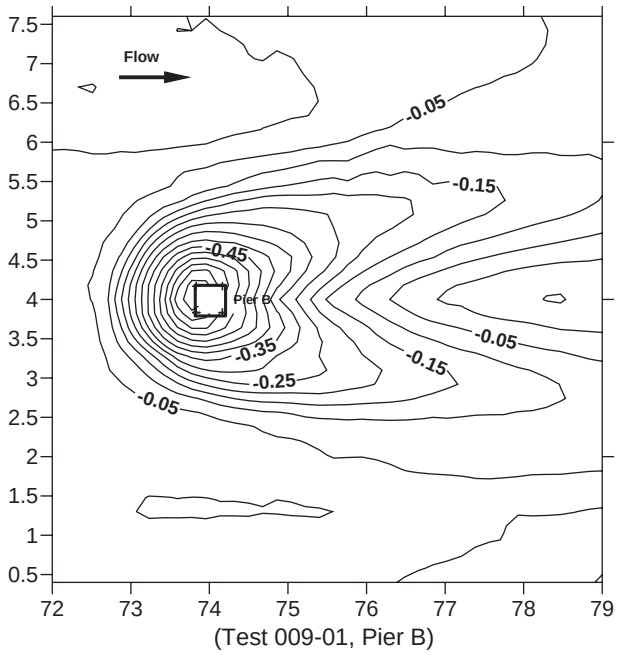

Figure 3.63. Typical scour contour map at square pier with no debris.

Rectangular debris clusters were fabricated with a range of dimensions as follows:

- Width: 1.0 to 6.0 ft (30 to 180 cm) (perpendicular to flow)
- Length: 1.0 to 4.0 ft (30 to 120 cm) (aligned with flow direction)
- Height: 0.33 to 1.0 ft (10 to 30 cm) (placed at various locations within the water column)

Debris clusters were fabricated both with and without roughness elements and filled with either wooden dowels to achieve 70% porosity or wadded geotextile swatches to achieve an essentially impermeable mass. Figure 3.64 is a photograph of a porous, permeable rectangular debris cluster that incorporates roughness elements. Dye tests performed at rectangular debris clusters showed that at the face of the debris mass, flow tended to plunge directly beneath the debris. Very little flow is shed around the sides of a rectangular debris cluster, as seen in the figure.

Table 3.15 summarizes the results of the rectangular debris tests. In this table, the actual approach velocity as measured by ADV and the measured approach flow depth are shown, because both velocity and depth during any particular test were typically slightly higher or lower than target conditions. The

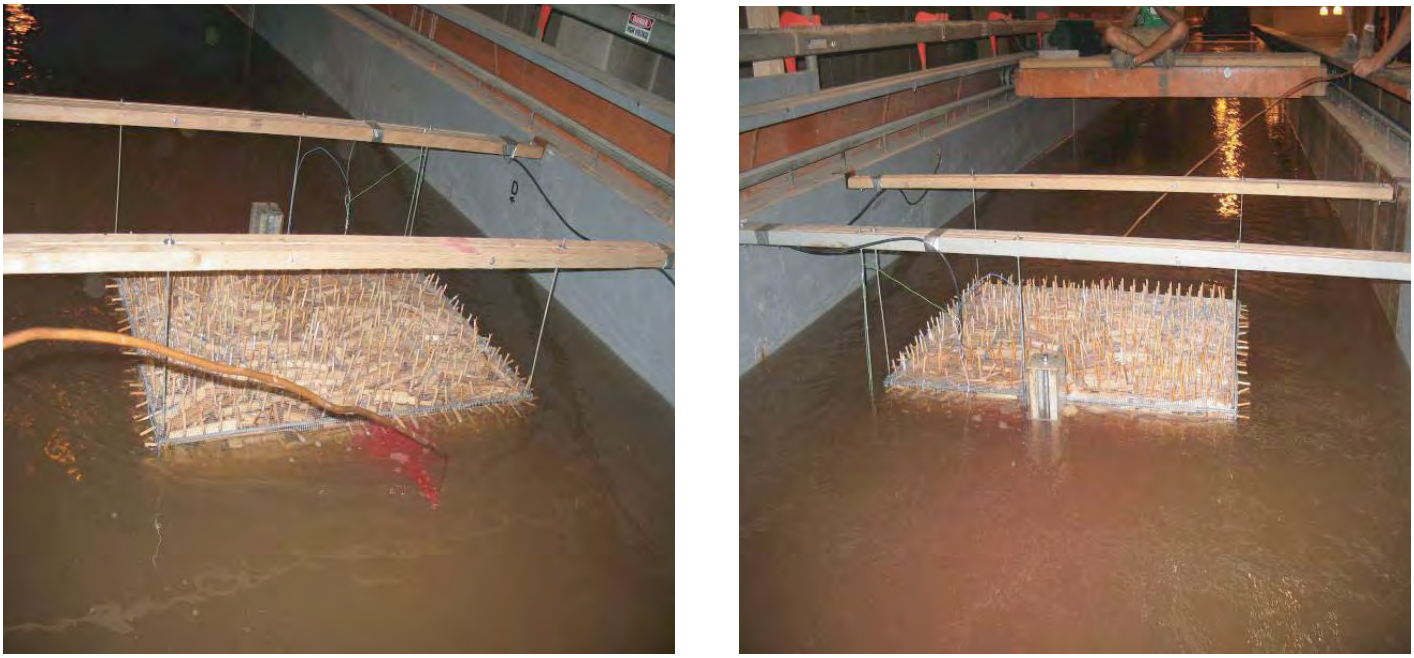

a. Upstream

b. Downstream (note upwelling flow and dye dispersal)

Figure 3.64. Typical plunging flow pattern (shown by dye) at a rectangular debris cluster.

table also shows the measured scour depths at the end of each test and the ultimate scour depth estimated by the Melville method.

Scour created by rectangular debris clusters typically resulted in a trough upstream of the pier created by the plunging flow, as shown in Figures 3.65 and 3.66. An important observation made during the course of the testing was that when the upstream extent of the debris was approximately equal to the depth of flow, the deepest part of the trough was coincident with the front face of the pier, significantly increasing the total scour at the pier itself. When the debris extended further than one flow depth in the upstream direction, the trough was moved further upstream as well, and scour at the pier face was less severe.

The depth of the upstream trough was found to be dependent on the frontal area of the debris mass (debris width times height). In many cases, the depth of the upstream trough was greater than the scour at the pier face. When the scour trough was located some distance upstream of the pier, the depth of the local scour at the pier face was sometimes greater and sometimes less than the baseline (no-debris) scour.

The lateral extent of scour created by rectangular debris clusters was directly related to the width of the cluster. The impact of the lateral scour extent on adjacent piers was not investigated during this study; however, the lateral scour caused by rectangular debris was directly related to the lateral extent of the debris. The side slopes of the scour trough (perpendicular to the flow direction) consistently ranged from 4H:1V to 6H:1V. For many of the tests with rectangular debris, the slope of the lateral scour trough was noted to intersect the flume walls on both sides of the pier.

In general, the scour processes described in the preceding paragraphs can be visualized by comparing idealized flow lines at a pier with no debris to those at a pier with a rectangular debris cluster. In Figure 3.67, the flow lines at an unobstructed pier are essentially uniform in the approach section. At the pier, the flow dives down the front face and spirals past the pier in the classic horseshoe vortex pattern.

In contrast, flow at a pier with a rectangular debris cluster is significantly obstructed and forced to plunge beneath the upstream face of the debris as shown in Figure 3.68. The plunging flow creates the upstream scour trough that was observed consistently during the laboratory testing program.

Because of the blockage created by the debris, some flow is forced around the sides as well. As the flow beneath the debris approaches the pier, the diving and spiral horseshoe patterns are still observed. Depending on the degree of blockage compared to the entire channel (flume) cross section, the relative strengths of the diving flow and horseshoe vortex may be greater or less than the unobstructed case.

Triangular/Conical Debris Clusters

A total of 14 tests were run under clear-water scour conditions with debris clusters having a triangular shape in plan view with a conical shape in profile. Three of those tests were conducted at a nominal (target) approach velocity of 0.7 V_{crit}, where V_{crit} was estimated to be 1.4 ft/s (0.43 m/s) for the initiation of

Table 3.15. Pier scour for rectangular debris tests.

Run No.	Pier	Debris Shape	Debris Location	Velocity Ratio V/V_c Target	Velocity Ratio V/V_c Meas.	Meas. Approach Depth (ft)	Test Duration (ft)	Measured Scour[1] (ft)	Estimated Ultimate Scour (ft)
4 in. (10 cm) Square Piers									
003_03	0.4	Rect	Surface	0.7	0.82	0.20	A	0.37	1.1
004_03	0.3	Rect	Surface	0.7	0.81	0.18	A	0.34	1.1
004_03	0.4	Rect	Surface	0.7	0.61	0.15	B	0.40	0.8
004_03	0.5	Rect	Surface	0.7	0.61	0.13	C	0.49	0.8
004_03	0.6	Rect	Surface	0.7	0.58	0.12	D	0.58	0.7
005_02	0.9	Rect	Surface	1.0	1.00	0.23	B	0.92	1.4
006_01	1	Rect	Surface	1.0	1.05	0.25	B	1.04	1.4
006_02	0.9	Rect	Surface	1.0	1.15	0.28	A	0.90	1.6
009_02	1.1	Rect	Surface	1.0	1.00	0.21	C	1.06	1.3
003_04	0.6	Rect	Surface	1.0	1.11	0.27	A	0.61	1.5
009_01	0.9	Rect	Surface	1.0	1.14	0.26	A	0.93	1.5
009_02	0.9	Rect	Surface	1.0	1.07	0.25	A	0.92	1.4
005_02	1	Rect	Surface	1.0	1.17	0.27	A	0.98	1.6
006_01	0.9	Rect	Surface	1.0	1.13	0.26	A	0.94	1.5
006_02	1	Rect	Surface	1.0	1.01	0.23	B	1.02	1.3
004_04	0.7	Rect	Surface	1.0	0.96	0.21	B	0.66	1.3
007_01	0.6	Rect	Surface	1.0	0.97	0.22	B	0.59	1.3
004_04	0.7	Rect	Surface	1.0	1.31	0.28	C	0.74	1.7
007_01	0.9	Rect	Surface	1.0	0.94	0.23	D	0.85	1.3
004_04	1	Rect	Surface	1.0	1.05	0.23	D	0.96	1.4
009_02	1.2	Rect	Surface	1.0	0.92	0.20	D	1.23	1.2
003_03	0.4	Wedge	Surface	1.0	0.67	0.15	D	0.41	0.9
007_02	0.9	Wedge	Surface	1.0	1.07	0.25	B	0.92	1.5
009_01	1.1	Wedge	Surface	1.0	0.99	0.21	C	1.08	1.3
007_02	0.8	Rect	Mid-Depth	1.0	1.40	0.24	C	0.8	1.3
005_02	0.9	Rect	Mid-Depth	1.0	1.39	0.25	A	0.9	1.4
006_01	1.2	Rect	Mid-Depth	1.0	1.42	0.22	B	1.2	1.3
006_02	0.8	Rect	Mid-Depth	1.0	1.33	0.23	C	0.8	1.4
004_04	0.4	Rect	Mid-Depth	1.0	1.66	0.23	C	0.4	1.4
005_02	0.4	Rect	Full Depth	1.0	1.39	0.22	C	0.4	1.3
006_01	0.5	Rect	Full Depth	1.0	1.41	0.22	C	0.5	1.3
006_02	0.5	Rect	Full Depth	1.0	1.37	0.21	C	0.5	1.3
009_01	0.8	Rect	Full Depth	1.0	1.35	0.22	D	0.8	1.3
005_01	0.7	Rect	Bed	1.0	1.66	0.28	A	0.7	1.6
1 in. (2.5 cm) Wall Piers (no skew)									
008_01	0.5	Rect	Full Depth		1.48	0.23	C	0.5	1.4
Multiple 0.5 in. (1.25 cm) Cylindrical Columns (no skew)									
008_01	0.4	Rect	Surface	1.0	1.02	0.23	D	0.35	1.4
008_02	0.5	Wedge	Surface	1.0	1.12	0.26	B	0.53	1.5
008_02	0.5	Rect	Mid-Depth	1.0	1.49	0.26	A	0.5	1.5

[1] Measured scour at Pier A was reduced by a factor of 1.23 to account for the observation that baseline scour was consistently larger at this pier.

motion of the bed material. The remaining 11 tests were conducted at a nominal velocity of 1.0 V_{crit}. Two of the tests (the first at 0.7 V_{crit} and the second at 1.0 V_{crit}) were conducted with the debris mass partially buried beneath the ambient bed level prior to the start of the test.

Triangular debris clusters were fabricated with a range of dimensions as follows:

- Width: 2.0 to 4.0 ft (60 to 120 cm) (perpendicular to flow)
- Length: 2.0 to 6.0 ft (60 to 180 cm) (aligned with flow direction)
- Height: 0.33 to 1.0 ft (10 to 30 cm) (placed at the surface or at the bed)

Debris clusters were fabricated both with and without roughness elements and filled with either wooden dowels to achieve 70% porosity, or wadded geotextile swatches to achieve an essentially impermeable mass. Figure 3.69 is a photograph of a porous, permeable triangular debris cluster that includes

(Test 004-03, Pier C)

Figure 3.65. Typical scour pattern at square pier with rectangular debris cluster.

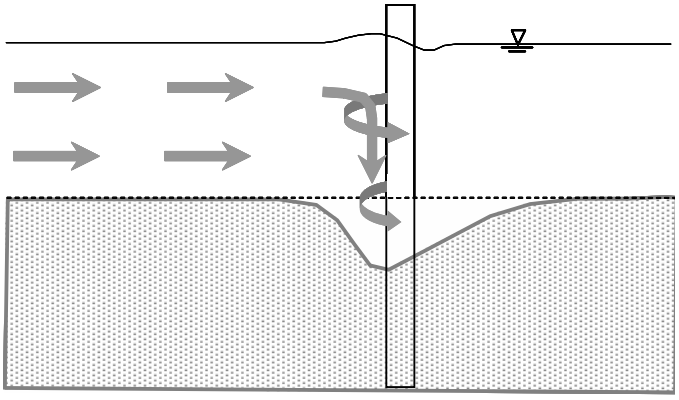

Figure 3.67. Idealized flow pattern at an unobstructed pier.

roughness elements. Dye tests performed at triangular clusters showed that at the centerline of the debris mass, flow tended to plunge beneath the debris but was also shed very readily around the sides of the debris, as seen in the figure.

Table 3.16 summarizes the results of the triangular debris tests. In this table, the actual approach velocity as measured by ADV and the measured approach flow depth are shown, because both velocity and depth during any particular test were typically slightly higher or lower than target conditions. The table also shows the measured scour depths at the end of each test and the ultimate scour depth estimated by the Melville method.

The scour pattern created by triangular debris clusters was markedly different from that exhibited by the rectangular clusters. **No scour troughs upstream of the pier were observed with any of the triangular debris clusters.**

The portion of the flow that plunges beneath a triangular/conical blockage is seen to be funneled towards the pier face, creating additional scour at the pier compared to the baseline condition. The scour at the pier face was found to be related to the thickness of the debris blockage at the pier face; i.e., a greater thickness of debris lodged directly against the pier created more scour at the pier face, with the triangular debris shapes.

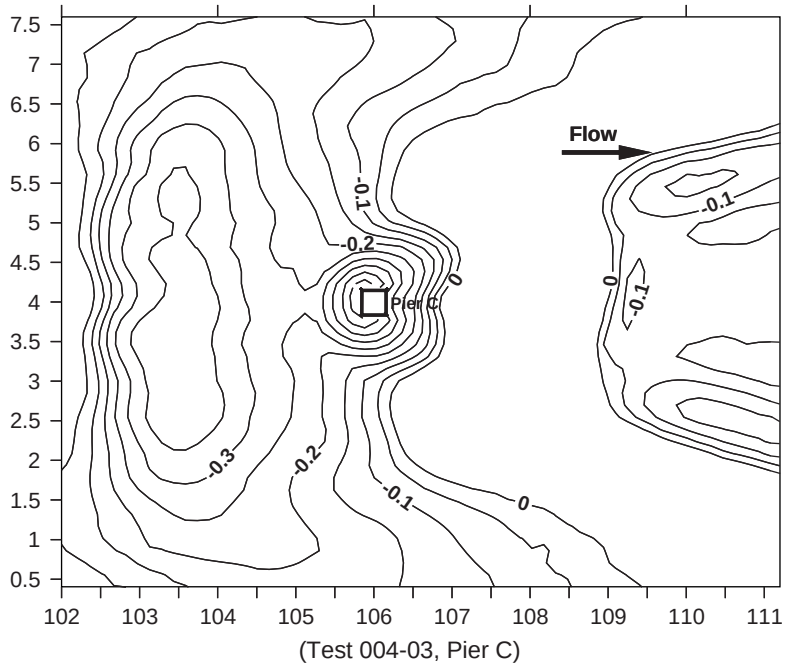

(Test 004-03, Pier C)

Figure 3.66. Typical scour contour map at square pier with rectangular debris cluster.

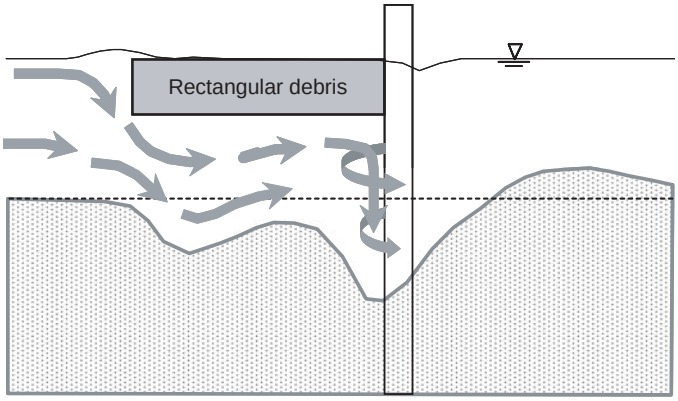

Figure 3.68. Idealized flow pattern at a rectangular debris cluster.

As with the rectangular debris tests, lateral extent of scour created by triangular debris clusters was directly related to the width of the cluster. However, the lateral extent of scour caused by a triangular debris cluster was shown to be greater than that of a rectangular one. This greater lateral extent appears to be caused by the shedding of flow around the triangular debris and has implications regarding adjacent piers or abutments.

Figures 3.70 and 3.71 illustrate typical scour patterns and contours created by triangular debris clusters. The slopes of the scour trough (oriented radially from the pier face) caused by triangular debris clusters consistently ranged from 2H:1V to 2.5H:1V.

An idealized flow pattern around a triangular debris cluster is shown in Figure 3.72. Note that the flow both plunges beneath the debris and is shed to the sides, as discussed previously.

Effect of Debris Roughness and Porosity on Scour

The laboratory studies revealed that the roughness and porosity of a debris mass do not significantly affect the pattern of scour or the magnitude of the scour depth at the pier face. For the range of these properties examined during this investigation, debris roughness and porosity can at most be considered second-order factors affecting pier scour and are much less important than (1) the size and shape of the pier and (2) the size, shape, and location (floating or buried) of the debris that collects on the pier. The effects of roughness and porosity are discussed in more detail in Section 3.7.4.

Summary

Laboratory-scale physical modeling of scour at debris-laden bridge piers was conducted using a range of pier types and widths, combined with different sizes and shapes of debris attached to the upstream pier face. In most (but not all) of the cases investigated, the presence of debris resulted in greater scour at the pier than the baseline (no-debris) condition.

Rectangular, blocky debris masses tended to produce the greatest scour at the pier when the extent ("length" dimension) of the debris upstream of the pier was on the order of one flow depth. This condition produced plunging flow that was directed toward the channel bed in the immediate vicinity of

a. Upstream

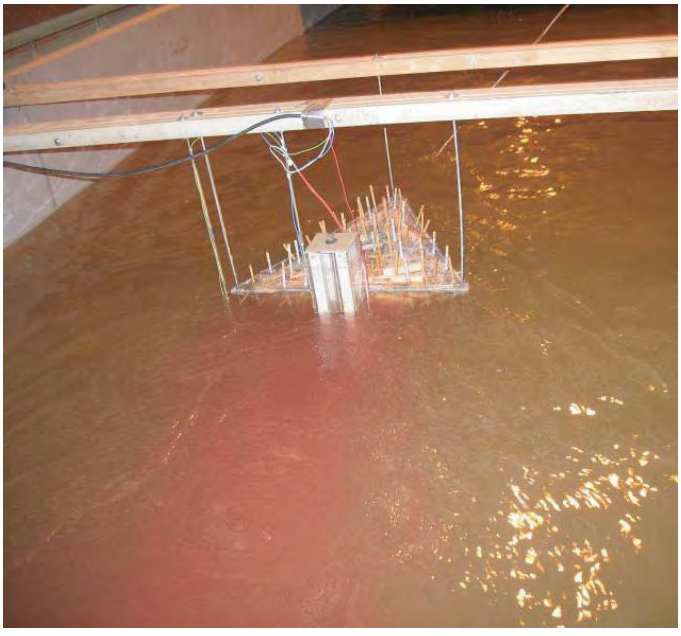

b. Downstream (note upwelling flow and dye dispersal)

Figure 3.69. Typical plunging flow with shedding around the sides (shown by dye and ripples) at a triangular debris cluster.

Table 3.16. Pier scour for triangular debris tests.

Run No.	Pier	Debris Shape	Debris Location	Velocity Ratio V/V_c		Meas. Approach Depth (ft)	Test Duration (ft)	Measured Scour[1] (ft)	Estimated Ultimate Scour (ft)
				Target	Meas.				
4 in. (10 cm) Square Piers									
003_03	0.4	Triangle	Surface	0.7	0.66	0.16	B	0.41	0.9
007_01	0.7	Triangle	Surface	1.0	1.08	0.26	A	0.71	1.5
003_04	0.7	Triangle	Surface	1.0	1.01	0.24	B	0.72	1.4
003_04	0.7	Triangle	Surface	1.0	0.99	0.22	D	0.69	1.3
007_02	0.8	Triangle	Surface	1.0	0.85	0.24	C	0.80	1.3
007_02	0.9	Triangle	Surface	1.0	1.07	0.25	A	0.93	1.4
009_02	1.2	Triangle	Surface	1.0	0.99	0.22	B	1.19	1.3
007_01	0.8	Triangle	Surface	1.0	1.04	0.23	C	0.77	1.4
003_03	0.1	Bur wedge	Surface	0.7	0.66	0.14	C	0.09	0.9
003_04	0.2	Bur wedge	Surface	2.0	0.99	0.21	C	0.21	1.3
005_01	0.2	Inv Cone on bed	Surface	3.0	0.94	0.20	C	0.19	1.2
1 in. (2.5 cm) Wall Piers (no skew)									
008_02	0.4	Triangle	Surface	1.0	1.07	0.23	C	0.37	1.4
008_02	0.5	Triangle	Surface	1.0	1.15	0.26	A	0.53	1.5

[1] Measured scour at Pier A was reduced by a factor of 1.23 to account for the observation that baseline scour was consistently larger at this pier.

the pier face, resulting in a worst-case scour condition. Total scour at the pier also tended to increase when the total frontal area of flow blockage (as a percentage of the cross-sectional area of the approach channel) was large. In that case, the debris-induced scour appeared to be similar to that created by pressure flow and contraction effects, for example, pressure flow beneath bridge decks that are submerged during floods.

Triangular debris clusters were also investigated, because the debris photographic archive revealed that this is another very common shape that can be produced in the field as drift accumulates at a pier. In a triangular configuration, the thickness of the debris is greater at the pier face, tapering upward and thinning toward the leading (upstream) point. This shape tended to produce more scour at the pier face compared to the baseline (no-debris) condition. In addition, triangular debris shapes produced more pronounced scour laterally outward from the sides of the pier, apparently because much of the debris-blocked flow tends to be shed around this shape compared to a rectangular, blunt-shaped blockage.

(Test 007-02, Pier A)

Figure 3.70. Typical scour pattern at square pier with triangular debris cluster.

Although the effect of lateral scour extent on adjacent piers was not investigated in detail, data collected from the laboratory tests yield valuable information in this regard. Both rectangular and triangular debris shapes resulted in lateral scour that was directly related to the width of debris blockage. Interestingly, the *lateral* side slopes of the debris-induced scour holes were relatively mild (ranging from about 6H:1V to 4H:1V) for rectangular debris compared to lateral side slopes produced by triangular debris (minimum 2.5H:1V).

Pier width normal to the flow direction is also important in determining the total scour depth at the pier face, even when the pier is loaded with a large amount of debris. Given the same size and shape of debris, a slender pier with debris will experience less total scour than a wider pier with the same amount of debris, for the same hydraulic conditions of the approach flow.

3.7 Scour Prediction at Bridge Piers with Debris Loading

3.7.1 Introduction

The laboratory testing program was designed and conducted to develop information on a variety of factors related to debris accumulations at piers that can potentially affect the

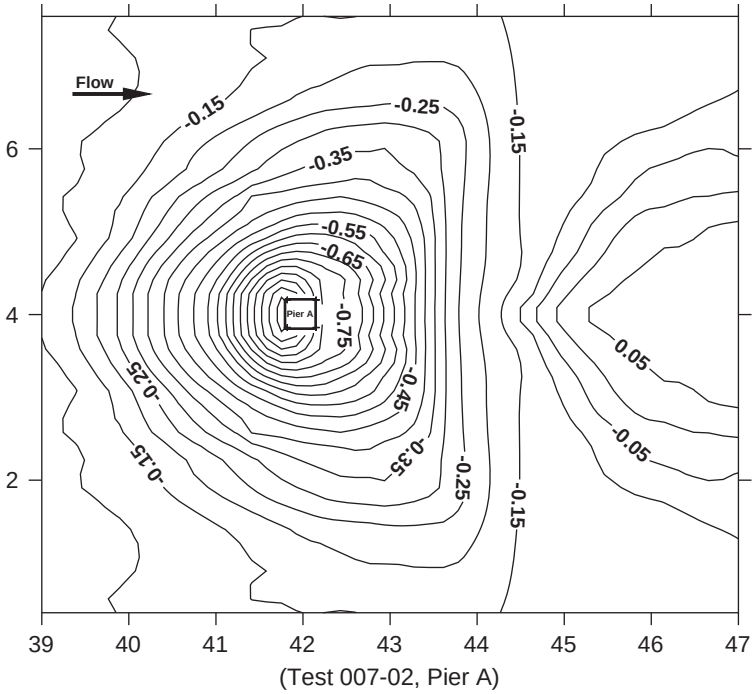

Figure 3.71. Typical scour contour map at square pier with triangular debris cluster.

depth of scour at the pier. The factors examined in this study included the following:

- Shape: Rectangular or triangular
- Size: Width, length, and thickness
- Location: Surface (floating), mid-depth, or bed (partially buried)
- Roughness: Smooth or roughened
- Porosity: Impermeable or 25% porosity
- Approach velocity: V/V_c ratios of 0.70 and 1.0

Selected combinations of the above factors were also tested; for example, a particular debris shape might be tested as (1) a smooth, impermeable body; (2) a smooth, porous body; (3) a rough, impermeable body; and (4) a rough, porous body.

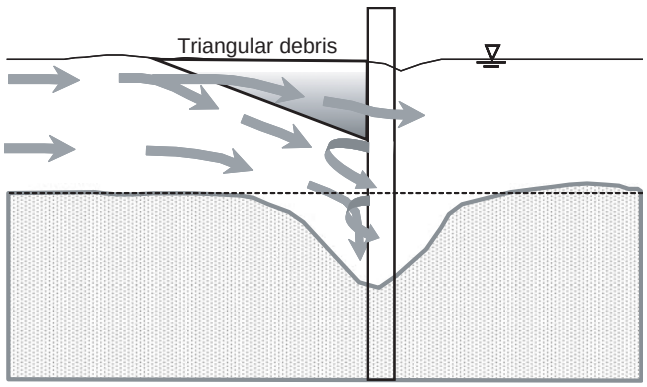

Figure 3.72. Idealized flow pattern at a triangular debris cluster.

All tests were conducted in the 8 ft wide (2.4 m) flume at CSU. Most of the tests were conducted using 4 in. (10.2 cm) square piers. Tests of selected debris shapes were also conducted using slender piers, consisting of 1 in. wide (2.5 cm) square-nosed wall piers and multiple 0.5 in. wide (1.3 cm) cylindrical column piers. However, tests using the slender piers were necessarily limited in number, and only a small subset of debris shapes could be examined with the resources available for this study.

The tests were not designed to represent any particular scale ratio. However, considering typical pier sizes and dimensions of debris accumulations found in the field and the photographic archive, a model to prototype scale ratio of approximately 1:10 to 1:30 can be considered a reasonable range for the tests conducted in the 8 ft (2.4 m) flume.

Factors *not* considered in the test program include the effect of bed material grain size, flow depth, live-bed conditions, and contraction scour. In addition, tests at different scales, including near-prototype scale ratios of approximately 1:2 to 1:4 were originally considered but were ultimately dropped from the program so that other factors could be investigated in more detail.

A total of 53 tests of debris-laden piers was run under clear-water scour conditions. These are generally categorized by debris shape and target approach velocity as follows:

- Rectangular debris shapes:
  - 0.7 V_{crit}: 5 tests
  - V_{crit}: 34 tests

- Triangular debris shapes:
  - 0.7 V_{crit}: 3 tests
  - V_{crit}: 11 tests

Most of the tests (35 tests) were conducted with the top surface of the debris at the water surface, forming a "raft." Selected tests were also performed with the debris located in the center of the water column, resting on the bed, or buried into the bed.

3.7.2 Equivalent Pier Width

The concept of *equivalent pier width* has been widely accepted as a way to quantitatively assess the extent to which debris affects scour at piers. Using the data collected from the laboratory program, this concept has been explored in great detail and appears to have the best promise for predicting the effect of debris on pier scour.

All pier scour prediction equations use pier width as a factor that contributes to the estimated scour depth. Intuitively, the accumulation of debris on a pier causes the pier to appear larger in the flow field, thereby increasing the total area blocked by obstruction. HEC-18 (Richardson and Davis 2001) uses the width, W, of the debris perpendicular to the flow direction to estimate the additional obstruction.

Dongol (1989) and Melville and Dongol (1992) provide an equation to calculate the "equivalent width," b_e, of a bridge pier that is loaded with debris. The equation uses both the width, *W*, and thickness, *T*, of the debris and is based on scour data from a limited number of tests (17 tests) in a laboratory flume. Only floating (surface) debris at cylindrical piers was tested, with the debris wrapped around the pier in all directions. The effect of the vertical location of the debris mass within the water column was not investigated. The equation to calculate equivalent pier width is:

$$b_e = \frac{K_{d1}(TW) + (y - K_{d1}T)a}{y} \tag{3.11}$$

where:

b_e = Effective width of the pier, ft (m)
K_{d1} = Dimensionless coefficient equal to 0.52 from laboratory tests (Dongol 1989)
T = Thickness of debris, ft (m)
W = Width of debris normal to flow, ft (m)
a = Pier width (without debris) normal to flow, ft (m)
y = Depth of approach flow, ft (m)

The effective width equation was compared to the results of the laboratory tests conducted at CSU under this study program. The **observed** effective width (denoted a_d^*) for all tests at 1.0 V_{crit} with debris at the water surface was determined from the CSU pier scour equation, using the equilibrium scour depth Y_{se} obtained from each test. The calculated value of b_e obtained from the Melville and Dongol equation was then plotted against a_d^* to determine how well the effective width equation predicts the actual effective width. Figure 3.73 presents the results of that comparison for both rectangular and triangular shapes.

Figure 3.73 indicates that the Melville–Dongol equation tends to overestimate the effective width of the pier when debris is present, particularly for triangular shapes. The Melville–Dongol equation does not take into account the shape of the debris mass (e.g., rectangular vs. triangular), nor does it consider the length, L, of the debris extending upstream from the pier. As discussed in Section 3.6, these aspects were observed to have an effect on the scour pattern as well as the total depth of scour at the pier face.

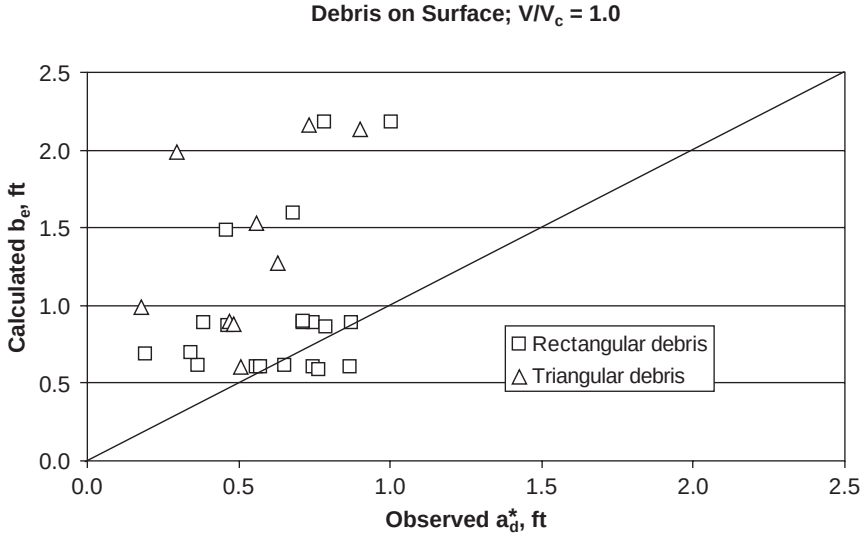

Figure 3.73. Comparison of the Melville and Dongol effective width to the observed effective width.

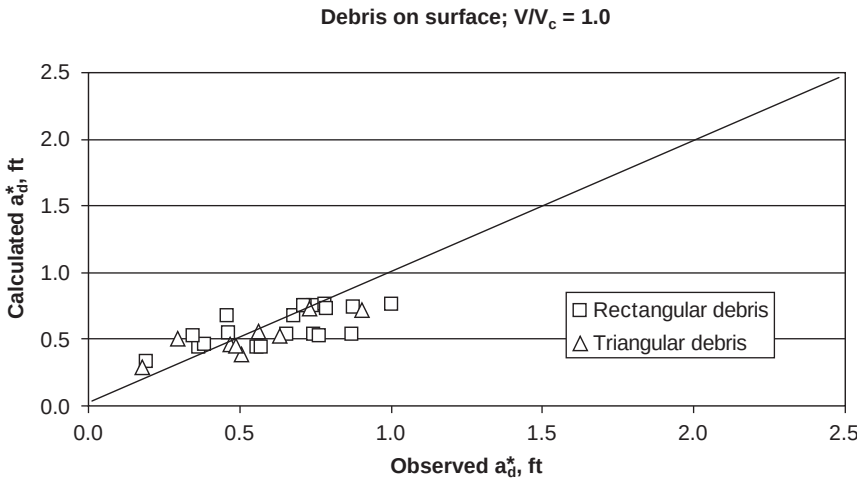

Figure 3.74. Comparison of the modified effective width to the observed effective width.

A modification to the equivalent width equation was therefore proposed and tested against the laboratory data. The proposed modification is denoted as "a_d^*" to distinguish it from the Melville and Dongol "b_e" and is given as:

$$a_d^* = \frac{K_{d1}(TW)(L/y)^{K_{d2}} + (y - K_{d1}T)a}{y} \tag{3.12}$$

where:

K_{d1} = Dimensionless coefficient optimized from laboratory test data

K_{d2} = Dimensionless exponent optimized from laboratory test data

L = Length of debris upstream from pier face, ft (m)

Other terms as are as defined previously.

Optimizing the coefficient K_{d1} and exponent K_{d2} to the observed laboratory data reveals that the shape and upstream extent of the debris do affect the resulting scour at the pier face. For rectangular debris shapes, K_{d1} and K_{d2} were found to be 0.39 and –0.79, respectively, whereas for triangular shapes, K_{d1} and K_{d2} were 0.14 and –0.17. **The coefficient K_{d1} is thus seen to be a shape factor, while the exponent K_{d2} is a factor that describes the intensity of the plunging flow created by the debris blockage.** The result of this comparison is presented in Figure 3.74 for both rectangular and triangular shapes.

Figure 3.74 shows that accounting for debris shape and length significantly improves the ability to predict the equivalent pier width (compare with Figure 3.73). Predicted and observed equilibrium scour depths are shown in Figure 3.75 for all runs with debris at the water surface and an approach velocity of 1.0 V_{crit}. In this figure, the CSU equation is used to

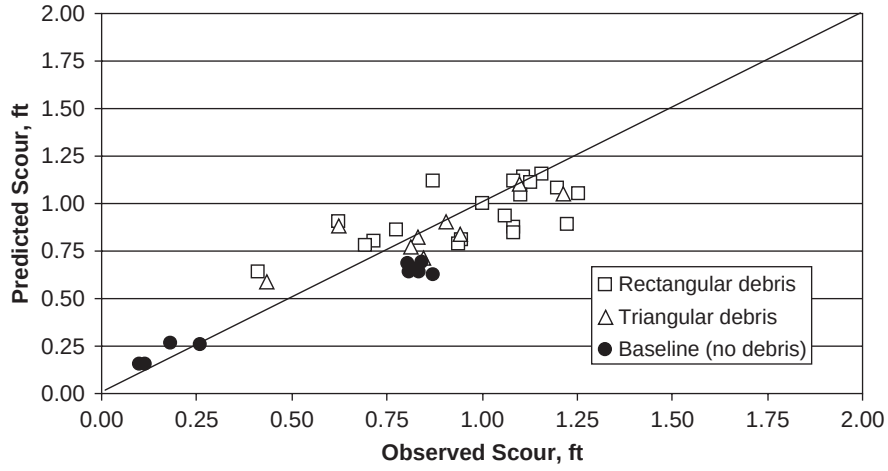

Figure 3.75. Comparison of observed scour to predicted scour using the modified equation for equivalent pier width.

predict ultimate clear-water scour at the pier face, with the equivalent pier width calculated using the modified version of the Melville–Dongol equation (Equation 3.12).

3.7.3 Recommended Design Equation

The previous section developed a predictive relationship to estimate local scour at a debris-laden bridge pier. The relationship was derived using an "equivalent width" concept by modifying the approach developed by Melville and Dongol. Figure 3.75 shows that the predictive equation, using optimized coefficients and exponents based on laboratory data, is essentially a best-fit relationship that underestimates the observed scour as often as it overestimates.

A relationship better suited to design should tend towards conservatism; that is, underestimation of the observed (i.e., actual) scour should be relatively rare. Based on the laboratory data developed for an approach velocity of 1.0 V_{crit}, the shape coefficient K_{d1} that provides overestimation 90% of the time (underestimating 10% of the observations) is 0.79 for rectangular debris shapes, and 0.21 for triangular shapes.

The recommended design equations for estimating an equivalent pier width for use with the CSU pier scour equation are, therefore:

$$a_d^* = \frac{K_{d1}(TW)(L/y)^{K_{d2}} + (y - K_{d1}T)a}{y} \quad \text{for } L/y > 1.0 \qquad (3.13)$$

and

$$a_d^* = \frac{K_{d1}(TW) + (y - K_{d1}T)a}{y} \quad \text{for } L/y \le 1.0 \qquad (3.14)$$

where:

K_{d1} = 0.79 for rectangular debris, 0.21 for triangular debris
K_{d2} = –0.79 for rectangular debris, –0.17 for triangular debris
L = Length of debris upstream from pier face, ft (m)
y = Depth of approach flow, ft (m)

Other terms are as defined previously.

The design or "envelope" values using the recommended equations are shown in Figure 3.76 for all runs with debris at the water surface and an approach velocity of 1.0 V_{crit}. In this figure, the CSU equation is used to predict ultimate clear-water scour at the pier face, using the equivalent pier width calculated by Equations 3.13 and 3.14 and the recommended K_{d1} and K_{d2} values presented above.

3.7.4 Effect of Debris Roughness and Porosity

The data from the laboratory research program indicate that roughness and porosity of the debris mass do not significantly affect the observed scour. The effects of roughness and porosity were investigated using a rectangular debris shape 2 ft wide by 1 ft long (0.6 m by 0.3 m). Nine tests were conducted with this shape mounted on the front of 4 in. (10.2 cm) square piers, with an approach velocity of 1.0 V_{crit}. An example of a smooth, impermeable debris shape is provided as Figure 3.77, and a rough, porous shape is shown in Figure 3.78.

The effect of roughness and porosity characteristics on scour was quantified using the ratio of scour depth caused by the debris to the baseline (no-debris) condition. The average scour ratio for all tests was 1.35, with a range of 1.28 to 1.48 and a standard deviation of only 5% about the mean. Figure 3.79 shows the results of these tests. At most, roughness and porosity can be considered second-order variables that are not significant compared to the size and shape of the debris mass.

3.7.5 Effect of Debris Location in the Water Column

The data from the laboratory research program indicate that the location of the debris in the water column affects the total depth of scour at the pier face. The effect of debris location was

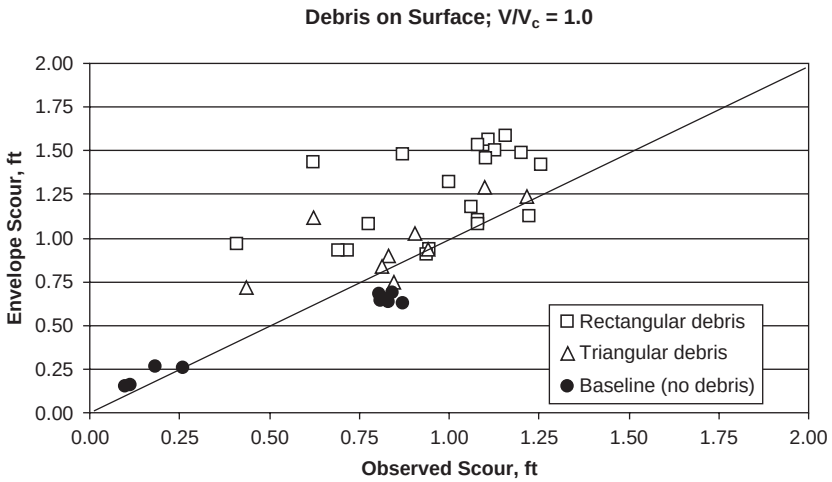

Figure 3.76. Comparison of observed scour to the recommended design equation using 90% envelope values.

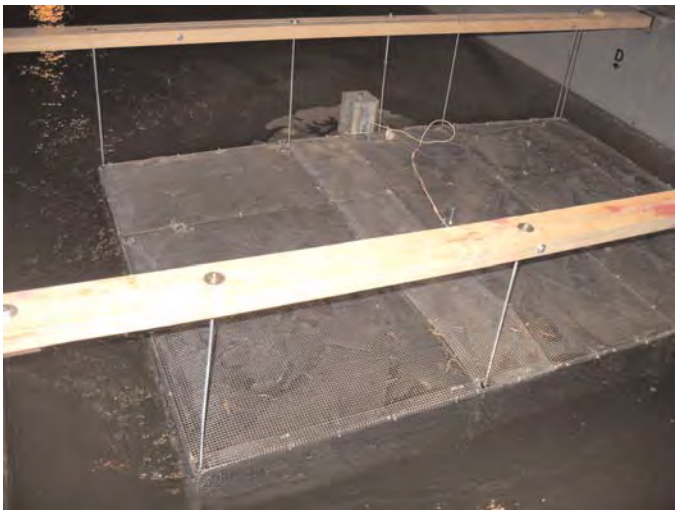

Figure 3.77. Example of a smooth, impermeable debris shape.

Figure 3.78. Example of a rough, porous debris shape.

investigated using two different rectangular debris shapes. The first shape was 2 ft wide by 2 ft long (0.6 m by 0.6 m), and the second was 1 ft wide by 1 ft long (0.3 m by 0.3 m). Fourteen tests were conducted with these shapes mounted on the front of 4 in. (10.2 cm) square piers, with an approach velocity of 1.0 V_{crit}.

Figure 3.80 shows a 1 ft by 1 ft rectangular debris shape on the bed in front of Pier D prior to testing. Figures 3.81 and 3.82 show the scour resulting from Test 009_01, a 72-hour test conducted with an approach velocity of 1.0 V_{crit}.

The effect of debris location in the water column on pier scour was quantified by the ratio of scour depth caused by the debris to the baseline (no-debris) condition. In general, the 2 ft wide by 2 ft long (0.6 m by 0.6 m) debris placed as a surface raft caused slightly greater scour at the 4 in. (10.2 cm) square piers compared to baseline conditions.

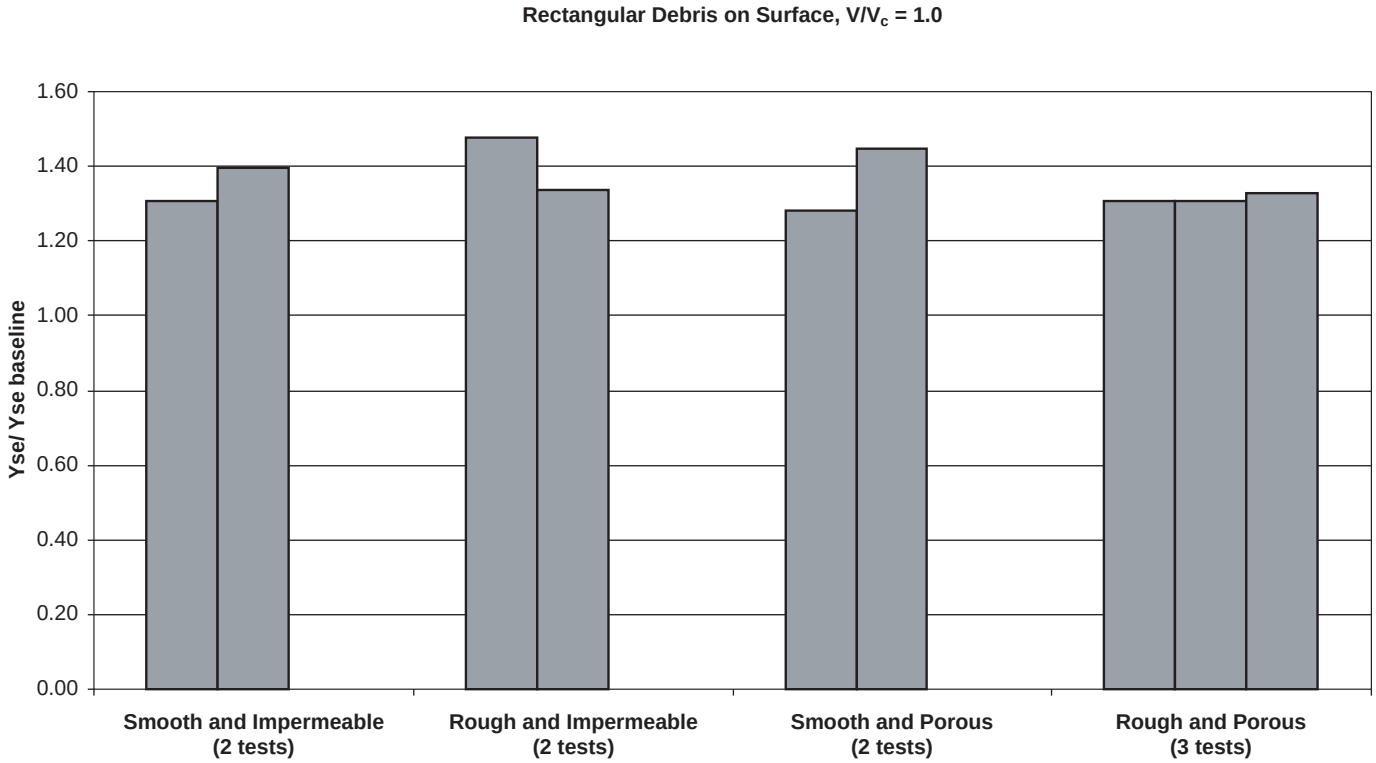

All tests utilized a rectangular debris shape, 2 ft wide by 1 ft long.

Figure 3.79. Effect of debris roughness and porosity on observed pier scour.

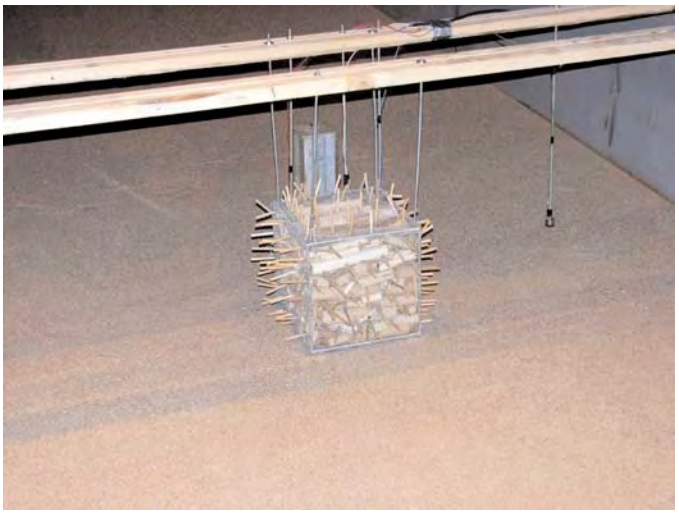

Figure 3.80. Pier D prior to Test 009_01.

In contrast, when this same shape was located at mid-depth in the flow, significantly less scour at the pier face was observed. This difference was presumably due to the relative distribution of flow over the debris compared to the plunging flow occurring beneath it. Similarly, when the debris was placed on the bed, less scour was observed at the pier face compared to baseline conditions. Figure 3.83 shows the results of the laboratory tests as a function of debris location in the water column.

3.7.6 Lateral Extent of Scour at Piers with Debris

When a debris mass accumulates at a pier, it typically initiates and grows from floating (usually organic) drift material. The laboratory tests conducted under this study

Figure 3.81. Pier D after Test 009_01, 72 hours at 1.0 V_{crit}.

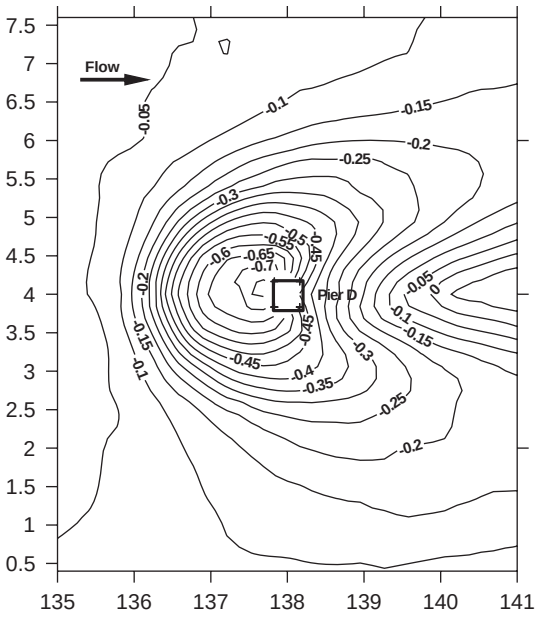

Figure 3.82. Maximum scour depth at the Pier D face after Test 009_01 is less than that obtained from the baseline (no-debris) condition.

program indicate that the lateral extent of the scour caused by floating debris rafts is directly proportional to the width of the raft.

The impact of the lateral scour extent on adjacent piers or abutments was not directly investigated in this study program. However, inferences in this regard can be drawn from the laboratory data collected:

- Rectangular debris: The lateral extent of scour created by rectangular floating debris extends outward from the edge of the debris (as measured from the pier face) at a slope ranging from about 4H:1V to 6H:1V.
- Triangular debris: The lateral extent of scour created by triangular floating debris extends outward from the edge of the debris (as measured from the pier face) at a slope ranging from 2H:1V to 3H:1V.

To estimate the impact on adjacent bridge elements (piers or abutments) caused by debris loading on a single pier, the recommended guidance is as follows:

1. Estimate the total scour at the debris-laden pier.
2. Extending from the edge of the debris, compute a lateral slope of 6H:1V for rectangular debris or 3H:1V for triangular debris.
3. Determine the scour prism using these values and determine the effect on adjacent bridge foundation elements.

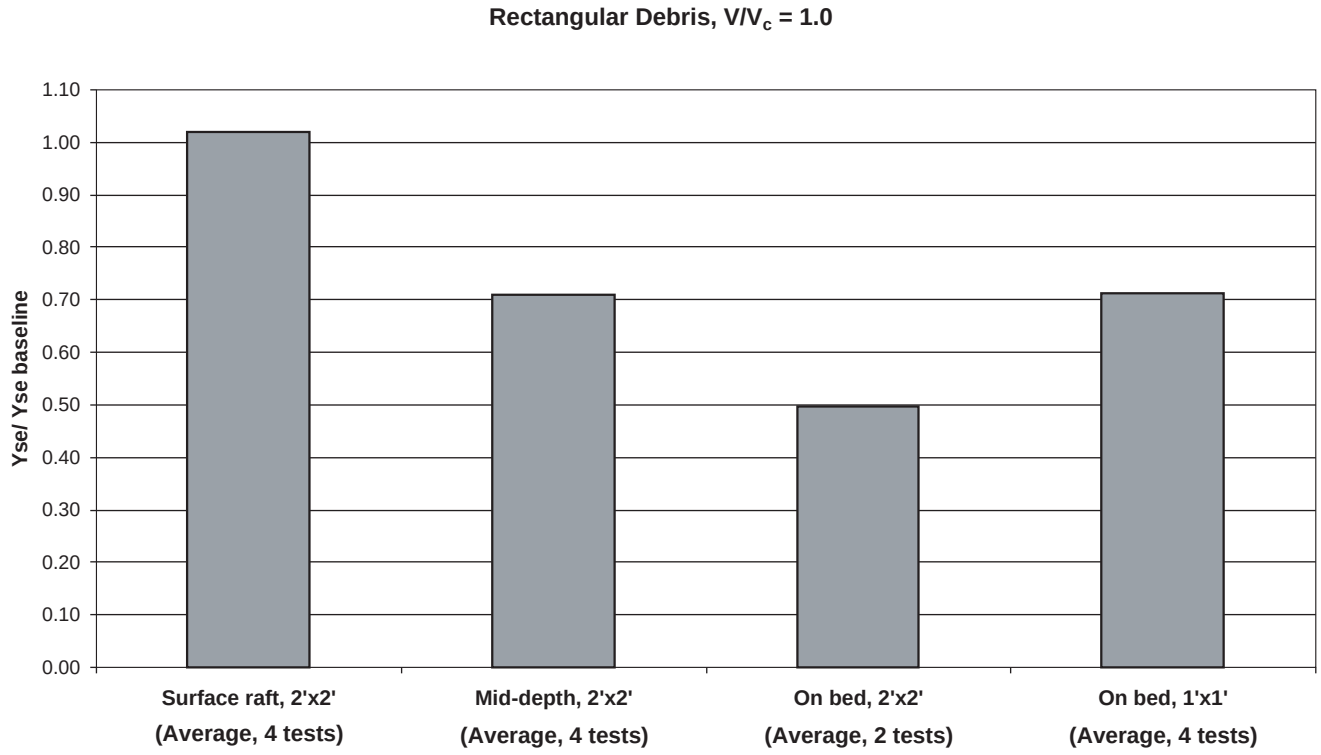

Figure 3.83. Effect of debris location in the water column on observed pier scour.

3.8 Incorporating Debris in Hydraulic Models

HEC-RAS (Brunner 2008) is a one-dimensional model that is the primary tool for simulating hydraulic conditions at bridges. The Finite-Element Surface Water Modeling System (FESWMS) (Froehlich 2002, rev. 2003) and RMA2 (Donnell et al. 2006) are used to simulate hydraulic conditions at bridges for more complex situations that require two-dimensional hydraulic analysis. The hydraulic effects of debris can be incorporated into each of these models. HEC-9 (Bradley et al. 2005) provides guidance on incorporating debris in hydraulic models. This section supplements the information in HEC-9.

3.8.1 HEC-RAS

In HEC-RAS, floating debris clusters can be added to bridge piers. Figure 3.84 shows a bridge crossing with a 6 ft high by 18 ft wide (1.8 by 5.5 m) debris cluster only at the center pier. Consistently sized debris clusters can be included at all piers or varying sizes can be input at individual piers. The debris cluster is centered on the pier and moves up and down with the water surface. It becomes fixed in place when it comes in contact with the low chord of the deck at the centerline of the pier. A debris raft can be simulated by setting the width dimensions of the debris clusters to form a continuous blockage. When floating debris is included at piers, HEC-RAS only includes the debris at the upstream face of the internal bridge sections. Debris that has accumulated on the bottom of the deck can be simulated by changing the low chord of the bridge deck. If the debris is only at the upstream face of the bridge, only the low chord of the upstream internal bridge section should be adjusted.

The HEC-RAS model includes four bridge hydraulic computation methods for low flow and two methods for high flow. Low flow is defined as flow through the bridge opening without the occurrence of either pressure flow (submerged deck) or roadway overtopping. The four low flow methods are energy (standard step method), momentum, WSPRO, and Yarnell. The two high flow methods are energy and pressure/weir. Each bridge hydraulic method incorporates the debris effects based on the hydraulic computation assumptions inherent to that method. For example, the energy method removes flow area at a bridge cross section based on the areas blocked by the embankments, piers, and abutments and includes wetted perimeter for each of these obstructions. In the energy method, the area and wetted perimeter of the debris cluster are included as part of the bridge pier obstruction. In the momentum method, the debris area is included in the drag force of piers in the force balance of the momentum solution at the bridge.

Just as the results of the HEC-RAS analysis differ based on the user-selected bridge hydraulic method, the effects of the debris also differ between the methods. For the example model shown in Figure 3.84, the debris increased the energy

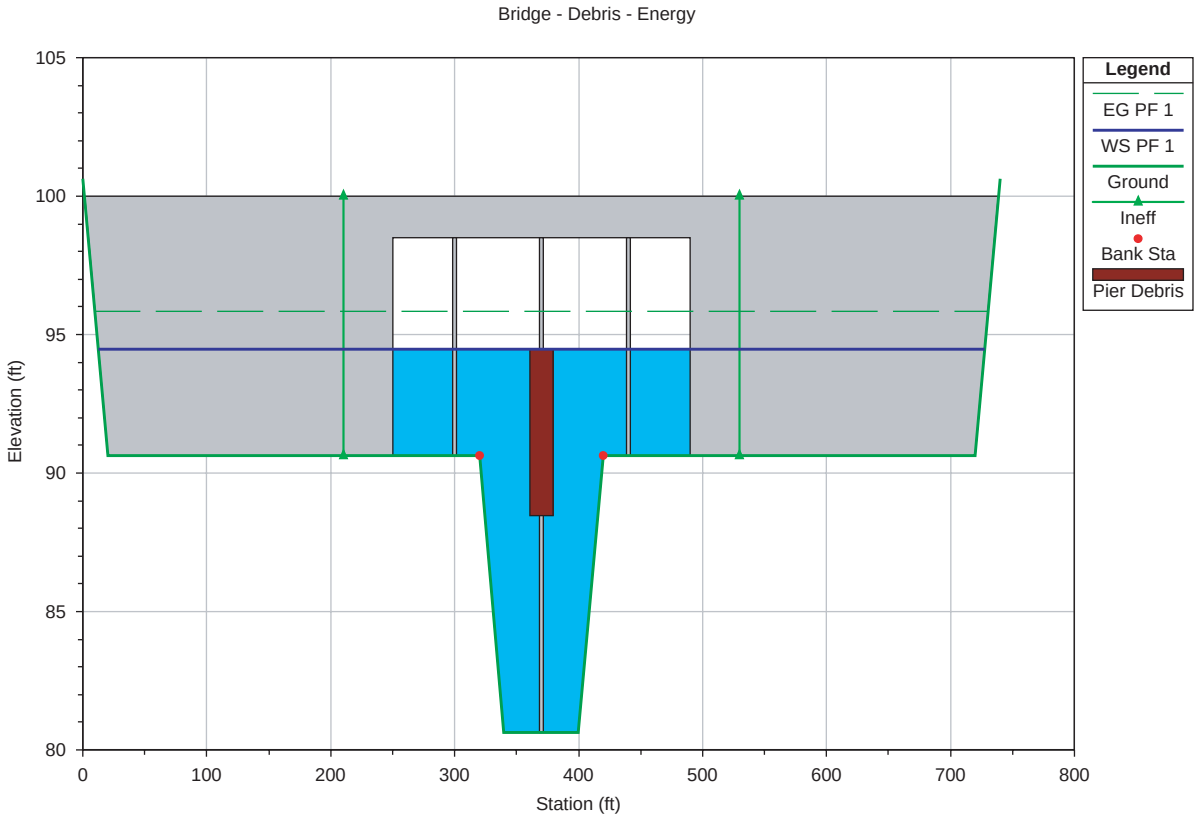

Figure 3.84. Debris cluster in the HEC-RAS hydraulic model.

grade upstream of the bridge by 0.06 ft (18.3 mm) for WSPRO, 0.10 ft (30.5 mm) for Yarnell, 0.14 ft (42.7 mm) for energy, and 0.18 ft (54.9 mm) for momentum. When the tailwater in the example model was increased to create a pressure and overtopping condition, the debris increased the upstream energy grade by 0.03 ft (9.1 mm) for pressure/weir and 0.04 (12.2 mm) for the energy method.

The bridge hydraulic method (energy, momentum, etc.) should be selected based on the suitability of that approach to the particular bridge crossing without considering debris. When debris is included, the same method should be used. If the momentum equation is used, then *NCHRP Report 445* (Parola et al. 2000) can be consulted for selection of the drag coefficient. Although the Parola report is directed at calculating debris forces on bridges, the guidance can be used in selecting the appropriate drag coefficients for debris in hydraulic modeling. If debris blocks a large portion of a bridge, the upstream and downstream cross sections adjacent to the bridge may need to include ineffective flow areas to represent areas that are not actively conveying flow.

HEC-RAS also includes scour computations in the Hydraulic Design menu. Debris only affects the scour results to the extent that it impacts the hydraulic results, such as a different hydraulic depth or flow distribution in the contraction scour calculation and a local depth or flow velocity in the pier scour calculation. The default pier width in the pier scour calculation is the pier width entered in the HEC-RAS bridge data editor. In the Hydraulic Design menu, the pier width value can be overridden so the value of a_d^* (the effective full-depth pier width computed as in Section 3.7) based on the debris dimensions can be used. As with any automated calculation, the results should be checked for accuracy.

While directly using a_d^* as the pier width in the HEC-RAS model may be tempting, this is not recommended. The hydraulic effect of debris is to block area. Therefore, the actual blocked area should be used in bridge hydraulic computations and a_d^* should be used only for scour calculations. The total area of blockage (debris plus the area of the remaining pier below the debris cluster) would not be expected to equal the area of the "effective width" pier.

3.8.2 Two-Dimensional Models

Two-dimensional finite-element models commonly used for bridge hydraulics (FESWMS and RMA2) use the momentum equation for hydraulic calculations. Actual pier dimensions and locations can be included directly in the FESWMS model. The model then computes the additional drag force

caused by the obstruction. To model debris in FESWMS, the user should calculate the total obstructed area of the pier and debris, divide by the flow depth, and use the resulting width as the pier width. This width is not the same as the effective width, a_d^*, used in the scour calculation. Even though the debris may be at the surface, the computed drag force does not account for the vertical location, so the computed hydraulic effect is the same regardless of the vertical location. *NCHRP Report 445* (Parola et al. 2000) can be consulted for selection of the drag coefficient.

To include the additional drag force in an RMA2 model is not as easy. In RMA2 (and FESWMS), the shear stress on the bed can be estimated from $\tau_o = \gamma y S$ and substituting the Manning equation for energy slope (assuming gradually varied flow, which is the assumption in these models). The resulting equation for shear stress is:

$$\tau_0 = \frac{\gamma n^2 V^2}{K_u^2 y^{1/3}} \tag{3.15}$$

where:

γ = Unit weight of water
n = Manning flow resistance coefficient
V = Velocity
Y = Flow depth (wide channel assumption)
K_u = 1.486 for U.S. customary units and 1.0 for SI

The resulting force on an element in the 2-D model network is approximately equal to the area of that element times the shear stress computed from the average velocity and depth for that element. To include the additional drag force caused by a pier and debris, one can calculate the drag force ($F_d = 0.5 C_d \rho A_p V^2$), add it to the bed force, and then back calculate an effective Manning n for that element that includes both forces. The resulting effective Manning n (n_e) can be computed without knowing velocity, because velocity squared is included in both forces and the equation for effective Manning n (n_e) is:

$$n_e^2 = n^2 + \frac{C_d A_p K_u^2 y^{1/3}}{2 g A_E} \tag{3.16}$$

where:

n = Manning n of the bed
C_d = Drag coefficient
A_p = Sum of the pier and debris cross-sectional areas for all the piers that are located within the element
A_E = Area of the element (in plan),
y = Average flow depth
g = Gravitational constant
K_u = 1.486 for U.S. customary units and 1.0 for SI

For example, if V is 5.0 ft/s (1.52 m/s), n is 0.030, C_d is 1.2, A_p is 45 ft^2 (4.18 m^2), y is 10 ft (3.0 m), and A_E is 400 ft^2 (37.2 m^2), then n_e would be 0.1043. As a check, the force on this element from bed stress alone is 118 lb (525 N), the drag force is 1310 lb (5827 N), for a total of 1428 lb (6352 N), and the force from the adjusted Manning n (n_e = 0.1043) is 1427 lb (6347 N) where the difference is due to rounding. An approximate overall hydraulic impact of piers and debris on a bridge can be included by using A_p equal to the sum of areas for all piers and debris at the bridge, y equal to the hydraulic depth of the bridge, and A_E equal to the total area (in plan) of the elements representing the bridge in the finite-element network.

Another way that piers can be included in 2-D models is to represent the pier with disabled elements in the finite-element network. This method is only used if the pier is large and the flow is significantly altered around the pier. If this method is used, then the dimensions of the disabled elements can be increased to account for debris blockage. This method would be most applicable to the situation where the debris predominantly blocks the water column. The width of the disabled element could also be estimated as the total area of the debris and pier divided by the flow depth.

To calculate pier scour from a 2-D model, the user would use the hydraulic results of the model combined with a_d^* determined as in Section 3.7. The value of a_d^* should not be used as the pier width for hydraulic calculations within the 2-D model.

3.9 Application Methodology and Examples

3.9.1 Methodology

The methodology for determining scour at a bridge with debris at the piers involves all of the steps that would be performed for any other bridge (see Richardson and Davis 2001) plus additional steps that relate to debris scour. The steps are summarized below:

1. Conduct a field reconnaissance to determine site conditions for hydraulic modeling, including the potential for debris production, debris delivery, key log dimensions, and existing debris accumulations (see the guidelines and flowcharts in Section 3.2).
2. Review bridge inspection reports for information on debris, including size and shape.
3. Contact bridge maintenance staff for information on debris removal, including size, frequency, and shape.
4. Based on the information obtained in the previous steps determine debris dimensions and shape that can be expected during extreme events. The existing bridge information can be used for analysis of replacement bridges,

but care must be taken to assess whether changes in span length, deck height, pier type, pier orientation, or pier placement would affect potential debris characteristics. For a new bridge crossing, the assessment should include other nearby bridges and differences in reach conditions for debris production and delivery as well as differences in structure type when determining the debris characteristics. The photographic archive (Appendix B) can also be used as a resource by comparing the bridge characteristics with photographs in the archive.

5. Perform hydraulic modeling (typically using HEC-RAS, see Section 3.8) with and without debris at the piers.
6. Compute scour for the pier without debris. If the pier is skewed, compute the projected width of the pier using a maximum pier length of 12 times the pier width per HEC-18 guidance (Richardson and Davis 2001).
7. Compute the effective pier width, a_d^*, for the selected debris dimensions using the equations in Section 3.7 and the hydraulic conditions from the with-debris model. If the pier is skewed, use the projected width as the pier width in the a_d^* calculation. (Note: This guidance is based on the judgment of the research team and not on laboratory investigation.)
8. If the length, L, of the debris cluster upstream of the pier exceeds the flow depth, y, also calculate a_d^* for L equal to y. This step is necessary because the plunging flow scour is greatest for $L/y = 1.0$, so this may be the controlling case for scour (see Section 3.6). When reducing the length, L, also adjust the width, W, and thickness, T, based on the expected debris conditions. In some cases, the width and thickness would not be decreased. The width should not be decreased to a value less than the key log length, and the thickness should not be decreased less than the expected rootwad diameter. If there is a large difference in the debris size, a third calculation for an intermediate debris cluster size may also be warranted.
9. Calculate pier scour with debris for the largest value of a_d^* obtained in Steps 7 and 8. Do not include the pier shape coefficient, K_1, or the skewed pier coefficient, K_2, in the HEC-18 equation for pier scour when making this calculation.
10. Check the scour estimates for reasonableness. For example, if the initial calculation of debris scour is for a rectangular cluster, a comparison could be made for a triangular cluster with the same dimensions.

3.9.2 Example Debris Scour Calculations

Steps 1 through 5

This example uses the South Platte River case study presented in Appendix D (Part 3) as the information for determining bridge conditions, probable debris characteristics, and hydraulic conditions. The case study results indicate that there is a high potential for debris production, high potential for debris transport and delivery, and a high potential for accumulation of debris at Pier 2, which is located in the center of the bridge near the middle of the channel. The span length is 112.9 ft (34.4 m), which is much longer than the key log length of 20 ft (6 m). Therefore, the debris is extremely unlikely to bridge between piers to form a raft. The key log diameter is approximately 1.5 ft (0.46 m) and rootwad sizes can exceed 6 ft (1.8 m). Inspection records of the existing bridge, a previous bridge at this location and nearby bridges indicate frequent debris accumulations.

The debris accumulation at Pier 2 for an extreme event is assumed to be 30 ft (9.1 m) wide, 6 ft (1.8 m) thick, and 20 ft (6.1 m) long. This size accumulation is based on the high debris accumulation potential, key log length, key log diameter, and rootwad size. The shape is assumed to be rectangular. The selection of the debris accumulation dimensions is based on engineering judgment using the key log dimensions and the assumption that the accumulation would be significant during a design event. These assumptions should be confirmed for reasonableness with bridge maintenance and inspection personnel (and/or by evaluating debris size and shape in the photographic archive in Appendix A).

The hydraulic conditions are calculated for a 100-year flood with and without debris loading. Without debris loading, the maximum channel velocity is 6.25 ft/s (1.91 m/s) and flow depth is 15.3 ft (4.66 m). When the hydraulic model is run to simulate debris loading, the maximum channel velocity is 6.17 ft/s (1.88 m/s) and the flow depth is 15.5 ft (4.72 m).

Because the length of the debris cluster exceeds the flow depth, the debris scour will also need to be computed for a length equal to the flow depth. It is assumed that this shorter debris pile is 26 ft (7.9 m) wide but remains 6 ft (1.8 m) thick and that the hydraulic conditions are the same as for the larger debris cluster.

The wall pier at this bridge has a width, a, of 1.5 ft (0.46 m); a length, L, of 43 ft (13.1 m); a 5° angle of attack; and a sharp nose (actually a debris deflector). Because the pier is more than 12 times the pier width, a maximum length of 12×1.5 ft = 18 ft (12×0.46 m = 5.5 m) is used per HEC-18 guidance. In the pier scour equation, the K_1 pier shape factor is 1.0 (because of the skew) rather than 0.9 for a sharp nose. The pier scour equation K_2 factor can be calculated based on HEC-18 guidance, or the projected width of the pier can be used in lieu of using K_2. K_3 is 1.1 based on an assumption of plane bed or small dunes expected on the South Platte River during extreme floods, and K_4 is 1.0 because armoring is not expected.

Guidance on obtaining the above information is contained in Steps 1 through 5 of the methodology outlined in the previous section.

Step 6

Compute pier scour without debris:

$$y_s = 2.0aK_1K_2K_3K_4\left(\frac{y}{a}\right)^{0.35} Fr^{0.43}$$

$$K_2 = \left[\mathrm{Cos}(\theta)+\left(\frac{L}{a}\right)\mathrm{Sin}(\theta)\right]^{0.65}$$

$$= \left[\mathrm{Cos}(5)+\left(\frac{18}{1.5}\right)\mathrm{Sin}(5)\right]^{0.65} = 1.6$$

$$Fr = \frac{V}{\sqrt{gy}} = \frac{6.25}{\sqrt{32.2\times 15.3}} = 0.28$$

$$y_s = 2.0\times 1.5\times 1.0\times 1.6\times 1.1\times 1.0\left(\frac{15.3}{1.5}\right)^{0.35}(0.28)^{0.43}$$

$$= 6.9\ \mathrm{ft}(2.1\ \mathrm{m})$$

Alternatively, the pier scour can be computed using the projected width and excluding K_2 from the pier scour equation.

The projected width of the pier without debris is:

$$a_{proj} = a\mathrm{Cos}(\theta)+L\mathrm{Sin}(\theta) = 1.5\mathrm{Cos}(5)+18\mathrm{Sin}(5)$$

$$= 3.1\ \mathrm{ft}(0.93\ \mathrm{m})$$

$$y_s = 2.0a_{\mathrm{proj}}K_1K_3K_4\left(\frac{y}{a_{\mathrm{proj}}}\right)^{0.35} Fr^{0.43}$$

$$y_s = 2.0\times 3.1\times 1.0\times 1.1\times 1.0\left(\frac{15.3}{3.1}\right)^{0.35}(0.28)^{0.43}$$

$$= 6.9\ \mathrm{ft}(2.1\ \mathrm{m})$$

Step 7

Determine the effective pier width with debris for the maximum debris dimensions. Maximum debris dimensions are $W = 30$ ft (9.1 m), $L = 20$ ft (6.1 m), and $T = 6$ ft (1.8 m) and the projected width of the pier should be used. For a rectangular debris cluster $K_{d1} = 0.79$ and $K_{d2} = -0.79$.

$$a_d^* = \frac{0.79TW\left(\frac{L}{y}\right)^{-0.79}+(y-0.79T)a_{\mathrm{proj}}}{y}$$

$$a_d^* = \frac{0.79\times 6\times 30\left(\frac{20}{15.5}\right)^{-0.79}+(15.5-0.79\times 6)3.1}{15.5}$$

$$= 9.7\ \mathrm{ft}(3.0\ \mathrm{m})$$

Step 8

Determine the effective pier width for the debris length equal to the flow depth. For a debris length equal to the flow depth, the debris dimensions are $W = 26$ ft (7.9 m), $L = 15.5$ ft (4.7 m), and $T = 6$ ft (1.8 m), where W and T are assumed based on the guidance in the previous section.

$$a_d^* = \frac{0.79TW+(y-0.79T)a_{\mathrm{proj}}}{y}$$

$$a_d^* = \frac{0.79\times 6\times 26+(15.5-0.79\times 6)3.1}{15.5} = 10.1\ \mathrm{ft}(3.1\ \mathrm{m})$$

Step 9

Calculate scour for a_d^* equal to the largest computed value of 10.1 ft (3.1 m) excluding K_1 and K_2 from the pier scour equation.

$$y_s = 2.0a_d^*K_3K_4\left(\frac{y}{a_d^*}\right)^{0.35} Fr^{0.43}$$

$$Fr = \frac{V}{\sqrt{gy}} = \frac{6.17}{\sqrt{32.2\times 15.5}} = 0.28$$

$$y_s = 2.0\times 10.1\times 1.1\times 1.0\left(\frac{15.5}{10.1}\right)^{0.35}(0.28)^{0.43} = 14.9\ \mathrm{ft}(4.54\ \mathrm{m})$$

Step 10

For comparison, compute the scour for a triangular debris accumulation with the same dimensions. Maximum debris dimensions are $W = 30$ ft (9.1 m), $L = 20$ ft (6.1 m), and $T = 6$ ft (1.8 m). For a triangular debris cluster, $K_{d1} = 0.21$ and $K_{d2} = -0.17$.

$$a_d^* = \frac{0.21TW\left(\frac{L}{y}\right)^{-0.17}+(y-0.21T)a_{\mathrm{proj}}}{y}$$

$$a_d^* = \frac{0.21\times 6\times 30\left(\frac{20}{15.5}\right)^{-0.17}+(15.5-0.21\times 6)3.1}{15.5}$$

$$= 5.2\ \mathrm{ft}(1.58\ \mathrm{m})$$

For a debris length equal to the flow depth, the debris dimensions are $W = 26$ ft (7.9 m), $L = 15.5$ ft (4.7 m), and $T = 6$ ft (1.8 m).

$$a_d^* = \frac{0.21TW+(y-0.21T)a_{\mathrm{proj}}}{y}$$

$$a_d^* = \frac{0.21\times 6\times 26+(15.5-0.21\times 6)3.1}{15.5} = 5.0\ \mathrm{ft}(1.58\ \mathrm{m})$$

Calculate scour for a_d^* equal to the largest computed value of 5.2 ft (1.58 m) excluding K_1 and K_2 from the pier scour equation.

$$y_s = 2.0 a_d^* K_3 K_4 \left(\frac{y}{a_d^*}\right)^{0.35} Fr^{0.43}$$

$$Fr = \frac{V}{\sqrt{gy}} = \frac{6.17}{\sqrt{32.2 \times 15.5}} = 0.28$$

$$y_s = 2.0 \times 5.2 \times 1.1 \times 1.0 \left(\frac{15.5}{5.2}\right)^{0.35} (0.28)^{0.43} = 9.7 \text{ ft} (2.96 \text{ m})$$

Summary

In summary, the pier scour would be 6.9 ft (2.1 m) without debris, 14.9 ft (4.5 m) with a rectangular debris cluster, and 9.7 ft (3.0 m) with a triangular debris cluster. The controlling condition for the rectangular cluster is when $L/y = 1.0$ (plunging flow coincident with the pier face) and, for the triangular cluster, the controlling condition is when the debris accumulation is at the maximum size.

3.10 Guidelines for Inspection, Monitoring, and Maintenance

3.10.1 Inspection

At bridges, debris characteristics can include single or multiple logs at a single pier, floating clusters at a pier, a floating raft spanning two or more piers, and submerged or sunken variations of these configurations. The debris jams compiled in the photographic archive (Appendix A) were compared to detailed measurements developed from field sites in Kansas and Colorado. This information, combined with a comprehensive review of the literature, has been used to develop guidelines for field inspectors in the assessment of debris at bridges.

Debris accumulates episodically at bridge piers, beginning as one or more logs, as shown in Figure 3.85. Single and multiple individual logs typically do not extend upstream for any significant distance and typically do not present a severe potential for creating additional scour at the pier.

However, if left unattended, more logs and branches will be caught and the jam will grow to become a mass of logs. The mass of logs then traps other floating debris, including relatively small branches, shrubs, twigs, etc. that would otherwise not hang up on a pier. A fully formed debris mass is shown in Figure 3.86 and represents a condition where a significant depth of additional scour at the pier can be expected.

Field inspectors and bridge maintenance personnel are uniquely positioned to detect and report potential hazards relating to debris buildup on bridge foundation elements. These individuals are aware of those bridges that tend to accumulate debris more frequently than other bridges in their district. Records of biennial bridge inspections, as well as maintenance records associated with debris removal, can reveal trends that will help identify debris-prone bridges.

Obviously, removing debris during the early stages of accumulation will minimize subsequent trapping of additional

Figure 3.85. Single- and multiple-log debris accumulations (photographs taken at low flow).

Figure 3.86. A fully developed debris mass creates significant scour potential.

debris that will eventually create a scour hazard; however, this approach is often not practical given limited maintenance resources. Guidance for inspectors includes the following elements:

- Inspection of debris conditions will usually consist of simple observations. However, during biennial bridge inspections, whenever possible, a thorough documentation of debris conditions should be made, including photographs and scour measurements. Underwater inspection near or beneath debris masses is extremely hazardous and is not advised, as discussed in the next section.
- When single- or multiple-log hangups are observed, a notation should be made in the inspection report and preventive maintenance should be requested. Although this condition does not represent a scour threat, it indicates that there is a potential for growth of the debris mass.
- The potential for debris recruitment from the stream banks or flood plain areas should be noted. Evidence of debris potential includes tree-lined banks that are undercut, leaning trees, and deadfall that may be swept into the stream at high flows. Areas previously affected by forest fires, beetle kill, or other circumstances that leave dead woody debris along or near the channel banks should be considered as having high potential for contributing floating material to the stream.
- If an initial hangup occurs at a bridge with a known history of debris problems, more frequent observations may be warranted, especially during or immediately after storm events or high flows. High flows recruit more floating debris that is likely to become trapped by the initial material. Keep in mind that debris arrives at bridges in bursts. Monitoring a debris mass is discussed in Section 3.10.2.
- When a debris mass is observed to have become more fully developed, expedited maintenance for removal should be scheduled. Maintenance is discussed in Section 3.10.3.
- Inspectors should also look for evidence of scour not only at the pier or piers where debris is accumulating, but also at adjacent foundation elements. Flow that sheds around a debris mass can exacerbate scour at adjacent piers or abutments and can cause erosion and instability of stream banks in the vicinity of the pier.

3.10.2 Monitoring

Monitoring a buildup of debris on bridge piers will typically begin with simple visual observations during the initial stages of debris accumulation. Existing debris masses at piers, particularly at bridges with a known history of debris problems, should be monitored more frequently than the biennial cycle, as mentioned in the previous section.

During high flows, observation of the entire extent of a debris buildup may be difficult, because the sides and leading edges may be submerged. However, during periods of low or "average" stream flows, the width and length of debris masses can be easily measured from the bridge deck with standard surveying equipment and methods, as described in the following paragraphs.

A theodolite or clinometer can be used to quickly determine the extent of a debris cluster from a bridge deck by measuring the instrument height above the water and declination angle (θ) to the leading edge of the debris cluster. The horizontal distance from the observer is $L = H/\tan(\theta)$. The distance should be measured at several radials (recording the azimuthal angle, α) from a position directly above the pier to determine the shape and lateral extent of the debris pile. For a height above the water surface measured to ± 1 ft and declination measured to $\pm 1°$, the calculated lengths should be accurate to within about 10%. This method can be used by DOTs to determine the extent of debris accumulations and is illustrated in Figure 3.87.

The thickness of debris is difficult to estimate when the water depth is greater than about 10 ft. During low flows, however, the debris-laden pier may be in shallow enough flow (or even dry, in many cases) such that a direct measurement can be made with a survey rod. **Diving around or under debris masses is extremely dangerous because of turbulence and unexpected currents in the vicinity of the debris, poor visibility, and the potential for becoming snagged or otherwise trapped underwater or being struck by a log. For these reasons, underwater inspection of a debris-laden pier is not advised.**

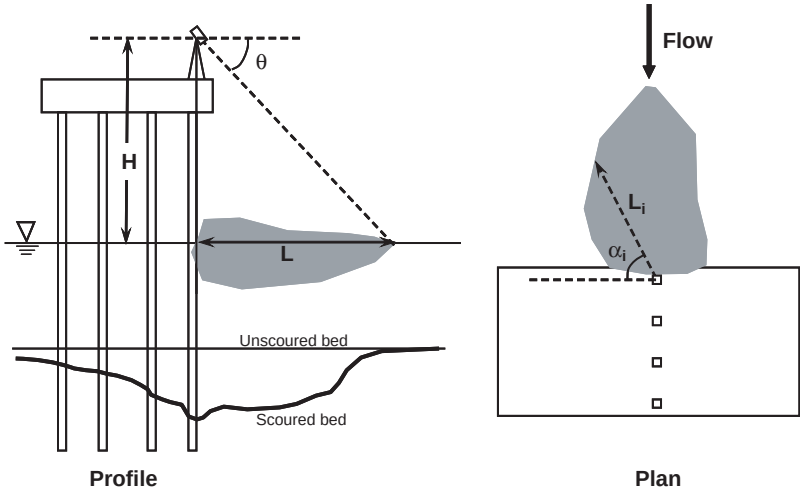

Figure 3.87. Survey method for measuring the upstream and lateral extent of debris.

3.10.3 Maintenance

Obviously, removing debris from a pier before it becomes a large, fully developed mass is desirable, but such removal is often impractical from a management and operations standpoint. As discussed in HEC-9 (Bradley et al. 2005), no specific guidelines for maintenance debris removal currently exist, instead "general maintenance practices . . . should involve regular inspections and cleaning, coupled with emergency removal of debris."

HEC-9 also suggests that priority should be given to bridges carrying interstate or other primary highways. The frequency of maintenance may be greater at these bridges compared to those carrying secondary highways or other roadways with lower average daily traffic. Obviously, a high priority should be given to bridges that are known to be prone to debris problems. Increased frequency of maintenance at these sites should be considered as well.

A maintenance plan that clearly defines the activities and responsibilities of inspectors and maintenance personnel should be developed for any structure that is susceptible to debris problems. Considerations for maintenance activities include the following:

- **Access:** It may be necessary to provide an area on one or both banks for mechanical equipment to reach the debris and remove it from the structure, ideally without having to disrupt traffic. Tracked vehicles can often be used after a flood event when the flow is very shallow or the affected pier is dry after flood waters recede. At large bridges with perennial flow, equipment may have to operate from a barge moored near the debris mass.
- **Debris disposal:** It is not acceptable to simply dislodge debris from a bridge and let it float downstream. Nor should debris be moved from the upstream side of a bridge to the downstream side. Debris may be temporarily placed on the banks or overbank flood plain areas, but it must be removed in a timely fashion so that it is not reintroduced to the stream during the next flood. Potential disposal options include using it as firewood or chipped wood or, if it is of high grade, using it for structural purposes. These disposal options are preferable to burying or burning it, as they may provide an opportunity for some financial return.
- **Countermeasures:** Countermeasures to control debris at bridge piers function in one of two ways: either trapping the debris upstream of the bridge or deflecting the debris away from the piers. Countermeasures have met with varying degrees of success and must themselves be inspected and maintained. However, they can serve to minimize the debris loading on the pier itself. Design guidance for debris countermeasures is described in detail in HEC-9. Types of countermeasures include:
  - Deflectors constructed of steel rails or steel piles filled with concrete placed upstream of the pier (Figure 3.88).
  - Debris fins consisting of a thin wall made of concrete, steel rails, or timber installed upstream of the pier and aligned with the flow (Figure 3.89).
  - In-channel debris basins, which are storage basins excavated in the stream bed upstream of the bridge. A row of posts to catch and hold floating debris must be included. After flood events, the debris stored in the basin must be removed.
  - Debris sweepers consisting of a buoyant cylinder mounted on the leading edge of a pier. The sweeper can slide up and down on a vertical metal pole and spins in the current. When debris encounters the spinning cylinder, it is kicked off to one side (Figure 3.90).

Source: Bradley et al. (2005)

Figure 3.88. Debris deflectors made of steel pipes filled with concrete.

Source: Bradley et al. (2005)

Figure 3.90. Spinning-type debris sweeper.

3.11 Implementation Plan

3.11.1 The Product

As described in more detail in the preceding sections, the products of this research include practical guidelines for predicting debris hazards at bridges and methods for predicting the depth, shape, and extent of scour at bridge piers resulting from debris accumulations.

3.11.2 The Market

The market or audience for the results of this research will be hydraulic engineers and maintenance and inspection personnel in state, federal, and local agencies with a bridge-related responsibility. These would include the following:

- State highway agencies
- Federal Highway Administration
- City/county bridge engineers
- Railroad bridge engineers
- U.S. Army Corps of Engineers
- Bureau of Land Management
- National Park Service
- Forest Service
- Bureau of Indian Affairs
- Any other governmental agency with bridges under their jurisdiction
- Consultants to the agencies above

Source: Bradley et al. (2005)

Figure 3.89. Timber debris fins with sloped leading edge.

3.11.3 Impediments to Implementation

A serious impediment to successful implementation of results of this research will be difficulties involved in reaching a diverse audience scattered among numerous agencies and institutions; however, this can be countered by a well-planned technology transfer program. Because of the complexity and geographic scope of the debris-related bridge scour problem and the diversity of bridge foundation geometries, a major challenge was to present the results in a format that can be applied by agencies with varying levels of engineering design capabilities and maintenance resources. Presenting the guidelines and methods in a format familiar to bridge owners, who are the target audience, will facilitate their use of the results of this research.

3.11.4 Leadership in Action

Through the National Highway Institute (NHI) and its training courses, FHWA has the program in place to reach a diverse

and decentralized target audience. For example, recommendations from this study could be considered for the next edition of HEC-18, "Evaluating Scour at Bridges," and NHI Course No. 135046, "Stream Stability and Scour at Highway Bridges."

TRB—through its annual meetings and committee activities, publications such as the *Transportation Research Record,* and periodic bridge conferences—can also play a leading role in disseminating the results of this research to the target audience.

AASHTO is the developer and sanctioning agency for standards, methods, and specifications. Thus, research results can be formally adopted through the AASHTO process. As a collective representation of individual state DOTs, AASHTO can also suggest any needed training to be developed by FHWA or others. The AASHTO Subcommittee on Bridges and Structures could provide centralized leadership through the involvement of all state DOT bridge engineers.

Regional bridge conferences, such as the Western Bridge Engineer Conference or the International Bridge Engineering Conferences, reach a wide audience of bridge engineers, manufacturers, consultants, and contractors. The groups would have an obvious interest in the effects of debris on bridges and their acceptance of the results of this research will be key to implementation by bridge owners.

3.11.5 Activities for Implementation

The activities necessary for successful implementation of the results of this research relate to technology transfer activities, as discussed in the previous section, and the activities of appropriate AASHTO committees.

3.11.6 Criteria for Success

The best criteria for judging the success of this implementation plan will be acceptance and use of the guidelines and methodologies that result from this research by state highway agency engineers and others with responsibility for design, maintenance, rehabilitation, or inspection of highway facilities. Progress can be gauged by peer reviews of technical presentations and publications and by the reaction of state DOT personnel during presentation of results at NHI courses. A supplemental critique sheet could be used during NHI courses to provide feedback on the applicability of the guidelines and suggestions for improvement.

The desirable consequences of this project, when implemented, will be more efficient planning, design, maintenance, and inspection of highway facilities considering the threat from debris. The ultimate result will be a reduction in the number of bridge failures and reduction in damage to highway facilities attributable to accumulation of debris on bridge piers.

CHAPTER 4

Conclusions and Suggested Research

4.1 Applicability of Results to Highway Practice

Approximately 83% of the 583,000 bridges in the National Bridge Inventory are built over waterways. Many, especially those on more active streams, will experience problems with scour, bank erosion, and channel instability during their useful life (Lagasse et al. 2001). The magnitude of these problems is demonstrated by the estimated average annual flood damage repair costs of approximately $50 million for bridges on the federal aid system.

Highway bridge failures caused by scour and stream instability account for most of the bridge failures in this country. A 1973 study for the FHWA (Chang 1973) indicated that about $75 million were expended annually up to 1973 to repair roads and bridges that were damaged by floods. Extrapolating the cost to the present makes this annual expenditure to roads and bridges on the order of $300 to $500 million. This cost does not include the additional indirect costs to highway users for fuel and operating costs resulting from temporary closure and detours and to the public for costs associated with higher tariffs, freight rates, additional labor costs and time. The indirect costs associated with a bridge failure have been estimated to exceed the direct cost of bridge repair by a factor of five (Rhodes and Trent 1993). Rhodes and Trent (1993) document that $1.2 billion was expended for the restoration of flood-damaged highway facilities during the 1980s.

Although it is difficult to be precise regarding the actual cost to repair damage to the nation's highway system from problems related to pier scour as a result of debris accumulation, the number is obviously very large. In addition, the costs cited in the preceding paragraphs do not include the extra costs that result from over design of bridge foundations that result from the inability to predict where and how debris will accumulate on bridge piers and calculate the resulting increase in pier scour. This lack of knowledge often results in overly conservative design.

The guidelines and methods that resulted from this research provide guidance to bridge owners for predicting and calculating the effects of debris on scour at piers. The end result will be a more efficient use of highway resources and a reduction in costs associated with the impacts of debris on highway facilities.

4.2 Conclusions and Recommendations

4.2.1 Overview

This research accomplished its basic objectives of developing guidelines for predicting the size and geometry of debris accumulations at bridge piers and methods for quantifying scour at bridge piers resulting from debris accumulations. The project produced results on two related problems: (1) predicting the accumulation characteristics of debris from potentially widely varying source areas, in rivers with different geomorphic characteristics, and on bridges with a variety of substructure geometries and (2) developing improved methods for quantifying the depth and extent of scour at bridge piers considering both the accumulation variables and the range of hydraulic factors involved.

Waterborne debris (or drift), composed primarily of tree trunks and limbs, often accumulates on bridges during flood events. Debris accumulations can obstruct, constrict, or redirect flow through bridge openings resulting in flooding, damaging loads, or excessive scour at bridge foundations. The size and shape of debris accumulations vary widely, ranging from a small cluster of debris on a bridge pier to a near complete blockage of a bridge waterway opening. Debris accumulation geometry is dependent on the characteristics and supply of debris transported to bridges, on flow conditions, and on bridge and channel geometry. The effects of debris accumulation can vary from minor flow constrictions to severe flow contraction resulting in significant bridge foundation scour.

At the outset of this study, only limited guidance was available on which to base critical public safety decisions during flooding on debris-prone rivers. There was a pressing need for accurate methods of quantifying the effects of debris on scour at bridge pier foundations for use by DOTs and other agencies in the design, operation, and maintenance of highway bridges.

4.2.2 Advances in the State of Practice

Guidelines for Debris Production and Delivery

As an extension of the original work by Diehl (1997) for the FHWA, expanded guidelines and detailed flowcharts are now available for estimating (1) the potential for debris production and delivery from the contributing watershed of a selected bridge and (2) the potential for accumulation on individual bridge elements. To facilitate the application of the guidelines, a case study of a debris-prone bridge on the South Platte River in Colorado is summarized in Chapter 3 and presented in detail in Appendix D. The case study also introduces and illustrates the use of Field Data Sheets for evaluating the potential for debris production and delivery from a given watershed. These sheets were developed specifically for the debris loading problem and provide a rapid and efficient approach to identifying the hydrologic, hydraulic, geomorphic, and vegetative factors relevant to the problem. When used as intended during a site reconnaissance, the data sheets will:

- Supply a methodological basis for field studies of the debris hazard
- Present a format for the collection of qualitative information and quantitative data on the stream system and its riparian corridor
- Supply the data and input information necessary to implement the engineering analysis of the debris hazard, and estimate the depth and extent of scour expected at a specific bridge pier under debris loading.

Although the sheets appear complex, they were designed to produce a comprehensive record of the morphology of the stream and its surroundings and to be applicable to a wide range of river types and sizes in diverse settings. With this in mind, one should resist the temptation to omit filling out part of the sheets for the purposes of expediency or because of perceived irrelevance, because the data may be used for other applications in the future. However, the sheets can be customized to a particular region, basin, or river through the removal of extraneous material rather than the omission of entire topics or sections.

Photographic Archive

As a basis for laboratory testing, the photographic archive introduced in Chapter 2 (see also Appendix A), the field pilot study of debris sites in Kansas (see Appendix C), and the South Platte River case study (see Appendix D) were examined to develop a limited number of debris shapes that represent the maximum number of configurations found in the field. These simplified, yet realistic, shapes that could be constructed and replicated with a reasonable range of geometric variables provided the physical characteristics of debris clusters needed for laboratory testing. Rectangular and triangular shapes with varying planform and profile dimensions were selected to represent prototype debris accumulations. To account for additional variables thought to be relevant to debris clusters in the field, a method to simulate both the porosity and roughness of the clusters was developed.

While the photographic archive in Appendix A provided the key to developing an efficient, comprehensive laboratory test program, the value of the archive will extend beyond the needs of this study. The archive provides a well-documented database on debris generation, movement, accumulation, and scour at bridges that can be used to inform and train design and maintenance personnel on debris-related hazards. As illustrated by example in the archive, supplemental data on a specific bridge can be acquired with relative ease using Internet and programmatic resources available to all DOTs (e.g., Google Earth™, Terraserver, the National Bridge Inventory).

Observations from Laboratory Testing

Laboratory-scale physical modeling of scour at debris-laden bridge piers was conducted using a range of pier types and widths, combined with different sizes and shapes of debris attached to the upstream pier face. In most (but not all) of the cases investigated, the presence of debris resulted in greater scour at the pier than the baseline (no-debris) condition.

Rectangular, blocky debris masses tended to produce the greatest scour at the pier when the extent ("length" dimension) of the debris upstream of the pier was on the order of one flow depth. This condition produced plunging flow that was directed toward the channel bed in the immediate vicinity of the pier face, resulting in a worst-case scour condition. Total scour at the pier was also significantly increased when the total frontal area of flow blockage (as a percentage of the cross-sectional area of the approach channel) was large. In that case, the debris-induced scour appeared to be similar to that created by pressure flow and contraction effects, for example, pressure flow beneath bridge decks that are submerged during floods.

Triangular debris clusters (conical in profile) were also investigated, because the debris photographic archive revealed that a triangle is another very common shape that can be produced in the field as drift accumulates at a pier. In a triangular configuration, the thickness of the debris is greater at the pier face, tapering upward and thinning toward the leading (upstream) point. This shape tended to produce more scour

at the pier face compared to the baseline (no-debris) condition. In addition, triangular debris shapes produced more pronounced scour laterally outward from the sides of the pier, apparently because much of the debris-blocked flow tends to be shed around this shape compared to a rectangular, blunt-shaped blockage.

Although the effect of lateral scour extent on adjacent piers was not investigated in detail, data collected from the laboratory tests yield valuable information in this regard. Both rectangular and triangular (conical) debris shapes resulted in lateral scour that was directly related to the width of debris blockage. Interestingly, the lateral side slopes of the debris-induced scour holes were relatively mild.

Pier width normal to the flow direction is also important in determining the total scour depth at the pier face, even when the pier is loaded with a large amount of debris. Given the same size and shape of debris, a slender pier with debris will experience less total scour than a wider pier with the same amount of debris, for the same hydraulic conditions of the approach flow.

Scour Prediction at Bridge Piers with Debris Loading

The laboratory testing program was designed and conducted to develop information on a variety of factors related to debris accumulations at piers that can potentially affect the depth of scour at the pier. The factors examined in this study included:

- Shape: Rectangular or triangular
- Size: Width, length, and thickness
- Location: Surface (floating), mid-depth, or bed (partially buried)
- Roughness: Smooth or roughened
- Porosity: Impermeable or 25% porosity
- Approach velocity: V/V_c ratios of 0.70 and 1.0

Selected combinations of the above factors were also tested; for example, a particular debris shape might be tested as (1) a smooth, impermeable body; (2) a smooth, porous body; (3) a rough, impermeable body; and (4) a rough, porous body.

All tests were conducted in the 8 ft (2.4 m) wide flume at CSU. Most of the tests were conducted using 4 in. (10.2 cm) square piers. Tests using slender piers (pile bent and wall piers) were also conducted, but were necessarily limited in number, considering the resources available for this study.

The tests were not designed to represent any particular scale ratio. However, considering typical pier sizes and dimensions of debris accumulations found in the field and the photographic archive, a model:prototype scale ratio of approximately 1:10 to 1:30 can be considered a reasonable range for the tests conducted in the flume. Factors not considered in the test program include the effect of bed material grain size, flow depth, live-bed conditions, and contraction scour. In addition, tests at different scales, including near-prototype scale ratios of approximately 1:2 to 1:4 were originally considered but were ultimately dropped from the program so that other factors could be investigated in more detail.

All pier scour prediction equations use pier width as a factor that contributes to the estimated scour depth. Intuitively, the accumulation of debris on a pier causes the pier to appear larger in the flow field, thereby increasing the total area blocked by obstruction. HEC-18 (Richardson and Davis 2001) uses the width of the debris perpendicular to the flow direction to estimate the additional obstruction.

The concept of *equivalent pier width* has been widely accepted as a way to estimate scour at complex piers and assess the extent to which debris affects scour at piers. Using the data collected from the laboratory program, this concept was validated as the best approach for predicting the effect of debris on pier scour.

Dongol (1989) and Melville and Dongol (1992) provide an equation to calculate the "equivalent width," b_e, of a bridge pier that is loaded with debris. The equation uses both the width and thickness of the debris and is based on scour data from a limited number of tests in a laboratory flume. Only floating (surface) debris at cylindrical piers was tested, with the debris wrapped around the pier in all directions. The effects of a debris mass with variable length, width, and thickness upstream of a bridge pier and the effect of the vertical location of the debris mass within the water column could not be predicted. Under this NCHRP study, these effects were investigated in detail and can now be considered when estimating the impact of debris on bridge pier scour.

Building on the algorithm originally proposed by Melville and Dongol and using an equivalent pier width, a_d^*, an improved predictive equation is now available. Considering the most common shapes of debris clusters found in the archive (rectangular in planform and profile, and triangular in planform but conical in profile), length, width, and thickness of the debris accumulation upstream of a bridge pier can now be considered. Different coefficients and exponents based on more extensive laboratory testing are recommended, but the basic form of the effective width equation is retained. The recommended equation is stable, can be adapted to most conditions found at bridge piers in the field, and complements the approach to estimating pier scour currently recommended in FHWA's HEC-18.

For the equivalent pier width equation, optimizing the coefficient K_{d1} and exponent K_{d2} to the observed laboratory data reveals that the shape and upstream extent of the debris do affect the resulting scour at the pier face. The coefficient K_{d1} in the effective pier width equation is thus seen to be a shape factor, while the exponent K_{d2} is a factor that describes

the intensity of the plunging flow created by the debris blockage. In addition, the methodology as formulated accounts for the occurrence of the upstream trough when a rectangular debris cluster extends upstream a distance, L, greater than the approach flow depth, y, as well as the observation of maximum scour when L equals y for a rectangular accumulation of debris.

The relationship derived using an "equivalent width" concept uses optimized coefficients and exponents based on laboratory data, but it is essentially a best-fit relationship that underestimates the observed scour as often as it overestimates. A relationship better suited to design should tend towards conservatism; that is, underestimation of the observed (i.e., actual) scour should be relatively rare. Consequently, design equations for estimating an equivalent pier width for use with the CSU pier scour equation using an "envelope" concept were derived. These equations for a_d^* are recommended for design.

Roughness and porosity of the debris mass have long been assumed to significantly affect the depth of scour at a bridge pier. This assumption was based largely on anecdotal data. The data from this laboratory research program indicate that roughness and porosity of the debris mass do not significantly affect the observed scour. At most, roughness and porosity can be considered second-order variables that are not significant compared to the size and shape of the debris mass.

The data also indicate that the location of the debris in the water column affects the total depth of scour at the pier face. The effect of debris location in the water column on pier scour was investigated using two different rectangular debris shapes and was quantified by the ratio of scour depth caused by the debris to the baseline (no-debris) condition. In general, rectangular debris cluster placed as a surface raft caused greater scour at the model square piers compared to baseline conditions. In contrast, when this same shape was located at mid-depth in the flow, significantly less scour at the pier face was observed. This was presumably due to the relative distribution of flow over the debris compared to the plunging flow occurring beneath it. Similarly, when the debris was placed on the bed, less scour was observed at the pier face compared to baseline conditions.

When a debris mass accumulates at a pier, it typically initiates and grows from floating drift material. The laboratory tests conducted under this study program indicate that the lateral extent of the scour caused by floating debris rafts is directly proportional to the width of the raft. The impact of the lateral scour extent on adjacent piers or abutments was not directly investigated; however, inferences in this regard can be drawn from the laboratory data collected:

- Rectangular debris: The lateral extent of scour created by rectangular floating debris extends outward from the edge of the debris at a slope ranging from about 4H:1V to 6H:1V.
- Triangular debris: The lateral extent of scour created by triangular floating debris extends outward from the edge of the debris at a slope ranging from 2H:1V to 3H:1V.

Both 1-D and 2-D hydraulic models have some capability to incorporate debris at a bridge pier. In a hydraulic model, the actual geometry of the debris cluster should be used, rather than incorporating any formulation of an effective pier width. The effective pier width is only used for scour calculations. It is recommended that hydraulic modeling be used to determine hydraulic variables in the bridge reach and that the effective pier width approach be used directly in the HEC-18 pier scour equation to estimate debris impacts.

Inspection, Monitoring, and Maintenance

General guidelines and considerations for inspection, monitoring, and maintenance of debris-prone bridges are discussed in Chapter 3. The major points include the following:

- Field inspectors and bridge maintenance personnel are uniquely positioned to detect and report potential hazards relating to debris buildup on bridge foundation elements. These individuals are aware of those bridges that tend to accumulate debris more frequently than other bridges in their district. Records of biennial bridge inspections, as well as maintenance records associated with debris removal, can reveal trends that will help identify debris-prone bridges.
- Obviously, removing debris from a pier before it becomes a large, fully developed mass is desirable, but this approach is often impractical from a management and operations standpoint.
- However, when single- or multiple-log hangups are observed, a notation should be made in the inspection report and preventive maintenance should be requested.
- A maintenance plan that clearly defines the activities and responsibilities of inspectors and maintenance personnel should be developed for any structure that is susceptible to debris problems.

4.2.3 Deliverables

As a result of this research, bridge owners now have documentation, guidelines, and analytical procedures to quantify the effects of debris-induced scour on bridge piers. These include the following:

- A fully documented database on debris and case studies, photographs, and data related to debris generation, movement, accumulation, and scour at bridges that can be used to inform and train design and maintenance personnel on debris-related hazards.

- Necessary guidelines for predicting the size, location, and geometry of debris accumulations at bridge piers.
- Methods for quantifying scour at bridge piers resulting from debris accumulations.
- Guidance for incorporating debris effects in 1-D and 2-D hydraulic modeling.
- Worked example problems and a case study illustrating the application of the guidelines and analytical methods.
- Suggestions for implementing the results of this research.

The end results of this research are practical, implementable guidelines for bridge owners that enhance their ability to predict debris-related hazards at bridges and design, operate, inspect, and maintain bridges considering those hazards.

4.3 Suggested Research

The observations of many researchers including Lyn et al. (2003b) would suggest that the recruitment, transport, and accumulation of debris appears to be a somewhat "random process," while the results of Manners et al. (2007) show that "the relationship between individual logs and complete debris jams is complex and nonlinear." Lyn also noted that the delivery of debris to a given site "seems to occur in bursts, rather than continuously, even during a flow event of extended duration" and that a possible explanation for this is that "the debris is not generated in the vicinity of the site, and the bursts result from different travel times from different contributing areas." They also concluded that "the transport of debris occurs rather intermittently with long periods of comparative inactivity punctuated by short periods of intense activity, generally on the rising limb of the hydrograph."

Both the field work and the debris photographic archive compiled for this study validate these findings. Any attempt to develop more definitive guidelines for predicting the site-specific geometry of a debris cluster at a particular bridge is not likely to yield meaningful results. However, this research had limitations in both time and budget that precluded conducting many of the laboratory tests originally planned. Tests of debris effects at a pile bent or long wall pier substructure with and without skew were not tested under this research. Also, time and budget did not permit fully exploiting the photographic archive.

Additional research is highly likely to yield important results on these topics. In addition, an expanded laboratory testing program would permit refining and expanding the applicability of the algorithm for predicting the depth and extent of scour at debris-prone bridges. Consequently, the following research is suggested:

- Using the examples in Appendix A as a model, expand the photographic archive of debris at bridges into a fully documented, searchable database for all sites currently in the archive. If resources are available, the archive could be expanded to include more sites.
- No laboratory tests were conducted for a debris length to flow depth ratio less than 1.0. For deep rivers, this ratio is likely to be less than 1.0, and additional tests are warranted.
- Conduct selected laboratory tests at a larger scale and include multiple-column (pile bents) and wall-type piers skewed to the flow direction. The prevalence of these pier types in the survey responses warrants these additional tests.
- Conduct laboratory tests at greater flow depths, because flow depth was not varied in this study. In addition, conduct higher velocity tests in the live-bed regime.
- Investigate in the laboratory the additional case representing a "true debris raft." The raft would extend the full width of the flume and far enough upstream to result in a uniform flow field at the pier.
- Further evaluate data from tests already completed under this study in order to develop guidance on potential impacts at adjacent piers or abutments or at a downstream bridge.
- Construct a realistic debris mass from natural materials (branches, rootwads, etc.) and test it in the laboratory to validate the prediction equations, because the equations were developed from tests that utilized "idealized" debris masses.
- Identify a debris-prone bridge on the South Platte River (sand bed channel); instrument it with fixed, telemetered scour-monitoring devices; and record the debris characteristics during and after each scour-producing event.
- Although debris mass dimensions and shape cannot be predicted for a specific bridge, measure individual debris masses in the field to evaluate whether specific debris mass dimensions can be correlated to the key log length and diameter, and rootwad size.

References

Abbe, T. B. and Montgomery, D. R. (1996). "Large Woody Debris Jams, Channel Hydraulics, and Habitat Formation in Large Rivers," *Regulated Rivers: Research and Management,* Vol. 12, pp. 201–221.

Abbe, T. B. and Montgomery, D. R. (2003). "Patterns and Processes of Wood Debris Accumulation in the Queets River Basin, Washington," *Geomorphology,* Vol. 51, pp. 81–107.

Abt, S. R., Dudley, S. J., and Fischenich, J. C. (1998). "Woody Debris Influence on Flow Resistance," *Proceedings of the 1998 ASCE Wetlands Engineering & River Restoration Conference,* Denver, CO.

Alonso, C. V. (2004). "Transport Mechanics of Stream-Borne Logs," *Riparian Vegetation and Fluvial Geomorphology, Hydraulic, Hydrologic, and Geotechnical Interactions,* American Geophysical Union, Washington, DC

Andrus, C. W., Long, B. A., and Froehlich, H. A. (1988). "Woody Debris and its Contribution to Pool Formation in a Coastal Stream 50 Years After Logging," *Canadian Journal of Fisheries and Aquatic Management,* Vol. 45, pp. 2080–2086.

Andrus, C. W. and Lorenzen, T. (1992). "Water Classification and Protection Project," Draft Report, Oregon Department of Forestry, Salem, OR.

Bailey, R. G. (1983). "Delineation of Ecosystem Regions," *Environmental Management,* Vol. 7, No. 4, pp. 365–373.

Bailey, R. G. (1995). "Descriptions of the Ecoregions of the United States," 2nd Edition, revised and expanded (1st Edition 1980), Miscellaneous Publication 1391 (rev.), Forest Service, U.S. Department of Agriculture, Washington DC, 108 p. (incl. 1:7,500,000 map).

Bailey, R. G. (1997). "Ecoregions Map of North America," Miscellaneous Publication Number 1548, Forest Service, U.S. Department of Agriculture.

Bailey, R. G. (2005). "Identifying Ecoregion Boundaries," *Environmental Management,* Vol. 34, Suppl. 1, pp. S14-S26.

Barton, K. E., Howell, D. G., and Virgil, J. F. (2003). "The North America Tapestry of Time and Terrain," pamphlet to accompany Geologic Investigations Series I-2720, U.S. Geological Survey, Washington, DC. (1:8,000,000 map).

Beechie, T. J. and Sibley, T. H. (1997). "Relationships Between Channel Characteristics, Woody Debris, and Fish Habitat in Northwestern Washington Streams," *Transactions of the American Fisheries Society,* Vol. 126, pp. 217–229.

Bilby, R. E. (1984). "Removal of Woody Debris May Affect Stream Channel Stability," *Journal of Forestry,* Vol. 82, pp. 609–613.

Bilby, R. E. and Ward, J. W. (1989). "Changes in Characteristics and Function of Woody Debris with Increasing Size of Streams in Western Washington," *Transactions of the American Fisheries Society,* Vol. 118, pp. 368–378.

Bilby, R. E. and Ward, J. W. (1991). "Characteristics and Function of Large Woody Debris in Streams Draining Old Growth, Clear-Cut, and Second-Growth Forests in Southwestern Washington," *Canadian Journal of Fisheries and Aquatic Sciences,* Vol. 48, pp. 2499–2508.

Bocchiola, D., Rulli, M. C., and Russo, R. (2008). "A Flume Experiment on the Formation of Wood Jams in Rivers," *Water Resources Research,* Vol. 44, W02408, 17 pp.

Bradley, J. B., Richards, D. L., and Bahuer, C. D. (2005). "Debris Control Structures—Evaluations and Countermeasures," Third Edition, Hydraulic Engineering Circular 9 (HEC-9), FHWA IF 04-016, Washington, DC., 179 p.

Braudrick, C. A. and Grant, G. E. (2000). "When Do Logs Move in Rivers?" *Water Resources Research,* 36(2), pp. 571–583.

Braudrick, C. A. and Grant, G. E. (2001). "Transport and Deposition of Large Woody Debris in Streams: A Flume Experiment," *Geomorphology,* Vol. 41, pp. 263–283.

Braudrick, C. A., Grant, G. E., Ishikawa, Y., and Ikeda, H. (1997). "Dynamics of Wood Transport in Streams: A Flume Experiment," *Earth Surface Processes and Landforms,* Vol. 22, pp. 669–683.

Brice, J. C., Blodgett, J. C., Carpenter, P. J., Cook, M. F., Craig, G. S., Jr., Eckhardt, D. A., Hines, M. S., Lindskov, K. L., Moore, D. O., Parker, R. S., Scott, A. G., and Wilson, K. V. (1978). "Countermeasures for Hydraulic Problems at Bridges, Volume 1—Analysis and Assessment," FHWA RD-78-162, FHWA, Washington, DC., 169 p.

Brunner, G. W. (2008). "HEC-RAS, River Analysis System User's Manual," Organization Report No. CPD-68, Hydrologic Engineering Center, U.S. Army Corps of Engineers, Davis, CA, 733 p.

Bryant, M. D. (1983). "The Role and Management of Woody Debris in West Coast Salmonid Nursery Streams," *North American Journal of Fisheries Management,* Vol. 3, pp. 322–330.

Buffington, J. M., Lisle, T. E., Woodsmith, R. D., and Hilton, S. (2002). "Controls on the Size and Occurrence of Pools in Coarse-Grained Forest Rivers," *River Research and Applications* 18:507–531.

Chang, F. F. M. (1973). "A Statistical Summary of the Cause and Cost of Bridge Failures," Federal Highway Administration, U.S. Department of Transportation, Washington, DC.

Chang, F. F. M. and Shen, H. W. (1979). "Debris Problems in the River Environment," FHWA RD-79-62. 67 p.

Chergui, H. and Pattee, E. (1991). "Breakdown of Wood in the Side Arm of a Large River: Preliminary Investigations," *Internationale*

Vereinigung für Theoretische und Angewandte Limnologie, Verhandlungen, Vol. 24, No. 3, pp. 1785–1788.

Cherry, J. and Beschta, R. L. (1989). "Coarse Woody Debris and Channel Morphology: A Flume Study," *Water Resources Bulletin,* Vol. 25, No. 5, pp. 1031–1036.

Collier, M. (2005). "Debris Free, Inc. Bridge Systems," Ojai, CA.

D'Aoust, S. G. and Millar, R. G. (2000). "Stability of Ballasted Woody Debris Habitat Structures," *Journal of Hydraulic Engineering,* Vol. 126, No. 11, pp. 810–817.

Daniels, M. D. and Rhoads, B. L. (2003). "Influence of a Large Woody Debris Obstruction on Three-Dimensional Flow Structure in a Meander Bend," *Geomorphology,* Vol. 51, pp. 159–173.

Diehl, T. H. (1997). "Potential Drift Accumulation at Bridges," FHWA RD-97-28, Turner-Fairbank Highway Research Center, Federal Highway Administration Research and Development, U.S. Department of Transportation, McLean, VA.

Diehl, T. H. and Bryan, B. A. (1993). "Supply of Large Woody Debris in a Stream Channel," *Proceedings of the 1993 National Conference on Hydraulic Engineering,* American Society of Civil Engineers, Vol. 1, pp. 1055–1060.

Dongol, M. S. (1989). "Effect of Debris Rafting on Local Scour at Bridge Piers," Report No. 473, School of Engineering, University of Auckland, Auckland, New Zealand.

Donnell, B. P., King, I., Letter, J. V., Jr., McAnally, W. H., and Thomas, W. A. (2006). "Users Guide to RMA2 WES Version 4.5," Coastal and Hydraulics Laboratory, Waterways Experiment Station, Engineer Research and Development Center, U.S. Army.

Downs, P. W. and Simon, A. (2001). "Fluvial Geomorphological Analysis of the Recruitment of Large Woody Debris in the Yalobusha River Network, Central Mississippi, USA," *Geomorphology,* Vol. 37, pp. 65–91.

Dudley, S. J., Fischenich, J. C., and Abt, S. R. (1998). "Effect of Woody Debris Entrapment on Flow Resistance," *Journal of American Water Resources Association,* Vol. 34, pp. 1189–1197.

Duncan, J. R. (2000). "Assessing the Structure of Debris Dams in Urban Stream Restoration and Management," *International Conference on Riparian Ecology and Management in Multi-Land Use Watersheds,* American Water Resources Association, August, pp. 305–310.

Elosegi, A., Diez, J. R., and Pozo, J. (1999). "Abundance, Characteristics, and Movement of Woody Debris in Four Basque Streams," *Archiv für Hydrobiologie,* Vol. 144, pp. 455–471.

Fenneman, N. M. (1917). "Physiographic Subdivision of the United States," *Proceedings of the National Academy of Sciences of the United States of America,* Vol. 3, pp. 17–22.

Fetherston, K. L., Naiman, R. J., and Bilby, R. E. (1995). "Large Woody Debris, Physical Process, and Riparian Forest Development in Montane River Networks of the Pacific Northwest," *Geomorphology,* Vol. 13, pp. 133–144.

Froehlich, D. C. (2002, rev. 2003). "Users Manual for FESWMS FST2DH Two-Dimensional Depth-Averaged Flow and Sediment Transport Model Release 3," University of Kentucky Research Foundation, Lexington, KY, Contract No. DTFH61-91-C-00093, 209 p.

Gippel, C. J. (1989). "The Hydraulic, Hydrologic, and Geomorphic Significance of Large Woody Debris (Snags) in Streams and Rivers," *Proceedings of the State of Our Rivers Conference,* 28–29 September 1989, Canberra, The Australian National University, Centre for Continuing Education.

Gippel, C. J. (1995). "Environmental Hydraulics of Large Woody Debris in Streams and Rivers," *Journal of Environmental Engineering,* Vol. 121, pp. 388–395.

Gippel, C. J., Finlayson, B. L., and O'Neill, I. C. (1996). "Distribution and Hydraulic Significance of Large Woody Debris in a Lowland Australian River," *Hydrobiologia,* Vol. 318, pp. 179–194.

Gippel, C. J., O'Neill, I. C., and Finlayson, B. L. (1992). "The Hydraulic Basis of Snag Management," Center for Environmental Applied Hydrology, University of Melbourne, Melbourne, 116 p.

Gregory, S. (1991). "Spatial and Temporal Patterns of Woody Debris Retention and Transport," *Bulletin of the North American Benthological Society,* Vol. 8, No. 1, p. 75.

Gregory, K. J., Davis, R. J., and Tooth, S. (1993). "Spatial-Distribution of Coarse Woody Debris Dams in the Lymington Basin, Hampshire, UK," *Geomorphology,* Vol. 6, pp. 207–224.

Haga, H., Kumagai, T., Otsuki, K., and Ogawa, S. (2002). "Transport and Retention of Coarse Woody Debris in Mountain Streams: An In Situ Field Experiment of Log Transport and a Field Survey of Coarse Woody Debris Distribution," *Water Resources Research,* Vol. 38, No. 8, 1126 p.

Hickin, E. J. (1984). "Vegetation and River Channel Dynamics," *Canadian Geographer,* XXVIII, 2, pp. 111–126.

Huizinga, R. J. and Rydlund, P. H., Jr. (2004). "Level II Bridge Scour Analysis for Structure L344 on State Route 129, Crossing Chariton River in Chariton County, Missouri," U.S. Geological Survey, Rolla, MO.

Hygelund, B. and Manga, M. (2003). "Field Measurements of Drag Coefficients for Model Large Woody Debris," *Geomorphology,* Vol. 51, pp. 175–185.

Jones, J. S. and Sheppard, D. M. (2000). "Local Scour at Complex Pier Geometries," *Proceedings ASCE 2000 Joint Conference on Water Resources Engineering and Water Resources Planning and Management,* July 3–August 2, Minneapolis, MN.

Keller, E. A. and Swanson, F. J. (1979). "Effects of Large Organic Material on Channel Form and Fluvial Processes," *Earth Surface Processes,* Vol. 4, pp. 361–380.

Keller, E. A. and Tally, T. (1979). "Effects of Large Organic Debris on Channel Form and Fluvial Processes in the Coastal Environment," In: Rhodes, D. D., and Williams, G. P. (Eds.), *Adjustments of the Fluvial System, Proceedings of the Tenth Annual Geomorphology Symposia,* Binghamton, New York, September 21–22, Kendall Hunt Publishing, pp. 361–390.

Keller, E. A. and MacDonald, A. (1983). "Large Organic Debris and Anadromous Fish Habitat in the Coastal Redwood Environment: The Hydrologic System," Technical Completion Report, California Water Resources Center, University of California, Davis.

Keller, E. A., MacDonald, A., Tally, T., and Merritt, N. J. (1985). "Effects of Large Organic Debris on Channel Morphology and Sediment Storage in Selected Tributaries of Redwood Creek, Northwestern California," In: Nolan, K. M., Kelsey, H. M., and Maron, D. C. (Eds.), *Geomorphic Processes and Aquatic Habitat in the Redwood Creek Basin, Northwestern California,* U.S. Geological Survey, Vicksburg, MS, 29 p.

Köppen, W. (1931). *Grundriss der Klimakunde,* Walter de Gruyter Co., Berlin, 388 p.

Kraft, C. E. and Warren, D. R. (2003). "Development of Spatial Pattern in Large Woody Debris and Debris Dams in Streams," *Geomorphology,* Vol. 51, pp. 127–139.

Lagasse, P. F. and Schall, J. D. (1980). "Final Report for Litigation Support on the Perkins Road Bridge Failure," prepared for Holt, Batchelor, Spicer, Ryan & Flynn, Memphis, TN.

Lagasse, P. F., Schall, J. D., Johnson, F., Richardson, E. V., Richardson, J. R., and Chang, F. (1991). "Stream Stability at Highway Structures," First Edition, Hydraulic Engineering Circular No. 20 (HEC-20), FHWA IP-90-014, Washington, DC, 195 p.

Lagasse, P. F., Schall, J. D., and Richardson, E. V. (2001). "Stream Stability at Highway Structures," Third Edition, Hydraulic Engineering Circular No. 20 (HEC-20), FHWA NHI 01-002, Washington, DC.

Lassettre, N. S. and Harris, R. R. (2001). "The Geomorphic and Ecological Influence of Large Woody Debris in Streams and Rivers," paper presented at Large Woody Debris Recruitment Modeling Workshop, University of California Cooperative Extension, April 29–30, 2002.

Laursen, E. M. and Toch, A. (1956). "Scour Around Bridge Piers and Abutments," Iowa Highway Research Board Bulletin No. 4, Iowa Institute of Hydraulic Research, Iowa City, IA.

Leighty, R. D. (2001). "Automated IFSAR Terrain Analysis System," Final Report, Defense Advanced Research Projects Agency (DOD), Information Sciences Office, Arlington, VA. (maps obtained from http://tapestry.usgs.gov/physiogr/physio.html)

Lienkaemper, G. W. and Swanson, F. J. (1987). "Dynamics of Large Woody Debris in Streams of Old-Growth Douglas Fir Forests," *Canadian Journal of Forest Research,* Vol. 17, pp. 150–156.

Likens, G. E. and Bilby, R. E. (1982). "Development, Maintenance, and Role of Organic-Debris Dams in New England Streams," General Technical Report PNW-141, Forest Service, U.S. Department of Agriculture.

Lyn, D. A., Cooper, T., Yi, Y.-K., Sinha, R., and Rao, A. R. (2003a). "Laboratory and Field Study of Single-Pier Debris Accumulation," Transportation Research Board 82nd Annual Meeting, Compendium of Papers.

Lyn, D. A., Cooper, T., Yi, Y.-K., Sinha, R., and Rao, A. R. (2003b). "Debris Accumulation at Bridge Crossings: Laboratory and Field Studies," School of Civil Engineering, Purdue University, Joint Transportation Research Program, Report No. FHWA/IN/JTRP-2003/10, 59 pp. (http://docs.lib.purdue.edu/jtrp/48).

Malanson, G. P. and Butler, D. R. (1990). "Woody Debris, Sediment, and Riparian Vegetation of a Subalpine River, Montana, U.S.A.," *Arctic and Alpine Research* 22, No. 2, pp. 183–194.

Manga, M. and Kirchner, J. W. (2000). "Stress Partitioning in Streams by Large Woody Debris," *Water Resources Research,* Vol. 36, No. 8, pp. 2373–2379.

Manners, R. B., Doyle, M. W., and Small, M. J. (2007). "Structure and Hydraulics of Natural Woody Debris Jams," *Water Resources Research,* Vol. 43, W06432, 17 pp.

McFadden, T. and Stallion, M. (1976). "Debris of the Chena River," CRREL Report 76-26, Alaska District, U.S. Army Corps of Engineers.

Melville, B. W. and Dongol, D. M. (1992). "Bridge Pier Scour with Debris Accumulation," *Journal of Hydraulic Engineering,* Vol. 118, No. 9, pp. 1306–1310.

Melville, B. W. and Coleman S. E. (2000). "Bridge Scour," *Water Resources Publications,* University of Auckland, Auckland, New Zealand.

Montgomery, D. R. and Piégay, H. (2003). Editorial—"Wood in Rivers: Interactions with Channel Morphology and Process," *Geomorphology,* Vol. 51, pp. 1–5.

Montgomery, D. R., Buffington, J. M., Smith, R. D., Schmidt, K. M., and Pess, G. (1995). "Pool Spacing in Forest Channels," *Water Resources Research,* Vol. 31, No. 4, pp. 1097–1106.

Montgomery, D. R., Massong, T. M., and Hawley, C. S. (2003). "Influence of Debris Flows and Log Jams on the Location of Pools and Alluvial Channel Reaches, Oregon Coast Range," *GSA Bulletin,* Vol. 115, No. 1, pp. 78–88.

Mueller, D. S. and Parola, A. C. (1998). "Detailed Scour Measurements Around a Debris Accumulation," ASCE Water Resources Engineering, pp. 234–239.

Murphy, M. L. and Koski, K. V. (1989). "Input and Depletion of Woody Debris in Alaska Streams and Implications for Streamside Management," *North American Journal of Fisheries Management,* Vol. 9, pp. 427–436.

Nakamura, F. S. and Swanson, F. J. (1993). "Effects of Coarse Woody Debris on Morphology and Sediment Storage of a Mountain Stream System in Western Oregon," *Earth Surface Processes and Landforms,* Vol. 18, pp. 43–61.

Nakamura, F. S. and Swanson, F. J. (1994). "Distribution of Coarse Woody Debris in a Mountain Stream, Western Cascade Range, Oregon," *Canadian Journal of Forest Research,* Vol., 24, pp. 2395–2403.

Parola, A. C., Hagerty, D. J., and Kamojjala, S. (1998a). *NCHRP Report 417: Highway Infrastructure Damage Caused by the 1993 Upper Mississippi River Basin Flooding.* TRB, National Research Council, Washington, DC.

Parola, A. C., Kamojjala, S., Richardson, J. and Kirby, M. (1998b). "Numerical Simulation of Flow Patterns at a Bridge with Debris," *Conference Proceedings,* ASCE Water Resources Engineering, Memphis, TN.

Parola, A. C., Apeldt, C. J., and Jempson, M. A. (2000). *NCHRP Report 445: Debris Forces on Highway Bridges,* TRB, National Research Council, Washington, DC.

Perham R. E. (1987). "Floating Debris Control; a Literature Review," U.S. Army Corps of Engineers, Cold Regions Research and Engineering Laboratory, Repair, Evaluation, Maintenance, and Rehabilitation Research Program Technical Report REMR-HY-2, Washington, DC, 63 p.

Perham, R. E. (1988). "Elements of Floating-debris Control Systems," U.S. Army Corps of Engineers, Cold Regions Research and Engineering Laboratory, Repair, Evaluation, Maintenance, and Rehabilitation Research Program Technical Report REMR-HY-3, Washington, DC, 69 p.

Piégay, H. (1993). "Nature, Mass and Preferential Sites of Coarse Woody Debris Deposits in the Lower Ain Valley (Mollon Reach), France," *Regulated Rivers: Research and Management,* Vol. 8, pp. 359–372.

Piégay, H. and Gurnell, A. M. (1997). "Large Woody Debris and River Geomorphological Pattern: Examples from S. E. France and S. England," *Geomorphology,* Vol. 19, pp. 99–116.

Piégay, H. and Marston, R. A. (1998). "Distribution of Large Woody Debris Along the Outer Bend of Meanders in the Ain River, France," *Physical Geography,* Vol. 19, pp. 318–340.

Piégay, H., Thevenet, A., and Citterio, A. (1999). "Input, Storage and Distribution of Large Woody Debris Along a Mountain River Continuum, the Drome River, France," *Catena,* Vol. 35, pp. 19–39.

Prasuhn, A. L. (1981). "Modeling Scour at Highway Bridges Due to Debris Accumulation," Canadian Society for Civil Engineering, *Proceedings Volume 1 of the 5th Canadian Hydrotechnical Conference,* May 26 and 27, 1981, Fredricton, New Brunswick, pp. 423–442.

Raudkivi, A. J. (1990). *Loose Boundary Hydraulics,* Pergamon Press, Oxford, UK, 538 pp.

Reihsen, G. and Harrison, L. J. (1971). "Debris Control Structures," Hydraulic Engineering Circular No. 9 (HEC-9), Federal Highway Administration Report No. EPD-86-106, Washington, DC.

Rhodes, J. and Trent, R. (1993). "Economics of Floods, Scour, and Bridge Failures," *Hydraulic Engineering, Proceedings of the 1993 ASCE National Conference,* Vol. 1, pp. 928–933.

Richardson, E. V. and Davis, S. R. (2001). "Evaluating Scour at Bridges," Fourth Edition, Hydraulic Engineering Circular No. 18 (HEC-18), FHWA NHI 01-001, Washington, DC.

Richardson, E. V., Simons, D. B., and Lagasse, P. F. (2001). "River Engineering for Highway Encroachments, Highways in the River Environment (HIRE)," Hydraulic Design Series No. 6, FHWA NHI 01-004, Washington, DC.

Richmond, A. D., and Fausch, K. D. (1995). "Characteristics and Function of Large Woody Debris in Subalpine Rocky Mountain Streams in Northern Colorado," *Canadian Journal of Fisheries and Aquatic Sciences,* Vol. 52, pp. 1789–1802.

Ringgold, P., Bollman, M., VanSickle, J., Barker, J. and Welty, J. (2000). "Predictions of Stream Wood Recruitment from Riparian Forests: Effects of Data Resolution," *International Conference on Riparian Ecology and Management in Multi-Land Use Watersheds,* American Water Resources Association, August, pp. 505–510.

Robinson, B. A. (2003). "Channel-Bank Conditions and Accumulations of Large Woody Debris along White River Between Anderson and Indianapolis, Indiana," USGS Open File Report 03-186.

Robison, E. G. (1988). "Large Woody Debris and Channel Morphology of Undisturbed Streams in Southeast Alaska," M. SC. Thesis (unpublished), Oregon State University, OR, 136 p.

Robison, E. G. and Beschta, R. L. (1990). "Identifying Trees in Riparian Areas That Can Provide Coarse Woody Debris to Streams," *Forest Science,* Vol. 36, No. 3, pp. 790–801.

Rollerson, T. and McGourlick, K. (2002). "Predicting Windthrow in Riparian Reserves in British Columbia," *Western Forester,* Vol. 47, No. 2, pp. 8–9.

Saunders, S. and Oppenheimer, M. L. (1993). "A Method of Managing Floating Debris," In: Shen, H. W., Su, S. T., and Wen, Feng, (Eds.), *Hydraulic Engineering '93, Proceedings of the 1989 National Conference on Hydraulic Engineering:* New York, American Society of Civil Engineers, pp. 1373–1378.

Schall, J. D. and Price, G. R. (2004). *NCHRP Report 515: Portable Scour Monitoring Equipment,* Transportation Research Board of the National Academies, Washington, DC.

Sedell, J. R., Bisson, P. A., Swanson, F. J., and Gregory, S. V. (1988). "What We Know About Large Trees That Fall Into Streams and Rivers," In: Maser, C., Tarrant, R. F., Trappe, J. M., and Franklin, J. F. (Eds.), *The Forest to the Sea: a Story of Fallen Trees,* General Technical Report PNW-GTR 229, Forest Service, U.S. Department of Agriculture.

Sedell, J. R. and Duval, W. S. (1985). *Influence of Forest and Rangeland Management on Anadromous Fish Habitat in Western North America, Volume 5: Water Transportation and Storage of Logs,* General Technical Report PNW-186, Forest Service, U.S. Department of Agriculture.

Sheppard, D. M., Mufeed, O., and Glasser, T. (2004). "Large Scale Clear-Water Local Pier Scour Experiments," *Journal of Hydraulic Engineering,* Vol. 130, No. 10, pp 957–963.

Shields, F. D., Jr. and Gippel, C. J. (1995). "Prediction of Effects of Woody Debris Removal on Flow Resistance," *Journal of Hydraulic Engineering,* Vol. 121, No. 4, pp. 341–354.

Simon, A., Bennett, S. J., and Neary, V. S. (2004). "Riparian Vegetation and Fluvial Geomorphology: Problems and Opportunities," *Riparian Vegetation and Fluvial Geomorphology, Water Science and Application 8,* American Geophysical Union, pp. 1–10.

Swanson, F. J. and Lienkaemper, G. W. (1978). "Physical Consequences of Large Organic Debris in Pacific Northwest Streams," General Technical Report PNW-69, Forest Service, U.S. Department of Agriculture.

Swanson, F. J., Lienkaemper, G. W., and Sedell, J. R. (1976). "History, Physical Effects, and Management Implications of Large Organic Debris in Western Oregon Streams," General Technical Report PNW-56, Forest Service, U.S. Department of Agriculture.

Swanson, F. J., Gregory, S. V., Sedell, J. R., and Campbell, A. G. (1982). "Land-Water Interactions: The Riparian Zone," In: Edmonds, R. L. (Ed.), *Analysis of Coniferous Forest Ecosystems in the Western U.S.,* Hutchison Ross, Stroudsberg, PA, pp. 267–291.

Tally, T. (1980). "The Effects of Geology and Large Organic Debris on Stream Channel Morphology and Process for Streams Flowing Through Old Growth Redwood Forests in Northwestern California," Ph.D. Dissertation, University of California, Santa Barbara, Santa Barbara, CA, 273 p.

Teply, M. E. (2001). "Tool to Relate Urban Land Use to Fish Production—Methodology to Quantify the Process of Wood Delivery," Technical Memorandum to Steve Cramer, S. P. Cramer and Associates, dated January 5, 2001.

Thorne, C. R. (1990). "Effects of Vegetation on Riverbank Erosion and Stability," In: Thornes, J. B. (Ed.), *Vegetation and Erosion—Processes and Environments,* John Wiley and Sons Ltd., Chichester, England, pp. 67–84.

Transportation Association of Canada (TAC) (2004). *Guide to Bridge Hydraulics,* Second Edition, Thomas Telford, London, 181 p.

Trewartha, G. T. (1968). *An Introduction to Weather and Climate,* Fourth Edition, New York: McGraw-Hill, 408 p.

U.S. Geological Survey (USGS) (2006). National Water Quality Assessment Program South Platte River Basin website, USGS website: http://co.water.usgs.gov/naqa/splt/

Van Sickle, J. and Gregory, S. V. (1990). "Modeling Inputs of Large Woody Debris to Streams from Falling Trees," *Canadian Journal of Forest Research,* Vol. 20, pp. 1593–1601.

Wallerstein, N. P. (2002). "Dynamic Model for Constriction Scour Caused by Large Woody Debris," *Earth Surface Process and Landforms* 28, p. 49.

Wallerstein, N. P. and Thorne, C. R. (1995). "Impact of Woody Debris on Fluvial Processes and Channel Morphology in Stable and Unstable Streams," U.S. Army Corps of Engineers, Waterways Experiment Station, Hydraulics Laboratory, Vicksburg, MS, Program 331, Flood Control Structures, Work Unit No. 32873, 104 p.

Wallerstein, N. P. and Thorne, C. R. (1998). "Computer Model for Prediction of Scour at Bridges Affected by Large Woody Debris," unpublished draft, University of Nottingham, UK.

Wallerstein, N. P and Thorne, C. R. (2004). "Influence of Large Woody Debris on Morphological Evolution of Incised, Sand-Bed Channels," *Geomorphology,* Vol. 57, pp. 53–73.

Wallerstein, N. P., Alonso, C. V., Bennett, S. J., and Thorne, C. R. (2001). "Distorted Froude-Scaled Flume Analysis of Large Woody Debris," *Earth Surface Processes and Landforms,* Vol. 26, No. 3, pp. 1265–1283.

Wallerstein, N. P., Alonso, C. V., Bennett, S. J., and Thorne, C. R. (2002). "Surface Wave Forces Acting on Submerged Logs," *Journal of Hydraulic Engineering,* Vol. 128, No. 3, pp. 349–353.

Wallerstein, N., Thorne, C. R., and Doyle, M. W. (1997). "Spatial Distribution and Impact of Large Woody Debris in Northern Mississippi," In: Wang, S. S. Y., Langendoen, F. D., and Shields, F. D., Jr. (Eds.), *Proceedings of the Conference on Management of Landscapes Disturbed by Channel Incision,* Oxford, MS, May 19–23, 1997, pp. 145–150.

Young, W. J. (1991). "Flume Study of the Hydraulic Effects of Large Woody Debris in Lowland Rivers," *Regulated Rivers: Research and Management,* Vol. 6, pp. 203–211.

Young, M. K. (1994). "Movement and Characteristics of Stream-Borne Coarse Woody Debris in Adjacent Burned and Undisturbed Watersheds in Wyoming," *Canadian Journal of Forest Research,* Vol. 24, pp. 1933–1938.

APPENDIX A

Debris Photographic Archive

Appendix A provides instructions for navigating and examples from the debris photographic archive. The appendix is available in *NCHRP Web-Only Document 148*. It can be found on the TRB website (www.trb.org) by searching for "NCHRP Web-Only Document 148".

APPENDIX B

Survey of Practitioners

This appendix contains instructions for viewing the NCHRP 24-26 questionnaire responses databases, the survey questionnaire, and the list of respondents to the survey. It is available in *NCHRP Web-Only Document 148*. It can be found on the TRB website (www.trb.org) by searching for "NCHRP Web-Only Document 148".

APPENDIX C

Field Pilot Study Report

This appendix contains the chronological trip summary of the field pilot study on four bridges in southeastern Kansas from April 25–28, 2005. The appendix is available in *NCHRP Web-Only Document 148*. It can be found on the TRB website (www.trb.org) by searching for "NCHRP Web-Only Document 148".

APPENDIX D

Field Data Sheets and Case Study

PART 1

Field Data Sheets

FIELD DATA SHEETS

FOR ASSESSING WOODY DEBRIS DELIVERY AND ACCUMULATION POTENTIAL AT A BRIDGE SITE

(To be used in conjunction with "Guidelines for Assessing Debris Production and Accumulation Potential")

1	**Date:**	**Project Personnel:**

A - BRIDGE LOCATION

3	**Street / Road Name:**	
4	**Bridge #:**	**River / Stream Name:**
5	**County and State:**	**Longitude / Latitude:**

B - DATA & INFORMATION THAT CAN BE COLLECTED PRIOR TO OR FOLLOWING A SITE VISIT

(1) SITE INFORMATION FROM TOPO MAPS, AERIAL PHOTOS, AND SURVEYS

(a) Upstream Watershed Characteristics

9	**Land-use:** Urban _____ Agricultural _____ Rural _____ Forested _____ Other _____	
10	**Man-made Disturbances (e.g. mining, logging, grazing, etc.):**	
11	**Natural Disturbances (e.g., landslides, forest fires, etc.):**	
12	**General Vegetation Patterns and Characteristics (describe):**	
13–14		

(b) Upstream Channel and Flood Plain Characteristics

16	**Upstream Reach Length:** feet / miles	**Flow Type:** Perennial _____ Ehemeral _____ Flashy _____
17	**Upstream Channel Sinuosity:**	**Upstream Channel Slope:**
18	**Average Upstream Channel Width at Crossings and/or Straight Reaches:** feet (top bank to top bank)	
19	**Average Upstream Channel Depth at Crossings and/or Straight Reaches:** feet (at bankfull)	
20	**Evidence of Active Meander Migration:** Yes ____ No ____	**Evidence of Active Bank Erosion/Retreat:** Yes ____ No ____
21	**Presence of :** Meander Cutoffs ____ Sloughs ____	**Bars and Other Major Sediment Deposits:**
22	**Was Reach Channelized:** Yes ____ No ____ Unknown ____	**Evidence of Regular Flooding:** Yes ____ No ____
23	**Visible Evidence of Active Debris Delivery, Transport, and Storage Along Upstream Channel:** Yes ____ No ____	
24–26	**Describe Existing Natural or Man-Made Barriers to Debris Delivery** (dams, diversions, bridges, rock outcrops, major constrictions etc.):	

(2) AVAILABILITY OF BRIDGE INFORMATION FROM STATE, COUNTY, OR LOCAL DOT (circle)

28	**Bridge Plans available for:**	**Bridge Inspection Records available for:**
29	*Current Bridge Site: Y N Nearby Bridge: Y N*	*Current Bridge Site: Y N Nearby Bridge: Y N*
30	**Bridge Maintenance Records available for:**	**Historic Ground Photos avaialable for:**
31	*Current Bridge Site: Y N Nearby Bridge: Y N*	*Current Bridge Site: Y N Nearby Bridge: Y N*
32	**Historic Aerial Photos available for:**	**Stream Flow Data or Records available for:**
33	*Current Bridge Site: Y N Nearby Bridge: Y N*	*Current Bridge Site: Y N Nearby Bridge: Y N*
34	**Scour Calculations available for:**	**Hydraulic Models available for:**
35	*Current Bridge Site: Y N Nearby Bridge: Y N*	*Current Bridge Site: Y N Nearby Bridge: Y N*

C - DATA & INFORMATION TO BE COLLECTED DURING A SITE VISIT & FIELD EXAMINATION

(1) OBTAIN GROUND PHOTOS AND DETAILED DESCRIPTIONS THAT DOCUMENT THE FOLLOWING

(a) Upstream Bridge Face and Structural Elements

	Bridge Openings	***Piers, Pilings, and footings***		***Abutments***
40	Number:	Type:		LEFT - Distance From Top Bank:
41	Width (ft):	Number:		Description:
42	Descriptions:	Skew to Flow (deg):		
43		Width (ft):	Nose:	
44		Descriptions:		
45				
46				RIGHT - Distance From Top Bank:
47				Description:
48–50				
51				

(b) General Bridge Reach Characteristics

Reach Location:

Straight _____ In Meander Bend - On US Limb _____ At Bend Apex: _____ On DS Limb _____ Flow Split _____

Skew to Flow (deg): Low Flow:_____ High Flow:_____ **Low Chord Height Above Streambed (ft):** Min. _____ Max. _____

Bed Material Type: Sand ___ Gravel ___ Cobble ___ Bldrs ___ **Thalweg Position at Bridge:**

Evidence of Scour (Debris Present ___ / Absent ___):

Scour Holes (Pier #):	Scour Hole Sizes (ft):	At Abutments (Location and Size):

Bars: Mid-channel Bar____ Point Bar____ Bank Attached Bar____ Sand____ Gravel____ Cobbles____ Boulders____

Existing Debris Accumulations:

On Flood Plain _____ On Bed _____ On Bars _____ On Banks _____ On Bridge Elements _____

Bankline Characteristics (LB = Left Descending Bank, RB = Right Descending Bank)

General Bank Face Shape: Convex _____ Concave _____ Vertical _____ Undercut/Overhanging _____

LB Toe Sediment Accumulation (Basal Endpoint Control): Significant _____ Moderate _____ Negligible _____

RB Toe Sediment Accumulation (Basal Endpoint Control): Significant _____ Moderate _____ Negligible _____

Bank Face/Slope Vegetation Type and Location:

LB: Trees___ Shrubs___ Grass___ Other___ Dense___ Mod.___ Sparse___ None___ Toe ___ Mid ___ Upper ___

RB: Trees___ Shrubs___ Grass___ Other___ Dense___ Mod.___ Sparse___ None___ Toe ___ Mid ___ Upper ___

Berms: LB ____ RB ____ Erosional ___ Depositional ___ **Inset Flood Plain:** LB ____ RB ____ Stable: Y___ N___

Vegetation on Berms/Inset Flood Plain: Yes ____ No ____ Trees___ Shrubs/Bushes___ Grasses___ Other ____

Additional Information:

Lateral Channel Stability & Active Bank Erosion Characteristics

Is General Bank Erosion Evident? Left Bank: Yes____ No____ Right Bank: Yes____ No____

	Intermittent	Continuous	In Bends	Reach-wide	In Toe	Whole Bank	Fluvial	Rotational	Cantilever	Saturation	Piping
Left Bank											
Right Bank											

If meander bends are present, are they actively migrating? Yes_____ No _____ Unsure _____

Additional Information:

Evidence of Vertical Channel Instability

Aggradation (berms, inset flood plain, overbank sedimentation, etc.): Yes____ No____ **Evidence:**

Degradation (headcuts, knickzone, vertical banks, exposed footings, etc.): Yes___ No___

(c) General Upstream Riparian Corridor Characteristics

Corridor Length (ft): Continuous _____ Intermittent _____ **Corridor Width (ft):** Avg_____ Max._____ Min._____

Spacing: Uniform ____ Irregular ____ **Density:** Dense ____ Mod. ____ Sparse ____ **Multistory?** Yes____ No____

Stage: Multi-generational ____ Even-Aged ____ **Typical Age:** Young____ Intermediate____ Mature____ Old Growth____

Debris Available from Flood Plain? Yes___ No___ **Tree Type:** Coniferous_____ Deciduous_____ **Healthy?** Y___ N___

Typical Species (if known):

Evident Debris Delivery Processes in Reach:

Bank Erosion/Failure___ Windthrow___ Landslides___ Flood Plain Input___ Disease/Insect Kill___ Logging___ DS Transport___

Estimate Potential for Debris Production:	***Estimate Potential for Debris Transport & Delivery:***
(See Flowchart A) High _____ Low _____	**(See Flowchart B)** High _____ Low _____

Additional Information:

101	**(d) Existing Debris Accumulation Characteristics at a Bridge Site**											
102	**Debris Accumulation Locations:** On Bars____ Bank Toe____ Top Bank____ Piers____ Abutments____											
103	**Type of Debris Accumulation on Bridge(s):**							**Typical Key Log Species:**				
104	Span Accumulation____ Pier Accumulation____ Both____							**Typical Key Log Length** (range - ft):				
105	**Root Wad Sizes** (range - ft):							**Typical Key Log Diameter** (range - ft):				
106	***Existing Debris Accumulations (Planform & Profile Descriptions)***											
107	**P&P Shape Abbreviations:** *Planform: T = Triangular R = Rectangular / Profile: C = Conical Cyl = Cylindrical IC = Inverted Cone*											
108	**At Bridge Piers/Abutments:**											
109	***Pier #***	***Abutment***	***1***	***2***	***3***	***4***	***5***	***6***	***7***	***8***	***9***	***Abutment***
110	P&P Shape	/	/	/	/	/	/	/	/	/	/	/
111	Width	/	/	/	/	/	/	/	/	/	/	/
112	Hgt/Depth	/	/	/	/	/	/	/	/	/	/	/
113	Length	/	/	/	/	/	/	/	/	/	/	/
114	**In Channel or Gap/Span (pier-to-pier):**											
115	***Span/Gap***	***Abut - 1***	***1-2***	***2-3***	***3-4***	***4-5***	***5-6***	***6-7***	***7-8***	***8-9***	***9-10***	***# - Abut***
116	P&P Shape	/	/	/	/	/	/	/	/	/	/	/
117	Width	/	/	/	/	/	/	/	/	/	/	/
118	Hgt/Depth	/	/	/	/	/	/	/	/	/	/	/
119	Length	/	/	/	/	/	/	/	/	/	/	/
120	***Estimate Debris Accumulation & Span Blockage Potential*** ***(see Flowcharts C and D)***											
121	**Bridge Pier/Abutment (#, see above):** Low _____ Med _____ High_____ Chronic _____											
122	**Pier-to-Pier Gap/Span (#, see above):** Low _____ Med _____ High_____ Chronic _____											
123	**Additional Information:**											
124												
125												
126												
127												
128												
129	**(e) Site Plan View Sketch (include important features and dimensions)**											
130												
131												
132												
133												
134												
135												
136												
137												
138												
139												
140												
141												
142												
143												
144												
145												
146												
147												
148												
149												
150												
151												
152												
153												
154												
155												
156												
157												
158												
159												

160	**(f) Cross Section Sketch of Upstream Bridge Face (looking downstream - include important features and dimensions)**
161–183	

184	**(g) Field Site Photo Log**	
185	***Photo #***	***Description***
186		
187		
188		
189		
190		
191		
192		
193		
194		
195		
196		
197		
198		
199		
200		
201		
202		

DESCRIPTION OF FIELD DATA SHEET ENTRIES

***** It is highly recommended that the user review and understand HEC-20 prior to conducting this assessment *****

Record the Date of the project and the main Personnel involved in the project.

Section A records specific information about the existing, replacement, or new bridge.

Provide as much information as possible about the bridge and its location. This information will be useful to others that review these sheets in the future.

Section B records information about the bridge site that can be obtained from various sources prior to or following the site evaluation.

Part B1 records information that can be acquired or measured from topo maps, aerial photos, or surveys.

Item B1a records the general characteristics of the watershed upstream of the bridge site.

Land use plays an important role in defining the types and extent of debris that may potentially be delivered to the site. Urban land use as well as logging, mining, overgrazing, forest fires, and landslides can be significant contributors to channel instability, bank erosion, and subsequently debris delivery.

Item B1b records the general upstream channel and flood plain characteristics.

The general characteristics of the upstream channel and flood plain can be acquired or measured from maps, aerial photos, and survey data. Prior to recording this information, the user should determine the appropriate reach length to be evaluated. This will generally be the reach between the current bridge site and the next upstream bridge site, dam, diversion, or other controlling structure OR an estimated distance over which most or all of the upstream area could potentially contribute debris during a major flow event. Sinuosity, which is the ratio of the channel length to the straight line valley length between two points, will control the distance over which debris will move along a channel (i.e., sinuous channels will impede the movement of debris). Slope can be estimated from maps or can be obtained from survey data. Channel width has the greatest control over debris transport, since debris that is longer than the width of a channel will probably not be transported very far from its source area. Depth also controls transport since floating of the debris is required, especially if the debris has root wads/balls attached. Exposed or shallow bars and in-channel sediment deposits can trap debris. Active channel migration and evident bank erosion are the primary contributors to debris delivery. Channels that have been straightened or channelized may be unstable and incising and can be active contributors of debris. Man-made or natural barriers may restrict the downstream movement of debris. Regular flooding can also supply debris from the flood plain.

Part B2 identifies the availability of existing bridge information that can be obtained from state, county, and/or local DOTs. Data should be obtained for the both the current bridge site, if available, and any nearby bridge, if close enough, to determine if there are any ongoing debris and stability problems in the reach.

The bridge plans will provide specific data and measurements for the various structural elements of the bridge. The bridge inspection records can be used to identify any long-term debris or channel stability problems that have occurred since construction.

Bridge maintenance records can provide information on past debris removal. Historic ground photos may show previous debris configurations and locations or past channel conditions that may be useful in identifying long-term changes tha have occurred.

Historic aerial photos can be used to identify long-term changes such as active meandering, changes in channel width, land use changes, etc. Stream flow data can be used to determine flood flow depths, extent, duration, velocity, and other factors that influence debris production, transport, and accumulation.

Scour calculations identify estimated scour without debris and can then be used to estimate the potential scour depth associated with debris. Hydraulic models can provide much of the channel and hydraulic information to be recorded on these sheets.

Section C records data and information to be collected on the bridge site during a site visit and field examination of the site.

Part C1 records the data, information, descriptions, and ground photos acquired during the site reconnaissance.

Item C1a records information on the morphology of the channel and structural elements of the upstream bridge face.

The data collected in this part includes pertinent data and information that defines the type of pier (e.g., column, wall, pile bent, etc.), the nose shape, the pier width, the skew of the piers to flow, and the number of bridge piers, openings, and abutments, their physical condition, their relationship to the channel, banks, and flood plain and any scour and debris problems that may be evident.

Item C1b records information on the general morphology, characteristics, and conditions at the bridge site.

Reach Location records the general planform of the channel at the bridge site, if it is situated on the upstream or downstream limb of a meander bend, the skew of the bridge to flow, the height of the low chord above the channel bed, the overall channel bed material that is being transported, and the thalweg position in the channel at the bridge site.

Evidence of Scour, if present, records the specific dimensions of the scour at the bridge piers and abutments. Scour may be dependent of whether or not debris is present.

Bars records whether or not bars are present at the site, the type of bar, and the dominant bar material composition.

Existing Debris Accumulations records the location of debris relative to the bridge site.

Bankline Characteristics provides information on bank stability, vegetative cover, the potential modes of bank failure, how debris may be recruited, and whether of not debris can be stored along the bankline in the upstream channel. The shape of a bank helps define the mode of failure such as undercutting with gravity failure (vertical or overhanging bank) or by rotational failures (concave bank) or by slow fluvial erosion (convex bank). Sediment buildup along the bank toe can temporarily buttress the bank from erosion, but is also indicative of active bank failures. Bank face vegetation can provide some measure of bank stability, but may also be susceptible to recruitment. Depositional berms or narrow floodplains inset into an entrenched floodway are indicative of past incision/degradation followed by recovery. Erosional berms may be indicative of recent incision/degradation. Unstable inset floodpains may be indicative of a new wave of incision. Vegetation on the inset berms and floodplains provide a source for recruitment.

Lateral Channel Stability & Active Bank Erosion Characteristics identifies the location, degree, and specific mode of active bank retreat and channel migration in the upstream channel. Active bank retreat and lateral migration are the modes of debris recruitment.

Vertical Channel Stability identifies whether aggradation or degradation is occurring in the upstream channel since both can contribute to debris recruitment. Degradation results in bank erosion and bank retreat, whereas aggradation can induce overbank flooding and lateral migration.

Item C1c records general information on the riparian corridor upstream of the bridge site. The characteristics of the corridor and its composition provide information on the potential extent and size of the debris that could be supplied to the bridge site. Provide a qualitative estimate of the potential for debris production (use **Flowchart A**) in the upstream reaches and for debris transport and delivery (use **Flowchart B**) to the bridge site .

Item C1d records general information on existing debris accumulations at a given bridge site.

General information is collected on the location of debris accumulations, the type of accumulation on a bridge, the Typical Key Log type and dimensions, and root wad sizes. Qualitative estimate of debris production and transport and delivery to bridge site is made.

Information on the plan and profile (P&P) shape, dimensions, and location of debris along an existing bridge is collected at each bridge element. Provide a qualitative estimate of the potential for debris accumlations on piers/abutments (use **Flowchart C**) and in gaps/spans (use **Flowchart D**). Be sure to incorporate information from available bridge data acquired from DOT (lines 27-35) in the debris accumulation estimations (lines 120-122).

Item C1e Site Plan View Sketch is drawn here and should include important features and dimensions.

Item C1f Cross Section Sketch of Upstream Bridge Face is drawn here. The sketch should be viewed in the downstream direction and should include important features and dimensions.

Item C1g Field Site Photo Log is used to record photos taken at the site. The descriptions of the photo and any important features in the photo are recorded here as well.

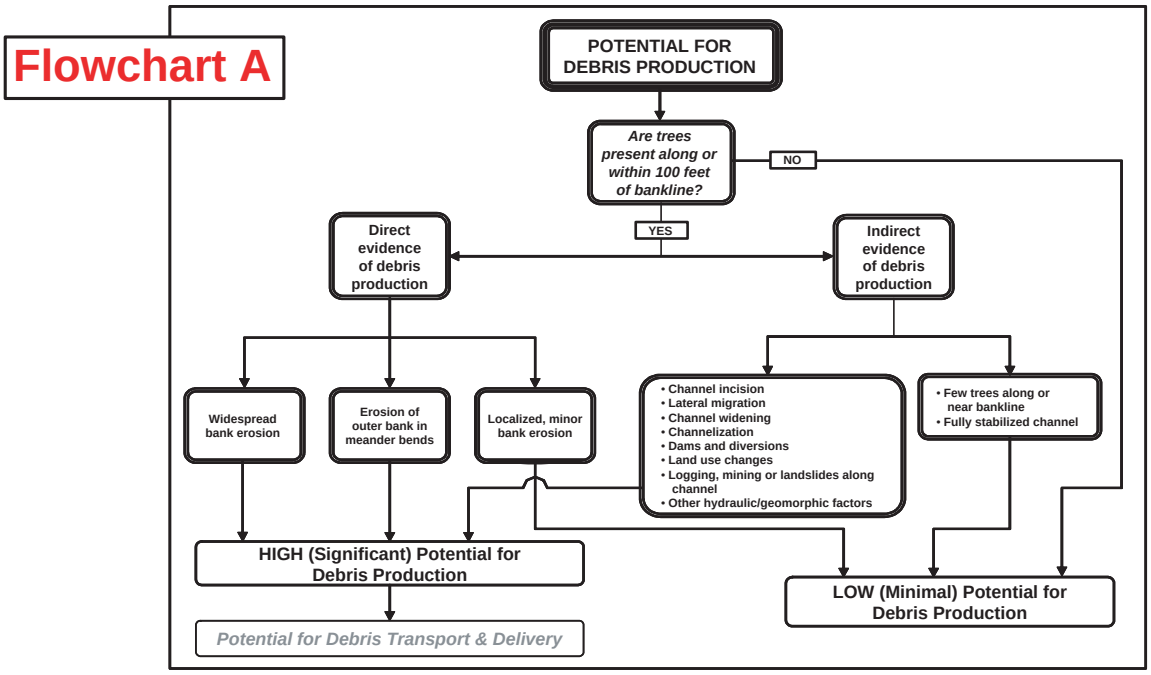

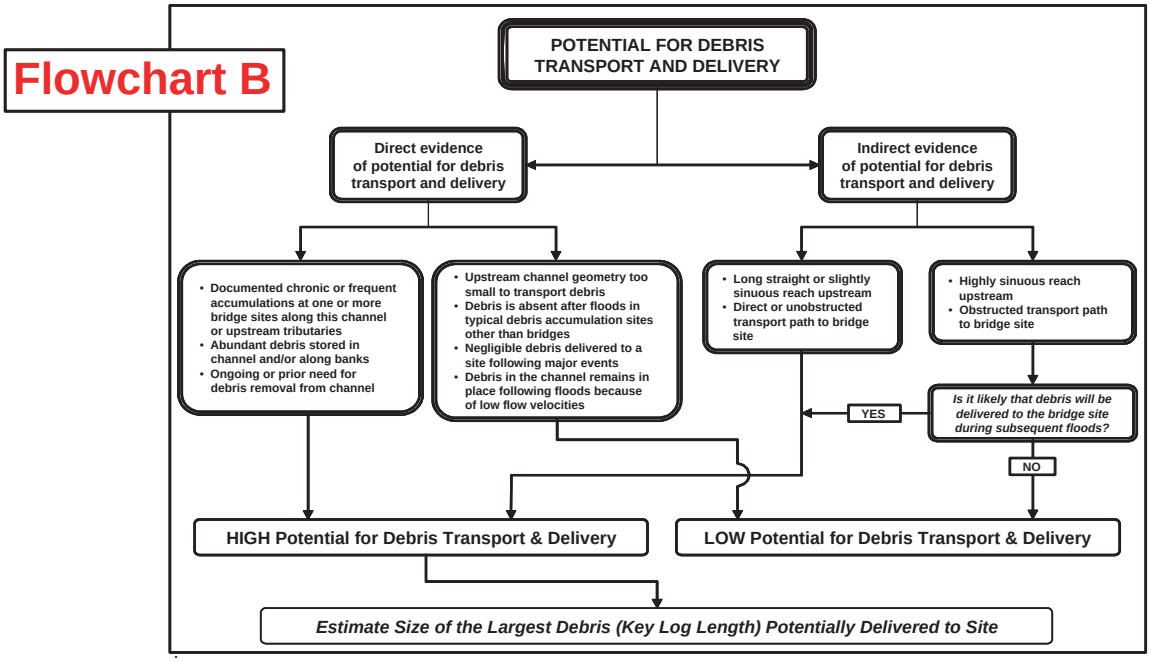

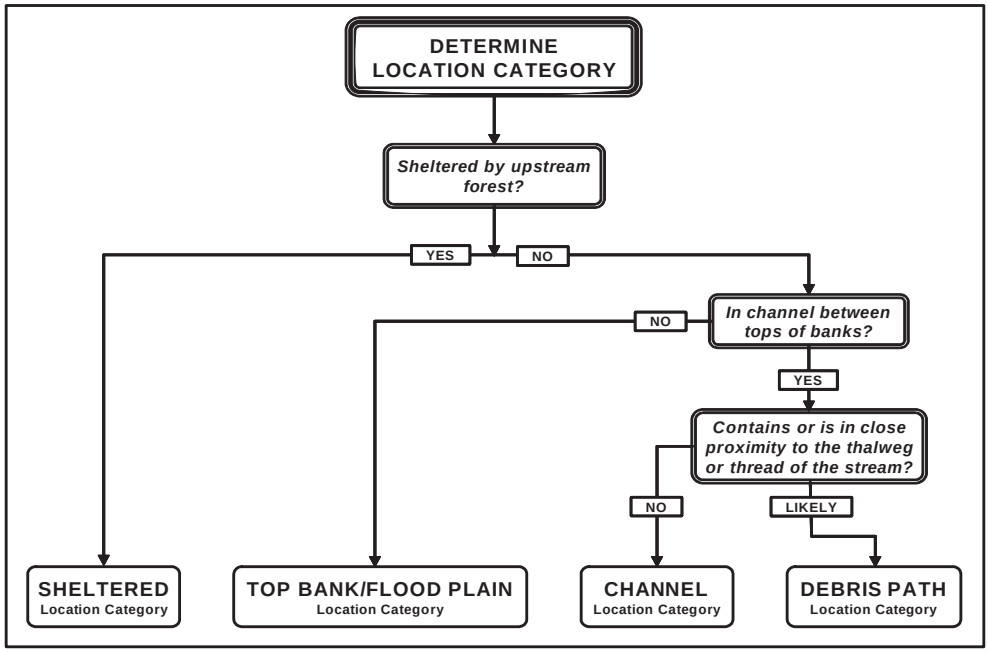

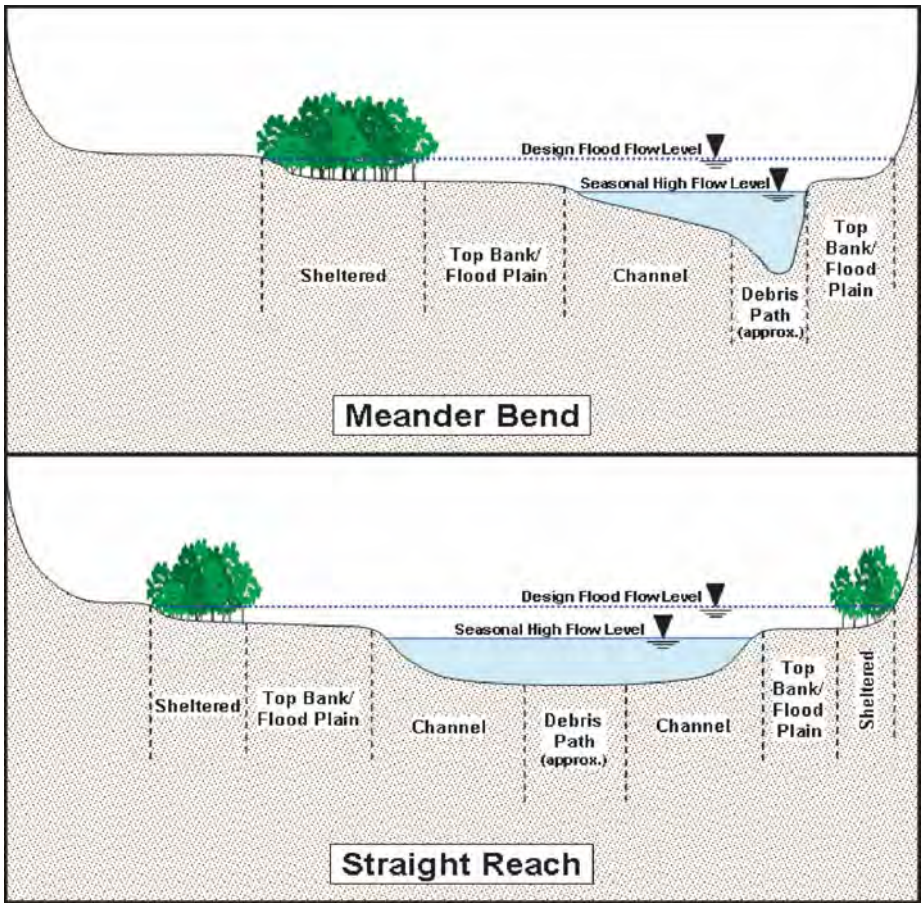

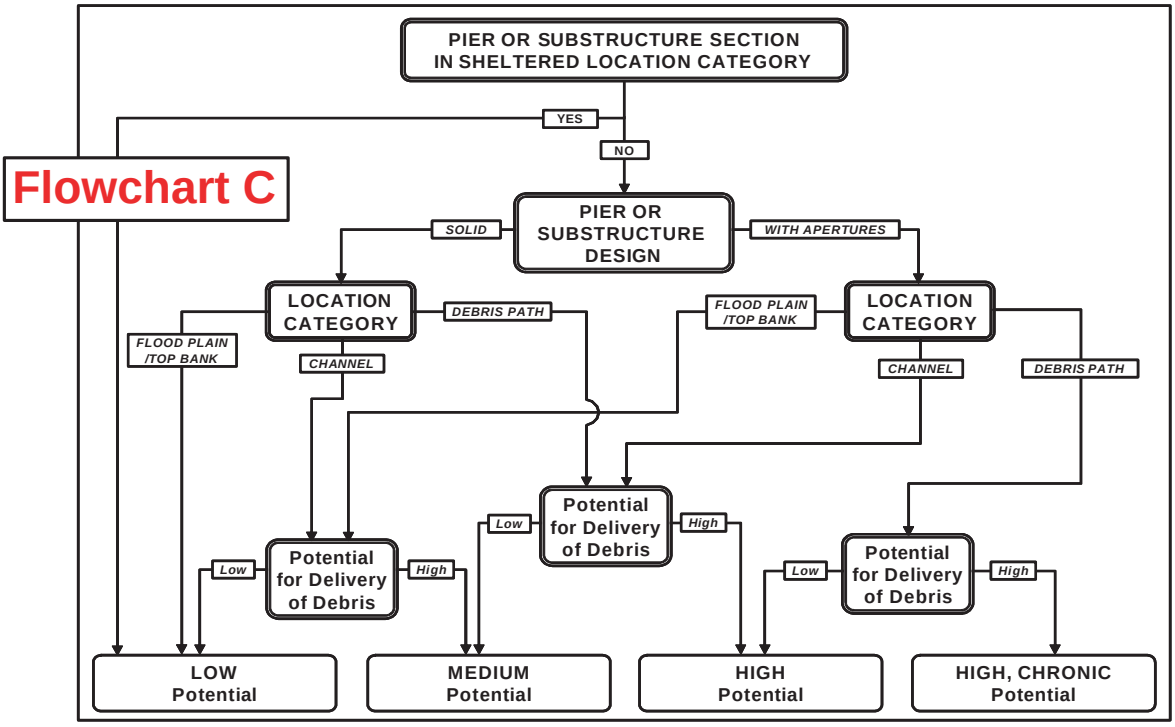

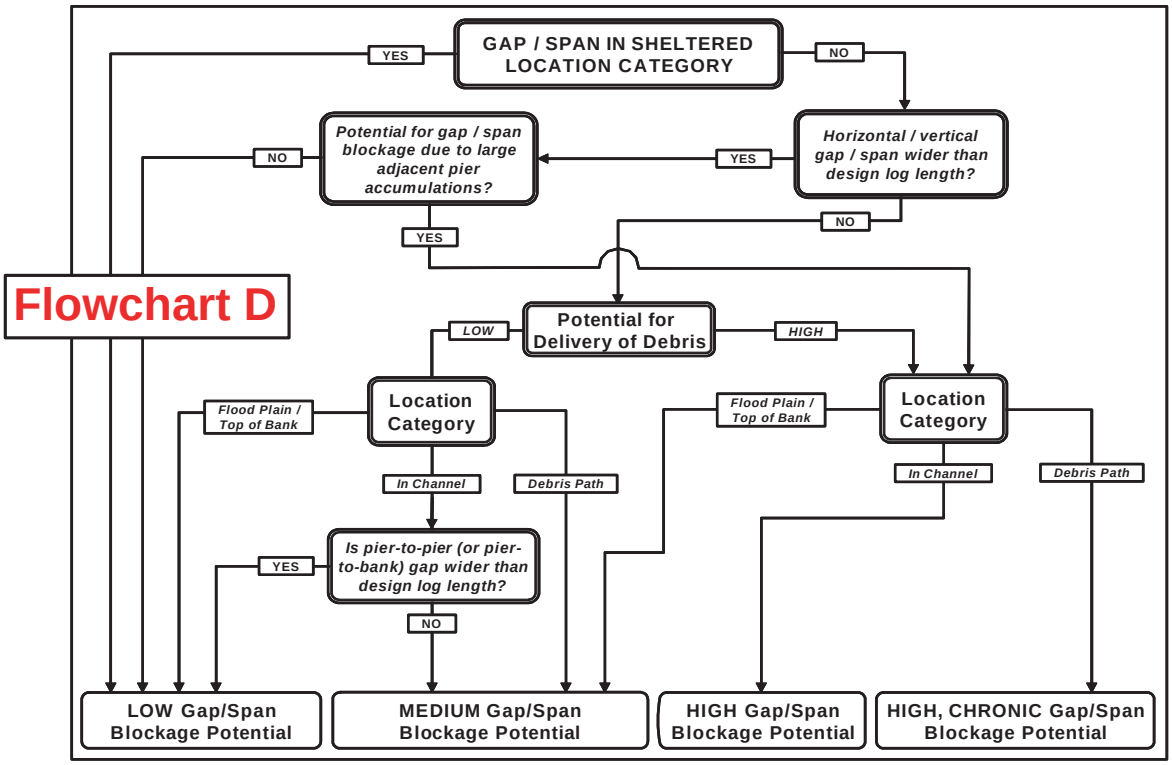

PART 2

South Platte River Site Reconnaissance and Preliminary Data Sheets

South Platte River between Greeley, CO, and Merino, CO (June 7, 2006)

D.1 Introduction

The intent of the field reconnaissance was to investigate potential case study locations on the South Platter River in Colorado. The Field Data Sheets were used to document site characteristics such as channel type and size, channel instability, bank erosion and retreat, and bank vegetation characteristics in detail. The purpose of the case study will be to provide an example of how the practitioner should apply the guidelines for assessing debris production and predicting debris accumulation at a bridge site developed in NCHRP Project 24-26.

D.2 South Platte River

Upstream of the potential study sites, the South Platte River Basin has a drainage area of approximately 14,600 mi^2. Figure D.1 shows a location map of the South Platte River Basin and contributing tributaries (see Attachment 1). Headwaters of the South Platte River are located in the central Colorado mountains where the mean annual precipitation is about 30 in., which includes approximately 300 in. of snowfall (USGS 2006). On the northern Colorado plains between Greeley and Sterling, Colorado, where the study sites are located, the mean annual precipitation is about 12 in., primarily in the form of rain that typically falls April through July.

The average June flow in the South Platte River in the corridor containing the potential study sites is 1,260 ft^3/s. During the field reconnaissance, the flow was approximately 90 ft^3/s at the USGS gage station in Fort Morgan. Unusually warm temperatures in May caused snowpack to melt faster than normal, resulting in an earlier runoff peak. In 2006, the South Platte River at Fort Morgan peaked in early May at 182 ft^3/s.

Land use in the corridor containing the potential study sites is primarily agriculture and some rangeland. Continuing moderate to severe drought conditions in Colorado have resulted in the need to shut off irrigation wells that draw from a shallow aquifer in the area in order to ensure minimum flow conditions in the South Platte River are maintained (ABC 2006). During the field visit, flow depths were observed to decrease moving downstream, despite the confluence with several tributaries, because of what appeared to be irrigation diversion.

D.3 Field Sites

Sixteen bridge sites were examined in a corridor of the South Platte River stretching from Greeley, Colorado, to Merino, Colorado; see Figure D.2 for a regional map. Two bridge sites were identified as potential candidates for case study locations (Figure D.3). These sites were the bridges carrying County Road 37 (RD-37) and County Road 50 (RD-50) over the South Platte River and are described in the following paragraphs. The other fourteen sites were eliminated for a number of reasons, which included:

- Stable banks did not contribute debris to channel.
- Several bridges had relief bridges that may reduce exposure to flood flows.
- Flow diversion drastically reduced channel flow.
- Older riparian vegetation was set back from the banks minimizing large woody debris in channel.

Bridge RD-37 has twelve sharp-nosed piers with narrow spans and a low bridge deck; four piers were located in the channel at the time of the site visit (Figure D.4). The Colorado Division of Water Resources (DWR) maintains a stream gage at this site, historical and recorded discharge data from this gage are shown in Figure D.5. Flow depth under Bridge RD-37 during the field visit was about 3.0 ft, overbank flow in this area occurs at 8.0 ft and bridge overtopping flow occurs at 10.0 ft (DWR 2006). A small amount of debris was observed on Pier 2, abundant amounts of debris were observed in the upstream channel and banks. The upstream banks were eroding and large trees were leaning into the channel (Figure D.6).

Bridge RD-50 has three sharp-nosed piers skewed approximately 5° to high flows and about 18 in. wide; two piers had debris buildup on the nose and sides (Figure D.7). The left and right abutments had about 1 ft diameter riprap protection, see Figure D.8. Riprap protection on the left bank extended about 300 ft upstream. Pier 1 is located on a mid-channel bar with moderate grass covering. A triangular debris pile consisting of several logs was located on the nose of Pier 1, with a small (less than 1 ft) scour hole (Figure D.9). Debris on Pier 2 consisted of a single log approximately 14 in. in diameter with a 4 to 6 ft rootwad aligned upstream (Figures D.10 and D.11). A debris pile and scour hole were observed on the right abutment, the scour hole was approximately 2 to 3 ft deep and 8 to 10 ft wide. Debris accumulation on the right abutment had no discernable key log but comprised several logs approximately 18 in. in diameter; one log had a 6 to 8 ft diameter rootwad aligned upstream (Figure D.12).

The bridge is located on the apex of a meander bend; see Figure D.13 for an aerial photograph. Upstream of Bridge RD-50, large woody debris was observed in the channel (Figure D.14). General bank erosion and evidence of bank failure was observed on the upstream right and left banks (Figure D.15).

Attachment 2 shows the completed Field Data Sheets for Bridge RD-50.

D.4 References

ABC News, The Denver Channel website, http://www.thedenverchannel.com/news/9317230/detail.html (June 3, 2006).

Colorado Division of Water Resources (DWR) website, http://www.dwr.state.co.us/Hydrology/flow_graph_standard.asp?ID=PLAKERCO&MTYPE=DISCHRG (June 12, 2006)

U.S. Geological Survey (USGS) National Water Quality Assessment Program, South Platte River Basin website, http://co.water.usgs.gov/nawqa/splt/ (June 9, 2006).

ATTACHMENT 1

Photographs

Source: USGS 2006

Figure D.1. South Platte River basin.

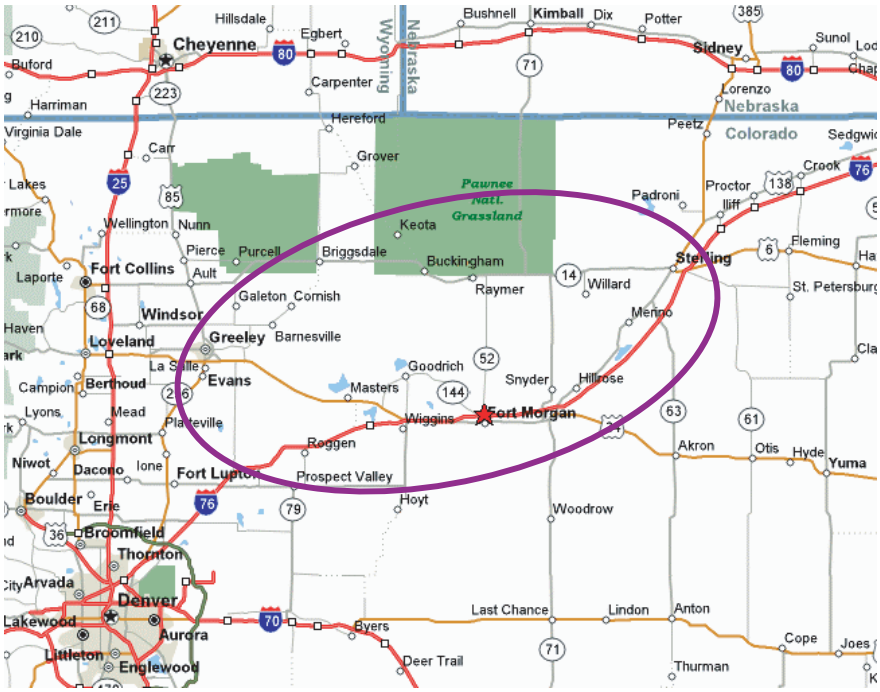

Figure D.2. Map showing area of Northern Colorado investigated for potential case study sites.

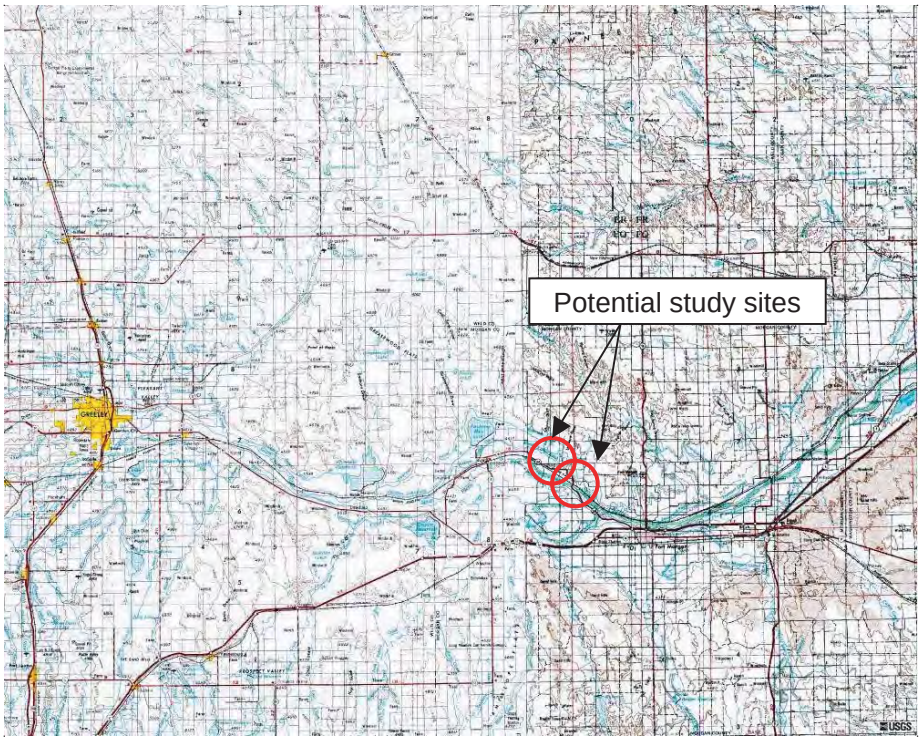

Figure D.3. Map of the South Platte River from Greely to Morin, Colorado.

Figure D.4. Looking downstream left bank to right bank at Bridge RD-37.

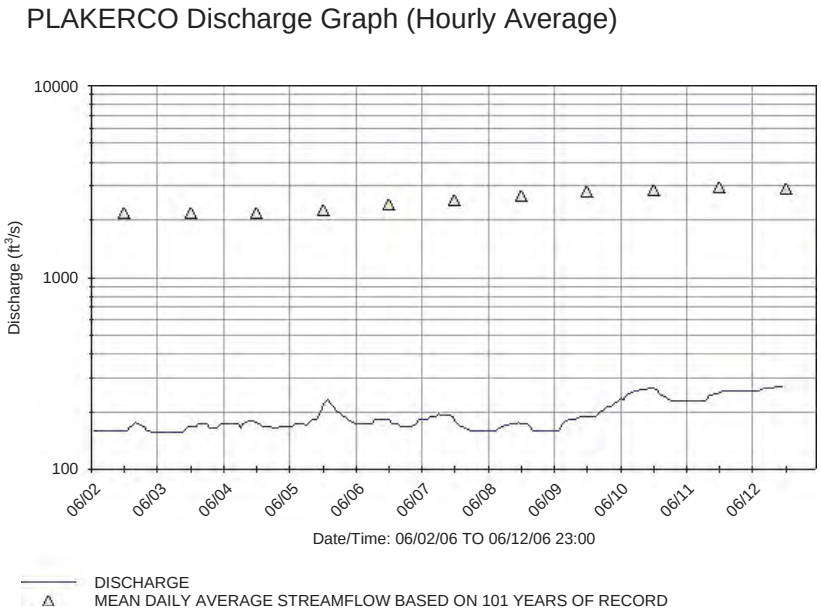

Source: DWR 2006

Figure D.5. Historic and recorded flow rates for Bridge RD-37.

Figure D.6. Looking upstream from Bridge RD-37.

Figure D.7. Looking upstream left bank to right bank at Bridge RD-50.

Figure D.8. Left abutment and Pier 1 on Bridge RD-50.

Figure D.9. Pier 1 with debris and scour hole.

Figure D.10. Pier 2 with debris.

Figure D.11. Looking down on Pier 2 and debris.

Figure D.12. Debris on right abutment.

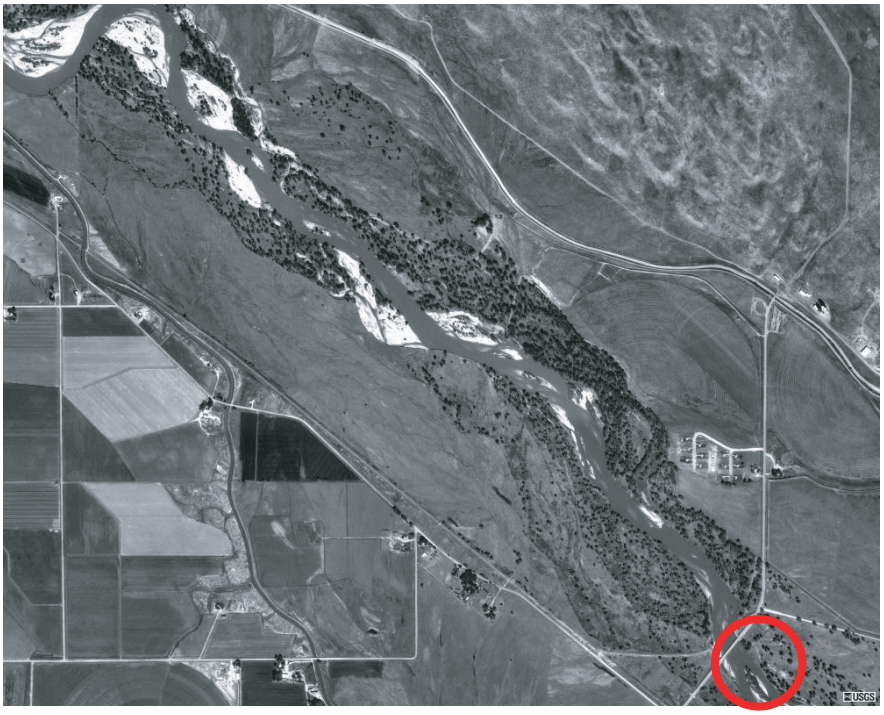

Figure D.13. Aerial view of Bridge RD-50 and the upstream corridor.

Figure D.14. Looking upstream from Bridge RD-50.

Figure D.15. Looking upstream from Bridge RD-50. Note riprap protection on left bank.

ATTACHMENT 2

Field Data Sheets Bridge WEL 50/67a
for assessing woody debris delivery
and accumulation potential at a bridge site

FIELD DATA SHEETS
FOR ASSESSING WOODY DEBRIS DELIVERY AND ACCUMULATION POTENTIAL AT A BRIDGE SITE

Date: June 7, 2006	Project Personnel: W. Spitz and L. Girard
A - BRIDGE LOCATION	
Street/Road Name: RD 50	
Bridge #:	River/Stream Name: South Platte River
County and State: Weld County, Colorado	Township/Range/Section: N 40° 24' 52.77", W 40° 20' 55.96"

B - DATA & INFORMATION THAT CAN BE COLLECTED PRIOR TO OR FOLLOWING A SITE VISIT

(1) SITE INFORMATION FROM TOPO MAPS, AERIAL PHOTOS, AND SURVEYS

(a) Upstream Watershed Characteristics

Land-use: Urban ____ Agricultural X Rural ____ Forested ____ Other ____

Man-made Disturbances (e.g. mining, logging, grazing, etc.): SOME GRAZING; IRRIGATION DIVERSIONS

Natural Disturbances (e.g., landslides, forest fires, etc.):

General Vegetation Patterns and Characteristics (describe): PRIMARILY NARROW RIPARIAN CORRIDOR ALONG BOTH BANKS, INTERMITTENT TO CONTINUOUS

(b) Upstream Channel and Flood Plain Characteristics

Upstream Reach Length: 1.0 feet / miles	Flow Type: Perennial X Ehemeral ____ Flashy ____
Upstream Channel Sinuosity: 1.2	Upstream Channel Slope: approx 0.0009
Average Upstream Channel Width at Crossings and/or Straight Reaches: 350 - 400' feet (top bank to top bank)	
Average Upstream Channel Depth at Crossings and/or Straight Reaches: 5 - 6'(?) feet (at bankfull)	
Evidence of Active Meander Migration: Yes X No ____	Evidence of Active Bank Erosion/Retreat: Yes X No ____
Presence of : Meander Cutoffs X Sloughs X	Bars and Other Major Sediment Deposits: BARS
Was Reach Channelized: Yes ____ No X Unknown ____	Evidence of Regular Flooding: Yes ____ No ____
Visible Evidence of Active Debris Delivery, Transport, and Storage Along Upstream Channel:	Yes X No ____

Describe Existing Natural or Man-Made Barriers to Debris Delivery (dams, diversions, bridges, rock outcrops, major constrictions etc.): TWO TIGHT MEANDER BENDS APPROX. 2.6 MILES UPSTREAM DIVERSION DAM APPROXIMATELY 3.8 MILES UPSTREAM

(2) AVAILABILITY OF BRIDGE INFORMATION FROM STATE, COUNTY, OR LOCAL DOT (check)

	Current Bridge Site:	Next Upstream Bridge:
Bridge Plans for:	✓	✓
Bridge Inspection Records for:	✓	✓
Bridge Maintenance Records for:	✓	✓
Historic Ground Photos for:	✓	✓
Historic Aerial Photos for:	✓	✓
Stream Flow Data or Records for:		✓
Scour Calculations for:		✓
Hydraulic Models for:		✓

C - DATA & INFORMATION TO BE COLLECTED DURING A SITE VISIT & FIELD EXAMINATION

(1) OBTAIN GROUND PHOTOS AND DETAILED DESCRIPTIONS THAT DOCUMENT THE FOLLOWING

(a) Upstream Bridge Face and Structural Elements

Bridge Openings	*Piers, Pilings, and footings*	*Abutments*
Number: 4	Type: sharp nosed wall piers	LEFT - Distance From Top Bank: Ø
Width (ft): 101	Number: 3	Description: approx. 1' diameter riprap protection EXTENDS U/S & D/S
Descriptions: 3 piers located in channel	Skew to Flow (deg): 5° at high water	
	Width (ft): 1.5 Nose: sharp	
	Descriptions: some riprap protection - appears incomplete	RIGHT - Distance From Top Bank: Ø
		Description: approx. 1' diameter riprap protection that extends ~300 ft upstream in bank

(b) General Bridge Site Characteristics

Reach Location:

Straight _____ In Meander Bend - On US Limb _____ At Bend Apex: X On DS Limb _____ Flow Split _____

Skew to Flow (deg): Low Flow: 15° High Flow: 5° **Low Chord Height Above Streambed (ft):** Min. _____ Max. _____

Bed Material Type: Sand X Gravel X Cobble ___ Bldrs ___ **Thalweg Position in Channel:** RB

Evidence of Scour (Debris Present X / Absent ___):

Scour Holes (Pier #):	Scour Hole Sizes (ft):	At Abutments (Location and Size):
#1 - 4/5 on left at nose #2 due to scour (small)	#2 - less than 1' #1 - less than 1'	Rabut: 2-8' deep, 8-10 ft wide

Bars: Mid-channel Bars X Point Bar X Bank Attached Bar X Sand X Gravel X Cobbles ___ Boulders ___

Existing Debris Accumulations:

On Flood Plain X On Bed X On Bars X On Banks X On Bridge Elements X

(c) General Upstream Channel Conditions

Stream Bed Characteristics

Bed Material Type: Sand X Gravel X Cobble ___ Bldrs ___ **Major Bedforms:** Sand Waves X Dunes ___ Other ___

Bars: Mid-channel Bars X Point Bars X Bank Attached Bars X Sand X Gravel X Cobble ___

Additional Information:
Stream observed during low flow, BRAIDED PATTERN @ LOW FLOW.
GAGE LOCATED APPROX. 4.5 MILES UPSTREAM

Bankline Characteristics (LB = Left Descending Bank, RB = Right Descending Bank)

General Bank Face Shape: Convex ___ Concave RB/LB Vertical ___ Undercut/Overhanging ___

LB Toe Sediment Accumulation (Basal Endpoint Control): Significant ___ Moderate U/S Negligible ___

RB Toe Sediment Accumulation (Basal Endpoint Control): Significant ___ Moderate US/DS Negligible ___

Bank Face/Slope Vegetation Type and Location:

LB:	Trees ___	Shrubs X	Grass X	Other ___	Dense ___	Mod. X	Sparse ___	None ___	Toe X	Mid ___	Upper ___
RB:	Trees X	Shrubs X	Grass X	Other ___	Dense ___	Mod. X	Sparse ___	None ___	Toe X	Mid ___	Upper ___

Berms: LB ___ RB ___ Erosional ___ Depositional ___ **Inset Flood Plain:** LB X RB X Stable: Y X N ___

Vegetation on Berms/Inset Flood Plain: Yes X No ___ Trees X Shrubs/Bushes X Grasses X Other ___

Additional Information:
NEWER MEANDERBELT & FLOODPLAIN INSET IN OLDER, HIGHER MEANDERBELT & FLOODPLAIN

Lateral Channel Stability & Active Bank Erosion Characteristics

Is General Bank Erosion Evident? Left Bank: Yes X No ___ Right Bank: Yes X No ___

	Intermittent	Continuous	In Bends	Reach-wide	In Toe	Whole Bank	Fluvial	Rotational	Cantilever	Saturation	Piping
Left Bank			X			X	X		X	X	
Right Bank			X			X	X			X	

If meander bends are present, are they actively migrating? Yes X No ___ Unsure ___

Additional Information:
extensive young vegetation on bars

Vertical Channel Stability

Aggradation (berms, inset food plain, overbank sedimentation, etc.): Yes ___ No X **Evidence:**

Degradation (headcuts, knickzone, vertical banks, exposed footings, etc.): Yes ___ No X

(d) General Upstream Riparian Corridor Characteristics

Corridor Length (ft): Continuous X Intermittent ___ **Corridor Width (ft):** Average 500 Max. 1000 Min. 300

Spacing: Uniform X Irregular ___ **Density:** Dense ___ Mod. X Sparse ___ **Multistory?** Yes X No ___

Stage: Multi-generational ___ Even-Aged X **Typical Age:** Young ___ Intermediate X Mature ___ Old Growth ___

Debris Available from Flood Plain? Yes X No ___ **Tree Type:** Conifererous ___ Deciduous X **Healthy?** Y X N ___

Typical Species (if known): Cottonwoods, WILLOWS

Evident Debris Delivery Processes in Reach:

Bank Erosion/Failure X Windthrow X Landslides ___ Flood Plain Input X Disease/Insect Kill ___ Logging ___ DS Transport X

Additional Information:

(e) Existing Debris Accumulation Characteristics

Debris Accumulation Locations: Upstream Bars X Bank Toe X Top Bank X Piers X Abutments X

Type of Debris Accumulation on Bridge(s): Span Accumulation X Pier Accumulation X Both X

Root Wad Sizes (range - ft): 3-6

Typical Key Log Species: Cottonwood

Typical Key Log Length (range - ft): 20'

Typical Key Log Diameter (range - ft): 1.4 - 1.6'

Existing Debris Accumulations (Plan & Profile Descriptions)

Shape Abbreviations: *Planform: T = Triangular R = Rectangular / Profile: C = Conical Cyl = Cylindrical IC = Inverted Cone*

At Bridge Piers/Abutments:

Pier #	*Abutment*	*1*	*2*	*3*	*4*	*5*	*6*	*7*	*8*	*9*	*10*
P&P Shape	/	T / NA	* /	/	/	/	/	/	/	/	/
Width	/	/	/	/	/	/	/	/	/	/	/
Hgt/Depth	/	2' / 3'	/	/	/	/	/	/	/	/	/
Length	/	/	/	/	/	/	/	/	/	/	/

Pier #	*11*	*12*	*13*	*14*	*15*	*16*	*17*	*18*	*19*	*20*	*Abutment*
P&P Shape	/	/	/	/	/	/	/	/	/	/	R / C
Width	/	/	/	/	/	/	/	/	/	/	8' / 10'
Hgt/Depth	/	/	/	/	/	/	/	/	/	/	7' / 8'
Length	/	/	/	/	/	/	/	/	/	/	25' / 30'

In Channel or Gap/Span (pier-to-pier):

Span/Gap	*Abut - 1*	*1-2*	*2-3*	*3-4*	*4-5*	*5-6*	*6-7*	*7-8*	*8-9*	*9-10*	*10-11*
P&P Shape	/	/	/	/	/	/	/	/	/	/	/
Width	/	/	/	/	/	/	/	/	/	/	/
Hgt/Depth	/	/	/	/	/	/	/	/	/	/	/
Length	/	/	/	/	/	/	/	/	/	/	/

Span/Gap	*12-Nov*	*12-13*	*13-14*	*14-15*	*15-16*	*16-17*	*17-18*	*18-19*	*19-20*	*20-21*	*# - Abut*
P&P Shape	/	/	/	/	/	/	/	/	/	/	/
Width	/	/	/	/	/	/	/	/	/	/	/
Hgt/Depth	/	/	/	/	/	/	/	/	/	/	/
Length	/	/	/	/	/	/	/	/	/	/	/

Additional Information:

*Single log accumulation on pier 2

Rabutment: 3-4, 18inch logs piled on riprap. One log with root wad, 7-8' diam.

No debris on Pier 3

(f) Additional Information

-At pier 3 the height from the channel bed to bottom of bridge deck was approx. 7ft.

(g) Site Plan View Sketch (include important features and dimensions)

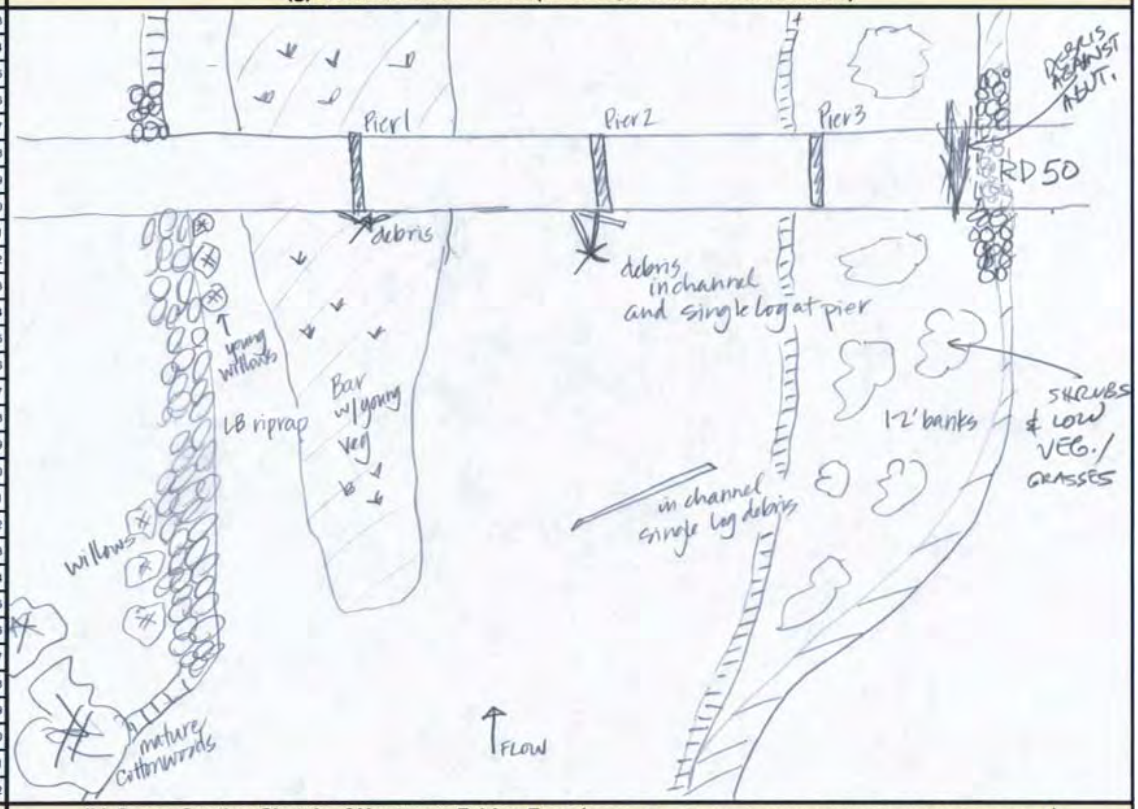

(h) Cross Section Sketch of Upstream Bridge Face (looking downstream - include important features and dimensions)

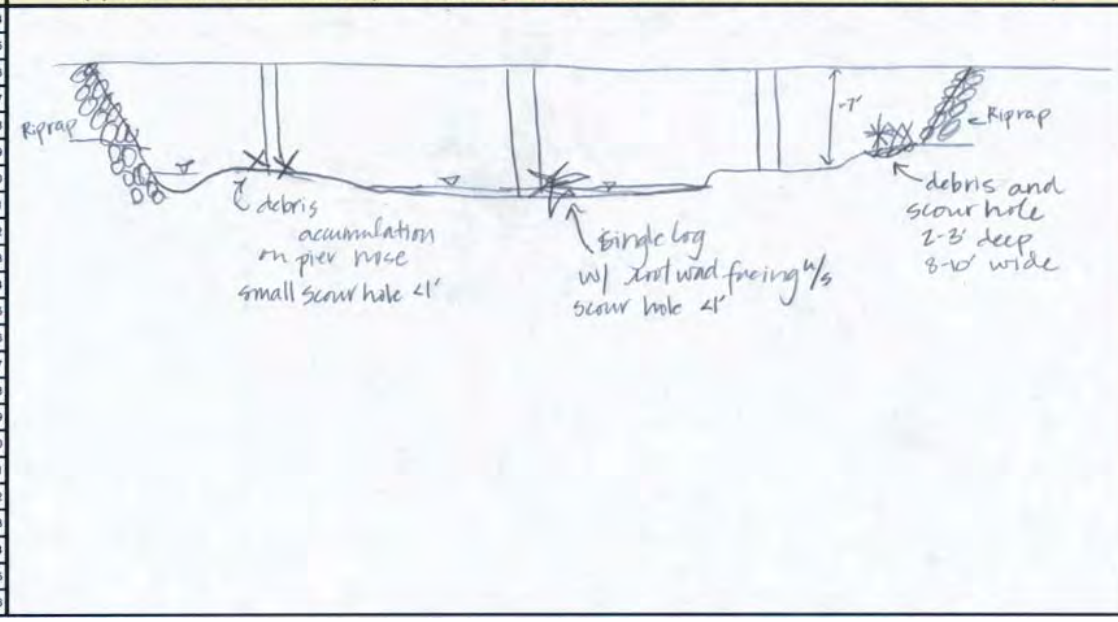

(i) Field Site Photo Log	
Photo #	**Description**
P1/12	view TL → TR showing debris on wall piers and u/s face of bridge
P1/13	view looking u/s, note debris in channel and on eroding banks
P1/14	view looking down on log w/ root wad and other debris on centerpier
P1/15,16	Pan looking u/s
P1/17	view d/s showing root wad on pier in P1/14 → single log debris
P1/18	view of log on TLB Pier
P1/19	view of debris on TRB abutment. Note scour hole (2-3' deep, 8-10' wide)
P1/20	view looking down on TLB Pier debris

DESCRIPTION OF FIELD DATA SHEET ENTRIES

***** It is highly recommended that the user review and understand HEC-20 prior to conducting this assessment *****

1	**Record the Date of the project and the main Personnel involved in the project**
2	**Section A** records specific information about the existing, replacement, or new bridge
3	Provide as much information as possible about the bridge and its location. This information will be useful to others that review these sheets in the future.
4	
5	
6	**Section B** records information about the bridge site that can be obtained from various sources prior to or following the site evaluation
7	**Part B1** records information that can be acquired or measured from topo maps, aerial photos, or surveys.
8	**Item B1a** records the general characteristics of the watershed upstream of the bridge site.
9	Land use plays an important role in defining the types and extent of debris that may potentially be delivered to the site. Urban land use as well as logging, mining, overgrazing, forest fires, and landslides can be significant contributors to channel ins
10	
11	
12	
13	
14	
15	**Item B1b** records the general upstream channel and flood plain characteristics.
16	The general characteristics of the upstream channl and flood plain can be acquired or measured from maps, aerial photos, and survey data. Prior to recording this information, the user should determine the appropriate reach length to be evaluated. This w
17	
18	
19	
20	
21	
22	
23	
24	
25	debris. Active channel migration and evident bank erosion are the primary contributors to debris delivery. Channels that have been straightened or channelized may be unstable and incising and can be active contributors of debris. Man-made or natural ba
26	
27	**Part B2** identifies the availability of existing bridge information that can be obtained from state, county, and/or local DOTs. Data should be obtained for the both the current bridge site, if available, and the next upstream bridge, if close enough, to d
28	The bridge plans will provide specific data and measurements for the various structural elements of the bridge. The bridge inspection
29	records can be used to identify any long-term debris or channel stability problems that have occurred since construction
30	Bridge maintenance records can provide information on past debris removal. Historic ground photos may show previous debris
31	configurations and locations or past channel conditions that may be useful in identifying long-term changes tha have occurred.
32	Historic aerial photos can be used to identify long-term changes such as active meandering, changes in channel width, land use changes, etc. Stream flow data can be used to determine flood flow depths, extent, duration, velocity, and other factors that i
33	
34	Scour calculations identify estimated scour without debris and can then be used to estimate the potential scour depth associated
35	with debris. Hydraulic models can provide much of the channel and hydraulic information to be recorded on these sheets.
36	**Section C** records data and information to be collected on the bridge site during a site visit and field examination of the site.
37	**Part C1** records the data, information, descriptions, and ground photos acquired during the site reconnaissance.
38	**Item C1a** records information on the morphology of the channel and structural elements of the upstream bridge face.
39	The data collected in this part includes pertinent data and information that defines the type of pier (e.g., column, wall, pile bent, etc.), the nose shape, the pier width, the skew of the piers to flow, and the number of bridge piers, openings, and abutm
40	
41	
42	
43	
44	
45	
46	
47	
48	
49	
50	
51	
52	**Item C1b** records information on the general morphology, characteristics, and conditions at the bridge site.
53	Reach Location records the general planform of the channel at the bridge site, if it is situated on the upstream or downstream limb of a meander bend, the skew of the bridge to flow, the height of the low chord above the channel bed, the overall channel b
54	
55	
56	
57	Evidence of Scour, if present, records the specific dimensions of the scour at the bridge piers and abutments. Scour may be dependent of whether or not debris is present.
58	
59	
60	
61	Bars records whether or not bars are present at the site, the type of bar, and the dominant bar material composition.
62	Existing Debris Accumulations records the location of debris relative to the bridge site.
63	
64	**Item C1c** records general information on the bed and bankline conditions and channel stability upstream of the bridge site.
65	Stream Bed Characteristics records pertinent information on bed material, bedforms, and bar types that can affect how and where debris accumulates in the upstream channel. Large bedforms and bars can migrate into the bridge reach and influence debris acc
66	
67	
68	
69	
70	

Bankline Characteristics provides information on bank stability, vegetative cover, the potential modes of bank failure, how debris may be recruited, and whether of not debris can be stored along the bankline in the upstream channel. The shape of a bank h

Lateral Channel Stability & Active Bank Erosion Characteristics identifies the location, degree, and specific mode of active bank retreat and channel migration in the upstream channel. Active bank retreat and lateral migration are the modes of debris rec

Vertical Channel Stability identifies whether aggradation or degradation is occurring in the upstream channel since both can contribute to debris recruitment. Degradation results in bank erosion and bank retreat, whereas aggradation can induce overbank f

Item C1d records general information on the riparian corridor upstream of the bridge site. The characteristics of the corridor and its composition provide information on the potential extent and size of the debris that could be supplied to the bridge sit

Item C1e records general information on existing debris accumulations at a given bridge site.

General information is collected on the location of debris accumulations, the type of accumulation on a bridge, the Typical Key Log type and dimensions, and root wad sizes.

Information on the plan and profile (P&P) shape, dimensions, and location of debris along an existing bridge is collected at each bridge element.

Item C1f Additional Information that may be deemed important is recorded here.

Item C1g Site Plan View Sketch is drawn here and should include important features and dimensions.

Item C1h Cross Section Sketch of Upstream Bridge Face is drawn here. The sketch should be viewed in the downstream direction and should include important features and dimensions.

Item C1i Field Site Photo Log is used to record photos taken at the site. The descriptions of the photo and any important features in the photo are recorded here as well.

PART 3

South Platte River Case Study: Final Data Sheets and Application of the Guidelines

Summary of Assessment of Debris Production, Transport, Delivery, and Accumulation Potential

Bridge WEL 50/67A *over South Platte River near Hardin, Weld County, Colorado*

Estimated potential for debris production: *HIGH*
Estimated potential for debris transport and delivery: *HIGH*
Estimated debris accumulation potential:
- Left Bank Abutment—*LOW*
- Pier 1—*MEDIUM*
- Pier 2—*HIGH*
- Pier 3—*HIGH*
- Right Bank Abutment—*LOW*

Estimated span blockage potential:
- Span 1—*LOW*
- Span 2—*LOW*
- Span 3—*LOW*
- Span 4—*LOW*

FIELD DATA SHEETS

FOR ASSESSING WOODY DEBRIS DELIVERY AND ACCUMULATION POTENTIAL AT A BRIDGE SITE

(To be used in conjunction with "Guidelines for Assessing Debris Production and Accumulation Potential")

Date: April 24, 2007 | **Field Personnel:** W. Spitz and L. Girard

A - BRIDGE LOCATION

Street / Road Name: Weld County Road CR 50 | **Nearest Town/City:** Hardin

Bridge ID / #: Bridge WEL 50/67A | **County and State:** Weld County, Colorado

River / Stream Name: South Platte River | **Longitude / Latitude:** -104.41466 / 40.34886

B - DATA & INFORMATION THAT CAN BE COLLECTED PRIOR TO OR FOLLOWING A SITE VISIT

(1) SITE INFORMATION FROM TOPO MAPS, AERIAL PHOTOS, AND SURVEYS

(a) Upstream Watershed Characteristics

Land-use: Urban _____ Agricultural __X__ Rural _____ Forested _____ Other _____

Man-made Disturbances (e.g. mining, logging, grazing, etc.): some grazing; irrigation diversions

Natural Disturbances (e.g., landslides, forest fires, etc.): None

General Vegetation Patterns and Characteristics (describe):
Primarily narrow, intermittent to continuous, riparian corridor along both banks. Relatively wide, grassy floodplain with some grazing.

(b) Upstream Channel and Flood Plain Characteristics

Upstream Reach Length: 1.0 miles | **Flow Type:** Perennial __X__ Ehemeral _____ Flashy _____

Upstream Channel Sinuosity: 1.2 | **Upstream Channel Slope:** 0.00123 (1994)

Average Upstream Channel Width at Crossings and/or Straight Reaches: 350 - 400 feet (top bank to top bank)

Average Upstream Channel Depth at Crossings and/or Straight Reaches: 5 - 6(?) ft (at bankfull), ~12 ft at flood stage

Evidence of Active Meander Migration: Yes __X__ No ____ | **Evidence of Active Bank Erosion/Retreat:** Yes __X__ No ____

Presence of : Meander Cutoffs __X__ Sloughs __X__ | **Bars and Other Major Sediment Deposits:** Bars

Was Reach Channelized: Yes _____ No __X__ Unknown _____ | **Evidence of Regular Flooding:** Yes ____ No __X__

Visible Evidence of Active Debris Delivery, Transport, and Storage Along Upstream Channel: Yes __X__ No ____

Describe Existing Natural or Man-Made Barriers to Debris Delivery (dams, diversions, bridges, rock outcrops, major constrictions etc.):
Two tight meander bends approx. 2.6 miles upstream; diversion dam approx. 3.8 miles upstream

(2) AVAILABILITY OF BRIDGE INFORMATION FROM STATE, COUNTY, OR LOCAL DOT (circle)

Bridge Plans available for: (attached)
Current Bridge Site: (Y) N *Nearby Bridge:* (Y) N

Bridge Inspection Records available for:
Current Bridge Site: (Y) N *Nearby Bridge:* (Y) N

Bridge Maintenance Records available for:
Current Bridge Site: (Y) N *Nearby Bridge:* (Y) N

Historic Ground Photos avaialable for:
Current Bridge Site: (Y) N *Nearby Bridge:* (Y) N

Historic Aerial Photos available for:
Current Bridge Site: (Y) N *Nearby Bridge:* (Y) N

Stream Flow Data or Records available for:
Current Bridge Site: (Y) N *Nearby Bridge:* (Y) N

Scour Calculations available for:
Current Bridge Site: Y (N) *Nearby Bridge:* (Y) N

Hydraulic Models available for:
Current Bridge Site: (Y) N *Nearby Bridge:* (Y) N

C - DATA & INFORMATION TO BE COLLECTED DURING A SITE VISIT & FIELD EXAMINATION

(1) OBTAIN GROUND PHOTOS AND DETAILED DESCRIPTIONS THAT DOCUMENT THE FOLLOWING

(a) Upstream Bridge Face and Structural Elements

Bridge Openings	*Piers, Pilings, and footings*	*Abutments*
Number: 4	Type: sharp nosed wall piers	LEFT - Distance From Top Bank: 0
Width (ft): 112.9-112.2-112.9-112.9	Number: 3	Description: Approx. 1-ft diameter riprap protection extends upstream and downstream. Upstream riprap in 173 ft long guidebank.
Descriptions: Vertical abutment cap wall with rock riprap spill-through abutment slopes.	Skew to Flow (deg): 5° at flood stage	
	Width (ft): 1.5 Nose: sharp	
	Descriptions: Some riprap protection of piers appears to have been dispersed or displaced. Piers are skewed 70° to bridge.	RIGHT - Distance From Top Bank: 0
		Description: Approx. 1-ft diameter riprap protection extends ~300 ft upstream and downstream. Upstream riprap in 173 ft long guidebank

(b) General Bridge Reach Characteristics

Reach Location:

Straight _____ In Meander Bend - On US Limb _____ At Bend Apex: __X__ On DS Limb _____ Flow Split _____

Skew to Flow (deg): Low Flow:__15°____ High Flow:___5°____ **Low Chord Height Above Streambed (ft):** Min. 7'(pier 3) Max. _____

Evidence of Scour (Debris Present _X_ / Absent ___):

Scour Holes (Pier #):	Scour Hole Sizes (ft):	At Abutments (Location and Size):
Pier #1 - downstream on left at nose Pier #2 - small	Pier #1 - less than 1 ft Pier #2 - less than 1 ft	RB Abutment, 2-3 ft deep, 8-10 ft wide

Existing Debris Accumulations:

On Flood Plain ___X___ On Bed ___X___ On Bars ___X___ On Banks ___X___ On Bridge Elements ___X___

Bars: Mid-channel Bar_X__ Point Bar_X__ Bank Attached Bar_X__ **Thalweg Position at Bridge:** right bank (RB)

Bankline Characteristics (LB = Left Descending Bank, RB = Right Descending Bank)

General Bank Face Shape: Convex _____ Concave _RB, LB_ Vertical _____ Undercut/Overhanging _____

LB Toe Sediment Accumulation (Basal Endpoint Control): Significant _____ Moderate __U/S__ Negligible _____

RB Toe Sediment Accumulation (Basal Endpoint Control): Significant _____ Moderate _U/S, D/S_ Negligible _____

Bank Face/Slope Vegetation Type and Location:

LB:	Trees___ Shrubs_X_ Grass_X_ Other___	Dense___ Mod._X_ Sparse___ None___	Toe _X__ Mid ___ Upper ___
RB:	Trees_X_ Shrubs_X_ Grass_X_ Other___	Dense___ Mod._X_ Sparse___ None___	Toe _X__ Mid ___ Upper ___

Berms: LB _____ RB _____ Erosional ___ Depositional ___ **Inset Flood Plain:** LB __X__ RB __X__ Stable: *Y* _X_ *N* ___

Vegetation on Berms/Inset Flood Plain: Yes _X__ No ____ Trees_X_ Shrubs/Bushes__X__ Grasses_X__ Other ____

Additional Information:

Stream observed during low flow - braided pattern at low flow. Gage located approx. 4.5 miles upstream. Current meander belt and flood plain inset into older, higher meander belt and flood plain is indicative of previous vertical instability, but is currently vertically stable. Extensive young vegetation on bars and lots of algae growth in channel.

Lateral Channel Stability & Active Bank Erosion Characteristics

Is General Bank Erosion Evident? Left Bank: Yes__X__ No____ Right Bank: Yes____ No____

	Intermittent	Continuous	In Bends	Reach-wide	In Toe	Whole Bank	Fluvial	Rotational	Cantilever	Saturation	Piping
Left Bank			X			X	X		X	X	
Right Bank			X			X	X			X	

If meander bends are present, are they actively migrating? Yes__X__ No _____ Unsure _____

Additional Information:

Aerial photos show numerous active meander bends upstream and active meander migration and point bar development. Active channel planform is borderline between braided and meandering.

Evidence of Vertical Channel Instability

Aggradation (berms, inset flood plain, overbank sedimentation, etc.): Yes____ No__X__ **Evidence:**

Degradation (headcuts, knickzone, vertical banks, exposed footings, etc.): Yes___ No__X_

(c) General Upstream Riparian Corridor Characteristics

Corridor Length (ft): Continuous __X___ Intermittent _____ **Corridor Width (ft):** Avg__500__ Max._1000__ Min.__300__

Spacing: Uniform __X__ Irregular ____ **Density:** Dense ____ Mod. _X__ Sparse ____ **Multistory?** Yes_X__ No____

Stage: Multi-generational ____ Even-Aged _X__ **Typical Age:** Young____ Intermediate_X__ Mature____ Old Growth____

Debris Available from Flood Plain? Yes_X_ No___ **Tree Type:** Conifererous_____ Deciduous___X__ **Healthy?** *Y* _X_ *N* ___

Typical Species (if known): Cottonwoods, willows

Evident Debris Delivery Processes in Reach:

Bank Erosion/Failure_X_ Windthrow_X_ Landslides___ Flood Plain Input_X_ Disease/Insect Kill___ Logging___ D/S Transport_X_

Estimate Potential for Debris Production:	***Estimate Potential for Debris Transport & Delivery:***
(See Flowchart A) High __X___ Low _____	**(See Flowchart B)** High __X___ Low _____

Additional Information:

(d) Existing Debris Accumulation Characteristics at a Bridge Site

Debris Accumulation Locations: On Bars__X__ Bank Toe__X__ Top Bank__X__ Piers__X__ Abutments__X__

Type of Debris Accumulation on Bridge(s):

Span Accumulation_____ Pier Accumulation_____ Both__X__

Root Wad Sizes (range - ft): >6 ft on Pier #2

Typical Key Log Species: Cottonwoods

Typical Key Log Length (range - ft): 18-20 feet

Typical Key Log Diameter (range - ft): 1.4-1.6 feet

Existing Debris Accumulations (Planform & Profile Descriptions)

P&P Shape Abbreviations: *Planform: T = Triangular R = Rectangular / Profile: C = Conical R = Rectangular IC = Inverted Cone*

At Bridge Piers/Abutments:

Pier #	*Abutment*	*1*	*2*	*3*	*4*	*5*	*6*	*7*	*8*	*9*	*Abutment*
P&P Shape	/	T / NA	1* /	/	/	/	/	/	/	/	/
Width	/	/	/	/	/	/	/	/	/	/	/
Hgt/Depth	/	2' / 3'	/	/	/	/	/	/	/	/	/
Length	/	/	/	/	/	/	/	/	/	/	/

In Channel or Gap/Span (pier-to-pier):

Span/Gap	*Abut - 1*	*1-2*	*2-3*	*3-4*	*4-5*	*5-6*	*6-7*	*7-8*	*8-9*	*9-10*	*# - Abut*
P&P Shape	/	/	/	/	/	/	/	/	/	/	R / IC
Width	/	/	/	/	/	/	/	/	/	/	8' / 10'
Hgt/Depth	/	/	/	/	/	/	/	/	/	/	7' / 8'
Length	/	/	/	/	/	/	/	/	/	/	25' / 30'

Estimate Debris Accumulation & Span Blockage Potential (see Flowcharts C and D)

Bridge Pier/Abutment (#, see above): Low _LB & RB Abut_ Med _____1_____ High____2 & 3____ Chronic _____

Pier-to-Pier Gap/Span (#, see above): Low ___All_____ Med _____ High_____ Chronic _____

Additional Information:

This field visit: Single log accumulation noted on Pier 2, no debris noted on Pier 3. On RB abutment, 3 to 4 18-inch diam. logs piled on riprap in scour hole, one log contains 7-8' diameter root wad.

Original bridge inspection records: Indicate consistant debris accumulation problem prior to bridge replacement in 1996.

Current bridge inspection records: In 1999, debris noted on upstream face at Pier 2; In 2002, debris noted at Span 4 and RB Abutment and photos show debris on downstream side of Span 3; In 2004, large trees noted at Pier 3 and RB Abutment; In 2006, debris and large trees noted on Piers 3 and 4 and RB Abutment.

(e) Site Plan View Sketch (include important features and dimensions)

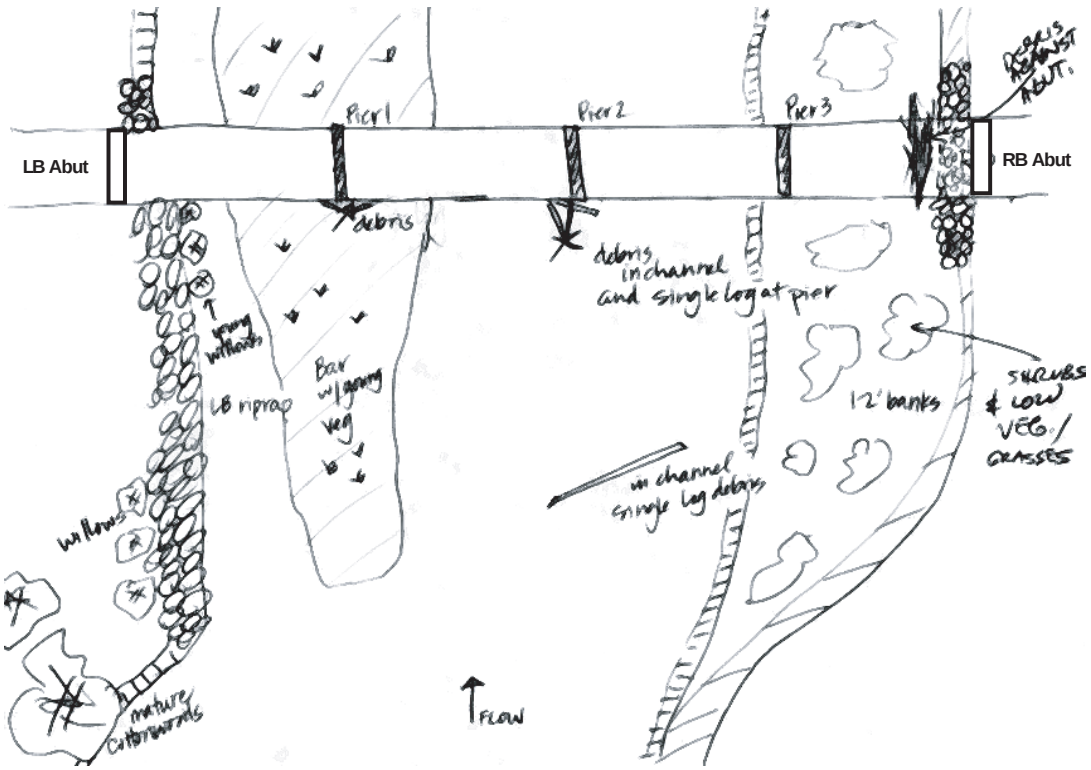

(f) Cross Section Sketch of Upstream Bridge Face (looking downstream - include important features and dimensions)

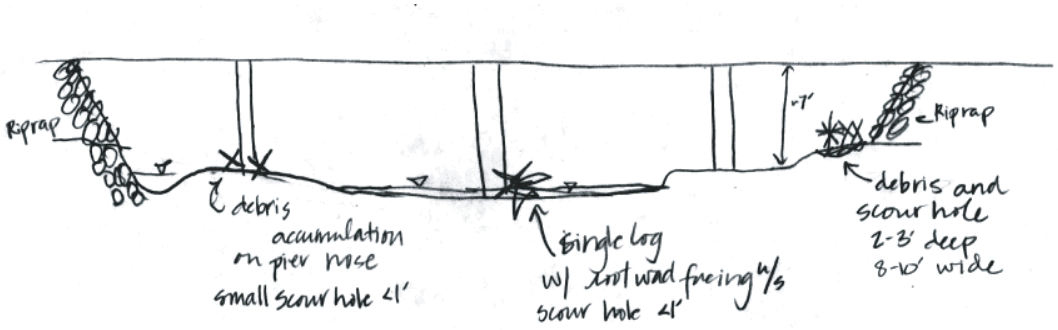

(g) Field Site Photo Log

Photo #	*Description*
P1/12	View TL to TR showing debris on wall piers and upstream face of bridge
P1/13	View looking upstream, note debris in channel and on eroding banks
P1/14	View looking down on log with root wad and other debris on center pier (Pier #2)
P1/15,16	Pan looking upstream
P1/17	View downstream showing root wad on Pier #2 = single log accumulation
P1/18	View looking toward Pier #1 and log along pier wall, root wad at pier nose
P1/19	View of debris on right bank abutment. Note scour hole around debris (2-3' deep, 8-10' wide)
P1/20	View looking down on Pier #1 debris accumulation at nose of pier

DESCRIPTION OF FIELD DATA SHEET ENTRIES

**** It is highly recommended that the user review and understand the concepts described in FHWA's HEC 20 prior to conducting this assessment ****

1	**Record the Date of the project and the main Personnel involved in the project.**
2	**Section A** records specific information about the existing, replacement, or new bridge.
3	Provide as much information as possible about the bridge and its location. This information will be useful to others that review these sheets in the future.
4	
5	
6	**Section B** records information about the bridge site that can be obtained from various sources prior to or following the site evaluation.
7	**Part B1** records information that can be acquired or measured from topo maps, aerial photos, or surveys.
8	**Item B1a** records the general characteristics of the watershed upstream of the bridge site.
9	Land use plays an important role in defining the types and extent of debris that may potentially be delivered to the site. Urban land use as well as logging, mining, overgrazing, forest fires, and landslides can be significant contributors to channel instability, bank erosion, and subsequently debris delivery.
10	
11	
12	
13	
14	
15	**Item B1b** records the general upstream channel and flood plain characteristics.
16	The general characteristics of the upstream channel and flood plain can be acquired or measured from maps, aerial photos, and survey data. Prior to recording this information, the user should determine the appropriate reach length to be evaluated. This will generally be the reach between the current bridge site and the next upstream bridge site, dam, diversion, or other controlling structure OR an estimated distance over which most or all of the upstream area could potentially contribute debris during a major flow event. Sinuosity, which is the ratio of the channel length to the straight line valley length between two points, will control the distance over which debris will move along a channel (i.e., sinuous channels will impede the movement of debris). Slope can be estimated from maps or can be obtained from survey data. Channel width has the greatest control over debris transport, since debris that is longer than the width of a channel will probably not be transported very far from its source area. Depth also controls transport since floating of the debris is required, especially if the debris has root wads/balls attached. Exposed or shallow bars and in-channel sediment deposits can trap debris. Active channel migration and evident bank erosion are the primary contributors to debris delivery. Channels that have been straightened or channelized may be unstable and incising and can be active contributors of debris. Man-made or natural barriers may restrict the downstream movement of debris. Regular flooding can also supply debris from the flood plain.
17	
18	
19	
20	
21	
22	
23	
24	
25	
26	
27	**Part B2** identifies the availability of existing bridge information that can be obtained from state, county, and/or local DOTs. Data should be obtained for the both the current bridge site, if available, and any nearby bridge, if close enough, to determine if there are any ongoing debris and stability problems in the reach.
28	The bridge plans will provide specific data and measurements for the various structural elements of the bridge. The bridge inspection records can be used to identify any long-term debris or channel stability problems that have occurred since construction.
29	
30	Bridge maintenance records can provide information on past debris removal. Historic ground photos may show previous debris configurations and locations or past channel conditions that may be useful in identifying long-term changes tha have occurred.
31	
32	Historic aerial photos can be used to identify long-term changes such as active meandering, changes in channel width, land use changes, etc. Stream flow data can be used to determine flood flow depths, extent, duration, velocity, and other factors that influence debris production, transport, and accumulation.
33	
34	Scour calculations identify estimated scour without debris and can then be used to estimate the potential scour depth associated with debris. Hydraulic models can provide much of the channel and hydraulic information to be recorded on these sheets.
35	
36	**Section C** records data and information to be collected on the bridge site during a site visit and field examination of the site.
37	**Part C1** records the data, information, descriptions, and ground photos acquired during the site reconnaissance.
38	**Item C1a** records information on the morphology of the channel and structural elements of the upstream bridge face.
39	The data collected in this part includes pertinent data and information that defines the type of pier (e.g., column, wall, pile bent, etc.), the nose shape, the pier width, the skew of the piers to flow, and the number of bridge piers, openings, and abutments, their physical condition, their relationship to the channel, banks, and flood plain and any scour and debris problems that may be evident.
40	
41	
42	
43	
44	
45	
46	
47	
48	
49	
50	
51	
52	**Item C1b** records information on the general morphology, characteristics, and conditions at the bridge site.
53	Reach Location records the general planform of the channel at the bridge site, if it is situated on the upstream or downstream limb of a meander bend, the skew of the bridge to flow, the height of the low chord above the channel bed, the overall channel bed material that is being transported, and the thalweg position in the channel at the bridge site.
54	
55	
56	Evidence of Scour, if present, records the specific dimensions of the scour at the bridge piers and abutments. Scour may be dependent of whether or not debris is present.
57	
58	
59	
60	Existing Debris Accumulations records the location of debris relative to the bridge site.
61	
62	Records whether or not bars are present at the site and the type of bar since bars can influence debris grounding and accumulation.
62	Bankline Characteristics provides information on bank stability, vegetative cover, the potential modes of bank failure, how debris may be recruited, and whether of not debris can be stored along the bankline in the upstream channel. The shape of a bank helps define the mode of failure such as undercutting with gravity failure (vertical or overhanging bank) or by rotational failures (concave bank) or by slow fluvial erosion (convex bank). Sediment buildup along the bank toe can temporarily buttress the bank from erosion, but is also indicative of active bank failures. Bank face vegetation can provide some measure of bank stability, but may also be susceptible to recruitment. Depositional berms or narrow floodplains inset into an entrenched floodway are indicative of past incision/degradation followed by recovery. Erosional berms may be indicative of recent incision/degradation. Unstable inset floodpains may be indicative of a new wave of incision. Vegetation on the inset berms and floodplains provide a source for recruitment.
63	
64	
65	
66	
67	
68	
69	
70	
71	
72	
73	

Lateral Channel Stability & Active Bank Erosion Characteristics identifies the location, degree, and specific mode of active bank retreat and channel migration in the upstream channel. Active bank retreat and lateral migration are the modes of debris recruitment.

Vertical Channel Stability identifies whether aggradation or degradation is occurring in the upstream channel since both can contribute to debris recruitment. Degradation results in bank erosion and bank retreat, whereas aggradation can induce overbank flooding and lateral migration.

Item C1c records general information on the riparian corridor upstream of the bridge site. The characteristics of the corridor and its composition provide information on the potential extent and size of the debris that could be supplied to the bridge site. Provide a qualitative estimate of the potential for debris production (use **Flowchart A**) in the upstream reaches and for debris transport and delivery (use **Flowchart B**) to the bridge site .

Item C1d records general information on existing debris accumulations at a given bridge site.

General information is collected on the location of debris accumulations, the type of accumulation on a bridge, the Typical Key Log type and dimensions, and root wad sizes. Qualitative estimate of debris production and transport and delivery to bridge site is made.

Information on the plan and profile (P&P) shape, dimensions, and location of debris along an existing bridge is collected at each bridge element. Provide a qualitative estimate of the potential for debris accumlations on piers/abutments (use **Flowchart C**) and in gaps/spans (use **Flowchart D**). Be sure to incorporate information from available bridge data acquired from DOT (lines 27-35) in the debris accumulation estimations (lines 120-122).

Item C1e Site Plan View Sketch is drawn here and should include important features and dimensions.

Item C1f Cross Section Sketch of Upstream Bridge Face is drawn here. The sketch should be viewed in the downstream direction and should include important features and dimensions.

Item C1g Field Site Photo Log is used to record photos taken at the site. The descriptions of the photo and any important features in the photo are recorded here as well.

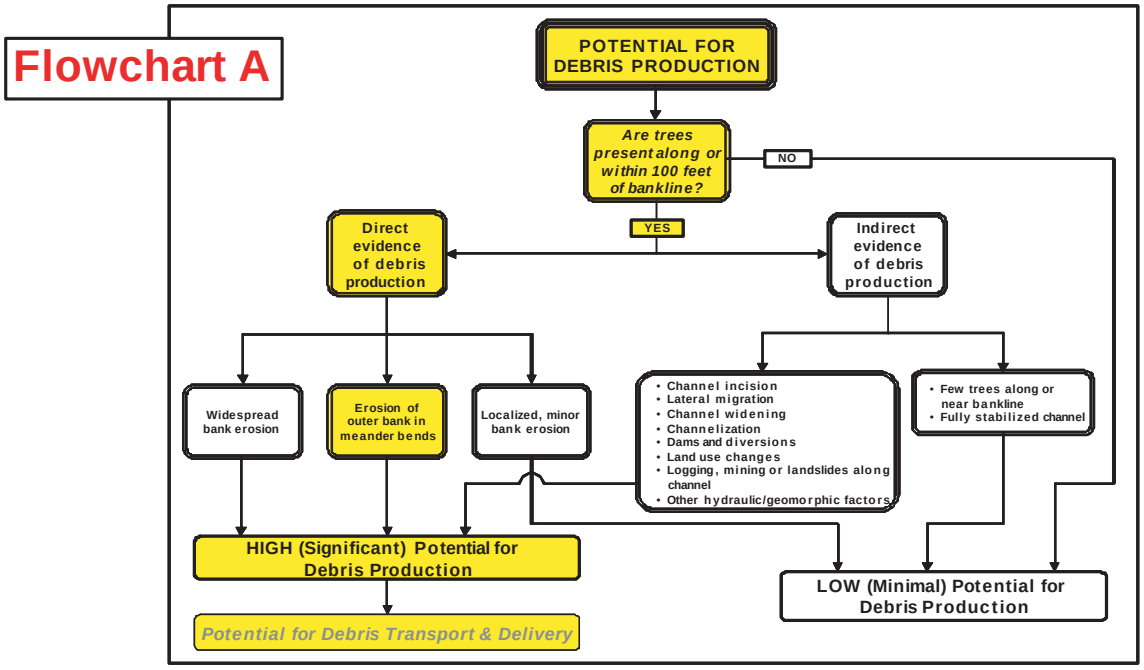

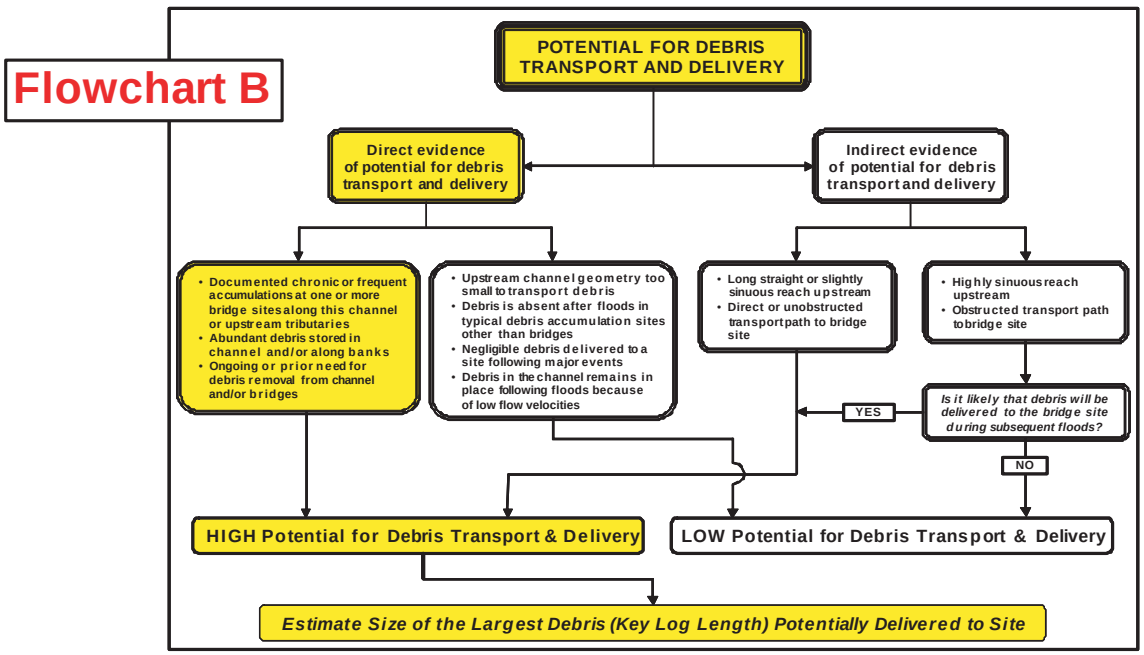

Locational Categories

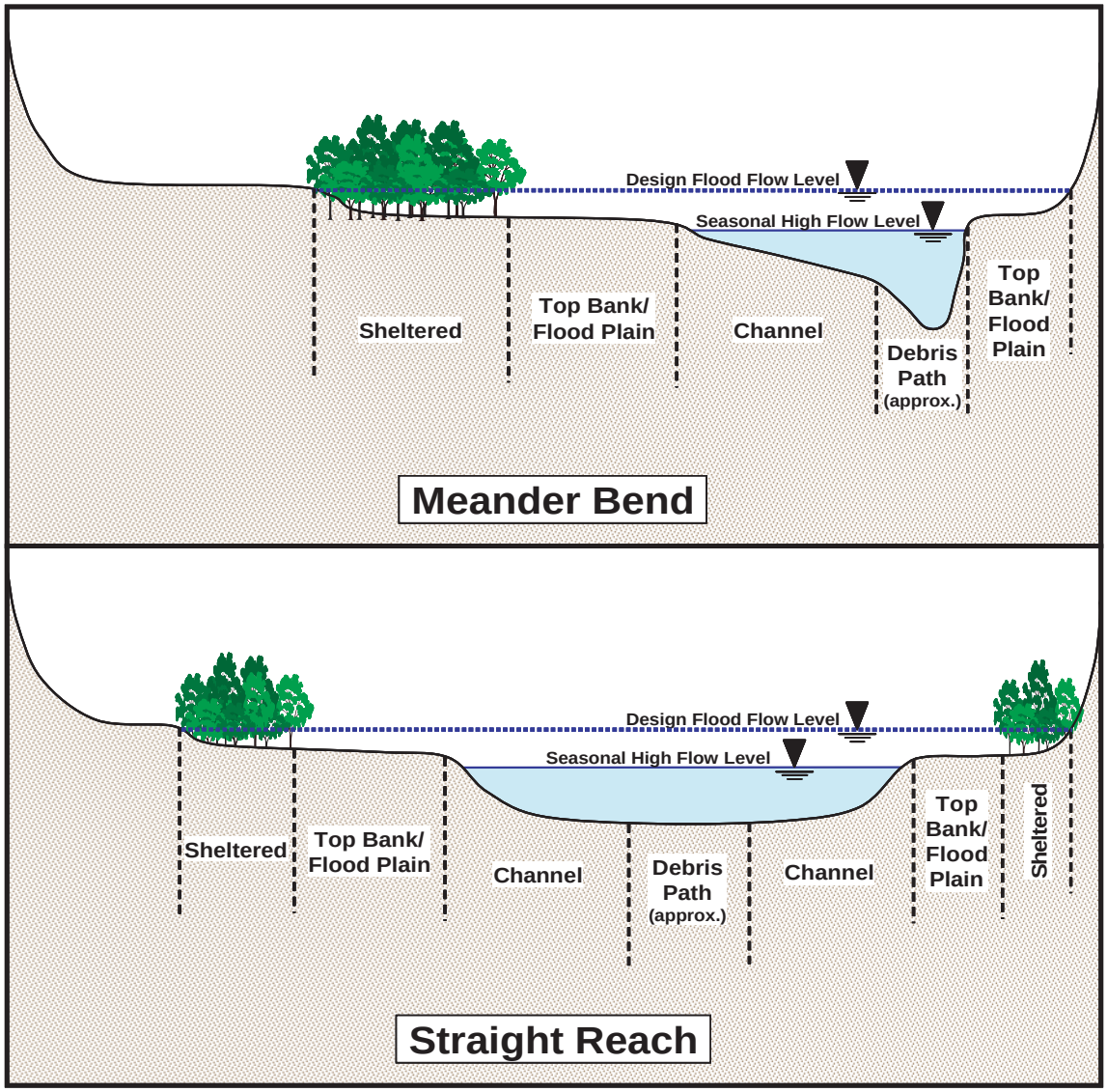

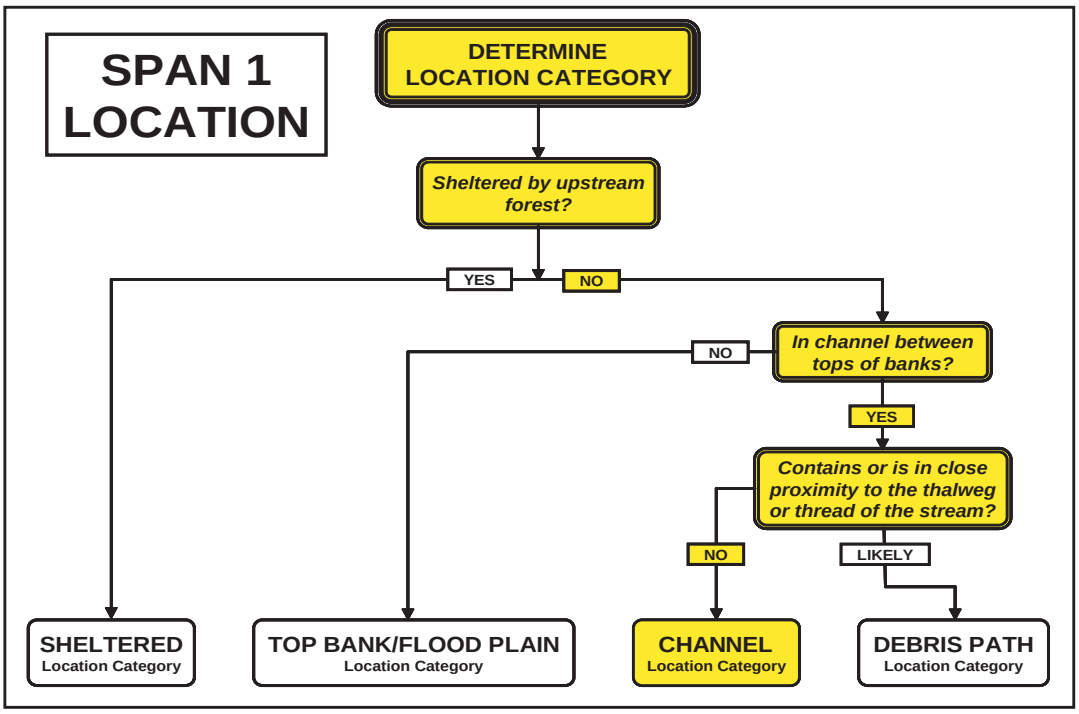

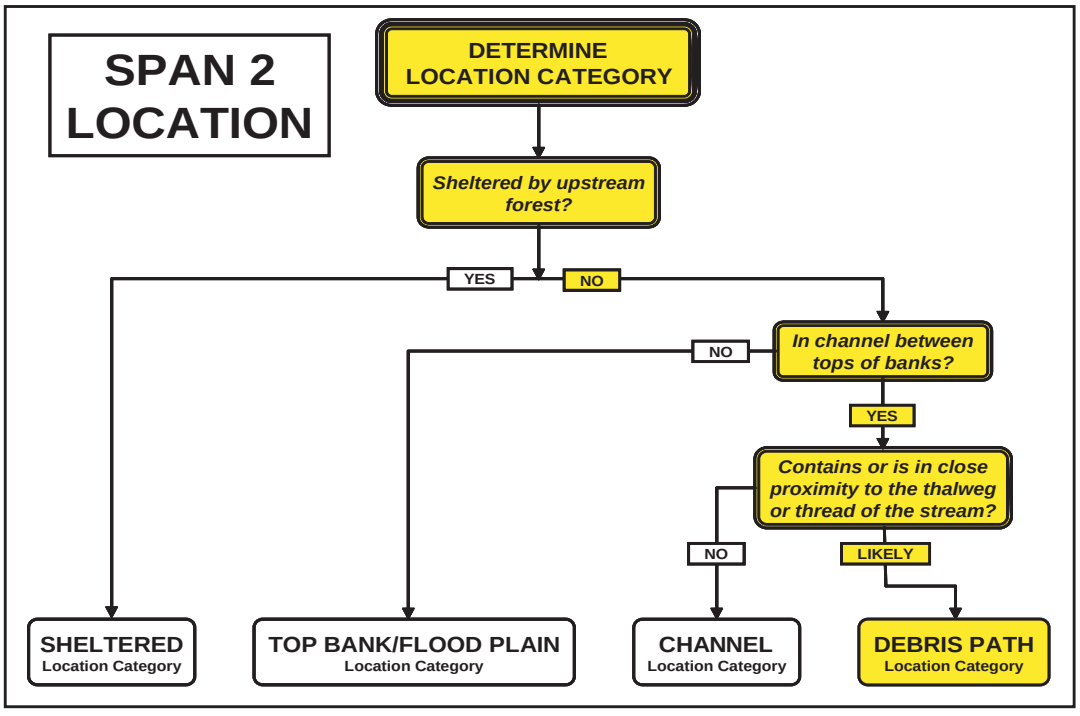

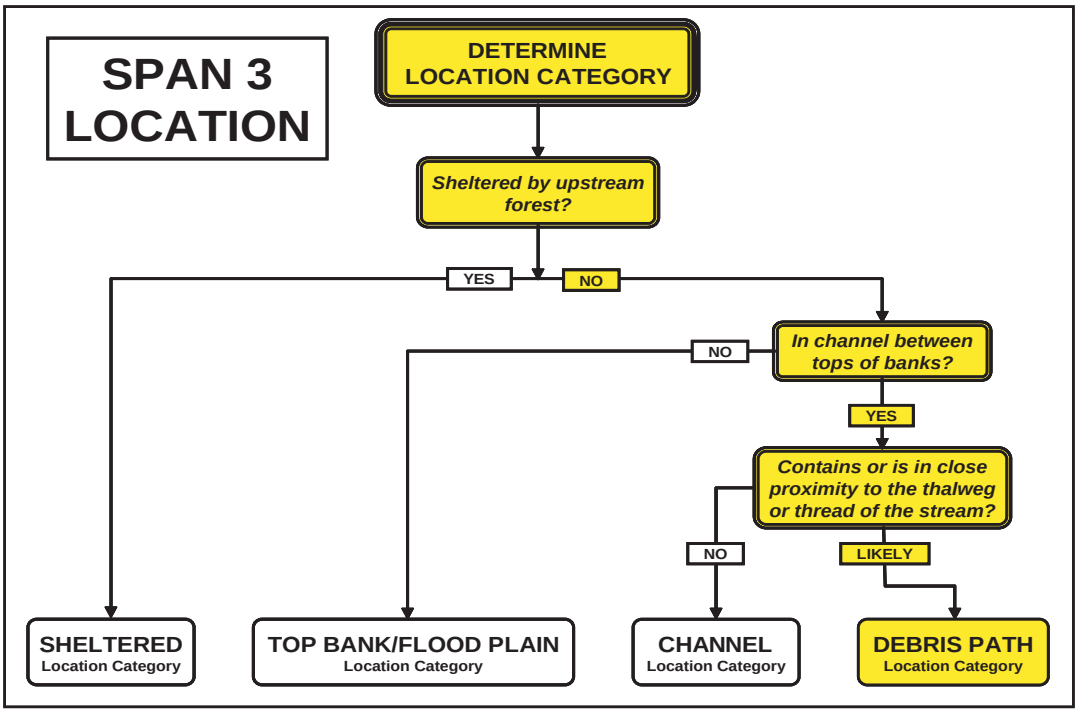

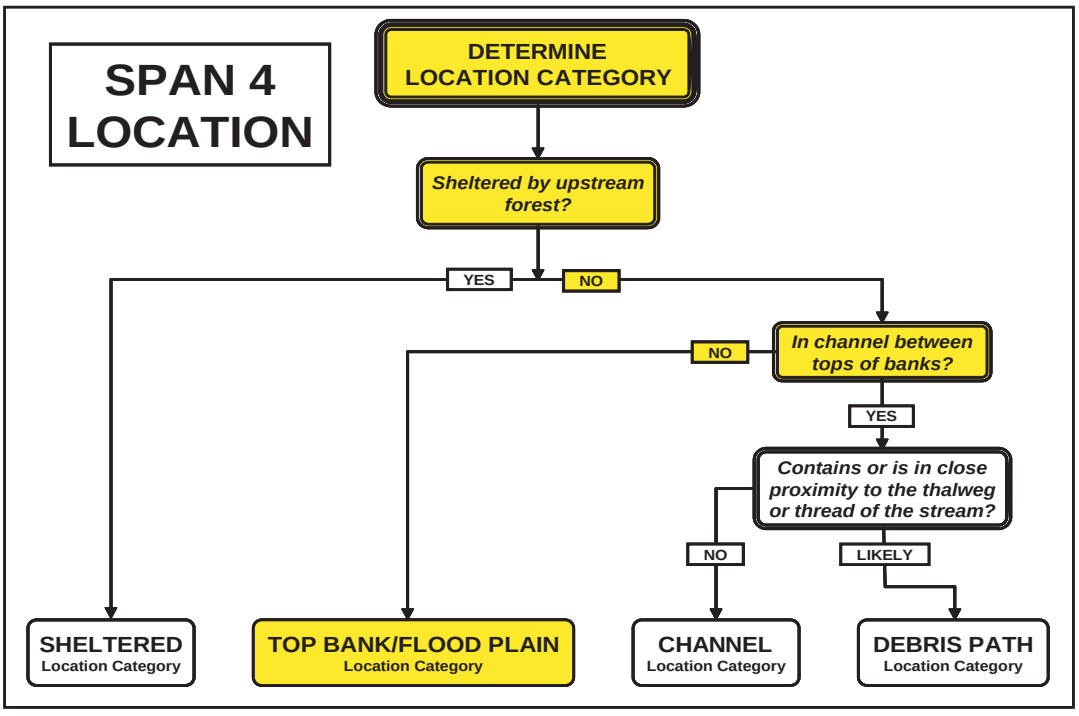

SPAN 1 BLOCKAGE POTENTIAL

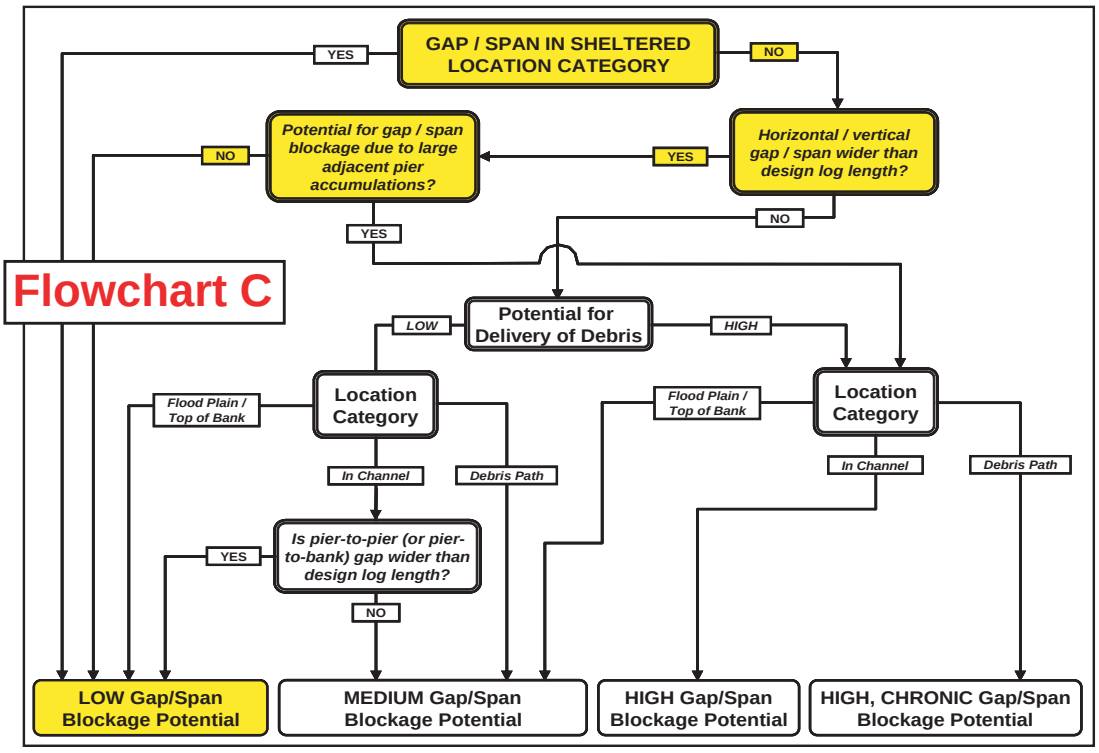

SPAN 2 BLOCKAGE POTENTIAL

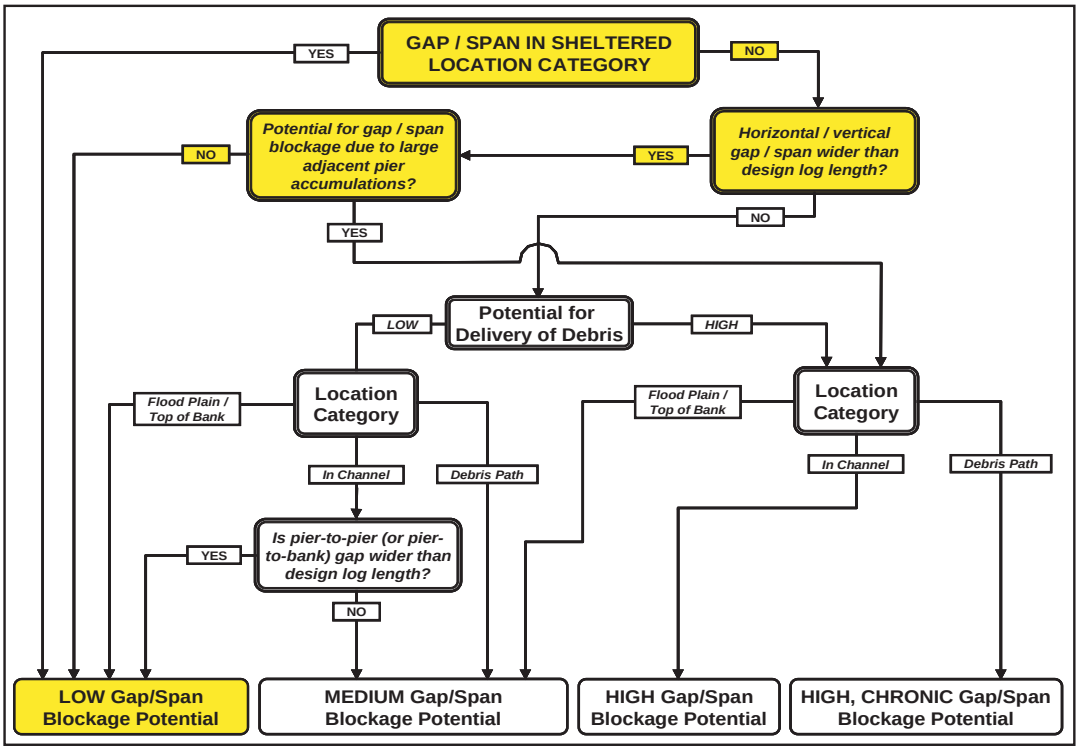

SPAN 3 BLOCKAGE POTENTIAL

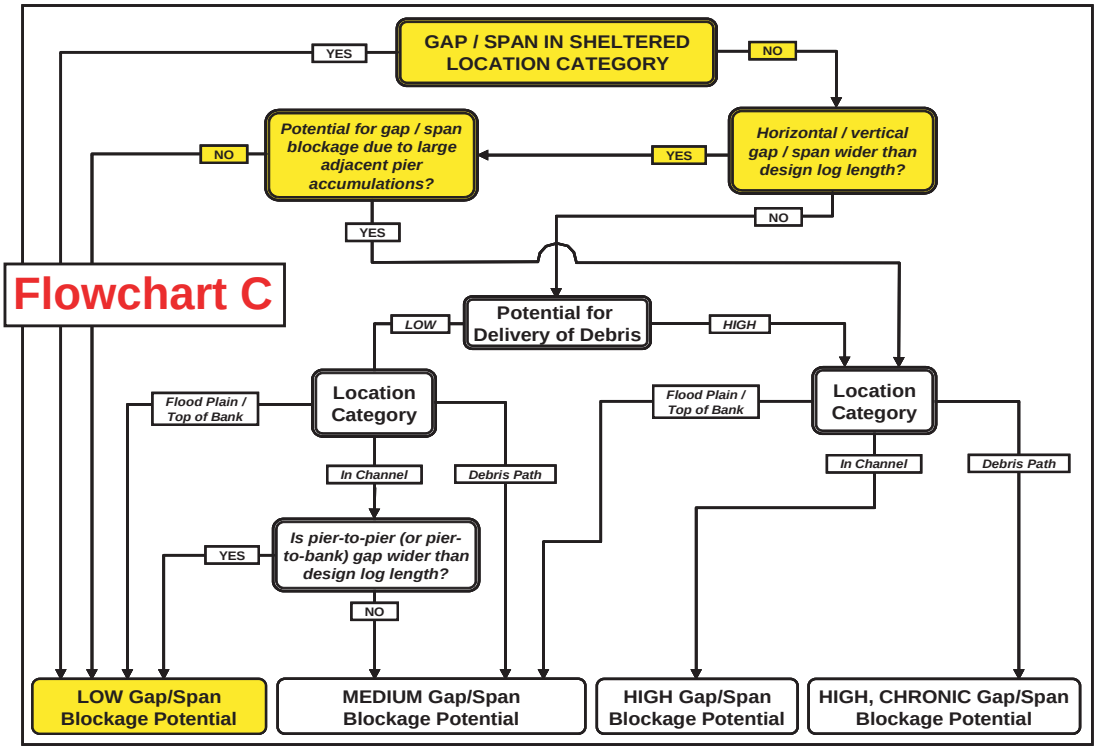

SPAN 4 BLOCKAGE POTENTIAL

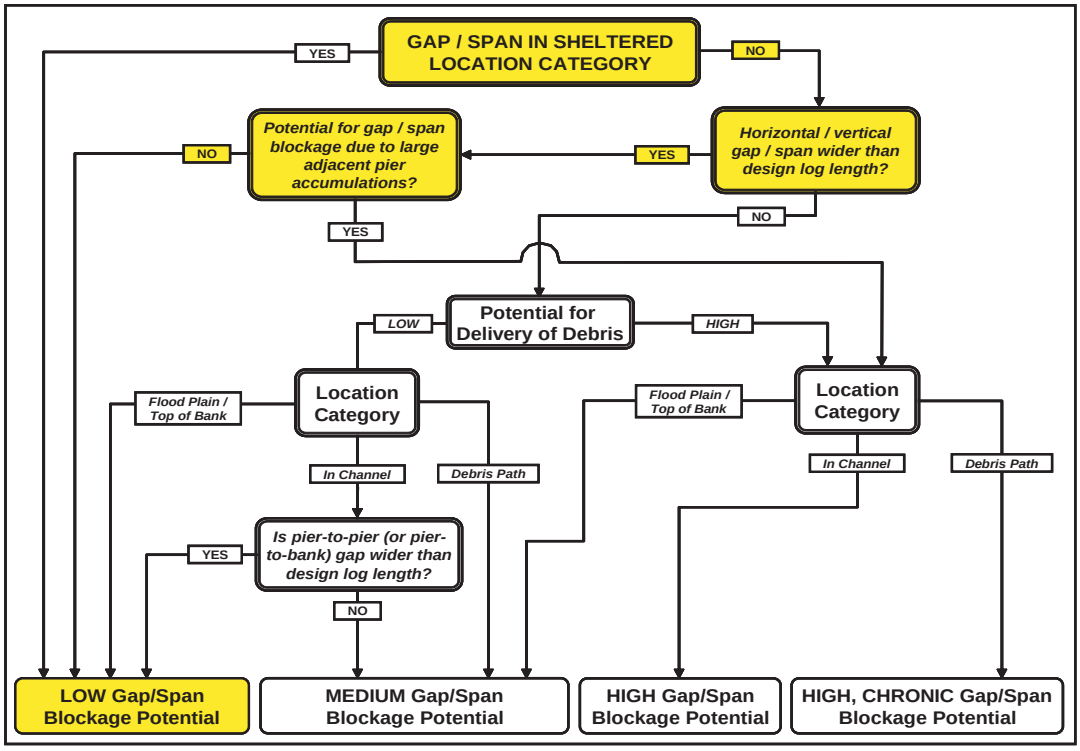

LB ABUTMENT ACCUMULATION POTENTIAL

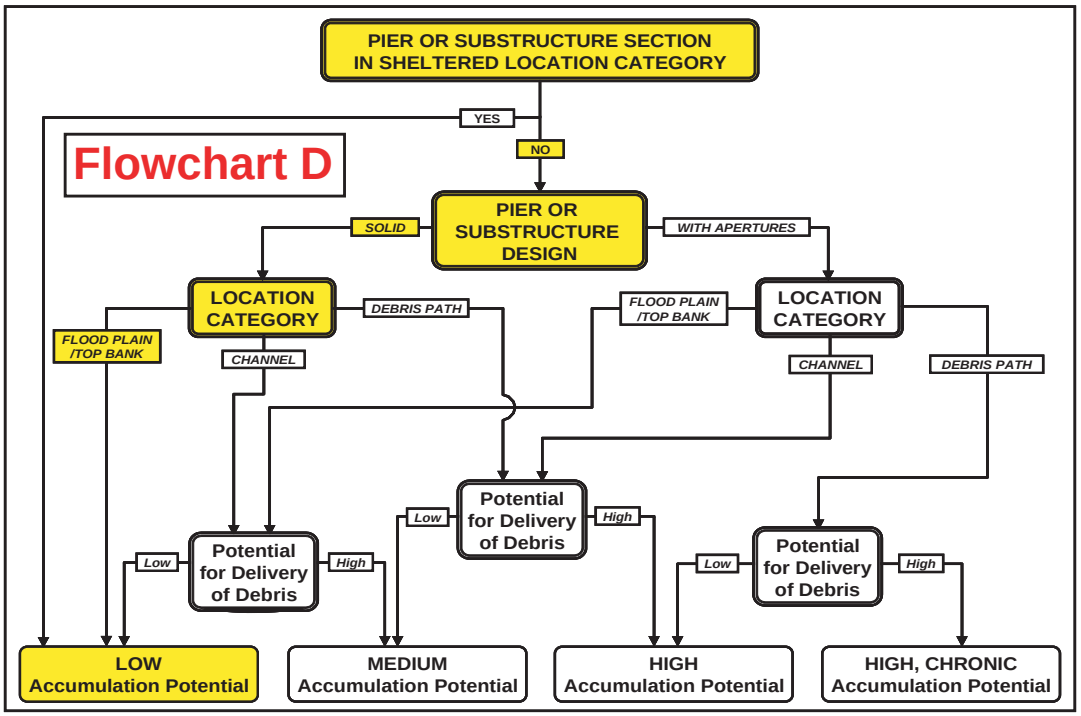

PIER 1 ACCUMULATION POTENTIAL

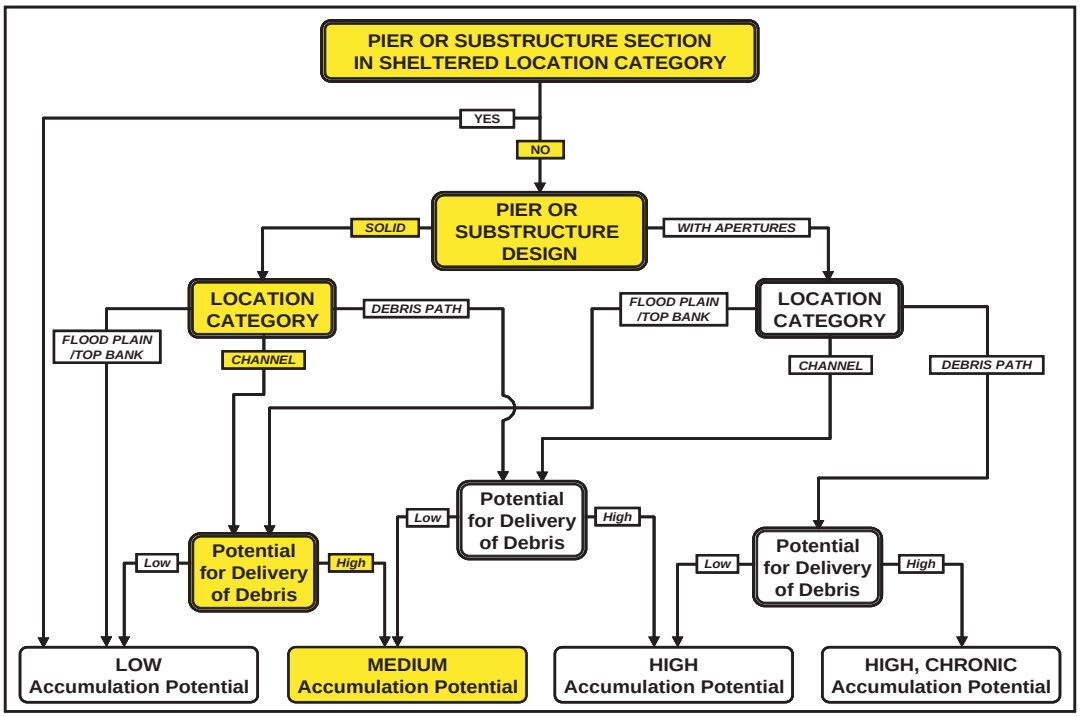

PIER 2 ACCUMULATION POTENTIAL

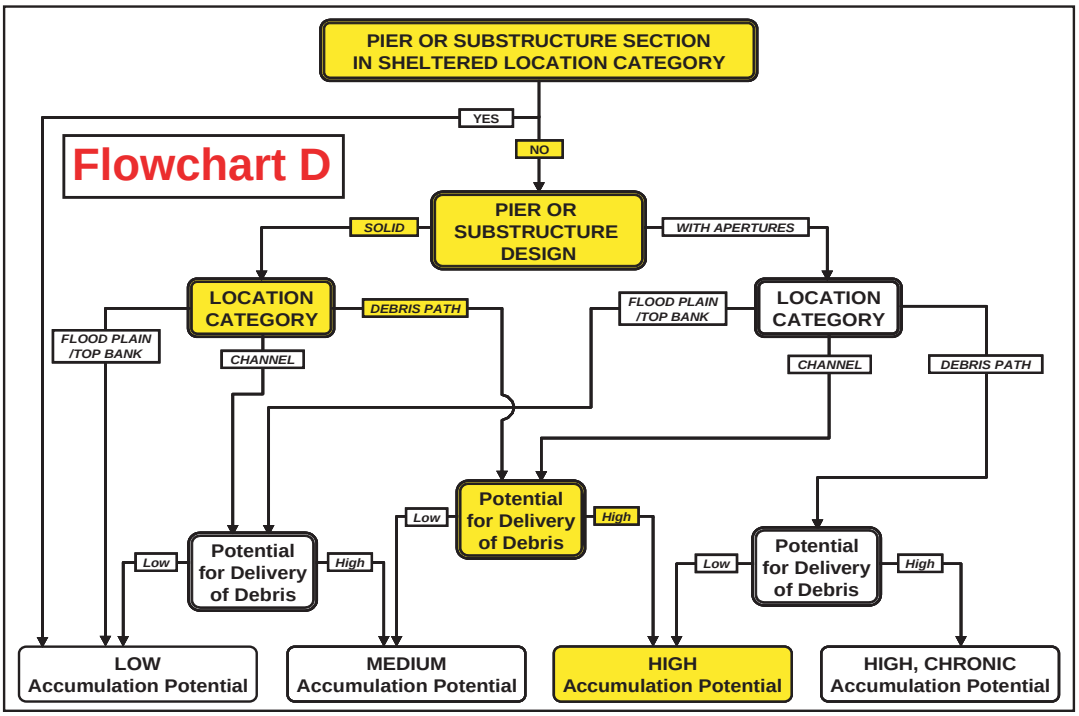

PIER 3 ACCUMULATION POTENTIAL

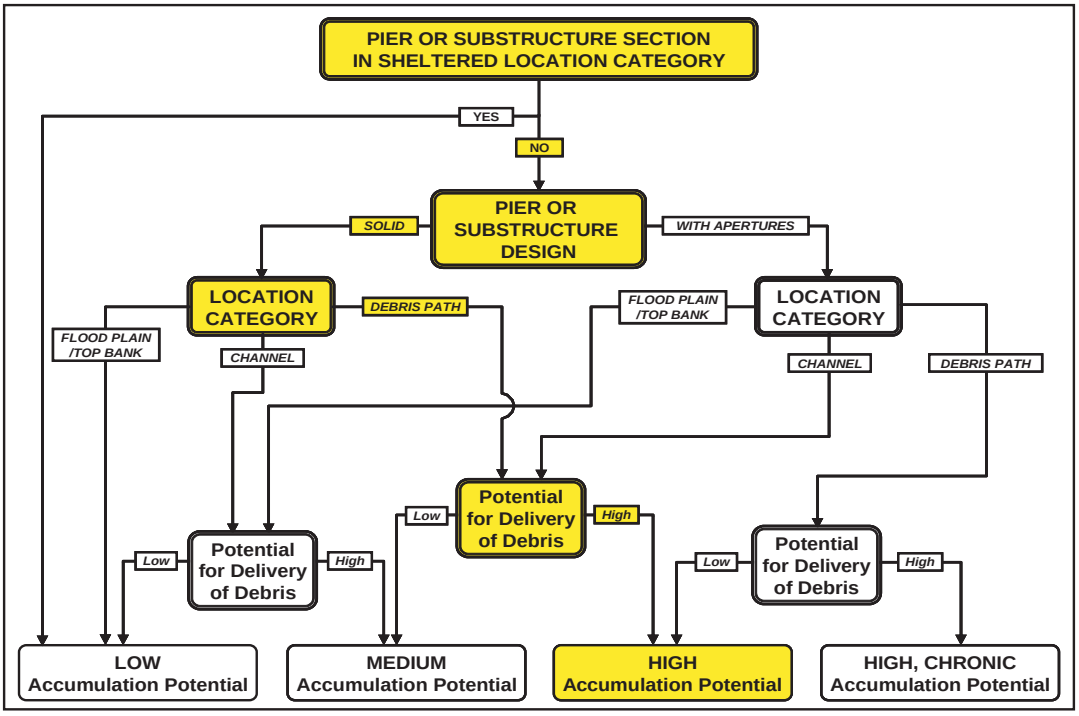

RB ABUTMENT ACCUMULATION POTENTIAL

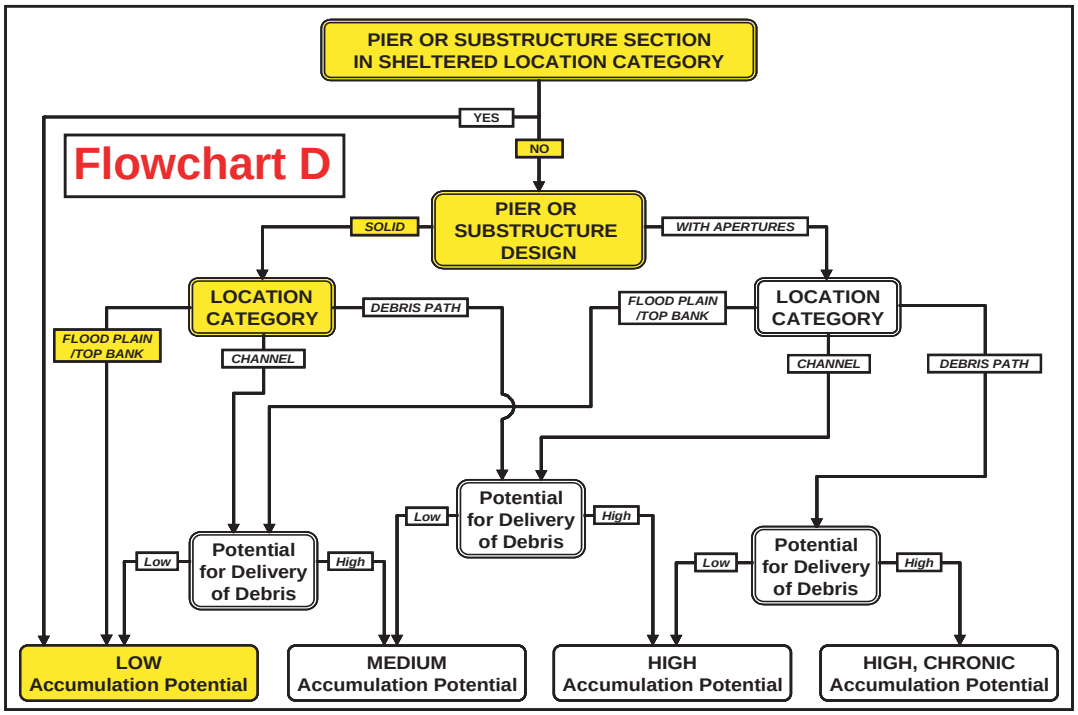

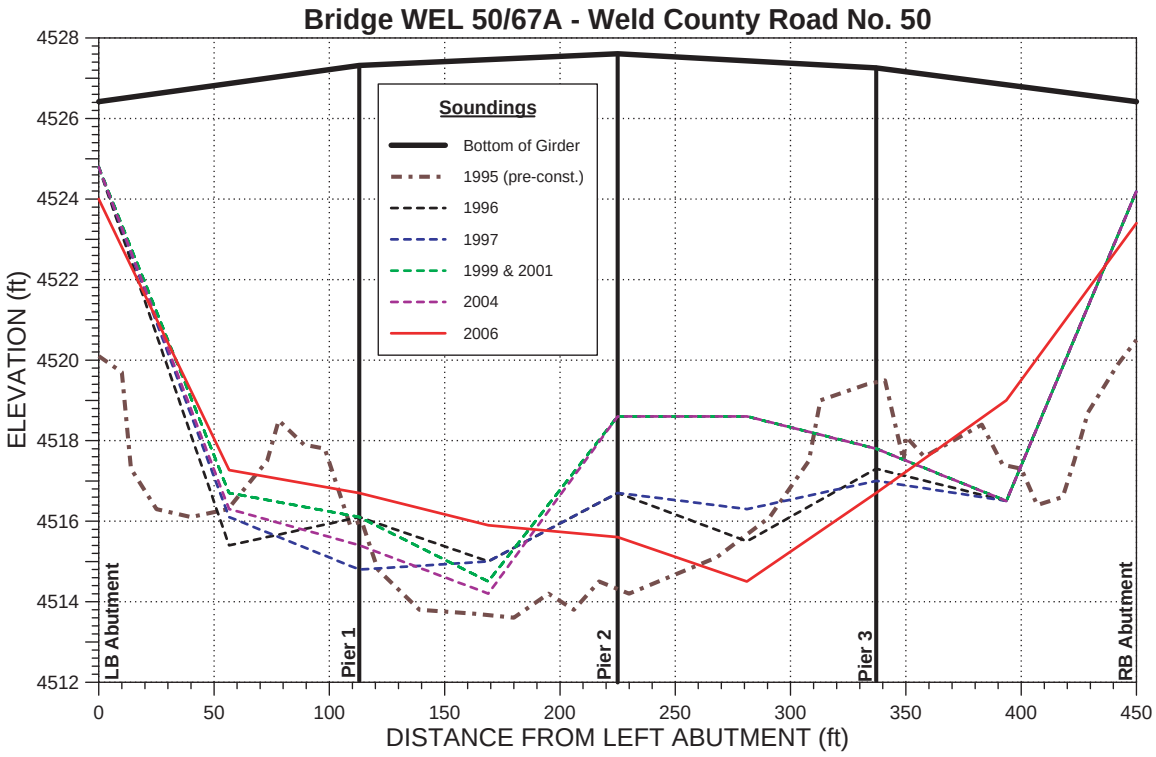

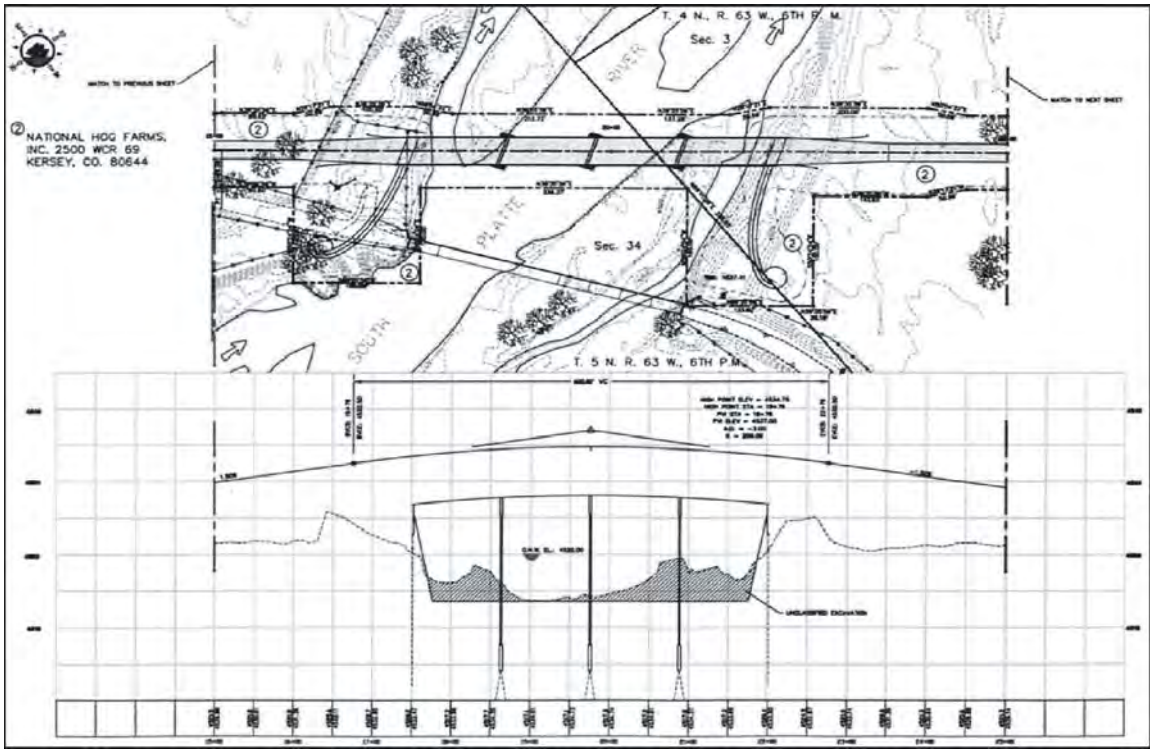

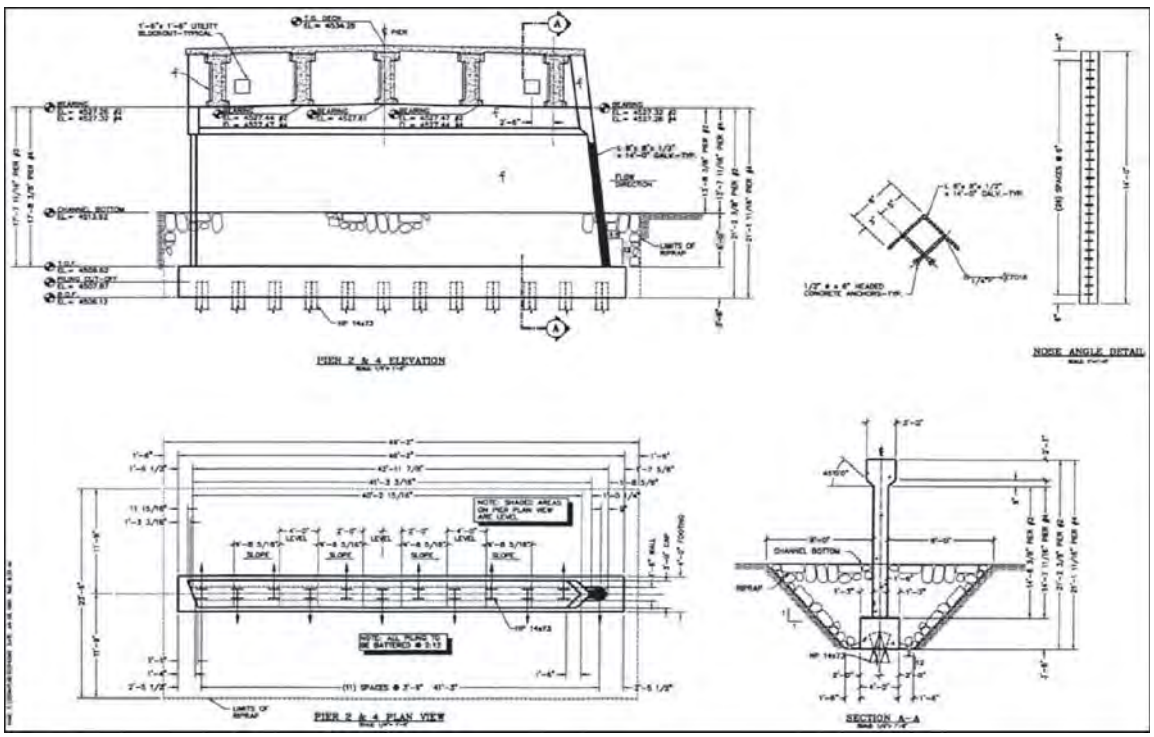

Zoyiopoulos and Associates, Inc.
Engineering Consultants
1011 42ND STREET EVANS, COLORADO 80620
PHONE: (970) 352-8000 FAX: (970) 330-8070

D-46

PART 4

Debris Scour Calculations

Steps 1 through 5

The case study of the South Platte River results indicate that there is a high potential for debris production, high potential for debris transport and delivery, and a high potential for accumulation of debris at Pier 2, which is located in the center of the bridge near the middle of the channel. The span length is 112.9 ft (34.4 m), which is much longer than the key log length of 20 ft (6 m). Therefore, the debris is extremely unlikely to bridge between piers to form a raft. The key log diameter is approximately 1.5 ft (0.46 m) and rootwad sizes can exceed 6 ft (1.8 m). Inspection records of the existing bridge, a previous bridge at this location and nearby bridges indicate frequent debris accumulations.

The debris accumulation at Pier 2 for an extreme event is assumed to be 30 ft (9.1 m) wide, 6 ft (1.8 m) thick, and 20 ft (6.1 m) long. This size accumulation is based on the high debris accumulation potential, key log length, key log diameter, and rootwad size. The shape is assumed to be rectangular. These assumptions should be confirmed for reasonableness with bridge maintenance and inspection personnel (and/or evaluating debris size and shape in the photographic archive in Appendix A).

The hydraulic conditions are calculated for a 100-year flood with and without debris loading. Without debris loading, the maximum channel velocity is 6.25 ft/s (1.91 m/s) and flow depth is 15.3 ft (4.66 m). When the hydraulic model is run to simulate debris loading, the maximum channel velocity is 6.17 ft/s (1.88 m/s) and the flow depth is 15.5 ft (4.72 m).

Because the length of the debris cluster exceeds the flow depth, the debris scour will also need to be computed for a length equal to the flow depth. It is assumed that this shorter debris pile is 26 ft (7.9 m) wide but remains 6 ft (1.8 m) thick and that the hydraulic conditions are the same as for the larger debris cluster.

The wall pier at this bridge has a width, a, of 1.5 ft (0.46 m); a length, L, of 43 ft (13.1 m); a 5° angle of attack; and a sharp nose (actually a debris deflector). Because the pier is more than 12 times the pier width, a maximum length of 12×1.5 ft = 18 ft (12×0.46 m = 5.5 m) is used per HEC-18 guidance. In the pier scour equation, the K_1 pier shape factor is 1.0 (because of the skew) rather than 0.9 for a sharp nose. The pier scour equation K_2 factor can be calculated based on HEC-18 guidance or the projected width of the pier can be used in lieu of using K_2. K_3 is 1.1 based on an assumption of plane bed or small dunes expected on the South Platte River during extreme floods, and K_4 is 1.0 because armoring is not expected.

Guidance on obtaining the above information is contained in Steps 1 through 5 of the methodology outlined in the previous section.

Step 6

Compute pier scour without debris:

$$y_s = 2.0aK_1K_2K_3K_4\left(\frac{y}{a}\right)^{0.35} Fr^{0.43}$$

$$K_2 = \left[\mathrm{Cos}(\theta) + \left(\frac{L}{a}\right)\mathrm{Sin}(\theta)\right]^{0.65}$$

$$= \left[\mathrm{Cos}(5) + \left(\frac{18}{1.5}\right)\mathrm{Sin}(5)\right]^{0.65} = 1.6$$

$$Fr = \frac{V}{\sqrt{gy}} = \frac{6.25}{\sqrt{32.2 \times 15.3}} = 0.28$$

$$y_s = 2.0 \times 1.5 \times 1.0 \times 1.6 \times 1.1 \times 1.0\left(\frac{15.3}{1.5}\right)^{0.35}(0.28)^{0.43}$$

$$= 6.9 \text{ ft } (2.1 \text{ m})$$

Alternatively, the pier scour can be computed using the projected width and excluding K_2 from the pier scour equation.

The projected width of the pier without debris is:

$$a_{\text{proj}} = a\text{Cos}(\theta) + L\text{Sin}(\theta) = 1.5\text{Cos}(5) + 18\text{Sin}(5)$$
$$= 3.1 \text{ ft } (0.93 \text{ m})$$

$$y_s = 2.0 a_{\text{proj}} K_1 K_3 K_4 \left(\frac{y}{a_{\text{proj}}}\right)^{0.35} Fr^{0.43}$$

$$y_s = 2.0 \times 3.1 \times 1.0 \times 1.1 \times 1.0 \left(\frac{15.3}{3.1}\right)^{0.35} (0.28)^{0.43} = 6.9 \text{ ft } (2.1 \text{ m})$$

Step 7

Determine the effective pier width with debris for the maximum debris dimensions. Maximum debris dimensions are $W = 30$ ft (9.1 m), $L = 20$ ft (6.1 m), and $T = 6$ ft (1.8 m) and the projected width of the pier should be used. For a rectangular debris cluster $K_{d1} = 0.79$ and $K_{d2} = -0.79$.

$$a_d^* = \frac{0.79TW\left(\frac{L}{y}\right)^{-0.79} + (y - 0.79T)a_{\text{proj}}}{y}$$

$$a_d^* = \frac{0.79 \times 6 \times 30\left(\frac{20}{15.5}\right)^{-0.79} + (15.5 - 0.79 \times 6)3.1}{15.5}$$
$$= 9.7 \text{ ft } (3.0 \text{ m})$$

Step 8

Determine the effective pier width for the debris length equal to the flow depth. For a debris length equal to the flow depth, the debris dimensions are $W = 26$ ft (7.9 m), $L = 15.5$ ft (4.7 m), and $T = 6$ ft (1.8 m), where W and T are assumed based on the guidance in the previous section.

$$a_d^* = \frac{0.79TW + (y - 0.79T)a_{\text{proj}}}{y}$$

$$a_d^* = \frac{0.79 \times 6 \times 26 + (15.5 - 0.79 \times 6)3.1}{15.5} = 10.1 \text{ ft } (3.1 \text{ m})$$

Step 9

Calculate scour for a_d^* equal to the largest computed value of 10.1 ft (3.1 m) excluding K_1 and K_2 from the pier scour equation.

$$y_s = 2.0 a_d^* K_3 K_4 \left(\frac{y}{a_d^*}\right)^{0.35} Fr^{0.43}$$

$$Fr = \frac{V}{\sqrt{gy}} = \frac{6.17}{\sqrt{32.2 \times 15.5}} = 0.28$$

$$y_s = 2.0 \times 10.1 \times 1.1 \times 1.0 \left(\frac{15.5}{10.1}\right)^{0.35} (0.28)^{0.43} = 14.9 \text{ ft } (4.54 \text{ m})$$

Step 10

For comparison, compute the scour for a triangular debris accumulation with the same dimensions. Maximum debris dimensions are $W = 30$ ft (9.1 m), $L = 20$ ft (6.1 m), and $T = 6$ ft (1.8 m). For a triangular debris cluster, $K_{d1} = 0.21$ and $K_{d2} = -0.17$

$$a_d^* = \frac{0.21TW\left(\frac{L}{y}\right)^{-0.17} + (y - 0.21T)a_{\text{proj}}}{y}$$

$$a_d^* = \frac{0.21 \times 6 \times 30\left(\frac{20}{15.5}\right)^{-0.17} + (15.5 - 0.21 \times 6)3.1}{15.5}$$
$$= 5.2 \text{ ft } (1.58 \text{ m})$$

For a debris length equal to the flow depth, the debris dimensions are $W = 26$ ft (7.9 m), $L = 15.5$ ft (4.7 m), and $T = 6$ ft (1.8 m).

$$a_d^* = \frac{0.21TW + (y - 0.21T)a_{\text{proj}}}{y}$$

$$a_d^* = \frac{0.21 \times 6 \times 26 + (15.5 - 0.21 \times 6)3.1}{15.5} = 5.0 \text{ ft } (1.52 \text{ m})$$

Calculate scour for a_d^* equal to the largest computed value of 5.2 ft (1.58 m) excluding K_1 and K_2 from the pier scour equation.

$$y_s = 2.0 a_d^* K_3 K_4 \left(\frac{y}{a_d^*}\right)^{0.35} Fr^{0.43}$$

$$Fr = \frac{V}{\sqrt{gy}} = \frac{6.17}{\sqrt{32.2 \times 15.5}} = 0.28$$

$$y_s = 2.0 \times 5.2 \times 1.1 \times 1.0 \left(\frac{15.5}{5.2}\right)^{0.35} (0.28)^{0.43} = 9.7 \text{ ft } (2.96 \text{ m})$$

Summary

In summary, the pier scour would be 6.9 ft (2.1 m) without debris, 14.9 ft (4.5 m) with a rectangular debris cluster, and 9.7 ft (3.0 m) with a triangular debris cluster. The controlling condition for the rectangular cluster is when $L/y = 1.0$ (plunging flow coincident with the pier face) and for the triangular cluster the controlling condition is when the debris accumulation is at the maximum size.

Abbreviations and acronyms used without definitions in TRB publications:

AAAE	American Association of Airport Executives
AASHO	American Association of State Highway Officials
AASHTO	American Association of State Highway and Transportation Officials
ACI–NA	Airports Council International–North America
ACRP	Airport Cooperative Research Program
ADA	Americans with Disabilities Act
APTA	American Public Transportation Association
ASCE	American Society of Civil Engineers
ASME	American Society of Mechanical Engineers
ASTM	American Society for Testing and Materials
ATA	Air Transport Association
ATA	American Trucking Associations
CTAA	Community Transportation Association of America
CTBSSP	Commercial Truck and Bus Safety Synthesis Program
DHS	Department of Homeland Security
DOE	Department of Energy
EPA	Environmental Protection Agency
FAA	Federal Aviation Administration
FHWA	Federal Highway Administration
FMCSA	Federal Motor Carrier Safety Administration
FRA	Federal Railroad Administration
FTA	Federal Transit Administration
HMCRP	Hazardous Materials Cooperative Research Program
IEEE	Institute of Electrical and Electronics Engineers
ISTEA	Intermodal Surface Transportation Efficiency Act of 1991
ITE	Institute of Transportation Engineers
NASA	National Aeronautics and Space Administration
NASAO	National Association of State Aviation Officials
NCFRP	National Cooperative Freight Research Program
NCHRP	National Cooperative Highway Research Program
NHTSA	National Highway Traffic Safety Administration
NTSB	National Transportation Safety Board
PHMSA	Pipeline and Hazardous Materials Safety Administration
RITA	Research and Innovative Technology Administration
SAE	Society of Automotive Engineers
SAFETEA-LU	Safe, Accountable, Flexible, Efficient Transportation Equity Act: A Legacy for Users (2005)
TCRP	Transit Cooperative Research Program
TEA-21	Transportation Equity Act for the 21st Century (1998)
TRB	Transportation Research Board
TSA	Transportation Security Administration
U.S.DOT	United States Department of Transportation